EVALUATION OF POWER SYSTEM STABILITY IN MULTIMACHINE POWER SYSTEM

Ph.D. Thesis

BHANU PRATAP SONI

(ID: 2014REE9503)

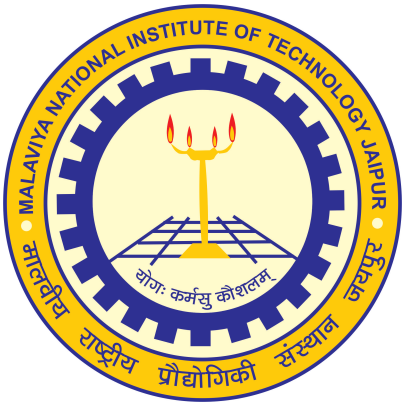

DEPARTMENT OF ELECTRICAL ENGINEERING

MALAVIYA NATIONAL INSTITUTE OF TECHNOLOGY JAIPUR

January 2020

EVALUATION OF POWER SYSTEM STABILITY IN MULTIMACHINE POWER SYSTEM

This thesis is submitted as a partial

fulfillment of the requirements for the degree of

Doctor of Philosophy

in Electrical Engineering

by

Bhanu Pratap Soni

(ID: 2014REE9503)

Under the Supervision of

Prof. Vikas Gupta

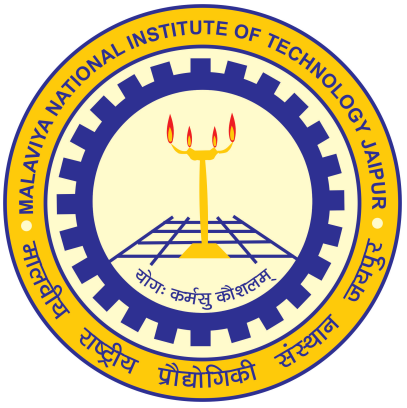

DEPARTMENT OF ELECTRICAL ENGINEERING

MALAVIYA NATIONAL INSTITUTE OF TECHNOLOGY JAIPUR

January 2020

DEPARTMENT OF ELECTRICAL ENGINEERING
MALAVIYA NATIONAL INSTITUTE OF TECHNOLOGY JAIPUR
INDIA, PIN-302017

Candidate's Declaration

I, **Bhanu Pratap Soni** (ID: 2014REE9503) declare that this thesis titled, ***"Evaluation of Power System Stability in Multimachine Power System"*** and work presented in it, is my own, under the supervision of Dr. Vikas Gupta, Department of Electrical Engineering, Malaviya National Institute of Technology, Jaipur (Rajasthan), India. I confirm that:

- This work was done wholly or mainly while in candidature for Ph.D degree at MNIT.
- No any part of this thesis has been submitted for a degree or any other qualification at MNIT or any other institution.
- Where I have consulted the published work of others, this is clearly attributed.
- Where I have quoted from the work of others, the source is always given. With the exception of such quotations, this thesis is entirely my own work.
- I have acknowledged all main sources of help.
- Where the thesis is based on work done by myself.

Date: January 11, 2020

Bhanu Pratap Soni
(ID: 2014REE9503)

DEPARTMENT OF ELECTRICAL ENGINEERING
MALAVIYA NATIONAL INSTITUTE OF TECHNOLOGY JAIPUR
INDIA, PIN-302017

Certificate

This is to certify that the thesis entitled ***"Evaluation of Power System Stability in Multimachine Power System"*** submitted by **Bhanu Pratap Soni** (ID: 2014REE9503) to Malaviya National Institute of Technology Jaipur for the award of the degree of **Doctor of Philosophy** in Electrical Engineering is a bonafide record of original research work carried out by him under my supervision.

It is further certified that:

i. The results contained in this thesis have not been submitted in part or in full, to any other University or Institute for the award of any degree or diploma.

ii. Mr. Bhanu Pratap Soni has fulfilled the requirements for the submission of this thesis.

Date: January 11, 2020

Dr. Vikas Gupta
Supervisor & Professor
Department of Electrical Engineering
Malaviya National Institute of Technology Jaipur

Acknowledgements

It gives me immense pleasure to acknowledge the help and contribution of the number of individuals who supported me during my Ph.D. work.

First, I would like to express my sincere gratitude and cordial thanks to my supervisor, ***Prof. Vikas Gupta*** for his valuable guidance, help and suggestions during my study and research work. It was an honour to work with him. I am gratefull to him for motivating me and being the guiding light. My special thanks to ***Prof. K. R. Niazi*** for his invaluable guidance and support. I will forever be oblized for the immense moral support given by them when i was facing tough time in my research.

Dr. Nitin Gupta, ***Prof. Rajive Tiwari*** and ***Prof. Harpal Tiwari***, deserve special thanks as my research evaluation committee members and advisors for providing me with valuable comments to give the required direction to my work.

In would like to thank ***Prof. Udaykumar R Yaragatti***, Director, MNIT Jaipur for extending all kinds of infastructural support and encouragement required during my Ph.D. I wish to express my thanks to ***Prof. Rajesh Kumar***, Head, Department of Electrical Engineering and ***Prof. Manoj Fozdar***, Convener DPGC, Department of Electrical Engineering, for encouraging me in all possible manners during the course of my Ph.D.

I wish to express my sincere thanks to Dr. S.L. Surana, Dr. Akash Saxena, Dr. Aniruddha Mukherjee, Dr. Kusum Verma, Dr. Shahbaz A. Siddiqui and Mr. Tara Chand Soni for their guidance and help.

My special thanks to my wonderful friends and fellow researchers Dr. Saurabh Ratra, Dr. Jayprakash Keshri, Dr. Pradeep Singh, Mr. Ajay Kumar and Mr. Nirav Patel and all others for revitalizing each day.

I also wish to thank all the faculty members of Electrical Engineering Department, MNIT, Jaipur for their help and constant moral support which enabled me to complete this work.

My family has always been supportive and encouraging. I give my jovial thanks to my parents and my wife Poorva Soni for their patience, cooperation, and understanding during the course of my Ph.D. work.

For any glitches or inadequacies that may remain in this work, the responsibility is entirely my own.

(Bhanu Pratap Soni)

Abstract

Existing power grids are moving towards smart and intelligent grids to achieve reliable, secure, stable and economic operation under the deregulated environment. The construction of next generation power systems need use of new technologies such as Phasor Measurement Units (PMUs), Internet on Things (IoT), Artificial Intelligence (AI) and Machine Learning (ML) based control methods, changes in operational practices and exploitation of existing infrastructure. The integration of the real time monitoring, accurate system health identification and fast & optimal preventive control action are the key characteristics for realizing smart, secure and stable power system.

Power system stability identification and its security are two major tasks in modern power system scenario for maintaining reliable and continuous supply to the consumers. The present trend towards deregulation and competitive environment motivate the utilities to utilize the existing generating, transmission and distribution resources to maximum extent. Moreover, due to economic and operational constraints modern power systems operate close to their stability limit and hence vulnerable to transient instability. Under such stressed operating conditions, even a small disturbance may endanger the system stability and may lead to instant failure of the power system. Therefore, there is an acute requirement of a comprehensive approach that is rapidly able to determine power system security state, transient stability state and can analyze the level of security and suggest appropriate control action within a safe time limit to ensure system security under all operating conditions. The study of contingency analysis and Transient Stability Assessment (TSA) studies are required to be re-investigated to develop effective operational strategies to improve the assessment speed, efficiency and reliability of the power system. Also, there is a need to develop Transient Stability and Security Constrained Optimal Power Flow (TSSCOPF) method to find optimal power flow. Therefore, this thesis is an attempt to address major issues like contingency analysis, security assessment, coherency analysis, TSA & TSSCOPF. Due to large number of operational and economic constraints involved, complexity and sensitivity towards the disturbances have increased. So, real time stability and security assessments are required to identify the stability state of the system to prevent it from collapse by taking appropriate remedial action.

In recent years, application of decision making paradigms based on supervised learning are in trend. The supervised learning mechanism requires input and output set, system features along with the set of optimal architecture configuration parameters of neural network such as, number of hidden layers, number of nodes and in some cases selection of kernel and biases. To make an intelligent choice employment of optimization algorithms are inevitable. These days' nature inspired algorithms are in trend due to their capability of solving complex problems. Recently a nature inspired algorithm based on behavior of grey wolves hunting behavior has been proposed. This algorithm suffers from poor convergence and entrapment in local minima. Keeping these limitations in mind an Intelligent Grey Wolf Optimizer (IGWO) is proposed in this work. First the algorithm is benchmarked on conventional functions which have the known characteristics such as minima, range and number of local and global minima. Having done validation of this the algorithm is employed for feature selection in contingency classification and solving transient stability and security constrained optimal power flow.

For implementing contingency analysis, the two well-known Performance Indices (PIs) namely, PI_{MVA} and PI_{VQ} have been used to measure the severity level of the contingency. Contingency is classified in two classes namely critical and non-critical by using these PIs. Employability of Artificial Neural Network (ANN) and meta-heuristic optimization algorithm for online security assessment and contingency analyses have been investigated in this thesis. Two different ANN-based methods namely, Feed Forward Neural Network (FFNN) and Radial Basis Function Neural Network (RBFNN) have been employed for on-line contingency classification.

This research work has been carried out to increase the classification accuracy and to reduce the computational time and complexity by employing IGWO based feature selection method. The effect of different optimization algorithm based feature selection methods namely GA, PSO, GWO, Binary GWO, and IGWO have been investigated and their performance has been compared with the proposed method. The effectiveness of the proposed method is demonstrated on IEEE 30-bus 6-generator and IEEE 39-bus 10-generator systems under multiple loading and operating conditions corresponding to single line outage contingency and the results are compared with the existing methods. The application results show that accuracy of proposed RBFNN with IGWO based feature selection method is much

better than the FFNN-based method for PIs estimation. Out of the applied different feature selection methods IGWO based feature selection method seems to be better suited for ANN training for PI prediction. The result of comparative study show that the proposed RBFNN with IGWO-based feature selection has better accuracy than the existing ANN-based methods. The proposed RBFNN gives excellent contingency classification with high accuracy even with very small feature subset and under varying topology of the network. Therefore, proposed RBFNN based method may serve as a promising tool for online contingency classification.

Identification of transient stability state in real-time and maintaining stability using preventive control technology are challenging tasks for a large power system while integrating constraints due to deregulation. Widely employment of Phasor Measurement Units (PMUs) in power system and development of Wide Area Management Systems (WAMS) give a relaxation to monitoring, measurement and control hurdles. This focuses on two research objectives; the first is Transient Stability Assessment (TSA) and the second is selection of the appropriate member for the control operation in unstable operating scenario. A model based on the artificial machine learning and PMU data is constructed for achieving both objectives. This model works through prompt TSA status with RBFNN and validates it with PMU data to determine the criticality level of the generators. To reduce the complexity of the model a Transient Stability Index (TSI) is proposed in this thesis. A RBFNN is proposed to determine stability status of system, coherent group, criticality rank of generator and preventive control action, following a large perturbation or fault. PMUs measure post-fault rotor angle values and these are used as inputs for training RBFNN. The proposed approach is demonstrated (validated) on IEEE 39-bus 10-generator, 68-bus 16-generator and 145-bus 50-generator test power systems successfully and the effectiveness of the approaches is discussed.

Further this thesis work also focuses on a control mechanism for the stability and security enhancement under transient unstable scenarios. This involves rescheduling of the generators with minimum increase in fuel cost in such a way that the all system security and transient stability constraints such as bus voltages, line loadings, reactive power generation, and rotor angle deviations remain within their respective permissible limits. To ensure secure operation proposed IGWO is applied to run TSSCOPF algorithm. To study the robustness and effectiveness, the proposed

method is demonstrated on the IEEE 30-bus 6-generator, IEEE 39-bus 10-generator test power systems successfully and results are compared with the other published algorithms.

The work carried out in this thesis for power system stability, contingency analysis and classification, coherency identification, transient stability assessment and IGWO-TSSCOPF based preventive control action may provide a comprehensive solution for both operation and control of the power system to enhance the system stability. At the end of the thesis conclusions drawn from the study are discussed and future scope of the present work is suggested.

Contents

List of Tables

List of Figures

Abbreviations

ABC	**A**rtificial **B**ee **C**olony
AI	**A**rtificial **I**ntelligence
ANFIS	**A**rtificial **N**euro-**F**uzzy **I**nterface **S**ystem
ANN	**A**rtificial **N**eural **N**etwork
CABC	**C**haotic **A**rtificial **B**ee **C**olony
CART	**C**lassification **A**nd **R**egression **T**ree
CCT	**C**rtical **C**learing **T**ime
CNN	**C**ascade **N**eural **N**etwork
COI	**C**entre **O**f **I**nertia
COA	**C**entre **O**f **A**ngles
DT	**D**ecision **T**ree
DSA	**D**ynamic **S**ecurity **A**ssessment
EMS	**E**nergy **M**anagement **S**ystem
EAC	**E**qual **A**rea **C**riterion
FCT	**F**ault **C**learing **T**ime
FFNN	**F**eed-**F**orward **N**eural Network
FFT	**F**ast **F**ourier **T**ransform
FILTRA	**FILT**ering, **R**anking and **A**ssessment
GA	**G**enetic **A**lgorithm
GWO	**G**rey **W**olf **O**ptimizer
IGWO	**I**ntelligent **G**rey **W**olf **O**ptimizer
HCA	**H**ierachical **C**luster **A**lgorithm

ISO	**I**ndependent **S**ystem **O**perator
LSSVM	**L**east **S**quare **S**upport **V**ector **M**achine
MLP	**M**ulti **L**ayor **P**erceptron
OPF	**O**ptimal **P**ower **F**low
PCA	**P**rincipal **C**omponent **A**nalysis
PEBS	**P**otential **E**nergy **B**oundary **S**urface
PI	**P**erformance **I**ndex
PNN	**P**robabilistic **N**eural **N**etwork
PSO	**P**article **S**warm **O**ptimization
RBF	**R**adial **B**asis **F**unction
TDS	**T**ime **D**omain **S**imulation
TEF	**T**ransient **E**nergy **F**unction
TSA	**T**ransient **S**tability **A**ssessment
T/S	**T**ransient **S**tability
TSSCOPF	**T**ransient **S**tability **S**ecurity **C**onstrained OPF
WAMS	**W**ide **A**rea **M**anagement **S**ystem

Symbols

$\Delta\omega_g$	Speed Deviation of g^{th} generator
P_{mg}	Input mechanical power of the g^{th} generator
P_{eg}	Output electrical power of the g^{th} generator
M_g	Moment of Inertia of g^{th} generator
D_g	Damping coefficient of g^{th} generator
$G_{gh} + jB_{gh}$	Transfer admittance between the g^{th} and h^{th} generator
δ_{COI}	Centre of Inertia Angle
δ_g	Rotor angle of the g^{th} generator
H_g	Inertia constant of g^{th} generator
δ_g^{COI}	Relative rotor angles with respect to COI
δ_{max}	Threshold value of rotor angle for transient stability limit
$\varphi(.)$	Activation function
b_k	Externally applies bias
x_j	Input signals
j	Synapse
φ_j	Radial basis function
μ_j	Vector determining the center of radial basis function
σ_j	Width of the radial basis function
W_{ko}	Bias term
y_k	Output signal of the neuron
P_{Dm}	Real power load demand at m^{th} bus
Q_{Dm}	Reactive power load demand at m^{th} bus

m	Load bus
x_n	Normalized input to the neural network
δ_{gh}	Rotor angle difference of most critical gen. g and least advance gen. h
ΔP_{G_g}	Change in real power output of the most advance generator g
$P_{G_g}^{pre}$	Pre-fault real power output of the generator g
$P_{G_g}^{initial}$	Initial power of generator g before rescheduling
P_g^{new}	New real power of generator g after rescheduling
$P_{G_g}^{min}$	Minimum limit of real power output of generator g
$P_{G_g}^{max}$	Maximum limit of real power output of generator g
$Q_{G_g}^{min}$	Minimum limit of reactive power output of generator g
$Q_{G_g}^{max}$	Maximum limit of reactive power output of generator g
V_h^{min}	Minimum limit of voltage at bus h of generaator g
V_h^{max}	Maximum limit of voltage at bus h of generaator g
δ_g^{min}	Minimum rotor angle for transient stability of generator g
V_g^{max}	Maximum rotor angle for transient stability of generator g
$g(t)$	Instantaneous value of the phasor
G_m	Maximum value of the phasor
G	Root mean square value of the phasor
ϕ	Instantaneous phase angle
J	Moment of inertia of the generator
ω_m	Rotor mechanical velocity
T_a	Accelerating torque
T_m	Mechanical torque
δ_i	Rotor angle of generator i
δ_{COA}	Centre of Angles
θ_g	Relative position of the rotor
P_g	Real power output of g^{th} generator

Chapter 1

Introduction

[*This section explains this work's background, context and motivation. It also describes this research's primary contribution and then the thesis structure.*]

Electrical power system provides the necessary infrastructure to generate electricity and deliver it to the consumers. Conventionally, the electricity is generated in large power plants that use different sources of energy such as fossil fuels (e.g. natural gas, oil and coal), converted fuels (e.g.,methane), nuclear fuels, and geothermal, hydro power, solar and wind power etc. [1]. The generated power is transferred through the transmission network at high voltage levels with either Alternating Current (AC) or Direct Current (DC). Then, the distribution networks distribute transmitted power to the consumer at medium and low voltage levels.

A secure and stable power system should be able to withstand contingencies and severe operating conditions without violating the specified operational limits (i.e. bus voltages, line loadings etc.) or compromising its post-contingency stability, so real time operation of power systems is becoming a major concern, where the system structure also changes along with the power demand. The fundamental goal of any power system is to supply uninterrupted, quality power, economically to its consumers. This concern crops up from the fact that electricity demand is growing continually in the present day competitive business environment.

The power network is charged to its limits with an rise in load, making it vulnerable to crash even under small disruption. These factors are creating a back-breaker

TABLE 1.1: Some notable wide-scale power outages around the world

References	**Country/Region**	**Date**	**Duration (hours)**	**Affected People (million)**	**Causes**
[2, 3]	Mexico & The USA	08-09-2011	12	2.7	Transmission line tripping
[4, 5]	Brazil	04-02-2011	16	53	Transmission line fault and fluctuated power flow
[6–8]	India	30-07-2012	15	620	Transmission line overload
[9]	Vietnam	22-05-2013	10	10	Crane operator
[10, 11]	Philippines	06-08-2013	12	8	Voltage collapse
[9, 12]	Thailand	2013	10	8	Lightning strike
[13]	Bangladesh	01-11-2014	24	150	HVDC station outage
[14, 15]	Pakistan	26-01-2015	2	140	Plant technical fault
[16]	Holland	27-03-2015	1.5	1	Bad weather conditions
[17, 18]	Turkey	31-03-2015	4	70	Power system failure
[19, 20]	Ukraine	21-11-2015	6	1.2	Power system failure
[19, 21]	Ukraine	23-12-2015	6	230	Cyber-attack
[22]	Kenya	07-06-2016	4	10	Animal shorted the transformer
[23]	Sri Lanka	03-03-2016	16	10	A severe thunderstorm
[24]	South Australia	28-09-2016	6.1	1.7	Storm damage to transmission infrastructure & cascading events
[25]	the US (NY)	01-03-2017	11	21	Cascading failure in transmission system
[26]	Uruguay	26-08-2017	4	3.4	Bad weather conditions lead to cascading failures

TABLE 1.2: An overview of the initial disturbances and the cascading events led to the major blackouts around the globe

References	**Blackout**	**Initial cause**	**Cascading Events**
[27, 28]	The US & Canada (2003)	East lake Generator tripping due to incorrect data from monitoring system	i—Transmission line trips after contact with a tree ii—Alarm system failure iii—345 kV Chamberli-Harding line sags on to a iv—Voltage dips and no AVR action v—Successive line trip due to under voltage
[29, 30]	Sweden–Denmark (2003)	1200 MW Nuclear power plant trips due to problems with steam valve	i— A double bus-bar fault on one of the substations ii—Transmission line tripping due to overload iii—Generator tripping due to under frequency iv—400 kV north-south interconnecting transmission line trips
[31, 32]	Italy (September 2003)	Tree flashover caused the tripping of a major transmission line	i—Automatic breaker failed to re-close due to synchronization problems ii—380 kV transmission line failure due to delayed re-dispatch of power iii—Loss of synchronism with the other parts of Europe iv—Frequency fell to 49 Hz and then to 47.5 in 2.5 min and generators tripped
[6, 8]	India (July 2012)	Circuit breaker on 400 kV	i—Tripping of Agra Bareilly breakers ii—Power failure cascading through the grid due to under voltage iii—The following day a relay failure occurred near Taj Mahal iv—Power stations across affected parts went offline
[9, 12]	Thailand (2013)	Failure in major AC tie-line	i—A 500 MW power station was interrupted ii—Major tie line for power distribution was affected iii—Further system generator tripped on under voltage and frequency
[13]	BPS (November 2014)	HVDC lines outage	i—Insufficient load shedding ii—Subsequent generator tripping on overload iii—Transmission lines disconnection due to under voltage
[22, 22]	Kenya (June 2016)	Monkey led to tripping of the transformer	i—Generators at the plant tripped on overload ii—180 MW lost from Gitaru iii—Voltage drop led to subsequent transmissions tripping

situation for the power engineers. Stressed conditions in an interconnected power system give rise to inter area oscillation. These oscillations should be taken care of very diligently as they grow otherwise system may collapse [33]. Tables 1.1 and 1.2 list some notable wide-scale power outages and cascading events around the world in this decade [34].

Several critical cascading failures have been listed in Table 1.2. It is therefore, important to come up with appropriate models which help in identifying critical disturbances in advance thereby eliminating blackout of power systems. Initially, the cause and the cascading process of blackouts must be known. Generally, a blackout usually starts as a single system failure, which can, hamper the continuity of operation, security and safety. This failure, in turn, may lead to cascading outages, thus affecting the stability of power system.

1.1 An Overview of Power System Stability

Power system is required to preserve its security and stability in order to meet the population's power requirement. Power system stability is the property of AC power systems that ensures that the system remains in working equilibrium due to both ordinary and abnormal operating circumstances. When used with reference to interconnected synchronous devices, working equilibrium relates to the operation of all devices in the scheme as synchronous, or common-frequency. A disruption may cause the loss of this synchronous conduct. In view of the frequency of occurrence during operation, the disturbance may be small and deemed normal or it may be serious and uncommon. IEEE/CIGRE joint task force [35] has described the definition of power system stability as:

"Power system stability is the ability of an electric power system, for a given initial operating condition, to regain a state of operating equilibrium after being subjected to a physical disturbance, with most system variables bounded so that practically the entire system remains intact."

Power system stability is traditionally categorized as voltage and rotor angle stability. Rotor angle stability can be categorized as large disturbance stability (transient) and small disturbance stability (signal).

1.2 Relationship between Power System Stability and Power System Security

The power system stability has been acknowledged as a major issue for the safe operation of the system since the 1920s [35]. The significance of this phenomenon has been shown by many significant blackouts triggered by power system instability [36, 37]. Usually, such failures are caused by a decreased level of security that makes the system fragile to a series of severe disturbances'. System safety has been approached through reliability and planning of system that could inherently be robust in the face of credible disturbances.

As power systems developed through continuous interconnection expansion, the use of modern techniques and controls, and improved operation under extremely stressed circumstances, various types of system instability have appeared. A power system is an extremely nonlinear system working in a setting that is constantly changing; loads, generator inputs and main working parameters are constantly changing. The health of the system depends on the operating conditions and the type of disturbance.

Reliability is the general goal in the planning and implementation of power systems. The power system must be safe most of the moment in order to be reliable. Security and stability are properties, that change with time and can be assessed by exploring the power system performance under a specific set of contingencies. For a stable power system, it is important that when system faced a disturbance (contingency), the system settles to new operating conditions such that no physical constraints are violated i.e. security is the main concern for power system stability. Thus power system security is essentially related to the stability of the power system under probable and credible contingencies. Therefore, classification of security follows the classification of power system stability.

1.3 Power System Security: Definition

The power system security is defined as, the ability of the system to withstand unexpected failures (contingencies) and continue to operate without interruption of supply to consumers. It is the key aspect in the planning and operational stage of a power system and also known as the security evaluation. Security evaluation is process in which explores the robustness of the system security standard in the existing and future state of a set of pre-selected contingencies.

1.3.1 Analysis of Power System Security

Power system security assessment may be classified in two significant assessments [35].

- *Static Security Analysis*—This is defined as the ability of the system to reach a steady state within the specified boundary limits following a contingency. This includes an ongoing assessment of the post-disturbance system circumstances to confirm that there is no violation of apparatus ratings and voltage limitations [38].
- *Dynamic Security Analysis*— This type of security assessment is also appears in the literature by the names of transient stability or rotor angle stability. These are mainly related to the ability of the synchronous generator of an multimachine power system to remain in synchronism after being subjected to a large disturbance. Synchronism of the system basically the ability to maintain/restore equilibrium between electromagnetic torque and mechanical torque of each synchronous generator in the system

This thesis work mainly focuses on the real time monitoring, assessment and control of the static security and transient stability of the power system. Therefore, this thesis attempts to address major issues like contingency analysis, static security assessment, transient stability assessment and stability enhancement method.

1.4 Static Security Assessment

With exponential increment in power demands, the components of power system are loaded to its permissible limits, and these condition making power system susceptible to collapse even under small disturbance. Also the competition between the supply companies has forced them to operate their system components under stressed operating condition closer to their security boundaries. Under such fragile conditions, any disturbance could endanger system security and may lead to system collapse. Therefore, the key issues before the electric utilities involve assessment, monitoring and control to decide, whether the current operating state of power system is secure or insecure. It is an aid to power system operator to maintain the stability of power system in order to prevent blackouts.

The term that power system is "secure" implies that not only are the present load requirements being met without any equipment overload or voltage problem, but it can also survive any reasonable future contingency without leading to equipment over-load, voltage degradation, system instability, service interruption, etc. This requires "security monitoring" of the present power system state and "contingency analysis" in real time. This analysis involves the simulation of all probable contingencies in which the system performance is detected. To identify the violation of the operational constraints with theirs severity level, each post-contingent scenario is assessed by solving AC load flow. There are various methods [39–95] used for contingency analysis for static security purpose such as conventional methods, ANN based method, other AI-based and hybrid methods etc. Traditional methods are computationally demanding and require exact information about every change in topology which is a difficult task. Sophisticated computer tools have become predominant in solving the difficult problems that arise in the areas of power system planning and operation. Among these computer tools ANNs have been extensively applied in recent years [43–75] in solving power system problems in many areas such as power system security assessment, contingency analysis, load forecasting etc. However, ANN needs to be re-investigated in order to improve its performance and to reduce computational time.

In this thesis ANN based approaches are investigated for contingency analysis

for the planning and operation of a power system as they have the ability to determine the value of severity indices (performance indices) with high accuracy and with in very less time almost instantaneously. The proposed method identifies the transmission lines and buses that violate the operational limits by employing the appropriate Performance Indices (PIs). To reduce the computational complexity and burden of the ANN, a meta heuristic based feature selection method is proposed in this thesis. The proposed approach is then tested on IEEE 30-bus 6-generator system and 39-bus 10-generator system with random load variation under varying topologies. Efforts have been made to improve the online contingency classification accuracy and reduce computational complexity and computation time by incorporating meta-heuristic based feature selection.

1.5 Transient Stability Assessment

The prime motive of the Transient Stability Assessment (TSA) is to determine the rotor angle of all the generators for the current operating condition for a set of probable contingencies. If the rotor angle of any generator or group of generators are found to violet the transient stability criteria, the system is termed as unstable (insecure) otherwise stable (secure). During normal operation, some unforeseen disturbance may occur which may not the part of the probable contingency set. These disturbances may endanger system stability as online assessment cannot be carried out for such unforeseen disturbances. Therefore the real time transient stability evaluation is also required to continuously monitor health (stability) of power system for unforeseen disturbance and to initiate timely and appropriate control measures automatically to ensure systems' stability.

One of the conventionally Time Domain Simulation (TDS) methods may be used for the TSA [96–101]. In TDS the set of non-linear dynamic equations are solved through numerical routines to obtain the rotor angle of all machines during disturbance and post-disturbance conditions. These methods can handle the detail system model and are therefore very accurate. But they are only used for offline applications and rarely utilized for online practices due to high computational time. Another conventional method for stability analysis of power systems by Lyapunov's

direct method has been addressed by M.A. Pai *et al.* in [35,38]. Direct methods are based on the post-fault system equations by a stability criterion [35, 38, 102–106]. But this method suffers from computational in accuracy for multi-machine power systems. A method based on Wide Area Management System (WAMS), energy function and Ad-joint Power system (APS) model was presented in [107]. The method is based on trajectory prediction by employing curve fitting technique. A corrected transient energy function based strategy for probabilistic TSA of power systems was proposed in [108]. An interval Taylor expansion based method was proposed to assess the transient stability in the presence of uncertainties in [109]. A modified form of swing equations and DC link dynamic equations to compute the critical clearing time for a given fault based on the center of angle evaluation was proposed in [110]. Employment of energy function based approaches enables the system operator with the information of degree of stability. Moreover, these approaches are fast and provide important information for selecting appropriate preventive control strategy. The major difficulty in traditional energy function based approaches is that they are applicable only for first swing instability [111]. Because of the limitations of these techniques, there has been excellent interest in implementing artificial intelligence and machine-based learning techniques that are ideal for real time applications. Due to their excellent classification capability and speed of ANNs, a lot of research works [72, 91, 112–118] have been carried out for assessment of power system health using ANNs.

In this thesis, Radial Function Basis Neural Network (RBFNN) has been employed for online TSA of power systems. The application of RBFNN for online TSA of power systems requires an appropriate and accurate Transient Stability Index (TSI) to determine the stability status under a given disturbance. A new TSI is proposed for determining the stability status of the current operating state in terms of synchronism of each generator under a given credible disturbance. The proposed index is based on the TDS solution of the swing equations and this index is a replica of the rotor angel trajectory of the generator. TSI values have been used for training of the RBFNN. The developed methodology has been tested on three different size power systems as IEEE 39-bus, 10-generator system, IEEE 68-bus, 16-generator system and 145-bus, 50-generator system. Efforts have been made to identify the criticality of the individual generator and generator coherent groups. Proposed methodology helps in overcoming the first instability and false alarming

problems. Work has been done to improve the classification accuracy and to reduce the computational time using proposed RBFNN.

Once the stability state is determined and it is found to be in unstable state, then a control action is required to bring the system back to the stable state. One of the control aspects of stability is known as the stability enhancement which is achieved by generator rescheduling with minimum fuel cost. The enhancement process relieves the overloaded lines from stress, reduce the burden on the critical generator which results in enhancement of power system stability. In order to operate the energy scheme stably and optimally, it is necessary to be stable under severe disturbances, i .e. system operation must satisfy the system security and transient stability constraints for a reliable operation. To ensure the stable and optimal solution, Transient Stability and Security Constrained Optimal Power Flow (TSSCOPF) come into the picture.

1.6 Transient Stability and Security Constraints Optimal Power Flow (TSSCOPF)

During the planning and operating stage of the power system, system operators have the main focus on the secure and optimal use of the system components. Optimal power flow (OPF) tool provides the solution under both constraints. In OPF method, production cost function is minimized as objective function via optimal values of the control variables, subject to the system security and limits of the system components. OPF constraints are divided into two categories inequality and equality constraints.

TSSCOPF is, however, a nonlinear optimization problem with both algebraic and differential equations in the time domain. It considers optimal and stable operations simultaneously. As a special requirement of the system, the initial or feasible operating point should be able to withstand the disturbance and can move to a new stable equilibrium state after the clearance of the disturbance without disturbing the equality and the inequality constraints. Due to huge dimension of TSSCOPF problem (especially, for system dealing with detailed machine models), it is really a

tough exercise to deal with this type of problem. For a given power system configuration, although the number of possible contingencies are numerous, there are a few critical contingencies that may cause instability. After analyzing and filtration, the major contingency is selected and the TSSCOPF procedure is applied to find out the optimal operating point.

In the past, classical optimization techniques such as interior point method [119], and Linear Programming (LP) [120] were employed for Transient Stability Constraints Optimal Power Flow (TSCOPF) solution. These techniques have many limitations and some drawbacks. They need an acceptable starting point that is close to the solution in order not to be stuck in local optimum and have poor convergence. In Ref. [120], a linear programming (LP) based computational procedure was developed to solve an algebraic NP problem. Therefore, many heuristic optimization techniques have recently become more and more attractive for researcher to obtain solution of TSCOPF problem. Some of them are Particle Swarm Optimization (PSO) [121], Genetic Algorithm (GA) [122], and Differential Evolution (DE) [123]. However the most important task is to incorporate in OPF operation both transient stability and security constraints subject to the severe disturbance.

Therefore in this thesis an attempt has been made to develop a meta heuristic based solution of the TSSCOPF to enhance the transient staility and static security of power systems. An OPF problem has been formulated as a constrained optimization problem by incorporating different constraints i.e. transmission, generation and stability constrains. A variant of a new meta heuristic algorithm Grey Wolf Optimizer (GWO) namely, Intelligent Grey Wolf Optimizer (IGWO) has been proposed and is employed to reschedule the generator with minimum fuel cost, such that the transient severity is minimized. The proposed approach is then tested on IEEE 30-bus 6-generator and 39-bus 10-generator system. In order to prove the accuracy of the IGWO algorithm, the results are compared with other state-of-the-art algorithms namely GA [121], PSO [121], ABC [124], CABC [124], WOA [125] and CWOA [125] algorithms. Efforts have been made to enhance the transient stability and security under the current operating condition subjected to optimal power generation.

Figure 1.1 represent the thesis structure. The thesis is divided into seven chapters, this chapter presents brief introduction of the terminologies used and research work carried out in this thesis with description of the research motivation.

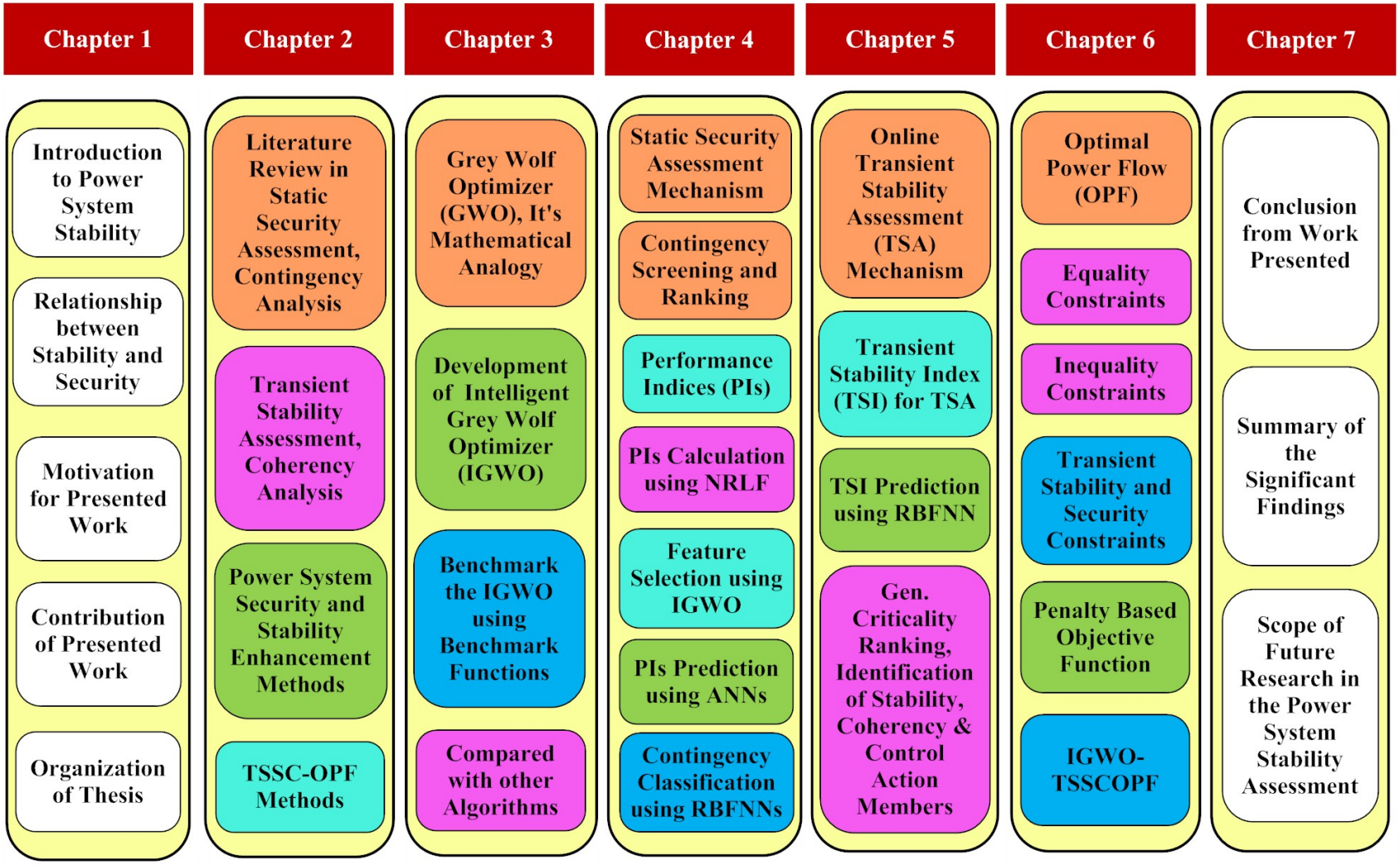

FIGURE 1.1: Thesis structure

Chapter 2 gives the detailed literature survey of the existing methods of the power system contingency analysis, transient stability analysis & its control methods and stability enhancement methods along with the limitations of these existing methods. Finally the research objectives framed are presented based on the literature survey.

Chapter 3 describes the development of an improved version of Grey Wolf Optimizer (GWO) named as Intelligent Grey Wolf Optimizer (IGWO). The details of the development along with the benchmarking of the proposed variant on different type of functions such as multi-modal, unimodal and fixed dimension are also presented.

Chapter 4 presents concept of contingency analysis of power system and the proposed ANN-based approach for ranking and screening. Simulation results and the performance evaluation of the proposed methodology for various test systems are presented.

Chapter 5 describes the proposed method for the real-time transient stability assessment. It also presents the proposed method for coherency identification, and coherency based preventive control technique. Applicability or proposed methods on standard IEEE test systems are also discussed.

Chapter 6 presents the design and implementation of Improved Grey Wolf Optimization (IGWO) for the TSSCOPF. The IGWO is implemented in order to reschedule the generator with minimum fuel cost such that the stability is maximized. In order to identify the efficiency of the proposed IGWO algorithm, the results obtained are compared with the other state-of-the-art algorithms.

In chapter 7 finally conclusions of the research work are presented along with the description of the future scope of this research work.

Chapter 2

Literature Survey

[*This chapter begins with the detailed literature survey of the existing methods of the power system contingency analysis, transient stability analysis & its control methods and stability enhancement methods along with the limitations of these existing methods. Finally the research objectives framed are presented based on the literature survey.*]

Power system failures triggered by instability cause considerable loss of power supply over large areas. Major blackouts may affect millions of consumers for several hours [34]. The recovery of normal operational conditions is a complicated process which requires a lot of time and efforts from control room personnel. For this reason, special attention is paid in providing sufficient stability margin in power systems both at the stage of network planning and at operational level. However it is not possible to prevent power system from collapse for all possible contingencies under all operating conditions. Moreover, unforeseen disturbance may occur in the system leading to the system failure. With the help of Phasor Measurement Units (PMUs) and Wide Area Management System (WAMS), it is now possible to measure and transmit phase and magnitude of the desired quantity to the control center from remote locations at very high speed and frequency. With this information it is possible to develop methods for analyzing the power system stability of the system in real-time and initiate the control action whenever the system is deemed to be unstable following a large disturbance.

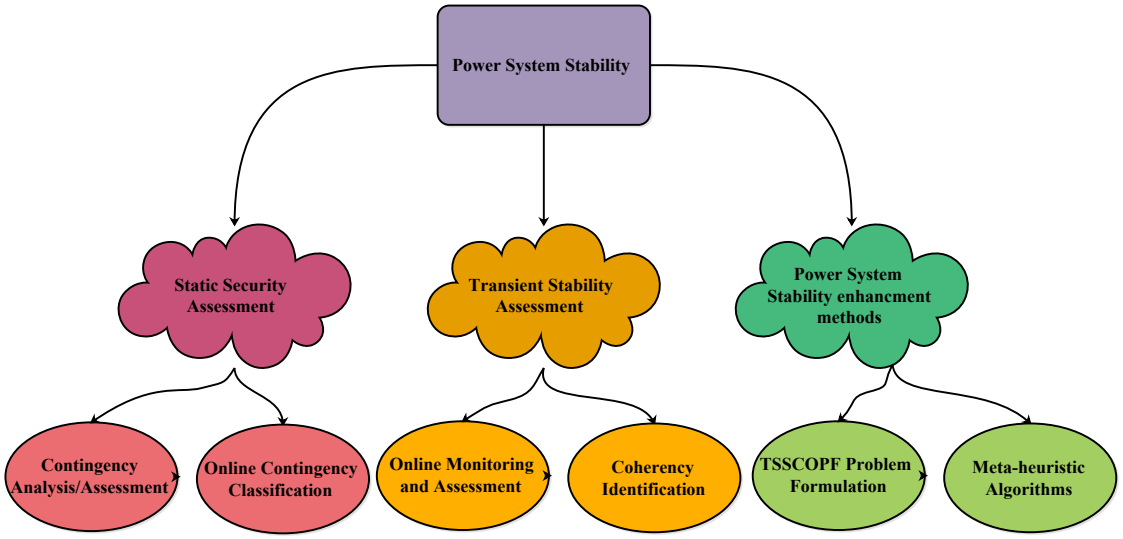

FIGURE 2.1: Study of power system stability

A lot of investigation work has been available in the field of power system stability and its enhancement, which has led to the development of various methodologies and approaches to deal with the problem. Figure 2.1 represent the main domains of the power system stability for the study and research purposes. For planning and operation of modern power system for specially stability point of view, there is a need to study the important issues like steady state security, transient stability and their enhancement methods. A brief literature survey related to the research work in these issues is presented in the following sections and based on the critical review of the literature, the research objectives are formulated.

2.1 Power System Static Security Assessment

In this section, a literature survey corresponding to the power system security assessment is presented. In the area of power system static security assessment, contingency analysis plays a vital role. The importance of the contingency analysis in way of the power system security assessment has been discussed in [126, 127]. The contingency analysis gives the information about the severity level of the power system state under a contingency.

2.1.1 Contingency Analysis

Evaluation of contingency is an important exercise for knowing about emergency conditions in power systems. Without understanding the severity and effect of a specific contingency, the system operator at Energy Management Systems (EMS) can not commence preventative measures. Assessment of contingency is an significant instrument for assessing system security. On the other side, prior forecast of critical contingencies (which may represent a future threat to system stability (voltage or rotor angle)) enables system operators to perform corrective actions and maintaining the power system in a secure state.

A lot of research work has been carried out [39, 43–68, 128–140] in this area in the past several decades. The various approaches for contingency analysis are broadly classified as: Conventional methods, ANN-based methods, other AI-based and hybrid methods etc.

2.1.1.1 Conventional Methods

In order to perform the contingency analysis, the system quantities are calculated for all probable contingencies. For this several load flow methods such as the Gauss-Seidal (GS), the Newton-Raphson (NR) and the Fast Decoupled (FD) [128] were used. These methods are very useful in order to obtain the load flow solutions under the contingency scenario, which helps to compute and rank the system severity. Most of the methods utilize a scalar quantity called the Performance Index (PI). Severity ranking given to the system contingency is based on the value of PI, which is the used to measure the contingency severity or system stress expressed in forms of the system parameters like reactive power and voltage magnitudes etc. Contingency with severity is given higher rank as compared to a contingency which is less severe. The application of the AC load flow in order to solve the outage cases with respect to the reactive power and voltage magnitudes are discussed in [129–133]. In the literature [39, 134], methods with higher accuracy are proposed in order to calculate the distribution factors based on the decoupled and the Newton-Raphson load flow methods using network sensitivities. The obtained factors are used to

compute the post-outage reactive power flows and the voltage magnitudes following a transmission line or a generator outage.

The AC load flow equations need to be solved for each contingency case in order to evaluate the limit violations. However, it is not feasible to perform online, because of the computational barrier. In order to overcome the barrier various approximate methods have been developed. There exist two techniques namely the explicit and the implicit techniques. The explicit methods [135–140] are the ranking methods, where the contingencies are ranked on basis of the order of severity using any PI.

Performance Indices

Most of the methods presented in literature for contingency screening and ranking are based on analytical techniques. Out of them PIs based methods are widely accepted [43–68]. The following section discusses about various performance indices capable of predicting the severity of contingencies and the power system security status. On the basis of literature review it is judged that the contingency ranking is performed by the scalar PI that measure the system security in terms of violation of transmission line loading and bus voltage. System behavior after contingencies is dynamic in nature and relying upon the loads at various loads at various buses, so it's observed that a critical contingency may be a non-critical one at some other loading condition. In order to evaluate the security by these approaches, it is necessary to compute the stress experienced by the system for a specific contingency which is termed as the severity. The severity is basically computed using the violations of the line flows, bus voltages etc. Over the years, the severity is referred by different names such as performance indices, the composite indices, the overall performance indices, the severity indices etc. Though the names appear different, they all compute the severity of the contingencies, but by considering different violations or by combining two types of severities. The indices which used to compute the severity are listed below.

1. *Severity Index:* This index computes the MVA line flow violations.
2. *Active power performance index:* This index computes the active power line flow violation.

3. *Voltage performance index:* This index computes the voltage violations at buses.

4. *Composite performance index:* This index computes the line flow and voltage violations as a single value.

5. *Static Severity index:* This index computes the MVA line flow violations.

The literature reveals the indices with the same name but a variation in the formulation in order to compute the severity based on the specific application. The most widely used indices are the active power and the voltage performance indices.

Contingency with highest severity is ranked as number one and going down the list with the least severity. Whereas, implicit methods use the network solutions in order to recognize the system violations and rank the severity for the various outages [40,141–146]. A partial system solution approach in [40,141,142] and an approximate approach in [143,146], were used to improve the computational speed. The method of concentric relaxation is introduced for the security monitoring. In this approach the system is treated as electrically rigid and gradually relaxed the results to compute the actual flexibility of transmission. These approaches consider only part of the system network in order to identify the branch flow violations. However, obtaining voltage violation is very complex. Thus, the authors in [147] have proposed complete bounding method to identify the line flow violations and the voltage violations. This method reduces the number of line flow computations and limits checking. The zero mismatch method [148] is proposed for quick power flow solutions by exploiting the difference in the convergence rate of individual nodes. Many PI-based method suffer from misclassification and false alarm. These methods are also highly complex and time consuming, hence not suitable for on-line applications.

2.1.1.2 ANN-based Methods

Conventionally, the method to contingency analysis and classification is carried out on the basis of the Performance Indices (PIs), which acquired by solving the load flow equations. The speed and accuracy of the security assessment method rely on the sort of methodology employed for the ranking approach. Thus, in past decade, the

literature has disclosed the implementation of the Artificial Neural Networks (ANN) to the static security assessment of the power system [43–75, 149–151]. The authors discuss the importance and applicability of the neural networks for the assessment and control of power system security [63, 84, 150, 151]. ANN's computing speed and generalization capacity makes it feasible for the smart power systems for the on-line security monitoring [152]. Swarup *et al.* [43] proposed a 3-layer perceptron network with back propagation learning technique for line flow and voltage contingency screening. The ranking and screening modules are composed of Feed-Forward Neural Network (FFNN) [44–46, 153]. The authors in [44, 46] have investigated a CNN, in which the filter and the ranking module are incorporated with a forward network, for quick line flow contingency screening and ranking.

The authors in [47–51,153] have investigate the methods, to estimate the security level for a pre-simulated contingencies data set using Radial Basis Function (RBF) network . A back propagation trained multi perceptron for power system contingency screening and static security assessment has been used in [53–59]. For line flow contingency ranking, a 3-layer perceptron ANN has been designed using back propagation learning technique in [52]. A method based on two-phase optimization neural network has been presented in [66] to compute the degree of insecurity and the voltage and angle at all the buses of the system corresponding to closest secure point.

In [67], ANN is being applied for ranking of critical contingencies. Application of Multilayer Perceptron (MLP), RBF Networks and Self-Organizing Feature Map (SOFM) is proposed in [68]. Chow *et al.* proposed a Hopfield model to solve the contingency classification problem in [149]. This method has demonstrated its feasibility in test cases, yet its assessment accuracy is highly dependent on the amount of training data. Application of Support Vector Machine (SVM) for power system static security assessment is proposed in [69–71, 73, 154]. However, despite their prominent properties, they are unsuitable for large data sets. Devaraj *et al.* [74] developed a set of FFNN to estimate the voltage stability level at different load conditions for the selected contingencies. Verma *et al.* [153] developed PIs based cotingency selection and ranking approach employing FFNN with different type of feature selection techniques. The use of MLP-ANN for contingency analysis, screening, ranking considering dynamic security has been investigated in [75–80].

2.1.1.3 Other AI-based and hybrid methods

Many Artificial Intelligence approaches and hybridization of different methods have also been explored by different authors to implement assessment problem more practical by mitigating the limitations of previously discussed methods. For fast voltage contingency ranking, of the most severe contingency for online applications in Energy Management System (EMS), model tree and hybrid decision tree based approaches were used in [81,82]. A Decision Tree (DT) for real time static security assessment is proposed in [83]. A hybrid model of ANN and Fast Fourier Transform (FFT) is used in [84] for contingency screening. Fuzzified multilayer perceptron network has been proposed in [85–87, 90] for voltage security based contingency analysis and ranking. Sobajic *et al.* [155] has developed a rule-based method for assessment of both single and multiple line-outages contingencies. A genetic based ANN for static security assessment has been proposed in [93]. An approach of using query-based learning in neural networks has been proposed in [94]. In [156], Particle Swarm Optimization (PSO) based method has been proposed for classification of power system security states.

2.1.2 Critical Review

The modern power system is a complex network which consists of several equipment, namely the transmission lines, the generators, the transformers etc. A power system network is said to be reliable, if it supplies quality power to consumers without interruption. Any disturbance will influence the system condition affecting the power supply or even damage the consumer appliances. Thus, the power system stability has become a major concern for the operational engineers. The conventional method of security assessment involves solving the set of nonlinear load flow equations and based on the AC load flow or sensitivity factors. These methods besides being complex, and computationally demanding require exact information about every change in topology. Computation time also makes them infeasible for real time security assessment of large power system networks. Now a days power systems are large and complex where tracking every possible change in topology seems to be a difficult task. The fuzzy, and DT- based solution are fast with better interpretability, but they lack adaptability as these methods provide rule-based solution that

are system specific. It is difficult to implement these methods because of the conflict between the faster solution and the accuracy of the solution. Methods based on ANN seems to have potential to provide effective solution of contingency analysis. However, the accuracy and the speed of the ANN based security evaluation methods depend on the type of methodology and the input variables taken for their training. A strong interaction among system variable resulting in highly complex relations between the input attributes and the output results is necessary. Thus, finding an appropriate feature set for ANN training seems to be a difficult task which directly affects ANN accuracy, complexity and computation time.

2.2 Transient Stability Assessment

For the reliable operation of power system, transient stability is the prime concern of the power system operator. The transient or large disturbance rotor angle stability is defined as the ability of the system to remain in synchronism immediately after large disturbance (such as loss of transmission line or generator) [33, 35]. Generally after large disturbance rotor angle of all the generators makes excursion from their pre-disturbance values, if the rotor angles increase/decrease monotonically without bound system is termed as transient by unstable; if however they oscillate between predefined threshold values the system is said to be transiently stable.

2.2.1 Online Transient Stability Assessment

For online assessment of the transient stability various methods have been reported in the literature, which are used for both offline and onlne purposes. These methods include Time Domain Simulation (TDS) [96–103, 157] based approaches, direct methods which are based on the energy functions [35,38,104–106,158–165]and ANN, SVM & Decision Tree (DT) based AI methods and other hybrid methods.

2.2.1.1 Time Domain Simulation (TDS) Methods

The dynamics of the rotation of the generator rotor is governed by the set of non-linear differential equations. The rotor angles of the machines can be explained as a function of time and their values can be obtained by solving these equations by numerical differential techniques such as trapezoidal method for pre-fault, during fault and post-fault periods [96–103,157]. It also provides the information of the state variables in steady state as well during transient period. The rotor angles obtained through numerical integration indicates the transient stability of the system. This is the most accurate and flexible method with respect to modelling of the power system, detailed model of power system can be considered for determining the rotor angles in the post-disturbance scenario [97]. However due to high computational burden, these methods are utilized for off-line purposes rather than for online applications. These methods does not provide information regarding the degree of instability/stability.

2.2.1.2 Direct Methods

The direct methods for stability analysis of power systems are based on the Lyapunov's stability criterion. These methods have not need to solving the system differential equations. Thus are computationally efficient but have limited to system modeling capability. These methods are generally based either on Lyapunov's second method [166] or Equal Area Criterion (EAC) [103,167]. The direct method based on Lyapunov function consists of defining in the state space a region of asymptotic stability for post fault stable equilibrium point and calculating the value of Lyapunov function. Stability is determined by comparing this value with agiven limit value. Lyapunov function used in the transient stability studies are functions of the energy type known as Transient Energy Function (TEF) [104–106, 158–165]. However, it is difficult to construct a suitable Lyapunov function for multi-machine power system. The EAC has also been applied as direct method for finding the transient stability state of the system [168]. The problem in implementing energy based methods for online security analysis is, difficulty in finding the function that defines the transient energy of the system. Time response of the state variable can not be obtained with these methods.

2.2.1.3 AI based Method

In recent years various AI based methods like Artificial Neural Network (ANN), Decision Tree (DT), Support Vector Machine (SVM), have been employed in the literature for evaluating the stability of the power system. Due to the capability in handling long series and large data satisfactorily and efficiently, AI based techniques were employed for the stability assessment. The developed methods have the human like learning capabilities and can map the complex input and output. The methods are developed to build classifier for the unseen scenarios for online application. In 1988, application of Artificial Neural Net (ANN) was first proposed for dynamic stability assessment of power system [91]. In [112–115, 169] Feed Forward Neural Network (FFNN) and MLP neural network based methods for Transient Stability Assessment (TSA) were proposed. Fisher discrimination as feature selection based neural network [170] was proposed for power system security assessment. Probabilistic Neural Network (PNN) [171–173] used as a classifier for evaluating transient stability. TSA of a single machine infinite bus using multi layer artificial neural network was presented in [174]. In [175] authors investigated the estimation of rotor angles of generators using ANNs and local PMU-based quantities for transient stability prediction. A method for prediction of generators' angles and angular velocities for TSA of multimachine power system was proposed using recurrent ANN [176]. Application of MLP ANNs in power system stability assessment using transient energy function was studied in [177]. For monitoring TSA considering system topology changes, multilayer FFNN trained with back propagation algorithm was investigated in [178]. The Critical Clearing Time (CCT) was used as an indicator for evaluation of system transient stability. In [179], authors investigated TSA of a power system using committee neural networks.

2.2.1.4 Hybrid and Other Methods

Hybrid neural network composed of Kohonen network and several radial basis networks [180] were used for assessing transient stability online. In [76, 181, 182] fuzzy logic and neural nets were used together for dynamic security assessment. In [171, 183, 184] different SVM based techniques were proposed for evaluating transient stability of power systems. Transient security assessment was accomplished by Kernel

ridge regression based method [185] using multivariate polynomial approximation. A DT based approach was presented in [186] for Dynamic Stability Assessment (DSA) and load shedding scheme was suggested for enhancing the dynamic performance. An online DSA [187] scheme using decision tree and phasor measurements was proposed, DTs provide online security assessment and preventive control strategy based on real time measurements through PMUs. Haque *et al.* [188] determined the first swing stability limit of multi-machine power system through Taylor series expansion. An online methodology was proposed in [189] for assessing the robustness of a power system from the point of view of transient stability, and a scalar transient stability index was derived. In [190], authors investigated the probabilistic transient stability assessment for online application using corrected transient energy margin. Ernst *at al.* [191] proposed a unified contingency Filtering, Ranking and Assessment approach (FILTRA) that relies on Single Machine Equivalent (SIME) in power system transient stability studies.

2.2.2 Coherency Identification

In the case of disturbance in a multi-machine power system, some of the machines have similar responses, meaning that the difference between their swing curves is so small that they can be considered to oscillate together in a coherent way. Coherency between generators is also an major aspect in dynamic performance of power systems, which has several applications including dynamic reduction of power systems and commissioning emergency safety an d govern strategies. Coherency based several methods have been proposed in literature for dynamic size reduction of power systems. These methods employing slow coherency concept [192], relation factor [193], Krylov subspace methods [194], Synchrony based algorithms [195–197] and applied on different small and large systems.

Many authors proposed methods [197–211] in the literature for identification of coherent behavior of generators and their classification, according to their similar behavior (TDS characteristics). After identification of the coherent groups, control strategies can be applied on them. In order to initiate any preventive control under stressed condition, it is desirable to discover the coherency between generators [198]. In general, coherency classification techniques can be divided mainly into two types.

The techniques that are placed in the first type are based on model reduction and require computation of the eigenvalues and eigenvectors of power system [197]. For example, a Synchronic Modal Equivalencing (SME) was proposed in [197] for structure preserving dynamic equivalencing of large power system models. Techniques that are placed in the second type are based on disturbances and use TDS to find coherent groups of generators. For example, several studies have used rotor trajectory index [199], Fourier spectrum [200] or fast Fourier dominant inter-area mode [201], principal component analysis [202], independent component analysis [203], hierarchical clustering methods [204–207], Fuzzy c-medoids algorithm [208,209], wavelet [210], and Hilbert-Huang transform [211] to identify coherent generators.

2.2.3 Critical Review

After the power system static security assessment, another most important aspect of the power system is TSA of the power system. Online TSA poses a great challenge for the power system operator under continuous changing system topology. The TDS and energy based direct methods are traditional methods for TSA. The TDS methods are computationally demanding for online applications even though they are more accurate. Also they require exact information about the topological changes which is cumbersome task for present day complex power systems. Employment of energy function based approaches enables the system operator with the information about degree of stability. In the existing TSA indices based methods, no effort has been made to obtain the relative stability of each machine with respect to COI. It is therefore necessary to analyze individual machine trajectory that carries important information on power system dynamic performance. Moreover, these approaches are fast and provide important information for selecting appropriate preventive control strategy. The major difficulty in energy function based approaches is that they are applicable only for first swing instability. Therefore due to the limitations of these methods, from the last three decades there has been rising interests in application of artificial intelligence and machine learning based methods for various power system problems, which are promising for online applications. The methods reported in the literature are fairly accurate and fast but applicable for fixed system topology only. Moreover in these methods emphasis has been on getting results with better accuracy i.e. whether the system is correctly classified as stable/unstable. However

finding the severity of the disturbance is also desirable in addition to accuracy for unstable operating scenarios.

For the control operation there is a need to identify the critical machine and non-critical machines which can effectively participate in the generator rescheduling during the unstable state of the system to ensure stable system operation. In large power systems, generally the information about coherency of generators can be effectively used to decide the participating generators for rescheduling to improve the transient stability of power systems. Usually methods discussed in literature for coherency identification generally require extensive calculation. Therefore further investigations are required for ANN applications in finding relative stability of each generator rather than finding the overall system stability as well as coherency identification for stable power system operation and control.

2.3 Power System Stability Enhancement Methods

Preventive control action based on rescheduling of generators subject to stability constraints for contingencies has been investigated for a number of years. The earliest work [212] investigated the maximum load-ability problem followed by an investigation into interface flow across tie lines [165]. In the papers transient energy margin concept and its sensitivity has been used to change in generation schedules. Since then a number of researches have appeared along these lines by extending the criteria to include Optimal Power Flow (OPF) [213] which is logical [214–216]. The other approach is to include the stability constraints as part of the OPF problem [120, 217]. In another word TSSCOPF is extension of Optimal Power Flow (OPF) with additional rotor angle and line flow inequality constraints.

TSSCOPF is, however, a nonlinear optimization problem with both algebraic and differential equations in the time domain. As a special requirement of the system, the initial or feasible operating point should withstand the disturbance and can move to a new stable equilibrium state after the clearance of the fault without disturbing the equality and the inequality constraints [218]. Due to huge

dimension of the TSSCOPF problem, it is really a tough exercise to deal with this type of problem. For a given power system configuration, although the number of possible contingencies are numerous, there are a few critical contingencies that may cause instability. Various optimization techniques have been evolved in the last two decades to solve the Transient Stability Constrained OPF (TSCOPF) problem. An improved genetic algorithm (GA) was proposed by Chan et al. [219] to solve multi-contingency TSCOPF problem where generator rotor angle constraints were additionally considered. An IPM method was introduced by Xia et al. [220] to efficiently perform the TSCOPF.

If the TSA detects that the system is vulnerable to an anticipated contingency, preventive Transient Stability Control (TSC) measures such as generation rescheduling should be taken to drive the system to the stable state. TSCOPF is becoming an effective tool for many problems in power systems since it simultaneously considers economy and dynamic stability of system operations. Generation rescheduling is a typical TSCOPF strategy used in [221, 222] to shift power from the most advanced generator to the least advanced generator so as to cause the system to move to a stable operating point. In the past, classical optimization techniques such as interior point method [119], and Linear Programming (LP) [120] were employed for TSCOPF solution. These techniques have many limitations. They need an acceptable starting point that should be close to the solution in order not to be stuck in local optimum and have poor convergence. The quality of solution substantially deteriorate because it depends on the initial conditions and the number of parameters in the problem. Additionally, as they have extremely limited capability to solve realistic power system problems, the mathematical relationships have to be simplified to obtain the solution of the problem. They are also weak in processing qualitative constraints. Therefore, many heuristic optimization techniques have recently become more and more attractive in OPF and TSCOPF solution for researchers. Moreover, in the recent past, various other nature-inspired optimization algorithms have been also designated and applied to solve the TSCOPF problem of power system. These includes Particle Swarm Optimization (PSO) [121], Genetic Algorithm (GA) [122], and Differential Evolution (DE) [123], Artificial Bee Colony (ABC) [124], Chaotic Artificial Bee Colony (CABC) [124], Whale Optimization Algorithm (WOA) [125] and Chaotic Whale Optimization Algorithm (CWOA) [125].

2.3.1 Critical Review

Apart from the assessment part of the power system stability, selection of appropriate control strategy is also a major concern to enhance the power system stability. From the literature survey it is observed that generation rescheduling is one of the control strategy for Power system stability enhancement. Research shows the application of several meta-heuristic algorithms are available to perform the economic load dispatch. However, the key factor in rescheduling the generators is the fuel cost incurred in a particular approach. The objective of security enhancement by rescheduling the generators with minimum fuel cost can be achieved with the design of an efficient algorithm. This factor motivated to develop an efficient algorithm for contingency constrained economic load dispatch for security enhancement.

From the above research background, it is observed that for security assessment ANN methods have advantage over classical methods. Thus, there is a scope for modeling neural networks for the prediction of severity of a contingency for static security and dynamic security assessment. Similarly, the literature review for the security and stability enhancement & control mechanism shows the use of many meta-heuristic algorithms for the optimal power flow and the generation rescheduling. But the important aspect which comes into picture in the control scenario is the cost incurred to perform the task by considering security aspect. This factor motivated to develop an efficient algorithm, which can reschedule the generators with minimum fuel cost, considering its static security and transient stability aspects under contingency scenario.

From the above discussion, it is clear that for the power system static security assessment, dynamic stability assessment and the enhancement, there is a need and scope to develop fast and efficient algorithmic techniques. The application of different algorithmic techniques for solving different aspects of power system stability is the main source of motivation for the present research work.

2.4 Research Objectives

After exhaustive literature survey and critical review of the existing methodologies the following research objectives are attempted in the present thesis work:

1. To develop a supervised learning based real time contingency classification engine incorporating an efficient method having reduced complexity and computational burden.
    i. To carry out comparative study of different contingency screening methods and develop a deep understanding in context to multi machine power network.
    ii. To develop an advance meta-heuristic algorithm with certain modifications to improve its optimization performance. Also to validate, the proposed modifications on different benchmark functions.
    iii. To check the applicability of proposed variant for feature selection problem.
    iv. To present a comparative analysis of different approaches employed for contingency screening on the basis of computational complexity and computation time.
2. To develop an algorithm to detect the critical state of individual generator on-line and to determine the coherency under varying operating conditions.
3. To develop an efficient online transient security assessment method for evaluating the system security under wide range of operating conditions for a set of probable contingencies.
    i. To develop a deep understanding of existing indices along with their advantages and limitations.
    ii. To propose a new index based on post-fault rotor trajectories for assessment of future state of power system.
4. To test the applicability of on-line transient security assessment method on different small, moderate and large standard power networks and also, to perform a comparative analysis between proposed index with others.

5. To develop and implement the meta–heuristic technique based approach for the transient stability and security constrained load dispatch for stability enhancement.

    i. To model a combined objective function for the transient stability and security based constrained optimal power flow.

    ii. To test the applicability of proposed method on standard power networks and to present comparison with other contemporary optimizers on the basis of fuel cost.

In this chapter literature survey of different methods of assessing static and dynamic security of power systems and their enhancement methods are presented. The critical analysis of literature survey has been carried out related with these aspects and research objectives have been formulated. The development of Intelligent Grey Wolf Optimizer (IGWO) and its benchmarking results are presented in following chapter.

Chapter 3

Development of Intelligent Grey Wolf Optimizer and Its Benchmarking

[*This chapter describes the development of an improved version of Grey Wolf Optimizer (GWO) named as Intelligent Grey Wolf Optimizer (IGWO). The details of the development along with the benchmarking of the proposed variant on different type of benchmark functions such as multi-modal, unimodal and fixed dimension are also presented.*]

3.1 Introduction

The trend of hybridizing and modifying Evolutionary Algorithms (EAs) has been on rise over the years [223, 224]. In the year 2014, a new meta-heuristic algorithm Grey Wolf Optimizer (GWO) was introduced by S. Mirjalili et.al. [225]. This algorithm is based on hunting strategy of grey wolf and follows the leadership hierarchy of grey wolves.

Recently this algorithm and its variants have been applied in many engineering applications. Ambient air quality classification has been performed with the help of GWO tuned Support Vector Machine (SVM) for different parts of India [226].

Application of GWO has been explored to solve Automatic Generation Control (AGC) [227] problem of two area power system. A binary version of GWO has been employed for unit commitment problem [228]. Binary version of GWO has also been implemented in feature selection for classification [229]. Hybrid GWO [230] was proposed to solve economic load dispatch for four different power systems. The authors [229] employed crossover and mutation operators to improve the performance of the existing version of GWO. From the literature review it is quite evident that for the solution of real world problems some meaningful modifications are required in the existing topologies of meta-heuristic algorithms. These modifications can help the optimizer to reduce computation time and can prove as redemption from the local minima trap. Many modifications have been suggested in the literature for improving the performance of GWO [228–233].

In this work, a new variant of GWO named as Intelligent Grey Wolf Optimizer (IGWO) is proposed to select the optimal features for artificial learning paradigm and to solve the optimal power flow. A sinusoidal truncated function along with opposition based learning is incorporated with GWO and experimented it over 22 benchmark functions (unimodal, multi-modal and multi-modal with fixed-dimension).

3.2 Grey Wolf Optimizer

The classical GWO is inspired by the leadership hierarchy and hunting mechanism of grey wolf. Three main steps of grey wolves are simulated in the algorithm, which are 1. Hunting (searching of prey) 2. Encircling prey 3. Attacking prey. This algorithm is based on the leadership hierarchy and hunting behavior of grey wolf. Grey wolves live in a pack and a fine example of leadership hierarchy. The pack is divided into four categories Alpha (dominant wolves) the decision makers, Beta the subordinate wolves, Delta the scouts, sentinels, elders, hunters, and caretakers and Omega the space goat or baby sitters. The mathematical analogy of hunting, encircling and attacking is presented in the following sections.

3.2.1 Encircling the Prey

The grey wolf encircle the prey and the mathematical equation for the same can be given as

$$\overrightarrow{D} = \left| \overrightarrow{C}.\overrightarrow{X_p}(t) - \overrightarrow{X}(t) \right| \tag{3.1}$$

$$\overrightarrow{X}(t+1) = \overrightarrow{X_p}(t) - \overrightarrow{A}.\overrightarrow{D} \tag{3.2}$$

Where t indicates the current iteration, $\overrightarrow{D}$ is distance vector between prey and wolf, $\overrightarrow{X_p}(t)$ is position vector of the prey and $\overrightarrow{X_p}(t+1)$ updation in the position of grey wolf in next iteration, $\overrightarrow{A}$, $\overrightarrow{C}$ are the coefficient vectors. These coefficient vectors are defined as $\overrightarrow{A} = 2\overrightarrow{a}.\overrightarrow{r_1} - \overrightarrow{a}$ and $\overrightarrow{C} = 2\overrightarrow{a}.\overrightarrow{r_2}$, where $\overrightarrow{a}$ decreases linearly from 2 to 0 and r_1 & r_2 are the random vectors in [0 1].

3.2.2 Hunting the Prey

In the search space the exact identification of the prey is not possible hence, the best three solutions are kept to oblige the social hierarchy (Alpha, Beta and Omega). The mathematical representation of this fact can be visualized in the Equations 3.3, 3.4 and 3.5.

$$\overrightarrow{D_\alpha} = \left| \overrightarrow{C_1}.\overrightarrow{X_\alpha} - \overrightarrow{X} \right| \ , \overrightarrow{D_\beta} = \left| \overrightarrow{C_2}.\overrightarrow{X_\beta} - \overrightarrow{X} \right| \ , \overrightarrow{D_\delta} = \left| \overrightarrow{C_3}.\overrightarrow{X_\delta} - \overrightarrow{X} \right| \tag{3.3}$$

$$\overrightarrow{X_1} = \overrightarrow{X_\alpha} - \overrightarrow{A_1}.(\overrightarrow{D_\alpha}) \ , \overrightarrow{X_2} = \overrightarrow{X_\beta} - \overrightarrow{A_2}.(\overrightarrow{D_\beta}) \ , \overrightarrow{X_3} = \overrightarrow{X_\delta} - \overrightarrow{A_3}.(\overrightarrow{D_\delta}) \tag{3.4}$$

$$\overrightarrow{X}(t+1) = \frac{(\overrightarrow{X_1} + \overrightarrow{X_2} + \overrightarrow{X_3})}{3} \tag{3.5}$$

The equations represent the position updation according to alpha, where $\overrightarrow{D_\alpha}, \overrightarrow{D_\beta}$ and $\overrightarrow{D_\delta}$ are the distances of the prey from α, β, δ wolves respectively and $\overrightarrow{X_1}, \overrightarrow{X_2}$ and $\overrightarrow{X_3}$ are positions of α, β, δ wolves respectively.

3.2.3 Attacking prey

This phase is responsible for exploitation and is handled by $\overrightarrow{a}$. The linear decrement in this parameter enables grey wolves to attack the prey while it stops moving.

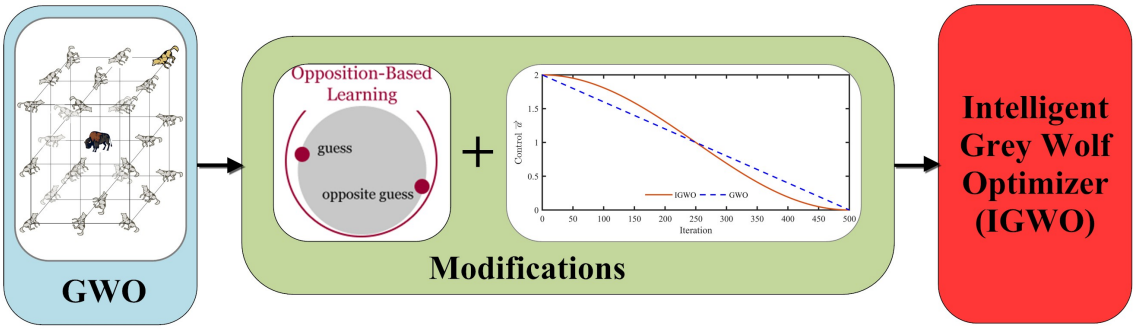

FIGURE 3.1: Block digram presentation of IGWO

Fluctuations in $\overrightarrow{A}$ is also controlled by $\overrightarrow{a}$ i.e. if the value of $\overrightarrow{a}$ is higher, then there are more fluctuations in vector $\overrightarrow{A}$.

3.3 Development of Intelligent Grey Wolf Optimizer (IGWO)

In this chapter two major modifications in GWO proposed to enhance the search capability i.e. better exploration and better convergence. The first modification which is designated by (GWO-M1) is the incorporation of control parameter variation through the sinusoidal truncated function for better exploration and exploitation. The second modification is to inculcate opposition based learning in the existing algorithm for better exploration. The algorithm with both these modifications is denoted by Intelligent Grey Wolf Optimizer (IGWO). Figure 3.1 shows the complete overview of the IGWO.

3.3.1 The Update in Control Vector

In the proposed IGWO both position and direction control of $\overrightarrow{a}$ have been allowed to vary in accordance with a truncated sinusoidal function rather than to decrease linearly as per Equations 3.6 and 3.7. After hunting, the grey wolves stop moving, this action is mimicked by linear decrement of $\overrightarrow{a}$. In proposed GWO trigonometric *sine* function is employed to mimic this behavior in an efficient manner. It can be observed from Figure 3.2 that during hunting period, at first half the values of $\overrightarrow{a}$

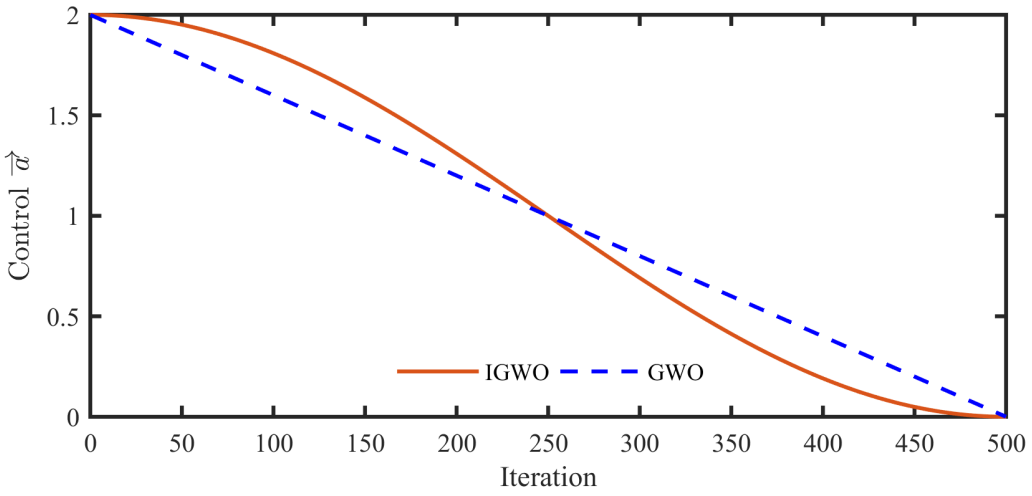

FIGURE 3.2: Control parameter variation through sinusoidal truncated function

associated with the modified version are higher and in later half it reduces more swiftly than the classical version. In a way, this modeling ensures better search capability with the higher value of $\vec{a}$ during hunting and mimics the behavior in a more efficient manner. This modification enables IGWO with better exploration and exploitation capabilities.

$$\theta_w = \pi \times \frac{Current\,Iteration}{Maximum\,Iteration} \tag{3.6}$$

$$a = 2 \times \left(1 - sin^2\left(\frac{\theta_w}{2}\right)\right) \tag{3.7}$$

Where θ_w is indicates the angular change of the wolf movement with respect to the current iteration (t).

3.3.2 Opposition Based Learning

In metaheuristic algorithms or in approximation problems, the search starts from a random point or initial guess and if the point is nearby to the optimal solution the convergence can be achieved faster. However, it is pragmatic to state that if we begin the search from a point which is very far away from the optimal solution the optimization routine/ approximation process will take more time and may become intractable. An opposition based learning approach was introduced by Hamid R.

Tizoosh in 2005 [234]. The approach states that the search for the solution should be in every direction simultaneously. A rich review of the application of opposition based learning in heuristic algorithm was presented in [235]. The popularity of the opposition based learning motivates the author to incorporate this modification in GWO algorithm. Basic concepts of opposition based learnings are discussed below.

Definition 1 Let $x \in [a, b]$ a real number, then the opposite number of x is defined by

$$\bar{x} = a + b - x \tag{3.8}$$

Definition 2 Let $A = (x_1, x_2, ..., x_Q)$ be a point in Q dimensional space, where $x_i \in R$, $\forall i \in \{1, 2, ..., Q\}$ and bounded by $[a, b]$, the opposite points matrix can be given by $\bar{A} = [\bar{x_1}, \bar{x_2}, \bar{x_3} ..., \bar{x_Q}]$. Hence

$$\bar{x_i} = [a_i + b_i - x_i] \tag{3.9}$$

To inculcate opposition based learning in the optimization following steps are used:

Step 1 Set the population size and maximum no. of iterations.

Step 2 Initialize the positions of grey wolves by randomly considering half of the population and remaining opposite population as per definition-2 in the search space.

Step 3 Calculate the fitness of each search agent which represents the distance of grey wolves from prey.

Step 4 Modify the positions of the grey wolves according to Equation 3.9.

In following section IGWO is benchmarked on unimodal, multi-modal standard benchmark functions [225, 236–240].

TABLE 3.1: Unimodal benchmark functions

Function	**Dim.**	**Range**	**Minimum Value**
$F_1(x) = \sum_{i=1}^{n} x_i^2$	30	[-100,100]	0
$F_2(x) = \sum_{i=1}^{n} \lvert x_i \rvert + \prod_{i=1}^{n} \lvert x_i \rvert$	30	[-10,10]	0
$F_3(x) = \sum_{i=1}^{n} \left(\sum_{j-1}^{i} x_j \right)^2$	30	[-100,100]	0
$F_4(x) = \max_i \{\lvert x_i \rvert \quad 1 \leq i \leq n$	30	[-100,100]	0
$F_5(x) = \sum_{i=1}^{n-1} [100(x_{i+1} - x_i^2)^2 + (x_i - 1)^2]$	30	[-30,30]	0
$F_6(x) = \sum_{i=1}^{n-1} ([x_i + 0.5])^2$	30	[-100,100]	0
$F_7(x) = \sum_{i=1}^{n-1} ix_i^4 + random[0,1]$	30	[-1.28,1.28]	0

TABLE 3.2: Multi-modal benchmark functions

Function	**Dim.**	**Range**	**Minimum Value**
$F_8(x) = \sum_{i=1}^{n} -x_i \sin\left(\sqrt{\lvert x_i \rvert}\right)$	30	[-500,500]	-418.9829×5
$F_9(x) = \sum_{i=1}^{n} [{x_i}^2 - 10\ \cos(2\pi x_i + 10)]$	30	[5.12,5.12]	0
$F_{10}(x) = -20\ \exp\left(-0.2\ \sqrt{\frac{1}{n}\sum_{i=1}^{n} {x_i}^2}\right) - \exp\left(\frac{1}{n}\sum_{i=1}^{n}\cos(2\pi x_i)\right) + 20 + e$	30	[-32,32]	0
$F_{11}(x) = \frac{1}{4000}\sum_{i=1}^{n} {x_i}^2 - \prod_{i=1}^{n}\cos\left(\frac{x_i}{\sqrt{i}}\right) + 1$	30	[-600,600]	0
$F_{12}(x) = \frac{\pi}{n}\{10\sin(\pi y_1) + A\} + \sum_{i=1}^{n} u(x_i, 10, 100, 4)$ $A = \sum_{i=1}^{n-1}(y_i - 1)^2[1 + 10\sin^2(\pi y_{i+1})] + (y_n - 1)^2$ $y_i = 1 + \frac{x_{i+1}}{4}$ $u(x_i, a, k, m) = \begin{cases} k(x_i - a)^m & x_i > a \\ 0 & -a < x_i < a \\ k(-x_i - a)^m & x_i < -a \end{cases}$	30	[-50,50]	0
$F_{13}(x) = 0.1\{sin^2(3\pi x_1) + A\} + \sum_{i=1}^{n} u(x_i, 5, 100, 4)$ $A = \sum_{i=1}^{n}(x_i - 1)^2\left[1 + \sin^2(3\pi x_i + 1)\right] + (x_n - 1)^2\left[1 + \sin^2(2\pi x_n)\right]$	30	[-50,50]	0

TABLE 3.3: Fixed-dimension multi-modal benchmark functions

Function	**Dim.**	**Range**	**Minimum Value**
$F_{14}(x) = \left(\frac{1}{500} + \sum_{j=1}^{25} \frac{1}{j + \sum_{i=1}^{2} (x_i - a_{ij})^6} \right)^{-1}$	2	[-65,65]	1
$F_{15}(x) = \sum_{j=1}^{11} \left[a_i - \frac{x_1 \left(b_i^2 + b_i x_2 \right)}{b_i^2 + b_i x_3 + x_4} \right]^2$	4	[-5,5]	0.00030
$F_{16}(x) = 4x_1^2 - 2.1x_1^4 + \frac{1}{3}x_1^6 + x_1x_2 - 4x_2^2 + 4x_2^4$	2	[-5,5]	-1.0316
$F_{17}(x) = \left(x_2 - \frac{5.1}{4\pi^2}x_1^2 + \frac{5}{\pi}x_1 - 6 \right)^2 + 10\left(1 - \frac{1}{8\pi}\right)\cos x_1 + 10$	2	[-5,5]	0.398
$F_{18}(x) = A(x) \times B(x)$ $A(x) = 1 + (x_1 + x_2 + 1)^2(19 - 14x_1 + 3x_1^2 - 14x_2 + 6x_1x_2 + 3x_2^2)$ $B(x) = 30 + (2x_1 - 3x_2)^2 \times (18 - 32x_1 + 12x_1^2 + 48x_2 - 36x_1x_2 + 27x_2^2)$	2	[-2,2]	3
$F_{19}(x) = -\sum_{i=1}^{4} c_i \exp\left(-\sum_{j=1}^{3} a_{ij}(x_j - p_{ij})^2 \right)$	3	[1,3]	-3.86
$F_{20}(x) = -\sum_{i=1}^{4} c_i \exp\left(-\sum_{j=1}^{6} a_{ij}(x_j - p_{ij})^2 \right)$	6	[0,1]	-3.32
$F_{21}(x) = -\sum_{i=1}^{5} \left[(X - a_i)(X - a_i)^T + c_i \right]^{-1}$	4	[0,10]	-10.1532
$F_{22}(x) = -\sum_{i=1}^{7} \left[(X - a_i)(X - a_i)^T + c_i \right]^{-1}$	4	[0,10]	-10.4028

3.4 Results and Discussions

In this section the proposed IGWO algorithm is tested on 22 benchmark functions. The functions are divided into three categories namely unimodal (F1-F7), multi-modal (F8-F16) and fixed dimension multi-modal (F17-F22) functions. The two variants namely GWO-M1 and IGWO of GWO along with the GWO are made to run 30 times on each benchmark function. For this experiment, the maximum number of iterations selected is 500, and search agents are 30. The mathematical definitions of these benchmark functions are given in Tables 3.1, 3.2 and 3.3 where "Dim." indicates dimension of the function, "Range" is the boundary of the function's search space, and "Minimum Value" is the optimum. These benchmark functions are the classical functions utilized by many researchers [236,237,241]. Despite the simplicity, these test functions to be able to compare the obtained results to those of the current meta-heuristics. The statistical results (mean and standard deviation) obtained from this experiment are shown in Tables 3.4 – 3.9.

TABLE 3.4: Comparison of optimization results obtained for the unimodal benchmark functions

	GWO [225]			GWO-M1			IGWO		
$F(x)$	**Stdv**	**Mean**	**p-values**	**Stdv**	**Mean**	**p-values**	**Stdv**	**Mean**	**p-values**
F1	2.85E-27	1.81E-27	N/A	9.93E-26	4.54E-26	3.86E-30	1.00E-25	5.55E-26	0.3363
F2	5.78E-17	9.66E-17	N/A	4.31E-16	7.19E-16	2.59E-32	7.82E-16	7.75E-16	0.6242
F3	2.09E-05	2.26E-05	N/A	0.001144	0.000186	1.75E-06	0.000763	9.93E-05	0.796
F4	1.63E-06	7.02E-07	0.0083	8.86E-07	8.98E-07	0.82	1.05E-06	1.08E-06	N/A
F5	0.789872	27.04077	0.16	0.664889	27.02188	0.09	0.642515	27.0042	N/A
F6	0.35082	0.801875	2.3E-04	0.350237	0.641103	0.7113	0.313278	0.6677	N/A
F7	0.001154	0.001995	0.07	0.001216	0.001935	0.03	0.001074	0.00182	N/A

3.4.1 Exploration and Exploitation Analysis

Tables 3.4, 3.5 and 3.6 are shown the comparison of the results for Unimodal, Multi-modal and Fixed dimension Multi-modal Benchmark Functions respectively. As per Table 3.4, the IGWO gives better results and outperforms GWO and GWO-M1 on function F5, F6 and F7. It is worth to mention here that unimodal functions are suitable for benchmarking the exploitation capability of the algorithm. From the results it can be observed that IGWO is a better choice. In comparison to unimodal functions, a number of optimal solutions exist in multi-modal functions. This fact makes the multi-modal functions enabled to benchmark the exploitation capability [225]. It may be noted that the unimodal functions are suitable for benchmarking exploitation. Therefore, results in Table 3.4 are show the superior performance of IGWO in terms of exploiting the optimum.

In contrast to the unimodal functions, multi-modal functions have many local optima with the number increasing exponentially with dimension. This makes them suitable for benchmarking the exploration ability of an algorithm. According to the results of Tables 3.5 and 3.6, IGWO is able to provide very competitive results on the multi-modal benchmark functions as well. It is observed from these results IGWO provides outperforming results on unimodal, multi-modal and multi-modal functions with fixed dimensions.

3.4.2 Statistical Analysis

To test the efficacy of the proposed variant IGWO a statistical non parametric Wilcoxon Rank Sum test [242] is performed with 5% significance level. The results of this test (p-values) along with the mean and standard deviation of the functions are shown in Tables 3.4, 3.5 and 3.6. 'N/A' (Not Applicable) has been written for the algorithm which has best performance for that particular function as the best algorithm can not be compared with itself [243]. Results presented in these tables reveals that IGWO outperforms for 13 out of 22 functions.

For functions F1, F2, F3, F10, F20, F21 and F22 GWO performs normally better whereas for rest of the functions i.e. F12 and F13 GWO-M1 performs a little better. Inspecting the results of this test, it is observed that GWO performs marginally better for functions F1, F2, F3 but the p-values obtained for IGWO are greater than 0.05. This shows that the GWO does not provide significant results as compared to IGWO on the other hand the p-values of GWO-M1 are much lower than 0.05

Table 3.5: Comparison of optimization results obtained for the multi-modal benchmark functions

	GWO [225]			**GWO-M1**			**IGWO**		
$F(x)$	**Stdv**	**Mean**	**p-values**	**Stdv**	**Mean**	**p-values**	**Stdv**	**Mean**	**p-values**
F8	777.7582	-5938.526	0.43	1019.180	-5898.140	0.28	950.3293	-5991.231	N/A
F9	7.658998	3.006042	3.4E-08	1.576759	1.321605	0.16	2.734441	1.270284	N/A
F10	1.88E-14	1.03E-13	N/A	4.53E-14	1.49E-13	2.4E-21	4.31E-14	1.64E-13	0.98
F11	0.011029	0.004714	0.40	0.009316	0.00172	0.82	0.005099	0.001994	N/A
F12	0.077122	0.041859	0.55	0.016073	0.039873	N/A	0.052673	0.042402	0.2523
F13	0.218983	0.636368	0.0015	0.204149	0.543674	N/A	0.21782	0.551296	0.52
F14	4.672684	4.258171	5.51E-05	4.515412	4.455777	0.29	3.741593	4.038417	N/A
F15	0.00695	0.004793	0.0164	0.007498	0.003829	0.47	0.00733	0.003662	N/A
F16	2.49E-08	-1.03163	3.76E-34	4.93E-11	-1.03163	0.1021	3.01E-11	-1.03163	N/A

Table 3.6: Comparison of optimization results obtained for the fixed dimension multi-modal benchmark functions

	GWO [225]			**GWO-M1**			**IGWO**		
$F(x)$	**Stdv**	**Mean**	**p-values**	**Stdv**	**Mean**	**p-values**	**Stdv**	**Mean**	**p-values**
F17	0.00013	0.397912	4.44E-27	0.000248	0.397954	0.4179	8.36E-05	0.397896	N/A
F18	4.71E-05	5.430034	0.1866	5.36E-05	4.620041	0.05	6.78E-05	3.00004	N/A
F19	0.002328	-3.86147	0.39	0.002652	-3.86167	0.79	0.002445	-3.86128	N/A
F20	0.084306	-3.28407	N/A	0.075858	-3.26297	0.05	0.089146	-3.26229	0.35
F21	2.273555	-9.34415	N/A	2.10046	-9.15418	3.48E-19	2.143705	-9.17025	0.97
F22	0.00105	-10.3479	N/A	2.87E-07	-10.0916	1.36E-30	7.45E-01	-10.297	0.70

TABLE 3.7: Comparison of IGWO with other algorithms on uni-modal benchmark functions

	IGWO		**PSO [244]**		**GSA [245]**		**DE [246]**		**EP [236]**	
	Stdv	**Mean**	**Stdv**	**Mean**	**Stdv**	**Mean**	**Stdv**	**Mean**	**Stdv**	**Mean**
F1	1.00E-25	5.55E-26	0.000202	1.36E-04	9.67E-17	2.53E-16	5.90E-14	8.20E-14	1.30E-04	5.70E-04
F2	7.82E-16	7.75E-16	0.045421	4.21E-02	0.194074	0.055655	9.90E-10	1.50E-09	0.00077	0.0081
F3	0.000763	9.93E-05	22.11924	70.1562	318.9559	896.5347	7.40E-11	6.80E-11	0.014	0.016
F4	1.05E-06	1.08E-06	0.317039	1.086481	1.741452	7.35487	0	0	0.5	0.3
F5	0.642515	27.0042	60.11559	96.71832	62.22534	67.54309	0	0	5.87	5.06
F6	0.313278	0.6677	8.22E-05	0.000102	1.74E-16	2.50E-16	0.00E+00	0.00E+00	0.00E+00	0.00E+00
F7	0.001074	0.00182	0.044957	0.122854	0.04339	0.089441	0.0012	0.00463	0.3522	0.1415

for these functions [243]. Similarly, for function F10, F20, F21 and F22 higher p-values (> 0.05) advocates that significant difference does not exist between the performance of IGWO and GWO. For function F12 and F13 the p-values associated with IGWO are again greater than 0.05 on the other hand, p-value of GWO for F-13 is less than 0.05 which shows that for this function, IGWO and GWO-M1 are suitable algorithms.

3.4.3 Convergence Analysis

Second column in Figure 3.3 shows the position of wolves around the best solution in search space over the course of iterations. To investigate the behavior of wolves, trajectory of first variable out of 30 variables is shown in the third column of the Figure 3.3. It can be noted from the trajectories that wolves slowly transit from exploration phase to exploitation phase. By application of opposition concept, half of the wolves placed randomly in search space and remaining half are placed as per the opposition rule. This action ensures the effective utilization of the search space during the exploration phase. This fact can be observed from the abrupt changes (transients) in the initial steps of iterations. These transients damped out gradually over the course of iterations. From the convergence analysis in Figure 3.3 (last column) it can be observed that the IGWO outperforms the GWO and GWO-M1.

Further a comparison of IGWO with PSO [244], Gravitational Search Algorithm (GSA) [245], Differential Evolution (DE) [246] and Evolutionary Strategies (ES) [236] have been carried out and it has been observed that the performance of IGWO

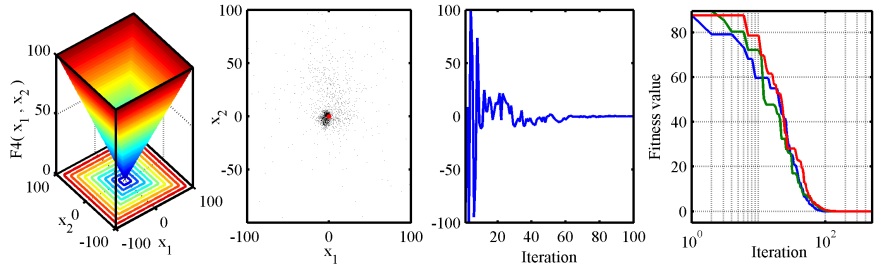

(a) F4

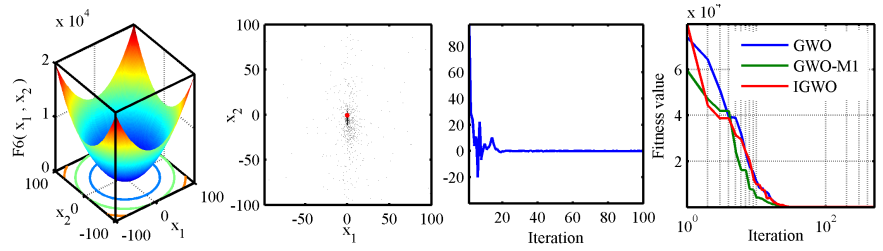

(b) F6

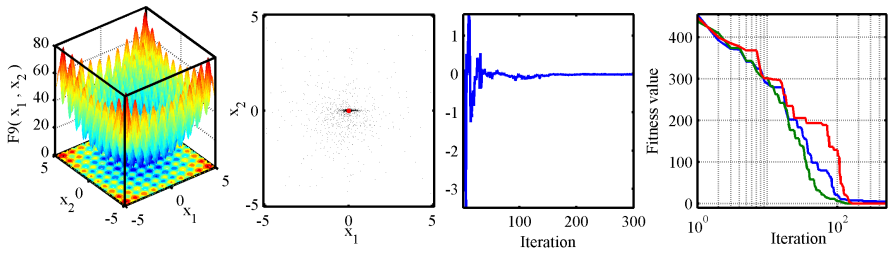

(c) F9

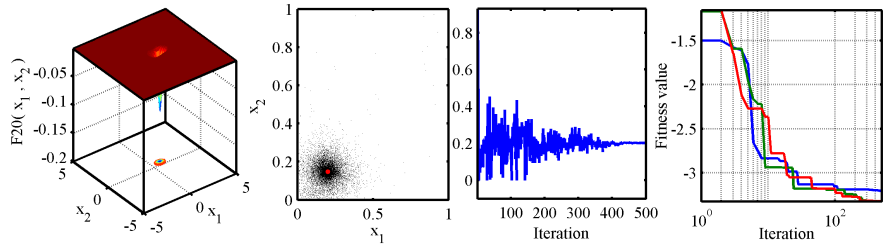

(d) F20

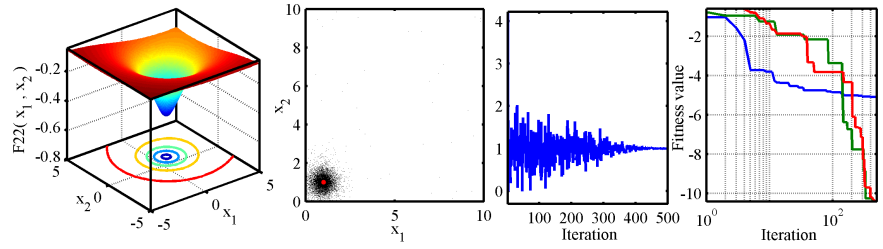

(e) F22

FIGURE 3.3: Search history and trajectory of the first particle in the first dimension

TABLE 3.8: Comparison of IGWO with other algorithms on multi-modal benchmark functions

	IGWO		**PSO [244]**		**GSA [245]**		**DE [246]**		**EP [236]**	
	Stdv	**Mean**	**Stdv**	**Mean**	**Stdv**	**Mean**	**Stdv**	**Mean**	**Stdv**	**Mean**
F8	950.3294	-5991.23	1152.814	-4841.29	493.0375	-2821.07	574.7	-11080.1	52.6	-12554.5
F9	2.734441	1.270284	11.62938	46.70423	7.470068	25.96841	38.8	69.2	0.012	0.046
F10	4.31E-14	1.64E-13	0.50901	0.276015	0.23628	0.062087	4.20E-08	9.70E-08	0.0021	0.018
F11	0.005099	0.001994	0.007724	0.009215	5.040343	27.70154	0	0	0.022	0.016
F12	0.052673	0.042402	0.026301	0.006917	0.95114	1.799617	8.00E-15	7.90E-15	3.60E-06	9.20E-06
F13	0.21782	0.551296	0.008907	0.006675	7.126241	8.899084	4.80E-14	5.10E-14	0.000073	0.00016

TABLE 3.9: Comparison of IGWO with other algorithms on fixed dimension multi-modal benchmark functions

	IGWO		**PSO [244]**		**GSA [245]**		**DE [246]**		**EP [236]**	
	Stdv	**Mean**	**Stdv**	**Mean**	**Stdv**	**Mean**	**Stdv**	**Mean**	**Stdv**	**Mean**
F14	3.741593	4.038417	2.560828	3.627168	3.831299	5.859838	3.30E-16	0.998004	0.56	1.22
F15	0.00733	0.003662	0.000222	0.000577	0.001647	0.003673	0.00033	4.50E-14	0.00032	0.0005
F16	3.01E-11	-1.03163	6.25E-16	-1.03163	4.88E-16	-1.03163	3.10E-13	-1.03163	4.90E-07	-1.03
F17	8.36E-05	0.397896	0	0.397887	0	0.397887	9.90E-09	0.397887	1.50E-07	0.398
F18	6.78E-05	3.00004	1.33E-15	3	4.17E-15	3	2.00E-15	3	0.11	3.02
F19	0.002445	-3.86128	2.58E-15	-3.86278	2.29E-15	-3.86278	N/A	N/A	0.000014	-3.86
F20	0.089146	-3.26229	6.05E-02	-3.26634	2.31E-02	-3.31778	N/A	N/A	0.059	-3.27
F21	2.143705	-9.17025	3.02E+00	-6.8651	3.74E+00	-5.95512	2.5E-06	-10.1532	1.59	-5.52
F22	7.45E-01	-10.297	3.09E+00	-8.45653	2.01E+00	-9.68447	3.90E-07	-10.4029	2.12	-5.53

is competitive. Results of this experiment are shown in Tables 3.7, 3.8 and 3.9 for Unimodal, Multi-modal and Fixed dimension Multi-modal Benchmark Functions respectively.

3.5 Summary

In this chapter development of an improved version of GWO named as Intelligent Grey Wolf Optimizer (IGWO) is discussed in detail. The crisp details of the development along with the benchmarking of the proposed variant on different type of functions such as multimodal, unimodal and fixed dimension are carried out. Following points, summarize the contributions of this chapter:

1. There is a scope of improvement in existing meta-heuristic techniques for many complex optimization problems. The developed IGWO perform better than his

respective standard model and existing meta-heuristic for the standard 22 benchmark functions.

2. The modifications suggested for improved algorithm are effectively contributing towards enhancing the convergence, accuracy and efficiency of the algorithm.

3. Proposed opposition based modification, disperses tentative solutions near the promising region so virtually reduces the problem search space of meta-heuristics. This feature makes the algorithms more efficient.

4. An efficient sinusoidal function has been employed to improve the bridging mechanism between the exploration and exploitation phase of GWO. Exploration and exploitation capabilities of GWO get enhanced with this newly developed mechanism. With this modification, the developed variant GWOM1 exhibits improved performance as compared with GWO.

5. Further, opposition based learning concept has been employed in the initialization phase of the GWO along with this sinusoidal bridging mechanism. The combined effect of these two modifications is positive and the implication of these modifications can be observed through the benchmarking results on various functions. The performance of the proposed variant has been validated on standard 22 benchmark functions of different properties and nature.

6. Following standard criterion have been chosen to demonstrate the effectiveness of the algorithm:

    i. Mean values of the objective function obtained from independent runs.

    ii. Standard deviation values of the objective function obtained from independent runs.

    iii. Statistical significance of the results obtained from independent runs.

    iv. Convergence characteristics.

7. Following are the major features of the IGWO:

    i. The proposed modification in control parameter guarantees the exploration and exploitation in an effective manner.

ii. Opposition based learning enables the IGWO, to utilize the search space in a very effective manner and hence ensures improved exploration.

8. It has been observed that the proposed variant IGWO shows promising results on majority of the benchmark functions. The superiority of this variant can be validated by optimal values of standard deviation, mean and p-value less than the significance level.

In following chapters, the application of the proposed variant on the feature selection and for solving transient stability constrained optimal power flow problem will be presented.

Chapter 4

Contingency Analysis and Its Classification

[*This chapter presents concept of static security assessment of power system and the proposed ANN-based approach for contingency ranking and screening. Simulation results and the performance evaluation of the proposed methodology for various test systems are presented.*]

4.1 Introduction

With the exponential growth in the power demand, secure operation of grid, congestion management, power quality, frequency, and power regulation etc. are the new challenges in front of the electricity supply industry [128]. The complexity and huge grid size, increase the insecurity of power systems. Therefore fast contingency assessment is of paramount importance in the power network to provide reliable and secure electricity supply to its customers. Contingency analysis is one of the most important tasks encountered by the planning and operation engineers of a bulk power system. Potential harmful disturbances that occur during the steady state operation of a power system are known as contingencies. The main objective behind the contingency analysis is to assess the post-contingent system health, effect of specified operating condition & disturbance and to warn the Independent System

Operator (ISO) about the system severe/critical contingencies that violate the equipment permissible operational limits and/or may drive the system towards insecurity and instability. There are various techniques employed for the contingency analysis and assess the system security [39–95]. Different algorithms have been developed for contingency analysis, majority of them are based on AC load flow calculations. These methods are considered as deterministic methods, which are more accurate than DC load flow methods. These approaches employed the simulation procedure instead of the actual change in the modeling. Load flow based methods have high accuracy but are more time consuming due to high computational burden. Since for power system planning, contingency analysis is the only tool to identify the possible insecure or overloading conditions, time and complexity are of paramount considerations. But for on-line contingency identification of large grid high computational time and complexity are considered pitfalls. Therefore, employing the traditional methods, on-line contingency analysis becomes a very difficult exercise as it requires fast solution with high accuracy. Following are the drawbacks and limitations of traditional power system contingency analysis [43]:

- AC load flow for all operating cases in the contingency set, results in high computation burden for these methods.
- Complexity is very high due to large amount of data that are used in calculation, diagnosis and learning.
- Analytical methods due to extensive data handling require large computational time to find the severity in the power system.
- Accuracy of these methods is also poor and rate of misclassification is high.

Conventional contingency analysis is more difficult for on-line operation hence there is a need of an advanced tool to solve the problem regarding accuracy, speed and capability to handle complexity that arises in the areas of the power system planning and operation. Among these advanced computational tools Artificial Neural Networks (ANNs) provide efficient computing models with the ability to solve nonlinear pattern matching problems. In this decade ANN has been employed by many researchers [39–75] to solve power system problems including the contingency

analysis and identification. Still this problem requires re-investigation in order to improve the performance with reduced computational time and burden.

In the following section, power system steady state security assessment and contingency screening & their ranking have been discussed.

4.2 Static Security Assessment

Static security is defined as the ability of the system to reach a state within the specified secure region following a disturbance (contingency). The Static Security Assessment (SSA) evaluates the post contingent steady state of the system neglecting the transient behavior and any other time dependent variations due to the changes in load generation conditions [35, 53]. SSA employing the load flow equations for various types of contingencies.

The steady-state load flow solution for evaluation of power system security of the network can be obtained by the following set of equations [33, 54].

$$\left.\begin{aligned} P_i &= P_{Gi} - P_{Di} \\ P_i &= V_i \sum_{j=1}^{N_B} V_j Y_{ij} \cos\left(\theta_{ij} - \delta_i + \delta_j\right) \end{aligned}\right\} \tag{4.1}$$

$$\left.\begin{aligned} Q_i &= Q_{Gi} - Q_{Di} \\ Q_i &= -V_i \sum_{j=1}^{N_B} V_j Y_{ij} \sin\left(\theta_{ij} - \delta_i + \delta_j\right) \end{aligned}\right\} \tag{4.2}$$

Where P_{Gi} and Q_{Gi} are the real and reactive power of the generators at bus i; P_{Di} and Q_{Di} are the real and reactive power demands at bus i;P_i and Q_i are the real and reactive power injected at bus i; V_i and δ_i are voltage magnitude and voltage angle at bus i; Y_{ij} is magnitude of ij^{th} element of bus admittance matrix of the system; θ_{ij} is angle of ij^{th} element of bus admittance matrix of the system; N_B is the number of buses in the system. Equations 4.1 and 4.2 are called Static Load Flow Equations (SLFEs).

The constraints for generator [33] during normal operating conditions of a power system as below:

$$\left.\begin{aligned} \sum_{i=1}^{N_B} P_{Gi} &= \sum_{i=1}^{N_B} P_{Di} + P_{Loss} \\ \sum_{i=1}^{N_B} Q_{Gi} &= \sum_{i=1}^{N_B} Q_{Di} + Q_{Loss} \end{aligned}\right\} \tag{4.3}$$

Where P_{Loss} and Q_{Loss}, are the real and reactive power losses in the transmission network.

For a secure operation of the power system, it is necessary that, all system variables must be with in specified security limits. Therefore, some inequality constraints always be force the system operation toward the secure limits and ensure the system secure. These constraints like all line MVA must be with in limits, all bus voltages must be with in limits and line MVA must not more then its maximum limits, all generator must be with in limits. These inequality constraints are as below:

$$\left.\begin{aligned} V_j^{\min} < V_j < V_j^{\max} \quad & \text{for } j = 1 \text{ to } N_B \\ S_l < S_l^{\max} \quad & \text{for } l = 1 \text{ to } N_L \\ P_{Gi}^{\min} < P_{Gi} < P_{Gi}^{\max} \quad & \text{for } i = 1 \text{ to } N_G \\ Q_{Gi}^{\min} < Q_{Gi} < Q_{Gi}^{\max} \quad & \text{for } i = 1 \text{ to } N_G \end{aligned}\right\} \tag{4.4}$$

Where V_j is the voltage at bus j; S_l is the apparent power of line l; N_B, N_L and N_G are the number of buses, transmission lines, and generators in the system respectively. Constraints (4.3) and/or (4.4) when referred to the post-contingency scenarios, are also known as security constraints.

Equation 4.3 corresponds to power balance requirements, while Equation 4.4 corresponds to system operation constraints, represented by limits imposed to bus voltage magnitudes, thermal limits of transmission lines and real and reactive power limits of generators.

The operation of the system is classified in two states as *"Secure"* state, if the constraints show in (4.3) and/or (4.4) are satisfied for a given operating condition and also for post-contingency conditions. If constraints (4.3) and/or (4.4) are not satisfied for at least one of the post contingency condition, the system operation is classified as *"Insecure"* state.

4.2.1 Approaches for the Static Security Assessment

The assessment of security is performed based on different approaches. The usage of specific approach depends on the requirements of the system security. The widely used approaches for security assessment are 1) contingency ranking approach and 2) classification approach, as shown in Figure 4.1.

In the ranking approach, the contingencies are ranked in descending order based on the severity. In the classification approach, the system security is classified into two classes secure and insecure. For appropriate corrective action, the classification of the security can be extended to multi-class such as secure, critically secure, insecure and highly insecure.

4.2.2 Contingency Screening and Ranking

As research done in past indicates that the computational burden faced in performing contingency analysis can be alleviated by performing contingency selection, screening, filtering and ranking. By simulating a number of probable outages a contingency data set is formed. Some contingencies from this data may lead to exceed the bus voltage limit or power system line overloads during the operation of power system. So there is need to identify these type of severe contingencies which may

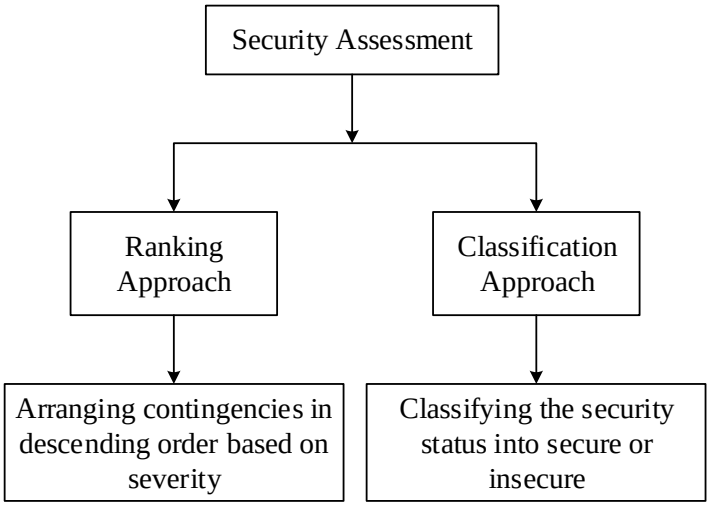

FIGURE 4.1: Classification of Security Assessment Approaches

lead system from secure state to insecure state. This identify process is referred to as contingency selection. After identifying the contingency, sort and rank them according to their severity is know as contingency ranking. Most of the literature on contingency ranking are based on analytical methods out of which Performance Indices (PIs) methods are widely accepted [43–68]. The following section discusses about various performance indices capable of predicting the severity of contingencies and the power system security status.

4.2.3 Performance Indices (PIs)

On the basis of literature review it can be observed that, the contingency ranking is performed by the scalar Performance Indices (PIs), which are used to evaluate the static security of the power system, help the operators to access the critical information about vulnerability of the power system components and the entire power system. In order to evaluate the security and contingency ranking by these approaches, it is necessary to compute the stress experienced by the system for a specific contingency which is termed as the severity. The severity is basically computed using the violations of the line flows, bus voltages etc. Over the years, the severity is referred by different names such as performance indices, the composite indices, the overall performance indices, the severity indices etc. Though the names appear different, they all compute the severity of the contingencies, but by considering different violations or by combining two types of severities. The indices which used to compute the severity are listed below [43–68].

1. *Severity Index:* This index computes the MVA line flow violations.
2. *Active power performance index:* This index computes the active power line flow violation.
3. *Voltage performance index:* This index computes the voltage violations at buses.
4. *Composite performance index:* This index computes the line flow and voltage violations as a single value
5. *Static Severity index:* This index computes the MVA line flow violations.

The literature reveals the indices with the same name but a variation in the formulation in order to compute the severity based on the specific application. The most widely used indices are the active power and the voltage performance indices.

In this chapter, for SSA following two scalar indices are investigated. One is based on Line MVA flow which is determined to estimate the extent of overload of lines. It is named as Line MVA Performance Index (PI_{MVA}). Second is used to scale the system stress in the form of generator reactive power limit violations and bus voltage limit violations. Its known as Line Voltage-Reactive Performance Index (PI_{VQ}).

4.2.3.1 Line MVA Performance Index PI_{MVA}

Loading conditions of the system have a high impact of the transmission line power flow, and its directly affect the network performance. Expression for the PI_{MVA} can be defined [52] by Equation 4.5.

$$PI_{MVA} = \sum_{i=1}^{N_L} \left(\frac{W_{Li}}{M} \right) \left[\frac{S_i^{post}}{S_i^{\max}} \right]^M \tag{4.5}$$

Where $S_i{}^{post}$ and S_i^{max} are the post contingency MVA flow and MVA rating of the i^{th} line respectively. Number of lines represented by N_L. Weighting factor $W_{Li} = 1$ is considered, and the order of the exponent for penalty function is represented by $M(= 2n)$. The classification of the PIs is directly depends on the value of the exponent n. Research reveals that if the value of n is higher, the chance for misclassification in the outages is less. This phenomenon, is known as 'masking effect' and selection of the value of n can be a significant problem. By using optimal selection of weights for PIs and higher order PIs, masking and mis-ranking effect can be reduced. The integer value n in this thesis has been taken as 4 [153].

4.2.3.2 Voltage Reactive Performance Index PI_{VQ}

In order to reflect the reactive power cap ability constraints of the generators and bus voltage limit violation in the contingency selection for voltage analysis, a generalized

voltage-reactive power performance index (PI_{VQ}) is employed. PI_{VQ} corresponding to each load pattern and for each single line outage indicating voltage deviation from the scheduled voltage at the load buses and reactive power violations at the generator buses, consists summation of two terms as defined [43] by Equation 4.6.

$$PI_{VQ} = \sum_{i=1}^{N_B} \left(\frac{W_{Vi}}{M}\right) \left[\frac{V_i - V_i^{sp}}{\Delta V_i^{Lim}}\right]^M + \sum_{i=1}^{N_G} \left(\frac{W_{Gi}}{M}\right) \left[\frac{Q_i}{Q_i^{\max}}\right]^M \tag{4.6}$$

Where

$$\Delta V_i^{Lim} = \frac{V_i^{\max} - V_i^{\min}}{2} \qquad M = 2n$$

W_{Vi} & W_{Gi} are the real non-negative weighting factors (= 1) and $M(= 2n)$ is the order of the exponent for penalty function. ${Q_i}^{\max}$ is the maximum limit for reactive power production of i^{th} generating unit N_G the number of generating units. In this study, the value of n was taken as 4 [153].

4.2.4 PIs Calculation for IEEE 30-Bus Power System using NR Load Flow

Table 4.1 shows the results of indices values for corresponding N-1 contingency outages for IEEE 30 bus system. The first column of table shows location of line outages. Similarly, the results associated with this line outage in terms of the PI_{MVA} and PI_{VQ} values are shown in adjacent column. For this study each possible contingency can be simulated and both the indices can be calculated. For the ranking purpose, both indices can be sorted. The entry which is having high numerical value of index is identified as critical one. Figure 4.2 shows contingency ranking according to the values of PI_{MVA} index. According to this analysis, outage of Line 6-8 is found to be the most critical as compared to other line outages at base case loading condition. For further investigation MVA line flow of all system line after the contingency outage of Line 6-8 are shown in Figure 4.3. This figure shows the plot of maximum MVA capacity and MVA line flow after the Line 6-8 outage. From this figure, it is observed that due to the contingency condition line MVA transmitting through Line 6-28 and Line 8-28 is found to be more than their respective maximum permissible

TABLE 4.1: PIs calculation for contingency ranking of IEEE 30-Bus System (Base load condition)

Line Outage	**Line MVA Performance Index by NRLF**	**Line Outage**	**Voltage Reactive Performance Index by NRLF**
L 6-8	2.3769	L 27-29	268.7099
L 8-28	1.4267	L 27-30	228.7603
L 10-22	0.5965	L 25-27	33.7834
L 15-23	0.5949	L 6-8	31.2691
L 27-28	0.5719	L 29-30	29.8197
L 10-20	0.4594	L 10-20	27.0174
L 23-24	0.4530	L 10-17	24.6846
L 15-18	0.3913	L 21-22	24.2273
L 27-30	0.3797	L 19-20	22.5485
L 12-16	0.3771	L 15-23	22.3476
L 4-6	0.3716	L22-24	22.3007
L 27-29	0.3653	L 12-14	22.0977
L 18-19	0.3569	L 15-18	21.9278
L 2-6	0.3555	L 23-24	21.8269
L 12-15	0.3554	L 10-21	21.4198
L 19-20	0.3515	L 12-15	21.3456
L 1-3	0.3513	L 5-7	21.3315
L 3-4	0.3478	L 10-22	21.3193
L 29-30	0.3407	L 27-28	21.3154
L 16-17	0.3405	L 2-4	21.3099
L 5-7	0.3396	L 2-6	21.3015
L 12-14	0.3387	L 1-3	21.2962
L 2-5	0.3371	L 3-4	21.2822
L 2-4	0.3361	L 14-15	21.2692
L 9-11	0.3352	L 2-5	21.2629
L1-2	0.3349	L 12-16	21.2261
L 14-15	0.3347	L 8-28	21.2229
L 4-12	0.3338	L 6-28	21.2173
L 9-10	0.3332	L 16-17	21.2167
L 6-9	0.3332	L 9-11	21.2097
L 6-10	0.3312	L1-2	21.2047
L 6-7	0.3271	L 6-10	21.1954
L22-24	0.3229	L 6-7	21.1842
L 21-22	0.3024	L 9-10	21.1802
L 10-17	0.2975	L 6-9	21.1801
L 24-25	0.2868	L 18-19	21.1599
L 6-28	0.2620	L 4-12	21.1359
L 10-21	0.2551	L 4-6	21.1052
L 25-27	0.2525	L 24-25	21.0823

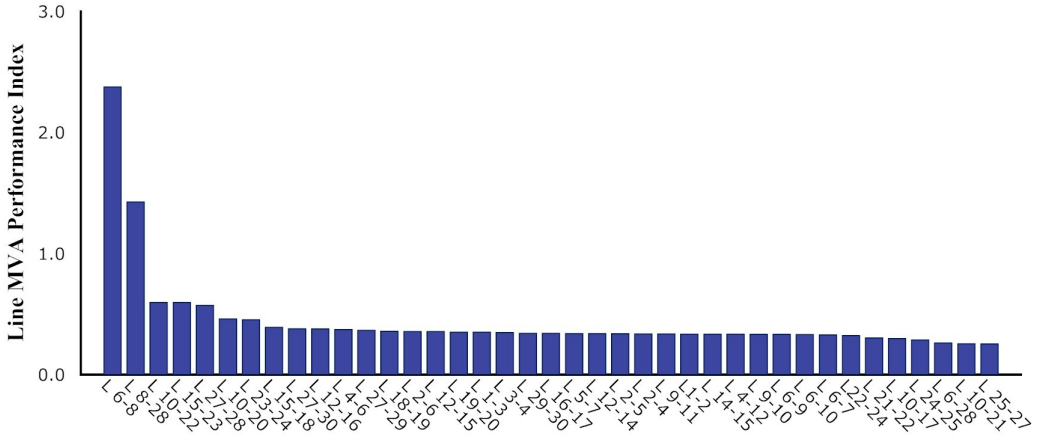

FIGURE 4.2: Contingency ranking of IEEE-30 bus system for PI_{MVA}

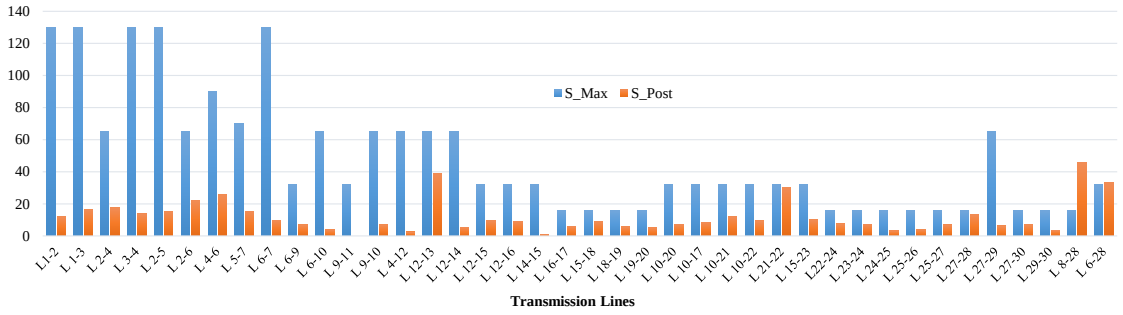

FIGURE 4.3: Line MVA of IEEE-30 bus system after the outage of line between buses 6-8

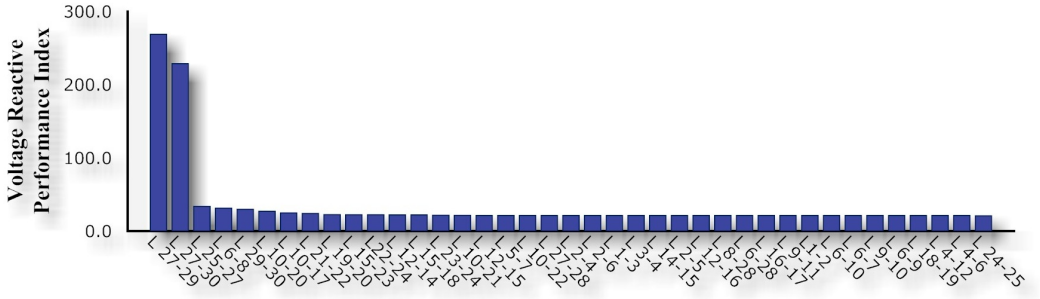

FIGURE 4.4: Contingency ranking of IEEE-30 bus system for PI_{VQ}

MVA transmission capability. This fact advocates line 6-8 is critical as far as line congestion point of view.

Figure 4.4 shows contingency ranking according to the values of PI_{VQ} index. According to this analysis, outage of Line 27-29 is found to be the most critical as

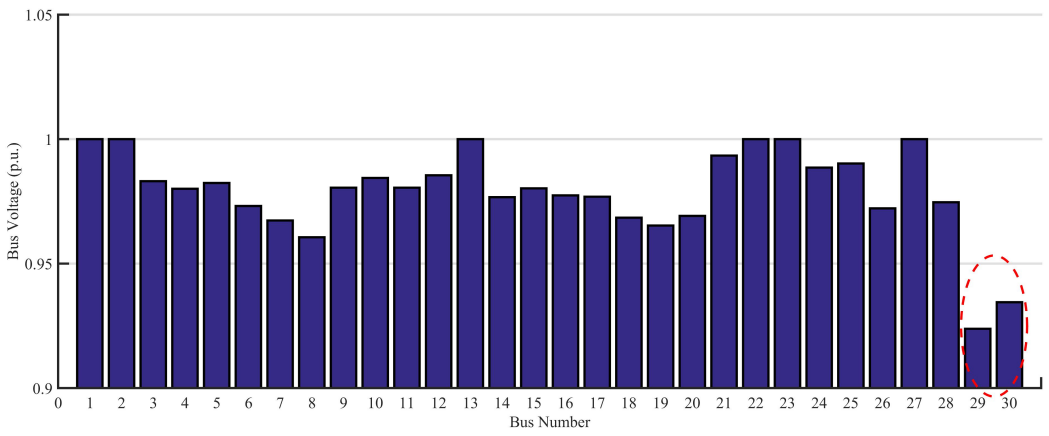

FIGURE 4.5: Bus voltages of IEEE-30 bus system after outage of line between buses 27-29

compared to other line outages at base case loading condition. For further investigation voltage at all buses after the contingency outage of Line 27-29 are shown in Figure 4.5. This figure shows the voltages at all bus terminals after the Line 27-29 outage. From this figure, it is observed that due to the contingency condition voltages at buses 29 and 30 are found to be less than their respective minimum permissible limit. This fact advocates line 27-29 is critical as far as voltage drop point of view.

4.2.5 PIs calculation for IEEE 39-Bus Power System using NR Load Flow

Table 4.2 shows the results of indices values for corresponding N-1 contingency outages for IEEE 39 bus system. The first column of table shows location of line outages. Similarly, the results associated with this line outage in terms of the PI_{MVA} and PI_{VQ} values are shown in adjacent column. For this study each possible contingency can be simulated and both the indices can be calculated. For the ranking purpose, both indices can be sorted. The entry which is having high numerical value of index is identified as critical one. Figure 4.6 shows contingency ranking according to the values of PI_{MVA} index. According to this analysis, outage of Line 21-22 is found to be most critical as compared to other line outages at base case loading

TABLE 4.2: PIs calculation for contingency ranking of IEEE 39-Bus System (Base load condition)

Line Outage	**Line MVA Performance Index by NRLF**	**Line Outage**	**Voltage Reactive Performance Index by NRLF**
L 21-22	6.2294	L 15-16	35.0169
L 13-14	1.5398	L 8-9	3.1679
L 10-13	0.6765	L 21-22	2.7237
L 23-24	0.6707	L 3-4	2.3233
L 6-11	0.6500	L 6-7	1.9899
L 26-27	0.5093	L 12-13	1.8266
L 10-11	0.4351	L 2-3	1.8227
L 16-21	0.4306	L 12-11	1.6717
L 4-14	0.2924	L 10-11	1.6086
L 5-6	0.2269	L 26-27	1.3716
L 16-17	0.1819	L 10-13	1.3710
L 1-2	0.1793	L 5-6	1.2693
L 4-5	0.1563	L 13-14	1.2372
L 17-18	0.1480	L 5-8	1.2050
L 26-29	0.1479	L 6-11	1.1635
L 28-29	0.1468	L 23-24	1.1560
L 6-7	0.1440	L 14-15	1.1307
L 15-16	0.1411	L 16-17	1.1161
L 2-25	0.1277	L 16-21	1.0985
L 5-8	0.1265	L 1-2	1.0952
L 2-3	0.1153	L 16-24	1.0948
L 1-39	0.1101	L 4-14	1.0834
L 25-26	0.1061	L 9-39	1.0717
L 16-24	0.0991	L 17-18	1.0383
L 3-18	0.0972	L 28-29	1.0376
L 14-15	0.0972	L 4-5	1.0193
L 22-23	0.0964	L 26-29	1.0150
L 3-4	0.0957	L 17-27	1.0021
L 8-9	0.0940	L 26-28	0.9935
L 7-8	0.0937	L 7-8	0.9903
L 26-28	0.0924	L 25-26	0.9876
L 12-11	0.0919	L 2-25	0.9836
L 12-13	0.0915	L 3-18	0.9750
L 17-27	0.0915	L 1-39	0.9675
L 9-39	0.0895	L 22-23	0.9470

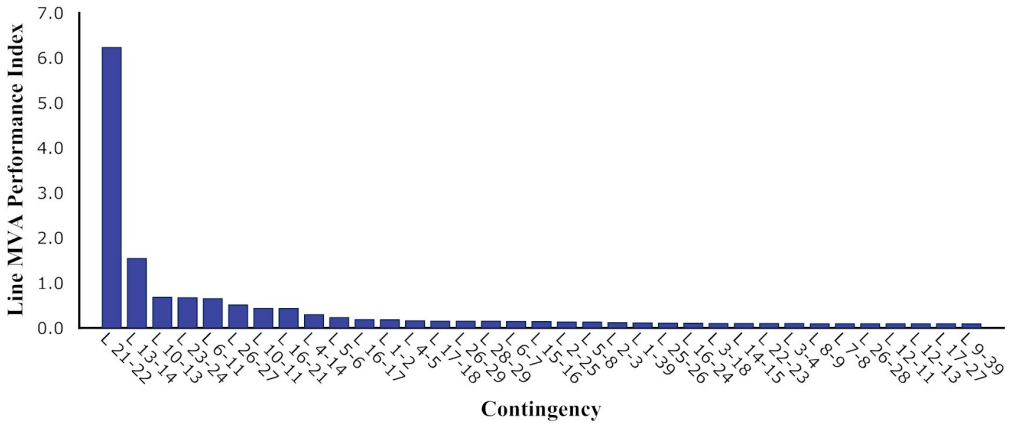

FIGURE 4.6: Contingency ranking of IEEE-39 bus system for PI_{MVA}

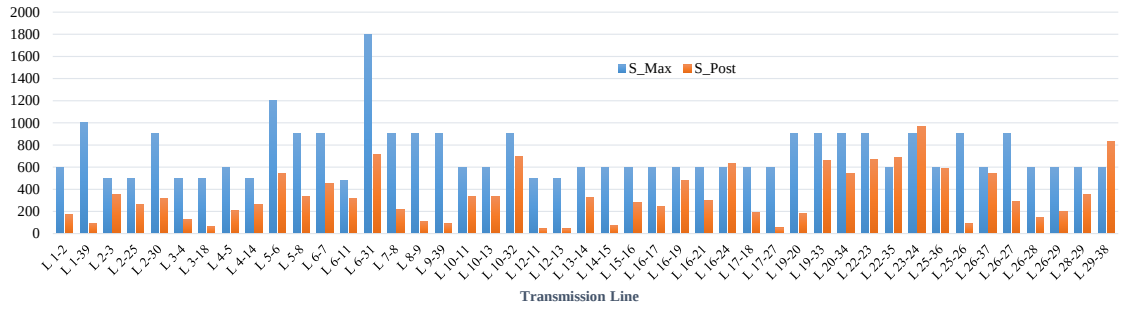

FIGURE 4.7: Line MVA of IEEE-39 bus system after the line outage of line between buses 21-22

condition. For further investigation MVA line flow of all system line after the contingency outage of Line 21-22 are shown in Figure 4.7. This figure shows the plot of maximum MVA capacity and MVA line flow after the Line 21-22 outage. From this figure, it is observed that due to the contingency condition line MVA transmitting through Lines 16-24, 22-35, 23-24 and 29-38 are found to be more than their respective maximum permissible MVA transmission capabilities. This fact advocates that Line 21-22 is critical as far as line congestion is concerned.

Figure 4.8 shows contingency ranking according to the values of PI_{VQ} index. According to this analysis, outage of Line 15-16 is found to be most critical as compared to other line outages at base case loading condition. For further investigation voltage at all buses after the contingency outage of Line 15-16 are shown in Figure 4.9. From this figure, it is observed that due to the contingency condition voltage at bus-15 is found to be less than their respective minimum permissible limit and

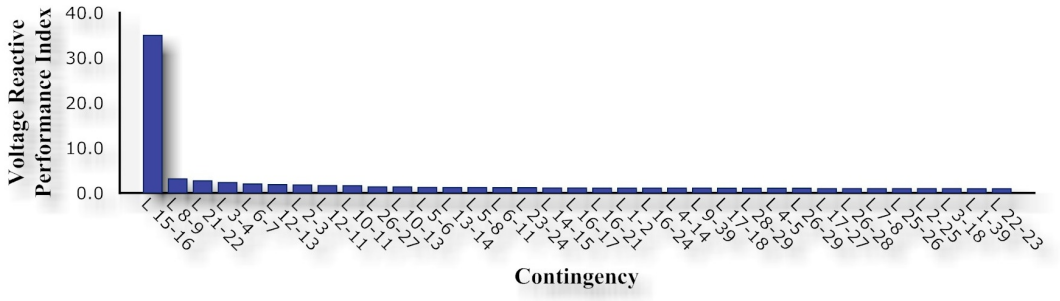

FIGURE 4.8: Contingency ranking of IEEE-39 Bus System for PI_{VQ}

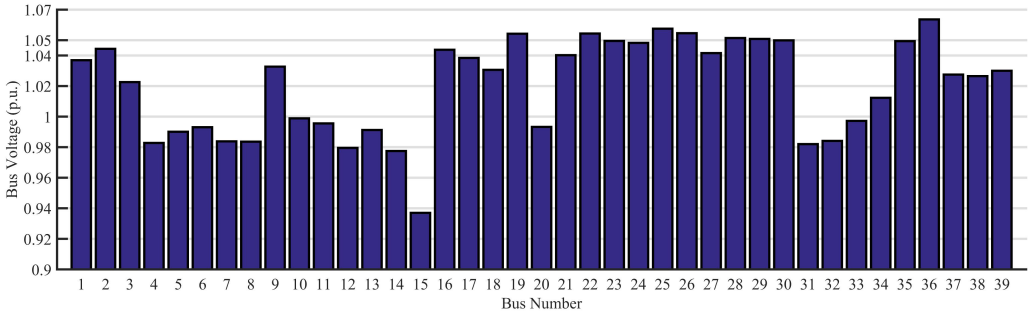

FIGURE 4.9: Bus voltages of IEEE-39 bus system after outage of line between buses 15-16

voltages at buses 19, 22, 25, 26 and 36 are found more than their respective maximum permissible limit. This fact advocates line 15-16 is critical as far as voltage point of view.

4.3 Proposed Methodology for Contingency Analysis using ANN

For contingency analysis Artificial Neural Network (ANN) has been highly used as discussed in [43–75]. The development of ANN, that is able to estimate the post-contingency severity from a series of pre-contingency data for contingency analysis is proposed in this chapter. The design of classification scheme using proposed ANN-based methods undergoes following sequence of operation [43]:

(i) Generation of the data for training and testing of the neural network.

(ii) Feature selection for selecting important attributes from the data.

(iii) Design of different Neural networks employing different architectures.

4.3.1 Data Generation

The data set should ideally represent all possible operating conditions and should be reliable. Reliable data generation is the most important step for the success of a neural network. Therefore, data is generated using the methodology proposed in the flowchart shown in Figure 4.10. The steps followed for data generation for security assessment and contingency analysis are:

Step 1 A large number of load patterns have been generated by randomly distributing the real and reactive loads on all the load buses. This exercise ensures that the data set is a representative of all possible operating conditions.

Step 2 During simulation, the system load has been changed from 1.0 (base case) per unit to 1.0 ± 0.05 per unit of base case.

Step 3 A contingency set consisting of all credible contingencies is considered. For each operating condition, a contingency is simulated. Single line outage is the most common event in a power system and hence, only one line outage at a time is considered here forming a set of $N_L - 1$ contingency, where N_L is the number of lines.

Step 4 Single line outage corresponding to each load pattern are simulated by AC load flow (Newton Raphson Power Flow) and the violation of operating limits of various components are checked. Keeping the load level constant, each contingency is simulated several times to obtain a wide range of operating scenarios. For this study each contingency is simulated 15 times for a selected load level.

Step 5 The post-contingency state of the system is stored for each contingency to calculate the performance indices, PI_{VQ} and PI_{MVA}. The obtained values are normalized between 0 and 1 for each contingent case.

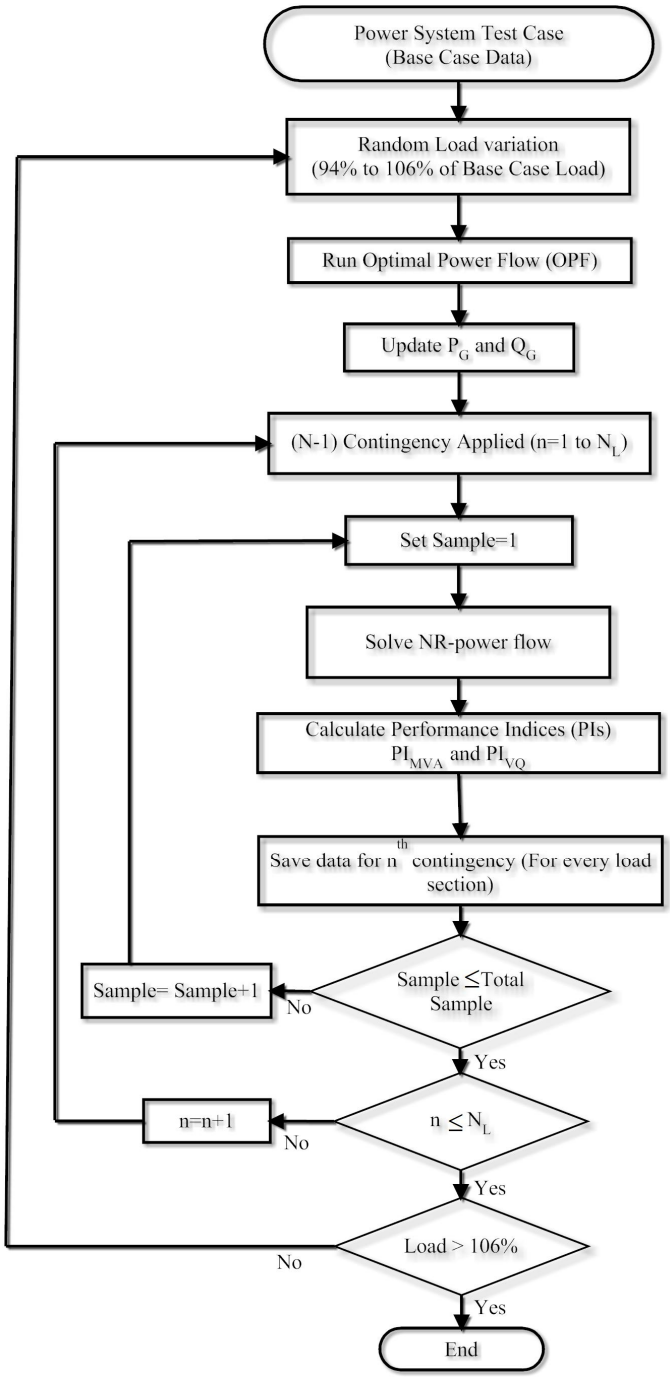

FIGURE 4.10: Flowchart of data generation for static security assessment and contingency analysis

Step 6 The system state, contingency type, and the corresponding security are noted for every operating point and for all the contingencies of a credible contingency set.

Step 7 The whole data set is suitably divided into training set and test set for performance evaluation purpose.

4.3.2 Data Normalization

The input/output training and testing set data are scaled in the range of 0 to 1 for each load pattern. In this thesis, each input or output parameter of x is normalized as x_n before being applied to the neural network as

$$x_n = \frac{0.8 \times (x - x_{\min})}{x_{\max} - x_{\min}} + 0.1 \tag{4.7}$$

Where x_{max} and x_{min} are the maximum and minimum values of data parameter x.

4.3.3 Feature Selection Using IGWO

Feature selection is a binary optimization problem. For the Intelligent Grey Wolf Optimizer (IGWO) based feature selection method, a binary version should be developed. In this work, a solution is represented as a one dimensional vector, where the length of the vector is based on the number of attributes of the original dataset. Each value in the vector (cell) is represented by '1' or '0'. Value '1' shows that the corresponding attribute is selected; otherwise the value is set to '0'.

Feature selection can be considered as a multi objective optimization problem where two contradictory objectives are to be achieved with minimal number of selected features and higher classification accuracy. The smaller is the number of features in the solution and the higher the classification accuracy. Each solution is evaluated according to the fitness function [247], which depends on the k-Nearest Neighbors (KNN) classifier [248] to get the classification accuracy of the solution and on the number of selected features in the solution. In order to balance between

the number of selected features in each solution (minimum) and the classification accuracy (maximum), the fitness function in Equation 4.8 is used in IGWO algorithm to evaluate search agents.

$$Fitness = \lambda_1 \gamma_R(D) + \lambda_2 \frac{|R|}{|N|} \tag{4.8}$$

Where $\gamma_R(D)$ represents the classification error rate of a given classier (the K-nearest neighbor (KNN) classifier is used here). Furthermore, $|R|$ is the cardinality of the selected subset and $|N|$ is the total number of features in the dataset, λ_1 and λ_2 are two parameters corresponding to the importance of classification quality and subset length, $\lambda_1 \in [0, 1]$ and $\lambda_2 = (1–\lambda_1)$ adopted from [229]. Generally, the monetary gain is the supreme motivation behind any investment along with the improvement of system performance.

4.3.4 Training and Testing Pattern

Off-line power flow calculation results corresponding to each contingent case are used to construct the training patterns. The load patterns were generated by randomly changing the load at each bus. Single line outage contingencies are considered in this work for online ranking, as these occur more frequently. Input features for ANN consists of pre-contingent variable and the PI values will be used as targets to perform contingency analysis. For this study, data consists of a large number of patterns that is normalized, shuffled and divided in two groups; one for training and the other for testing.

4.3.5 Selection of Neural Network Architecture

The neural network architecture selected for online security evaluation are Feed Forward Neural Network (FFNN) and Radial Basis Function Neural Network (RBFNN). The applicability of these two ANN-based methods has been investigated under different operating and contingency condition with IGWO based feature selection method. Initially these neural networks have been trained for estimation of PI value.

TABLE 4.3: PI based contingency classification for screening and ranking

Class/Rank	PI Range	Static Security Status
I: Most Critical	>0.8	Insecure (0)
II: Critical	0.4-0.8	Insecure (0)
III: Less Critical	0.2-0.4	Insecure (0)
IV: Non Critical	<0.2	Secure (1)

The neural network which gives the best results will further employed for contingency classification.

4.3.6 Contingency Classification States

First, the values of PI are determined, after this classification of the contingency on the basis of their PI values. Neural Network classification task is completed by classifying the contingencies either as secure or insecure in accordance with Table 4.3, that finally gives the ranking for all the contingencies on the basis of their PI values.

Class-I contingencies indicate that they are never safe under any operating condition and require immediate attention. Presence of these contingency causes major violations grenerator's active and reactive power limits, voltage limits of buses and the thermal limits of transmission lines.

Class-II contingencies indicate that they are not safe since there is major violation of all or some operating constraints respectively depending upon the operating condition and these contingencies require proper preventive control measures such as generator rescheduling or load shedding.

Class-III contingencies indicate that they are less critical but there are minor violations of some system constraints depending upon the operating conditions and these contingencies become safe with proper control measures.

Class-IV contingencies indicate non-critical contingencies that never drives the power system into insecure state. Here, all the critical contingencies (Class I to III) are indicated by '0' and Non critical contingencies (Class-IV) are indicated by '1'.

4.4 Simulation and Results

The proposed strategy is tested over two standard power systems namely IEEE 30-bus 6-generator and IEEE 39-bus 10-generator systems. IEEE 30-bus test system has 6-generators and 41-transmission lines. Bus number 1 is taken as slack bus for this system. Whereas, IEEE 39-bus test system has 10-generators and 46-transmission lines. Bus number 39 is taken as slack bus for this system. The line and bus data of the systems are given in the Appendix A. All the simulations are carried out using MATLAB [249], MatPower [250] with Intel Core i3, 2.5 GHz, 6 GB RAM.

4.4.1 Data Generation

To analyses the line contingency and ranking for IEEE 30-bus test system 4305 patterns were generated from 7 operating cases by varying the loads at all the buses and generation randomly in the range of $94\% - 106\%$ of their base case values (in steps of the 2%). For each system topology, corresponding to 7 operating cases and 41 single line outage are simulated 15 times to obtain different operating conditions resulting in total 4305 ($7 \times 41 \times 15$) patterns.

For IEEE 39-bus test system 4830 patterns were generated from 7 operating cases by varying the loads at all the buses and generation randomly in the range of $94\% - 106\%$ of their base case values (in steps of the 2%). For each system topology, corresponding to 7 operating cases and 46 single line outage are simulated 15 times to obtain different operating conditions resulting in total 4830 ($7 \times 46 \times 15$) patterns.

Contingency analysis has been performed by utilizing the pre-outage data to determine the PIs for each loading case corresponding to each outage at a time. Out of total samples, 135 samples and 285 samples are excluded from the training data where Newton Raphson (NR) power flow solution failed to converge for 30-bus system and 39-bus system respectively. A total of 4170 and 4545 samples have been taken to analyze the performance (training and testing) of the proposed ANN-based methods for 30-bus test system and 39-bus test system respectively.

4.4.2 Feature Selection

The input attributes selected are normally measured and processed in real time using state estimator results and PMUs. The selected features should contain adequate information about the health of power system from security point of view. Therefore, pre-contingent active and reactive power generation of all generators: $P_{G(1:NG)}$ and $Q_{G(1:NG)}$, real and reactive load at buses $P_{D(1:NB)}$ and $Q_{D(1:NB)}$ are considered as input features. Here N_G is the number of generators and N_B is the number of load buses in the system.

For IEEE 30-bus system, the number of generators are 6 and the number of dispatched loads are 20 (Total Variables: 52). Whereas, for IEEE 39-bus system, the number of generators are 10 and the number of dispatched loads are 21 (Total Variables: 62). Now it is required to select adequate features, out of these total variables i.e 52 and 62 for IEEE 30-bus and 39-bus systems respectively. The initial feature sets for IEEE 30-bus test system and IEEE 39-bus test system are shown in Equations 4.9 and 4.10 respectively.

$$FS_i = [P_{G1:6}, Q_{G1:6}, P_{D1:20}, Q_{D1:20}] \quad \text{(Total 52 features)} \tag{4.9}$$

$$FS_i = [P_{G1:10}, Q_{G1:10}, P_{D1:21}, Q_{D1:21}] \quad \text{(Total 62 features)} \tag{4.10}$$

Generally, the monetary gain is the supreme motivation behind any investment along with the improvement of system performance. IGWO is employed to select the minimum number of features with highest accuracy. To obtain results of feature selection, 30 independent runs are performed for this approach. The maximum number of iterations is set to 100. During this feature selection method, the k-NN classifier (where k=5 [229]) is used as evaluator in the wrapper FS approach. Total dataset is randomly divided into two sets, 80% of the samples are used for training and the remaining 20% samples are employed for the tasting purpose. We also experimented the effect of the population size on performance and accuracy of the IGWO for prediction with high accuracy. So the IGWO is tested over the different population sizes (*i.e.* 10, 20, 30, 40, 50). Accuracy results of IGWO with different population sizes for PI_{MVA} and PI_{VQ} represented in Figures 4.11 and 4.12 respectively.

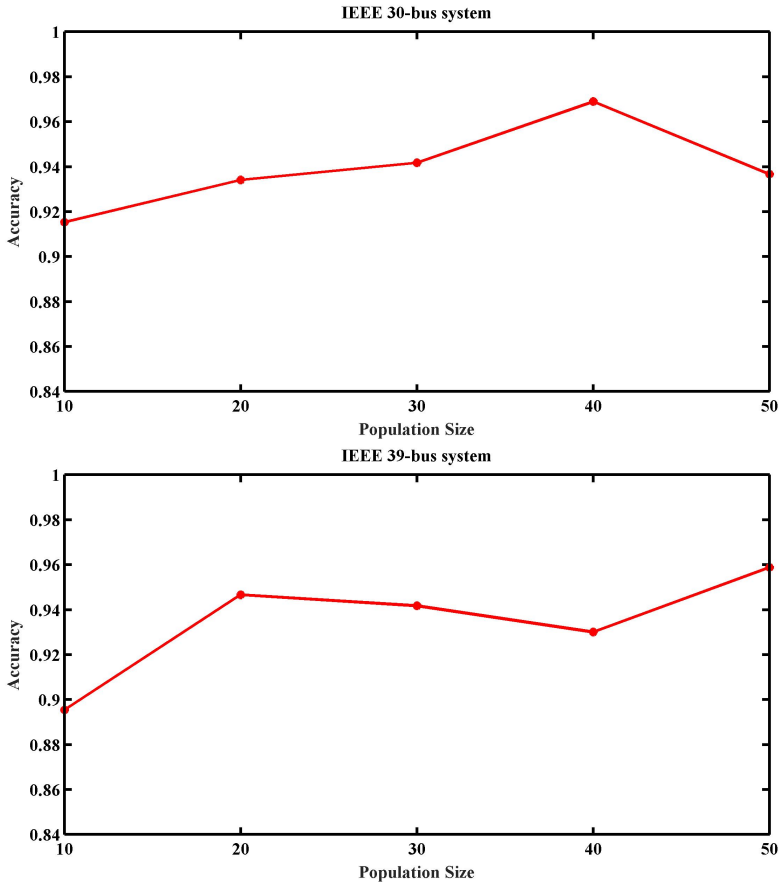

FIGURE 4.11: Accuracy results of IGWO with different population sizes for IEEE 30-bus and 39-bus systems (PI_{MVA})

TABLE 4.4: Comparison between the proposed approaches based on average classification accuracy (PI_{MVA})

Algorithm	IEEE 30 Bus System		IEEE 39 Bus System	
	Average Accuracy	StdDev	Average Accuracy	StdDev
GA [251]	0.8974	0.0088	0.8854	0.0036
PSO [244]	0.9567	0.0053	0.9498	0.0031
GWO [225]	0.9505	0.0064	0.9518	0.0056
BGWO [229]	0.9480	0.0040	0.9513	0.0183
IGWO	**0.9685**	**0.0006**	**0.9616**	**0.0011**

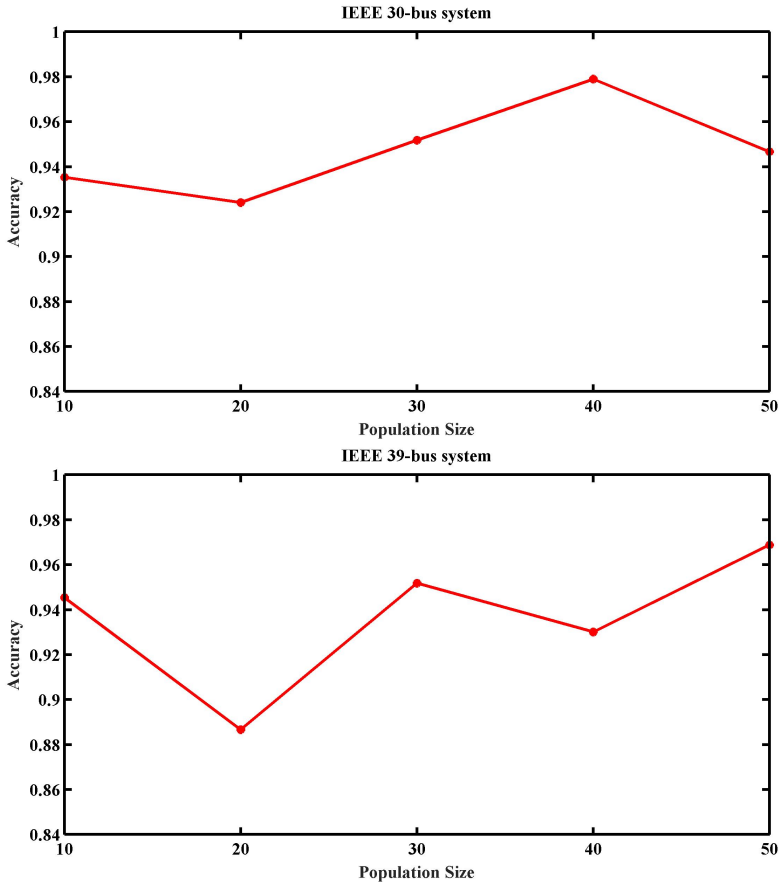

FIGURE 4.12: Accuracy results of IGWO with different population sizes for IEEE 30-bus and 39-bus Systems (PI_{VQ})

TABLE 4.5: Comparison between the proposed approaches based on average classification accuracy (PI_{VQ})

Algorithm	IEEE 30 Bus System		IEEE 39 Bus System	
	Average Accuracy	StdDev	Average Accuracy	StdDev
GA [251]	0.8754	0.0041	0.9014	0.0054
PSO [244]	0.9422	0.0084	0.9407	0.0046
GWO [225]	0.9274	0.0023	0.9312	0.0074
BGWO [229]	0.9317	0.0064	0.9211	0.0121
IGWO	**0.9564**	**0.0012**	**0.9716**	**0.0020**

TABLE 4.6: Best obtained results of GA, PSO, GWO and it's variants concerning fitness values, classification Accuracy (Acc), and Number of selected Features (NF) (PI_{MVA})

Algorithm	**IEEE 30 Bus System**			**IEEE 39 Bus System**		
	Fitness Value	**Acc**	**NF**	**Fitness Value**	**Acc**	**NF**
GA [251]	0.0179	0.9671	13	0.1275	0.9517	17
PSO [244]	0.1461	0.9711	17	0.0157	0.9814	21
GWO [225]	0.0597	0.9703	6	0.0332	0.9762	10
BGWO [229]	0.1812	0.9785	10	0.0943	0.9629	15
IGWO	**0.0042**	**0.989**	**9**	**0.0076**	**0.974**	**10**

TABLE 4.7: Best obtained results of GA, PSO, GWO and it's variants concerning fitness values, classification Accuracy (Acc), and Number of selected Features (NF) (PI_{VQ})

Algorithm	**IEEE 30 Bus System**			**IEEE 39 Bus System**		
	Fitness Value	**Acc**	**NF**	**Fitness Value**	**Acc**	**NF**
GA [251]	0.0179	0.9471	13	0.1275	0.9517	17
PSO [244]	0.1461	0.9611	17	0.0157	0.9844	21
GWO [225]	0.0597	0.9603	6	0.0332	0.9762	10
BGWO [229]	0.1812	0.9685	10	0.0943	0.9629	15
IGWO	**0.0042**	**0.974**	**8**	**0.0076**	**0.982**	**11**

TABLE 4.8: Feature selected using IGWO for contingency analysis using PI_{MVA}

System	**Initial Feature Set** FS_i	**Final Selected Feature Set** FS_{f1}	**Dimensionality Reduction (%)**
IEEE 30 Bus System	$P_{G1:6}, Q_{G1:6}$, $P_{D1:20}, Q_{D1:20}$ (Total:52 features)	$P_{G1}, Q_{G3}, Q_{G4}, Q_{G5}$, $Q_{G6}, P_{D1}, P_{D5}, Q_{D2}$, Q_{D3} (Total:9 features)	82.69
IEEE 39 Bus System	$P_{G1:10}, Q_{G1:10}$ $P_{D1:21}, Q_{D1:21}$ (Total:62 features)	$P_{G10}, Q_{G1}, Q_{G2}, Q_{G4}$ $Q_{G6}, Q_{G7}, Q_{G10}, P_{D1}$, P_{D6}, Q_{D21} (Total:10 features)	83.87

TABLE 4.9: Feature selected using IGWO for contingency analysis using PI_{VQ}

System	Initial Feature Set FS_i	Final Selected Feature Set FS_{f1}	Dimensionality Reduction (%)
IEEE 30-Bus System	$P_{G1:6}, Q_{G1:6}$, $P_{D1:20}, Q_{D1:20}$ (Total: 52 features)	$P_{G1}, Q_{G3}, Q_{G4}, Q_{G5}$, $Q_{G6}, P_{D3}, P_{D5}, Q_{D4}$ (Total: 8 features)	84.6
IEEE 39-Bus System	$P_{G1:10}, Q_{G1:10}$ $P_{D1:21}, Q_{D1:21}$ (Total: 62 features)	$P_{G10}, Q_{G1}, Q_{G3}, Q_{G4}$, $Q_{G6}, Q_{G8}, Q_{G10}, P_{D3}$, P_{D8}, Q_{D19}, Q_{D23} (Total: 11 features)	82.25

k-Nearest Neighbor (KNN) [252], a common and simple method is used for classification. KNN is a supervised learning algorithm that classifies an unknown sample based on the majority of the k-nearest neighbor category. Classifiers do not use any model for k-nearest neighbors and are determined solely based on the minimum distance from the query instance to the training samples. The KNN method is simple and easy to implement hence it is used for a classification and to ensure the goodness of the selected features.

4.4.3 Determination of Performance Indices

In order to investigate the performance of FFNN and RBFNN, diiferent architectures of the both networks have been trained using the stored data set with selected features. Following different networks have been investigated for the both IEEE 30-bus power system and IEEE 39 bus power system.

(A) IEEE 30-bus 6-generator power system

(A.1) FFNN-1 for PI_{MVA} determination using data set with IGWO based feature selection.

(A.2) FFNN-2 for PI_{VQ} determination using data set with IGWO based feature selection.

(A.3) RBFNN-1 for PI_{MVA} determination using data set with IGWO based feature selection.

(A.4) RBFNN-2 for PI_{VQ} determination using data set with IGWO based feature selection.

(B) IEEE 39-bus 10-generator power system

(B.1) FFNN-1 for PI_{MVA} determination using data set with IGWO based feature selection.

(B.2) FFNN-2 for PI_{VQ} determination using data set with IGWO based feature selection.

(B.3) RBFNN-1 for PI_{MVA} determination using data set with IGWO based feature selection.

(B.4) RBFNN-2 for PI_{VQ} determination using data set with IGWO based feature selection.

For the above mentioned FFNN-1 and RBFNN-1 networks, the number of inputs is same as the number of the features in the selected feature set as per Table 4.8 and for FFNN-2 and RBFNN-2 networks, the number of inputs is same as the number of the features in the selected feature set as per Table 4.9 for IEEE 30-bus power system and IEEE 39-bus power system. The value of PIs are output of ANNs. Different type of FFNNs combinations have been investigated with different combination of the hidden layers and trained using Levenberg-Marquardt Algorithm (LMA). Several RBFNNs have been investigated with different values of Gaussian spread parameter. The results of the investigation for FFNN and RBFNN are summarized in Tables 4.10, 4.12 and Tables 4.11, 4.13 respectively. After the determination of the PI value, the next step to find out the contingency class on the basis of their PI values.

The average error of test results obtained for IEEE 30-bus system from the FFNN and RBFNN for PI_{MVA} and PI_{VQ} respectively are shown in Tables 4.10 and 4.11. From these tables, following observations can be made for the 30-bus test system.

- For PI_{MVA} determination the average training error and average testing error of FFNN are 1.8126% and 2.6184% respectively. Whereas the average training error and average testing error of RBFNN are 1.0277% and 1.3751% respectively.

TABLE 4.10: Average error of test results proposed from FFNN classifier for PI_{MVA} and PI_{VQ} with IGWO based feature selection (IEEE 30-Bus Test System)

Sr. No.	Architecture h1-h2-h3-o or h1-h2-o	Number of features selected	Total Number of Sample	Number of Sample		Error (%)	
				Train Set	Test Set	Train Set	Test Set
A.1 (PI_{MVA})	30-15-10-1	9	4170	3500	670	1.2412	1.9451
	30-15-10-1	9	4170	3000	1170	2.3142	3.0145
	30-10-10-1	9	4170	3500	670	1.0241	2.0941
	30-10-10-1	9	4170	3000	1170	2.6712	3.420
				Average Error (%)		**1.8126**	**2.6184**
A.2 (PI_{VQ})	30-15-10-1	8	4170	3500	670	2.4147	2.6411
	30-15-10-1	8	4170	3000	1170	2.1434	2.6524
	30-10-10-1	8	4170	3500	670	1.2457	1.9876
	30-10-10-1	8	4170	3000	1170	2.0142	2.6521
				Average Error (%)		**1.9545**	**2.4833**

TABLE 4.11: Average error of test results proposed from RBFNN classifier for PI_{MVA} and PI_{VQ} with IGWO based feature selection (IEEE 30-Bus Test System)

Sr. No.	Network (Spread Constant)	Number of features selected	Total Number of Sample	Number of Sample		Error (%)	
				Train Set	Test Set	Train Set	Test Set
A.3 (PI_{MVA})	N1(8)	9	4170	3500	670	1.1103	1.8465
	N2(9)	9	4170	3000	1170	1.0120	1.3451
	N3(7)	9	4170	3500	670	1.0314	1.2147
	N4(9)	9	4170	3000	1170	0.9571	1.0942
				Average Error (%)		**1.0277**	**1.3751**
A.4 (PI_{VQ})	N5(10)	8	4170	3500	670	1.0245	1.1278
	N6(8)	8	4170	3000	1170	1.3256	1.4547
	N7(9)	8	4170	3500	670	1.9854	1.9949
	N8(7)	8	4170	3000	1170	1.4512	1.9875
				Average Error (%)		**1.4466**	**1.6412**

- For PI_{VQ} determination the average training error and average testing error of FFNN are 1.9545% and 2.4833% respectively. Whereas the average training error and average testing error of RBFNN are 1.4466% and 1.6412% respectively.

The average error of test results obtained for IEEE 39-bus system from the FFNN and RBFNN for PI_{MVA} and PI_{VQ} respectively are shown in Tables 4.12 and 4.13. From these tables, following observations can be made for the 39-bus test system.

TABLE 4.12: Average error of test results proposed from FFNN classifier for PI_{MVA} and PI_{VQ} with IGWO based feature selection (IEEE 39-Bus Test System)

Sr. No.	Architecture h1-h2-h3-o or h1-h2-o	Number of features selected	Total Number of Sample	Number of Sample		Error (%)	
				Train Set	Test Set	Train Set	Test Set
B.1 (PI_{MVA})	30-15-10-1	10	4545	3500	1045	1.1142	1.7412
	30-15-10-1	10	4545	3000	1545	1.2273	2.5332
	30-10-10-1	10	4545	3500	1045	1.1556	2.7423
	30-10-10-1	10	4545	3000	1545	2.2547	2.3451
				Average Error (%)		**1.4379**	**2.3404**
B.2 (PI_{VQ})	30-15-10-1	11	4545	3500	1045	1.4124	1.7852
	30-15-10-1	11	4545	3000	1545	2.3712	2.5423
	30-10-10-1	11	4545	3500	1045	1.4278	1.9854
	30-10-10-1	11	4545	3000	1545	2.2123	2.4258
				Average Error (%)		**1.8560**	**2.1846**

- For PI_{MVA} determination the average training error and average testing error of FFNN are 1.4379% and 2.3404% respectively. Whereas the average training error and average testing error of RBFNN are 1.1118% and 1.1604% respectively.
- For PI_{VQ} determination the average training error and average testing error of FFNN are 1.8560% and 2.1846% respectively. Whereas the average training error and average testing error of RBFNN are 1.1042% and 1.1873% respectively.

First, the values of PI are determined, after this classification of the contingency on the basis of their PI values. Neural Network classification task is performed by classifying the contingencies either as secure or insecure in accordance with Table 4.3, that finally gives the ranking for all the contingencies on the basis of their PI values. On the basis of PI values , three different severity levels have been considered that also provides the ranking of the contingencies; Class-I (Highly Critical Contingencies), Class-II(Critical Contingencies) and class-III (Non-Critical contingencies). The output determines whether a pattern belongs to a particular Class: I to III indicating the ranking of contingencies and the system security status. For some line outage, load flow solution failed to converge at some loading condition. Such line outage are placed at the top of the ranking list. Thus contingency screening, ranking and security assessment are performed at the same time.

TABLE 4.13: Average error of test results proposed from RBFNN classifier for PI_{MVA} and PI_{VQ} with IGWO based feature selection (IEEE 39-Bus Test System)

Sr. No.	Network (Spread Constant)	Number of features selected	Total Number of Sample	Number of Sample		Error (%)	
				Train Set	Test Set	Train Set	Test Set
B.3 (PI_{MVA})	N1(8)	10	4545	3500	1045	0.9410	1.0345
	N2(10)	10	4545	3000	1545	1.1321	1.0514
	N3(14)	10	4545	3500	1045	1.0174	1.2143
	N4(12)	10	4545	3000	1545	1.3567	1.3415
				Average Error (%)		**1.1118**	**1.1604**
B.4 (PI_{VQ})	N5(12)	11	4545	3500	1045	1.0041	1.0249
	N6(8)	11	4545	3000	1545	1.0347	1.0894
	N7(8)	11	4545	3500	1045	1.1241	1.3210
	N8(10)	11	4545	3000	1545	1.2541	1.3142
				Average Error (%)		**1.1042**	**1.1873**

It is found from the results shown in Table 4.10 to Table 4.13 that RBFNN is better suited for the classification of contingencies as compared with FFNN for both 39-bus and 30-bus power system. So in next step for the classification only RBFNN has been proposed for the contingency analysis.

The RBFNN is selected for on-line contingency assessment and ranking. The normalized values of IGWO based selected features from pre contingent real and reactive power output of generators (P_G & Q_G)and real and reactive demand at all the load buses (P_D & Q_D) are considered as input features for training of the RBFNN. The PIs of the system PI_{MVA} and PI_{VQ} are taken as the output features. Single line outage contingencies are considered in this work for online ranking, as they are most frequent in occurrence.

The number of inputs to the network is equal to the number of training features the input feature set FS_f obtained using IGWO for determining PI_{MVA} and PI_{VQ}. Once the training of the neural network is successfully accomplished, the estimation of PI for unknown load patterns is almost instantaneous.

Each input vector $[y_i]$ is of the following form:

$$[y_i] = \text{Selected Final Input Feature Set, } FS_{f1} \text{ or } FS_{f2} \tag{4.11}$$

The output vector $[y_o]$ of the proposed model determine PIs, as

$$\left.\begin{array}{l}[y_{o1}] = [PI_{MVA}] \text{ from RBFNN-1} \\ [y_{o2}] = [PI_{VQ}] \quad \text{from RBFNN-2}\end{array}\right\} \tag{4.12}$$

Since the same contingency, some cases may be critical from PI_{VQ} point of view and non-critical from index PI_{MVA} is used to assess security and similarly for some other cases security margin is found to critical from PI_{MVA} point of view and non0critical from index PI_{VQ}. Therefore,separate ranking is obtained for both indices PI_{MVA} and PI_{VQ} employing two RBFNNs as shown in . For each case, the performance indices are obtained off-line by AC load flow calculation.

4.4.4 Performance Evaluation of Proposed Radial Basis Function Neural Network for Contingency Analysis

With selected features employing IGWO method, contingency analysis is performed for the IEEE 30-bus system and IEEE 39-bus system. The performance evaluation of the proposed RBFNN-based method for contingency analysis of both systems is indicated in Tables 4.14, 4.15, 4.16 and 4.17 with different RBFNN architectures and different size of input patterns. The value of various training parameters have been taken as the default values provided by the available software [249]. The classifier performance is evaluated by classifying the patterns in test set, which generated randomly. The accuracy of system operating state classifications can be evaluated by determining the following measures [76, 95].

- *False Alrms (%)*-cases in which system operating state is classified as insecure, when it is a secure state.

$$\text{False Alarms (\%)} = \frac{\text{Number of 1's classified as 0}}{\text{Total number of secure samples}} \times 100$$

- *Missed Alrms (%)*-cases in which system operating state is classified as secure, when it is an insecure state.

$$\text{Missed Alarms (\%)} = \frac{\text{Number of 0's classified as 1}}{\text{Total number of insecure samples}} \times 100$$

- *Classification Accuracy (%)*-percentage of samples classified correctly.

$$\text{Classification Accuracy (\%)} = \frac{\text{Number of samples classified correctly}}{\text{Total number of samples}} \times 100$$

In power system security evaluation, the false alarms do not bring any harm to power system operation. While in case of missed alarms, effects of system operation become unknown leading to the failure of control actions [76,95,253]. Therefore, the classification system must be efficiently designed to meet this requirement that the missed alarms are kept as minimum as possible.

The performance evaluation and classification results of the proposed RBFNN model for PI_{MVA} for IEEE 30-bus test system and IEEE 39-bus test system with feature selection based on IGWO is shown in Table 4.14 and Table 4.16 respectively. The Classification Accuracy, False Alarms and Missed Alarms percentage are calculated on the basis of total samples falling in the secure or in secure class. The given contingencies falling in I, II, III and IV on the basis of PI value are 'static insecure', and those in class IV are 'static secure'.

The performance evaluation and classification results of the proposed RBFNN model for PI_{VQ} for IEEE 30-bus test system and IEEE 39-bus test system with feature selection based on IGWO is shown in Tables 4.15 and 4.17 respectively.

For Tables 4.14, 4.16, 4.15 and 4.17, it may be observed that of all the trained RBFNNs give excellent classification accuracy of is nearly 99% with very less contingency classification time. It is important to note that this classification accuracy is

TABLE 4.14: Performance evaluation of proposed RBFNN-1 classifier for PI_{MVA} (IEEE 30-Bus Test System)

Network/ (Spread Constant)	**Number of Samples**		**Classification Accuracy** (%)	**False Alarms** (%)	**Missed Alarms** (%)	**Total Training Time (sec)**	**Testing Time/Sample (sec)**
	Train Set	**Test Set**					
N1(10)	3500	670	99.104	0.969	0.649	11.4313	1.273×10^{-4}
N2(10)	3000	1170	99.230	0.661	1.140	10.6512	1.744×10^{-4}
N3(12)	3500	670	98.805	1.162	1.298	11.2146	1.291×10^{-4}
N4(8)	3000	1170	99.487	0.441	0.760	10.7714	1.341×10^{-4}

Number of Features Selected=9 Total Number of Sample=4170

obtained on unseen samples. Therefore, proposed RBFNN-based method may serve as promising tool for online contingency classification.

Some the sample results of contingency classification based on PI_{MVA} and PI_{VQ} obtained from proposed best RBFNN models with IGWO based selected features for IEEE 30-bus test system and IEEE 39-bus test system are shown in Tables 4.18, 4.19 and Tables 4.20, 4.21 respectively. As shown in these Tables 4.18, 4.19, 4.20, and

TABLE 4.15: Performance evaluation of proposed RBFNN-2 classifier for PI_{VQ} (IEEE 30-Bus Test System)

Network/ (Spread Constant)	**Number of Samples**		**Classification Accuracy (%)**	**False Alarms (%)**	**Missed Alarms (%)**	**Total Training Time (sec)**	**Testing Time/Sample (sec)**
	Train Set	**Test Set**					
N5(9)	3500	670	99.253	0.749	0.735	11.5314	1.743×10^{-4}
N6(8)	3000	1170	99.316	0.648	0.816	11.2452	1.324×10^{-4}
N7(10)	3500	670	98.656	1.310	1.470	11.4512	1.451×10^{-4}
N8(9)	3000	1170	99.401	0.432	0.816	10.7314	1.244×10^{-4}

Number of Features Selected=8 Total Number of Sample=4170

TABLE 4.16: Performance evaluation of proposed RBFNN-3 classifier for PI_{MVA} (IEEE 39-Bus Test System)

Network/ (Spread Constant)	**Number of Samples**		**Classification Accuracy (%)**	**False Alarms (%)**	**Missed Alarms (%)**	**Total Training Time (sec)**	**Testing Time/Sample (sec)**
	Train Set	**Test Set**					
N1(9)	3500	1045	98.947	0.868	1.412	12.5213	1.732×10^{-4}
N2(10)	3000	1545	99.805	0.208	0.170	11.4714	1.414×10^{-4}
N3(12)	3500	1045	99.043	1.103	0.847	11.6142	1.351×10^{-4}
N4(8)	3000	1545	99.093	0.939	0.851	11.4512	1.984×10^{-4}

Number of Features Selected=10 Total Number of Sample=4545

TABLE 4.17: Performance evaluation of proposed RBFNN-4 classifier for PI_{VQ} (IEEE 39-Bus Test System)

Network/ (Spread Constant)	**Number of Samples**		**Classification Accuracy (%)**	**False Alarms (%)**	**Missed Alarms (%)**	**Total Training Time (sec)**	**Testing Time/Sample (sec)**
	Train Set	**Test Set**					
N5(9)	3500	1045	99.043	0.814	1.298	11.9562	1.411×10^{-4}
N6(12)	3000	1545	98.964	1.002	1.096	10.8541	1.247×10^{-4}
N7(12)	3500	1045	99.138	0.814	0.974	11.4256	1.325×10^{-4}
N8(8)	3000	1545	99.158	0.901	0.731	11.8742	1.741×10^{-4}

Number of Features Selected=11 Total Number of Sample=4545

4.21 , the classification of PIs in a particular class indicates its ranking considered in Table 4.3.

The conclusion for sample results of IEEE 30-bus system shown in the Table 4.18 can be summarized as:

1. For line outage 15-18, it is found that system is always insecure at 98% of base case, 104% of base case, and 106% of base case. This indicates that the occurrence of this contingency with the above loading conditions, results in system insecurity due to the major violations of the operational constraints. In the event of this outage line flows are affected on a number of lines. The contingency ranking for this line outage varies from class I to III depending upon the loading condition.

2. For line outage 10-20, it is found that system is insecure at base case, 102% of base case, and 106% of base case. Due to the occurrence of this line outage, there is overloading of some transmission lines resulting in system thermal limit violations. The severity rank of this contingency varies from class I to III depending upon the loading condition.

3. Similar interpretation can be drwan for other line outages on the basis of system operational limit violations considered for PI_{MVA} determination.

Some other conclusions for the sample results for the cases of IEEE 30-bus system are shown in the Tables 4.18 and 4.19 can be summarized as:

1. For sample result for 106%, base case, and 104% of base case, it is found that operational constraints are violated for outage of line 10-20, resulting in system insecurity as both the PIs are in insecure classes.

2. The classification of both PIs in a particular class indicates its ranking. The sample contingent case corresponding to 96% of base case with line outage 27-29 having rank-III (PI_{MVA}), the system is found to be less critical from overloading point of view. However it is critical from bus voltage limit violation point of view having rank-II (PI_{VQ}). The power system is insecure for this case and therefore, overload capabilities of transmission lines must be taken

TABLE 4.18: Sample results for PI_{MVA} estimation from proposed RBFNN method with IGWO based selected features for IEEE 30-Bus System

Pattern No.	System Load (% of base case load)	Outage No.	PI_{MVA}		Class/Rank	
			NR	RBFNN-1	NR	RBFNN-1
95	94	1-3	0.7455	0.7345	II	II
1013	98	15-18	0.5675	0.5843	II	II
1248	102	10-20	0.2827	0.2889	III	III
1861	106	15-18	0.3675	0.3715	III	III
2025	102	12-16	0.6523	0.6712	II	II
2247	96	24-25	0.1241	0.1284	IV	IV
2653	104	15-23	0.8612	0.8741	I	I
2849	106	10-20	0.6472	0.6361	II	II
3254	96	27-29	0.3324	0.3289	III	III
3341	104	15-18	0.8112	0.8069	I	I
3556	104	16-17	0.4587	0.4642	II	II
4124	100	10-20	0.8412	0.8581	I	I

TABLE 4.19: Sample results for PI_{VQ} estimation from proposed RBFNN method with IGWO based selected features for IEEE 30-Bus System

Pattern No.	System Load (% of base case load)	Outage No.	PI_{VQ}		Class/Rank	
			NR	RBFNN-2	NR	RBFNN-2
452	96	27-29	0.6174	0.6231	II	II
1152	106	10-20	0.8148	0.8204	I	I
1454	98	1-3	0.5641	0.5708	II	II
1920	100	10-20	0.3241	0.3312	III	III
2141	100	27-29	0.1247	0.1189	IV	IV
2465	102	16-17	0.7754	0.7605	II	II
2747	106	10-20	0.6632	0.6698	II	II
3014	104	27-29	0.1847	0.1963	IV	IV
3266	102	16-17	0.1434	0.1393	IV	IV
3458	104	23-24	0.5541	0.5423	II	II
3742	94	24-25	0.2364	0.2319	III	III
4136	102	10-20	0.6745	0.6614	II	II

in to account during the operation and planning stages in order to avoid such critical incidents.

The conclusions for sample results of IEEE 39-bus system are shown in the Table 4.20 can be summarized as:

1. For line outage 21-22, it is found that system is always insecure at 98% of base case, 102% of base case, and 106% of base case. This indicates that the occurrence of this contingency with the above loading conditions, results in system insecurity due to the major violations of the operational constraints. In the event of this outage line flows are affected on a number of lines. The contingency ranking for this line outage varies from class I to III depending upon the loading condition.

2. For line outage 1-2, it is found that system is insecure at base case, 102% of base case, and 106% of base case. Due to the occurrence of this line outage, there is overloading of some transmission lines resulting in system thermal limit violations during insecure operating cases. The severity rank of this contingency is either insecure class II or III depending upon the loading condition.

3. Similar interpretation can be drawn for other line outages on the basis of system operational limit violations considered for PI_{VQ} determination.

Some other the conclusion for the sample results for the cases of IEEE 39-bus system shown in the Tables 4.20 and 4.21 can be summarized as:

1. For sample result for base case, 102% of base case and 106% of base case, it is found that operational constraints are violated for outage of line 1-2, resulting in system insecurity as both the PIs are in insecure classes.

2. The classification of both PIs in a particular class indicates its ranking. The sample contingent case corresponding to 104% of base case with line outage 16-17 having rank-I (PI_{MVA}), the system is found to be most critical from overloading point of view. However it is not critical from bus voltage limit violation point of view having rank-IV (PI_{VQ}). The power system is insecure for this case and therefore, overload capabilities of transmission lines must be

TABLE 4.20: Sample results for PI_{MVA} estimation from proposed RBFNN method with IGWO based selected features for IEEE 39-Bus System

Pattern No.	System Load (% of base case load)	Outage No.	PI_{MVA}		Class/Rank	
			NR	RBFNN-3	NR	RBFNN-3
4394	98	21-22	0.6457	0.6341	II	II
46	104	22-35	0.1245	0.1189	IV	IV
847	106	21-22	0.2925	0.2853	III	III
4015	106	1-2	0.2235	0.2354	III	III
3549	98	1-39	0.8575	0.8412	I	I
3840	102	19-33	0.1834	0.1778	IV	IV
3181	100	1-2	0.7451	0.7345	II	II
490	100	4-14	0.2143	0.2236	III	III
788	102	21-22	0.8841	0.8795	I	I
1493	102	1-2	0.3928	0.3855	III	III
1986	104	16-17	0.8345	0.8445	I	I
1078	102	10-32	0.1542	0.1625	IV	IV

TABLE 4.21: Sample results for PI_{VQ} estimation from proposed RBFNN method with IGWO based selected features for IEEE 39-Bus System

Pattern No.	System Load (% of base case load)	Outage No.	PI_{VQ}		Class/Rank	
			NR	RBFNN-4	NR	RBFNN-4
4394	106	21-22	0.4612	0.4712	II	II
1013	100	1-2	0.8341	0.8245	I	I
1248	104	16-17	0.1480	0.1556	IV	IV
1861	104	19-33	0.1741	0.8621	I	I
2025	102	1-2	0.2365	0.2478	III	III
2247	96	13-14	0.4512	0.4635	II	II
2641	106	1-2	0.3265	0.3345	III	III
2849	98	4-14	0.5238	0.5347	II	II
3254	100	16-17	0.8623	0.8574	I	I
3341	100	21-22	0.7453	0.7389	II	II
3556	104	16-17	0.2350	0.2459	III	III
4124	94	10-32	0.1128	0.1356	IV	IV

taken in to account during the operation and planning stages in order to avoid such critical incidents.

3. It is observed that PI predicted by the proposed RBFNNs are very near to required values of PI obtained from the NR method. The contingency ranking results reveals that rank predicted by both proposed RBFNNs and the NR method are almost same.

4. The verification of the results with conventional NR method indicates the effectiveness of the proposed RBFNN method for contingency screening and ranking.

5. The ranking results obtained with the proposed RBFNN-based methods may alert the power system operaters of potential overloads and voltage violations at any instant.

4.5 Comparison of the Proposed Method with Existing ANN-based Methods

The results of proposed method are compared with other existing methods in Tables 4.22 and 4.23. These tables show the comparative results for IEEE 30-bus system and 39-bus system in terms of number of input features, testing time, number of test samples, classification error and classification accuracy. It is evident that the classification accuracy obtained with the proposed method is higher than the existing ANN-based methods [95, 153, 254, 255]. The proposed approach provides fast computation of voltage reactive performance index, and MVA performance index and

Table 4.22: Comparison results for contingency analysis of IEEE 30-Bus Test System

Type of ANN	**Feature Selection Method**	**No. of Input Features**	**Testing Time/ Sample (sec)**	**Classification Error (%)**	**Classification Accuracy (%)**
RBFNN [254]	-	-	-	11.12	88.88
RBFNN [Proposed Method]	**IGWO**	**9**	**1.341×10^{-4}**	**0.513**	**99.487**

TABLE 4.23: Comparison results for contingency analysis of IEEE 39-Bus Test System

Type of ANN	**Feature Selection Method**	**No. of Input Features**	**Testing Time/ Sample (sec)**	**Classification Error (%)**	**Classification Accuracy (%)**
MLP [255]	Sequential Forward Selection	20	2.3×10^{-4}	16.49	83.51
MSVM [95]	Sequential Forward Selection	17	-	9.42	90.58
FFNN [153]	Divergence	18	1.67×10^{-4}	0.60	99.40
FFNN [153]	Fisher's Class Separability & Correlation Analysis	35	1.259×10^{-4}	0.32	99.68
RBFNN [Proposed Method]	**IGWO**	**10**	$\mathbf{1.414}\times10^{-4}$	**0.20**	**99.80**

MLP: Multi Layer Perceptron; MSVM: Multiclass Support Vector Machine

Once the network is trained and evaluated, this method can provide a fast contingency screening and requires much less calculations as compared to the traditional methods.

4.6 Summary

In this chapter an attempt has been done to employ supervised learning architecture for ranking and classification of the probable contingencies. In supervised learning approaches feature selection process is very critical because these approaches are employed for online applications considering this fact in mind meta-heuristic based distinct feature selection approach has been proposed in this chapter and the application results are presented for two systems as IEEE 30-bus system and IEEE 39-bus system. Based on this chapter following conclusions may be drawn:

1. For feature selection task, new version of GWO algorithm named as IGWO has been proposed and employed for performing feature selection task. It has been observed that proposed IGWO based feature selection technique shows promising results, when it is compared with previously published approaches.

2. The efficacy of proposed feature selection mechanism has been tested on two standard IEEE power networks. The supervised architecture is framed with two standard neural network topologies that are FFNN and RBFNN. It is observed

that with the help of proposed feature selection method both networks perform well in prediction of PIs. It has also been observed that RBFNN obtains better accuracy hence it has been further used for classification of the contingency.

3. With the help of proposed supervised architecture the computational complexity has been drastically reduced, it has also been observed that the proposed method is also helpful in dimensionally reduction. This fact is supported by the entries with less value of execution time for training, testing and validation.

4. Proposed supervised architecture has been tested over unseen critical contingencies. The results of simulations have been expressed in terms of missed, false alarms and classification accuracy. It has been observed that proposed RBFNN based method exhibit superior performance with high accuracy and very less number of false alarms. These results make this sup arch for online applications.

5. The proposed RBFNN methods gives excellent contingency classification of more than 99% even with a very small feature subset. Therefore, proposed RBFNN-based method may serve as a promising tool for online contingency classification.

In the next chapter assessment of transient stability with the help of a supervised learning method (RBFNN) will be discuss in details.

Chapter 5

Identification of Generator Criticality and Transient Instability

[*This chapter describes the RBFNN based method for the real-time transient stability assessment. It also presents the proposed method for coherency identification, and coherency based identification of members for preventive control technique. Applicability or proposed methods on standard IEEE test systems are also discussed.*]

5.1 Introduction

The transient stability is one of the most important issue at Energy Management System (EMS) to maintain reliable & uninterrupted operation, prevent cascading failures, avoid power system instability and large-area blackouts. Due to the deregulation, limited investment in the generation and transmission, and competitive business environment, the transmission lines are operating near their permissible limits. With this cropped up concern, planning of foolproof system is a prerequisite. In recent years several cases of grid failure have been experienced throughout the world. Tables 1.1 and 1.2 list some notable wide-scale power outages and cascading events [34]. There is a pressing need to develop fast and more accurate online

stability evaluation methods which could analyze the level of stability and suggest appropriate control action well in time to ensure power system transient stability under all operating conditions. However operating condition is found to be unstable, then system stability takes over system economy. and preventive action may be taken to bring the state in secure operating state even if cause some loss of economy.

Power system Transient Stability Assessment (TSA) has become a major concern for modern electric utilities which are operating closer to their security limits due to deregulation, competitive business environment, economic and operational constraints. Modern power systems are dynamic in nature, where the network topology is changing continuously with varying load demand. With increase in load, the power system is loaded to its limit leading to loss of synchronism and system collapse even under minor disturbance [35]. In real time operation, the operating conditions, loading conditions are quite different from those assumed at planning stage. Thus, to prevent system from failure due to any possible hard contingency the operator access and monitor the health of power system by simulating different contingencies in advance and keep the preventive control action in mind. This whole process is called Transient Stability Assessment (TSA) and preventive control. The TSA involves monitoring and assessment of the rotor angles of the generators under abnormal operating conditions. The dynamic behavior of the power system under probable contingency is studied based on these rotor angle behavior.

In the past, various methods based on energy functions [35, 38, 104–106, 158–165], Time-Domain Simulations (TDS) [96–103, 157] and hybrid methods have been proposed by various researchers for TSA. TDS based methods consists of simulating during and post-fault behaviors of the system for a given disturbance and observing the angular swings of the machines to estimate security status [103]. However, this method is difficult to implement for on-line TSA mainly due to heavy computational burden. Another conventional method for stability analysis of power systems by Lyapunov's direct method has been addressed by M.A. Pai et.al. [35,38]. Direct methods are based on the post-fault system equations by a stability criterion [35, 38, 102–106]. But this method suffers from computational in accuracy for multi-machine power systems. A method based on Wide Area Management System (WAMS), Energy function and Ad-joint Power system (APS) model was presented in [107], the method was based on trajectory prediction by employing curve fitting

technique. A corrected transient energy function based strategy for probabilistic TSA of power systems was proposed in [108]. An interval Taylor expansion based method was proposed to assess the transient stability in the presence of uncertainties in [109]. A stochastic power system model based on stochastic differential equations (SDEs) was proposed to take into account the uncertain factors [256]. A modified form of swing equations and DC link dynamic equations to compute the critical clearing time for a given fault based on the center of angle evaluation was proposed in [110]. Employment of energy function based approaches enables the system operator to get information regarding degree of stability. Moreover, these approaches are fast and provide important information for selecting appropriate preventive control strategy. However, the bottlenecks in the energy function based approaches are characterization of stability boundary and definition of fault dependent region of attraction locally around controlling unstable equilibrium points. The major difficulty in energy function based approaches is that they are applicable only for first swing instability [111].Therefore due to the limitations of these methods, there have been great interests in applying artificial intelligence and machine learning based methods, which are promising for online application. Extensive research have been made for assessment of power system health using ANNs due to its excellent classification capability and speed [72, 91, 112–118].

The ANN based TSA methods requires generation of reliable data set using most accurate TDS techniques. So TDS based approaches along with the application of supervised framework are still preferred over other approaches. Following are the advantages of TDS based methods.

- These approaches are simple and are applicable to general power system models.
- The time domain response of all state variables can be obtained in post, pre and during fault states. This information is beneficial for both planning and operating states. The operator can interpret the simulation results at any point of time.

TDS provide the details about the generators rotor angles' deviation during the post, pre and during fault states. However, interpretation of these information for

the purpose of the assessment is a complicated task. The ANN based assessment methods needs the transient stability status in the form of some numerical values and therefore, one of the purpose of online TSA is to compute an index which provide the numerical values which are replica of the transient stability of the power system under contingencies. This index is helpful for power engineer to gain insight into stability related problems and to take proper operational decisions. In the current decade, many researchers have proposed different severity indices for online assessment of dynamic security of the large power systems [97, 118, 199, 257–261]. Rotor Trajectory Index (RTI) has been employed in approaches for ranking and re-dispatching generation of the generating machines [199, 257]. In [261] a small signal stability index is proposed for power network dynamic assessment by employing TDS. The value of this index is calculated by the system's eigenvalues. This is determined using dynamic simulation. An index is proposed in [260] for Dynamic Security Assessment (DSA). In [260], a practical and heuristic index is proposed for fast contingency ranking. These indices are based on transient stability status in large power systems. Some limitation of these methods as under:

- Due to the usage of rotor angle values directly, the method put heavy computational burden.
- The prediction of the real time transient state of the power can be done successfully by published methods, but these methods are used only as a classifier.
- The stability status of the individual generator for any contingency cannot be determined by these methods.
- For the control action like generator rescheduling, the knowledge of the individual generator state (either stable or unstable) with high accuracy is mandatory.
- For large power systems large simulation time is required for monitoring the system health [35].
- Due to first swing instability [35] wrong assessment of transient stability has been observed.

- However, there is still one major limitation in machine learning-based TSA techniques, existing work tends to employ a fix time frame data and a particular fix instant value of dynamic data for modeling the supervised learning engine.

From the literature, it is evident that a numerical indicator which is composed of major state variables of the power system is able to indicate the stability status of the power system. This fact has become major motivation to derive a new indicator for stability status. For determination of stability status a bulk power system is segregated into small equivalent groups of generators. To overcome the above said limitations in previous proposed approaches, these approaches need improvements for accurate identification of the generator criticality and transient instability of the system.

Cascading outages are major threats to the secure and stable operation of power systems. During cascading failures, the interconnection between different electric areas is weakened and the system working generators are divided in several groups according to their behavior [262]. These groups are known as coherent groups of generators. Some groups are very sensitive to the disturbance and some are unaffected by the disturbance. To initiate a preventive control action for enhance the power system stability under disturbance, information about the generator coherent group are primarily required.

As stated, generator coherency has a considerable application in power system operation and control. The concept of coherent groups of generators is based on the similar behavior of TDS responses of generators when they are subjected to a perturbation [33]. This phenomenon is called coherency. In this consideration, generators that have the similar post-disturbance rotor angle deviation or speed variation characteristics are called coherent and are placed in the same group. The generator's dynamic response under disturbances can also be recognized by the deviations in phase angles of voltage or/and current phasor of the system. Hence, it is required to monitor and examine the relationship or similarity of rotor angle deviation to find coherent nature of the power system components.

Several methods have been introduced in the literature for identification of coherent behavior of generators and their classification, according to their similar behavior

(TDS characteristics). After identification of the coherent groups, control strategies can be applied on them. In order to initiate any preventive control under stressed condition, it is desirable to discover the coherency between generators [198]. In general, coherency classification techniques can be divided mainly into two types. The techniques that are placed in the first type are based on model reduction and required computation of the eigenvalues and eigenvectors of power system [197]. For example, a Syn-chronic Modal Equivalencing (SME) was proposed in [197] for structure preserving dynamic equivalencing of large power system models. Techniques that are placed in the second type are based on disturbances and use TDS to find coherent groups of generators. For example, several studies have used Rotor Trajectory Index (RTI) [199] has been used. Fourier spectrum [200] or fast Fourier dominant inter-area mode [201], principal component analysis [202], independent component analysis [203], hierarchical clustering methods [204–206] and [207], Fuzzy c-medoids algorithm [208, 209], wavelet [210], and Hilbert-Huang transform [211] to identify coherent generators.

Generally, real time TSA is an approach to find the fast and accurate prediction of the system stability status (either stable or unstable) in real time by considering the future behavior of the generator under the disturbed operating condition. In the literature various topologies were proposed to forecast the system stability status by using different types of artificial intelligence based techniques [154, 263–267]. The coherency and stability state prediction were carried out by using rotor angle values through RBFNN in [263]. Due to the usage of rotor angle values directly, the method put heavy computational burden. Hashiesh et. al. [264] proposed a supervised learning technique for transient stability state prediction by ANN. The prediction of the real time transient state of the power can be done successfully by the above discussed methods, but these methods are used only as classifier. The stability status of the individual generator for any contingency cannot be determined by these methods. For the control action like generator rescheduling, the knowledge of the individual generator state (either stable or unstable) with high accuracy is mandatory. However, there is still one major research gap in machine learning-based TSA techniques. The existing work tends to employ a fix time frame data and a particular fix instant value of dynamic data for modeling the supervised learning engine. On the basis of the critical review, authors are motivated to propose a new severity index which can normalize the values of post fault rotor angle deviations in

a specified range for precise classification of coherent groups and transient stability status with low computation burden.

The main requirement of real time TSA is that it should be fast enough to allow timely initiation and implementation of appropriate preventive and emergency control action [263] to prevent possible loss of stability. It is desired that future stability status should be known with in few cycles from Fault Clearing Time (FCT) after the fault. It is reasonable to believe that initial variations of rotor angles of generators carry sufficient information about prospective stability status of power system. Therefore, by observing the initial rotor trajectory it is possible to predict the prospective stability status. However. larger the period of initial observation better is the success rate of prediction.

In this chapter an RBFNN based method is proposed for online TSA of power system for a probable set of contingency. An new Transient Stability Index (TSI) is proposed to scaling the severity of the transient instability and identifying the stability status of each generator in term of their synchronism. The proposed TSI is based on time domain solution of the swing equation that is used for the assessing the transient stability of the power system. The online stability under varying operating condition is determined through RBFNN based approach predicting the TSI values for all the generators for given operating conditions and then evaluating the transient stability state. The input of the proposed RBFNN are the variation of rotor angle values of all the generators (available through PMUs installed at high side of generating bus) with respect to δ_{COI} from FCT+0.01s to FCT+0.05s. The rotor angles after a large disturbance gives the information of transient stability state of the system. If any generator goes "out of step", the operating state is declared "unstable" state, else "stable". The predicted output of RBFNN is employed to determine stability status of system, coherent group, criticality rank of generator and preventive control action, when system following a large perturbation or fault. The proposed method is independent of the fault location and the type of fault and depend only upon the post-fault data obtained through PMUs in real time at centralized control center. The applicability of comprehensive scheme of TSA has been tested on IEEE 39-bus, 10-generator, IEEE 68-bus, 16 generator and 145-bus, 50-generator systems under wide operating conditions and application results are presented. In the following section mathematical formulation for TSA is presented.

5.2 Problem Formulation for Transient Stability Assessment

The main objective of the transient stability analysis is to identify the ability of a power system to remain in equilibrium after the severe disturbance. The aim of TSA to assess the dynamic behavior of a power system accurately and efficiently.

5.2.1 Power System Dynamics

TDS method is used to solve the differential equations involved in power system stability analysis. The Overall system model of TDS is shown in Figure 5.1. TDS of power system with dynamic disturbance is required for TSA to find whether system maintains synchronism during disturbance or not. This decision is taken by monitoring the movement of trajectories of rotor angles during a perturbation period. The swing equation shows the transient behavior of the system [33, 102]. If the trajectories of rotor angle of either single generator or a group of generators are found to increase without limit with reference to remaining machines, then the system is unstable. Another phenomenon, if rotor angles of all working system generators remain bounded within their respective permissible limits, then system is considered as stable [102]. Vahdati et al. [268] describe mathematical representation of the detailed system dynamics. In this study, the multi machine classical model for transient stability analysis is used.

$$\frac{d\delta_j}{dt} = \Delta\omega_j \qquad j = 1, 2, ..., N_G \tag{5.1}$$

$$\frac{d\Delta\omega_j}{dt} = \frac{1}{M_j}\left(P_{mj} - P_{ej} - D_j\Delta\omega_j\right) \tag{5.2}$$

$$P_{ej} = G_{jj}E_j^2 + \sum_{k=1,\, k\neq j}^{n} E_j E_k \left\{ G_{jk}\cos\left(\delta_j - \delta_k\right) + B_{jk}\sin\left(\delta_j - \delta_k\right)\right\} \tag{5.3}$$

where, $G_{jk} + jB_{jk}$ is transfer admittance between the j^{th} and k^{th} generators, M_j is moment of inertia, P_{ej} is electrical power output, D_j is damping coefficient, P_{mj} is mechanical power input, $\Delta\omega_j$ is rotor speed deviation, δ_j is rotor angle for j^{th}

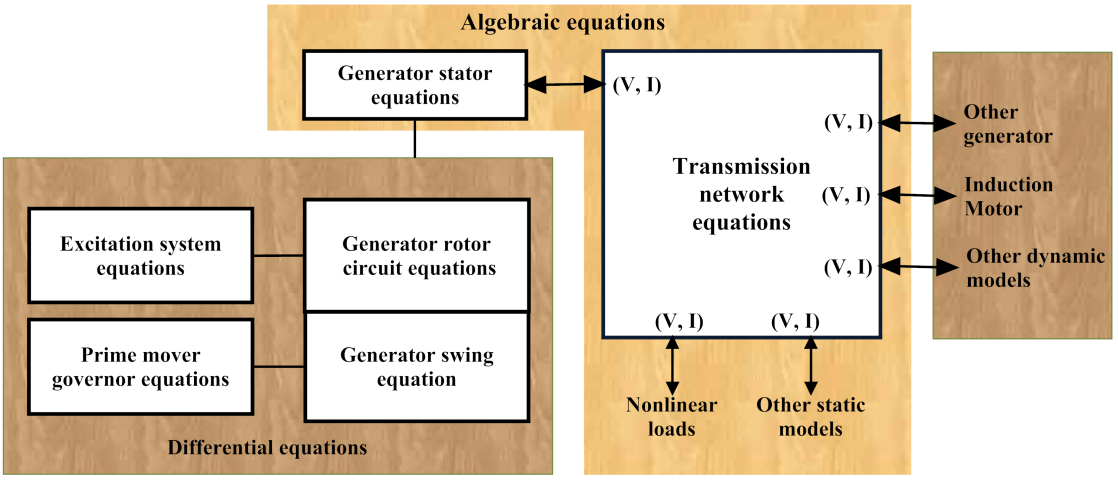

FIGURE 5.1: The overall system model of TDS

generator, δ_k is rotor angle of k^{th} generator. The deviation between generator rotor angles with reference to time t can be found by using the set of swing Equations 5.1, 5.2 and 5.3.

In the projectile transient phenomena, inertial center of system is taken as reference frame for calculations. The generators' rotor angles with respect to center of inertia (COI) [269] are used to detect whether the system is stable or not. For a system having N_G-generators with inertia constant M_j and rotor angles δ_j of j^{th} generator then the inertial center δ_{COI} is determined by Equation 5.4.

$$\delta_{COI}(t) = \frac{1}{M_{total}} \sum_{j=1}^{N_G} M_j \delta_j(t) \tag{5.4}$$

5.2.2 Proposed Transient Stability Assessment

With the wide application of the Phasor Measurement Units (PMU) and Wide Area Measurement System (WAMS) in power system, TSA is possible in real time. The real time measurements based transient instability detection methods used to employ the post fault power angle trajectories for many decades [263]. The power angle deviation is used as transient stability indicator. If it increases monotonically and cross the predefined threshold value, then power system is transiently unstable.

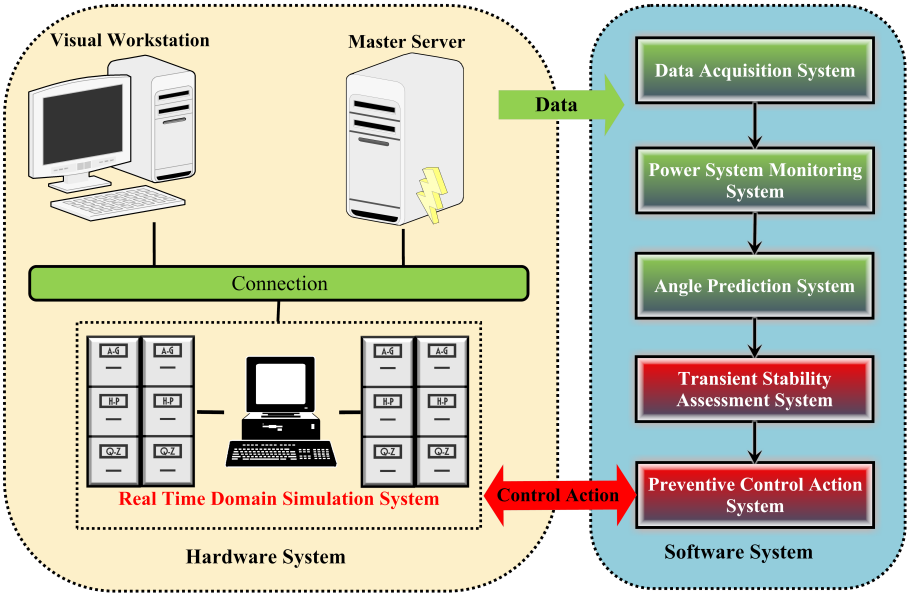

FIGURE 5.2: Proposed transient stability assessment model

The frame structure of real time power system TSA model mainly consists of two systems, viz. hardware system and software system as shown in Figure 5.2. Hardware includes the master server, the visual work station and communication interface as well as control action actuating devices. Software system includes the data acquisition system, the power system monitoring system, the generator rotor angle prediction system, the transient instability identifier system and the preventive/emergency control action system.

A numerical integration technique such as Runge-Kutta method can be used to solve swing equation. The T/S status is determined by monitoring the swing in rotor angle trajectories and deviation in rotor angle with respect to the constraint for transient instability is given as Equation 5.5.

$$\Delta\delta_{j,COI} = |\delta_j - \delta_{COI}| \leq \delta_{\max} \quad j = 1, 2, \ldots, N_G \tag{5.5}$$

Here $\delta_{\max}$ is maximum allowable value of relative rotor angle for secure operation. The PMUs are installed on the high side of generating buses to monitor generator rotor angles [270]. The data are transferred to the central control location every cycle with 1-μs accuracy and is utilized for real-time calculations for this study. During the case of disturbance if relative rotor angle $\Delta\delta_{j,COI}$ violates $\Delta\delta_{j,COI}$ ($\geq \delta_{\max}$) in a time interval [0, $t_{\max}$], the system is considered as insecure (1) else is considered

secure (0). For this work maximum allowable value of relative rotor angle for secure operation $\delta_{\max}$ is taken as 120^0 [271–273].

5.2.3 Proposed Transient Stability Index

Rotor angle trajectory of any generator is a replica of transient behavior of that generating unit. Application of PMUs and WAMS makes it possible to determine rotor angle values which can be used to detect the synchronism state of a generating unit in real time. The synchronism status of the generating machines for every insecure contingency needs to be discovered with less computational burden and time. Therefore, the rotor angle trajectory based severity index, called Transient Stability Index (TSI) is proposed in this chapter to assess the severity of any operating condition following a disturbance. TSI is determined from TDS and defined for any j^{th} generator as:

$$TSI_j = 1 - \frac{\delta_{\max} - \Delta\delta_{j,COI}(\tau)}{|\delta_{\max} + \Delta\delta_{j,COI}(\tau)|} \tag{5.6}$$

Where, $\Delta\delta_{j,COI}(\tau)$ is the final value of rotor angle deviation in degrees at the end of simulation time.

TSI can be used to assess the stability of power system, to rank the criticality and individual stability status of the generators and coherency among generators. Hence, it indicates the synchronizing condition of the system for a given hard contingency. The numerical value of TSI is an indicator of the unstable or stable system state of the power system respectively.

$$Generator\ Stability\ Status = \begin{cases} Unstable & if\ TSI \geq 1 \\ Stable & if\ TSI < 1 \end{cases} \tag{5.7}$$

5.2.4 Proposed Methodology for Online TSA using ANN

TDS is the well established and accurate method for TSA. It can handle detailed modeling of the system and provides most accurate information of power system variables in post-disturbance scenarios but it is computationally very demanding. Moreover, the TDS methods requires complete information about all the dynamic

and static variables of power system to predict the security status of a current operating state. Modern power systems are large and complex therefore, it is not possible to keep a track of all minor changes occurring in topology and control variables and therefore TDS methods are not suitable for on-line applications. However, these methods can be used to generate accurate off-line data covering wide range of operating scenarios for training ANN. ANN has widely used for the TSA as reported in the literature. The proposed method is used an predictor, which predict the TSI values. These predicted TSI values employed to classifies the operating states of a power system into secure and insecure classes. In this thesis, a more efficient TSA scheme is proposed which determines the on-line transient stability state of the system for probable disturbance through Transient Stability Index (TSI), which is based on the rotor angle deviations using Radial basis function Neural Network (RBFNN). The development of RBFNN topology capable of predicting the post-disturbance severity from pre-contingent data for TSA is proposed in this section. The method can be used on-line for the unseen operating scenarios when the system is still in secure state and rank the possible contingencies for particular operating conditions in decreasing order of the severity through predicted values of the TSI.

5.2.5 Data Generation

The primary objective of data generation is to obtain all possible operating states of the power system. The off-line database consists of large number of randomly varied load patterns covering wide range of scenarios for credible contingencies. The selection of critical contingencies depends upon the knowledge of the operator about the probability of their occurrence and severity. The rotor angle values of the generator after fault clearing time i.e. (FCT+0.01s to FCT+0.05s) are considered as input features of the neural network and the values of TSI at the end of the simulation and out of step time are taken as output targets. The steps for generating offline data using TDS for online TSA are as follows:

Step 1 Run Optimal Power Flow (OPF) on the given test system at base case, obtain and set the optimal generation.

Step 2 Set random total load of the system between 95%-105% of the base case.

Step 3 Set pattern $I = 1$.

Step 4 Randomly vary the real and reactive load of each bus of the system.

Step 5 Create a thre phase fault, perform TDS for given load pattern.

Step 6 Record the rotor angles with respect to COI, $\delta_{j,COI}(t)(g = 1, 2, ..., N_G)$ at each time step during simulation.

Step 7 According to the $\delta_{j,COI}(t)$ TSI is calculated.

Step 8 Is $\delta_{j,COI}(t) > 120^0$ or $TSI > 1$, the system for the given operating conditions contingency J is transient unstable (1) otherwise transient stable (0).

Step 9 Is pattern $count = max$? Yes, go to next step (x) else $I = I + 1$ and go to step (iv).

Step 10 All cases simulated? Yes, divided the total patterns into train set and test set for RBFNN otherwise, Increase the total load by 2.5% and go to step 3.

5.3 Proposed Radial basis Function Neural Network

Radial basis Function Neural Network (RBFNN) architecture is proposed for on-line TSA of power system. RBFNN is used due to its nonlinear mapping capability, structural simplicity and better training efficiency can be effectively used for predicting the post-disturbance TSI values with pre-disturbance data. Radial basis function (RBF) networks were introduced into the neural network literature by Lowe *et.al* [274]. RBFNN is the class of single nonlinear hidden layer feed forward neural networks which have nonlinear mapping capability and use radial basis function as activation function. The output of the network is a linear combination of radial basis functions of the inputs and neuron parameters.

An RBFNN with a supervised learning mechanism is made up of a set of neurons configured in a connected network consisting of three layers, namely, input layer, hidden layer and output layer. The input layer is actually an input vector with

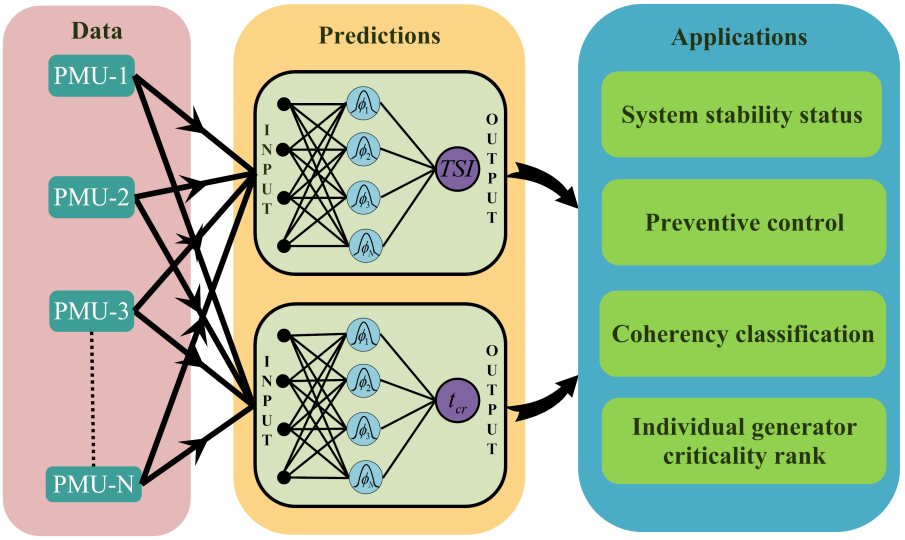

FIGURE 5.3: Proposed Radial Basis Function Neural Network (RBFNN)

each element representing a feature, while the hidden layer consists of Radial Basis Function Neurons (RBFNs) and the output layer consists of Linear Neurons (LNs). The structure of RBFNN includes $X = (x_1, x_2, x_3, \ldots, x_d)^T$ a d-dimensional input vector. $C = (c_1, c_2, c_3, \ldots, c_d)^T$ a center vector, $\|X - C\|$ distance between X and C, $\varphi(X, C, \sigma)$ a Gaussian basis function with input X as variable and center C and width σ as parameters, and y the output of the neuron. The Gaussian basis function [47] is of the form:

$$\varphi(X, C, \sigma) = \exp\left(-\frac{\|X - C\|^2}{2\sigma^2}\right) \tag{5.8}$$

where $\|X - C\|$ is the Euclidean distance expressed as:

$$\|X - C\| = \sqrt{\sum_{i=1}^{d} (x_i - c_i)^2} \tag{5.9}$$

Figure 5.3 shows the architecture of the proposed RBFNN, in which neurons are linked together to form a 3-layer network. In the network, all the neurons in the hidden layer are linked with the input layer and also to the every neuron in the output layer. Links exist between two adjacent layers only, and there is no link in the same layer and between any two non-adjacent layers. The working process of the network can be divided into three phases. At first, an external input X being

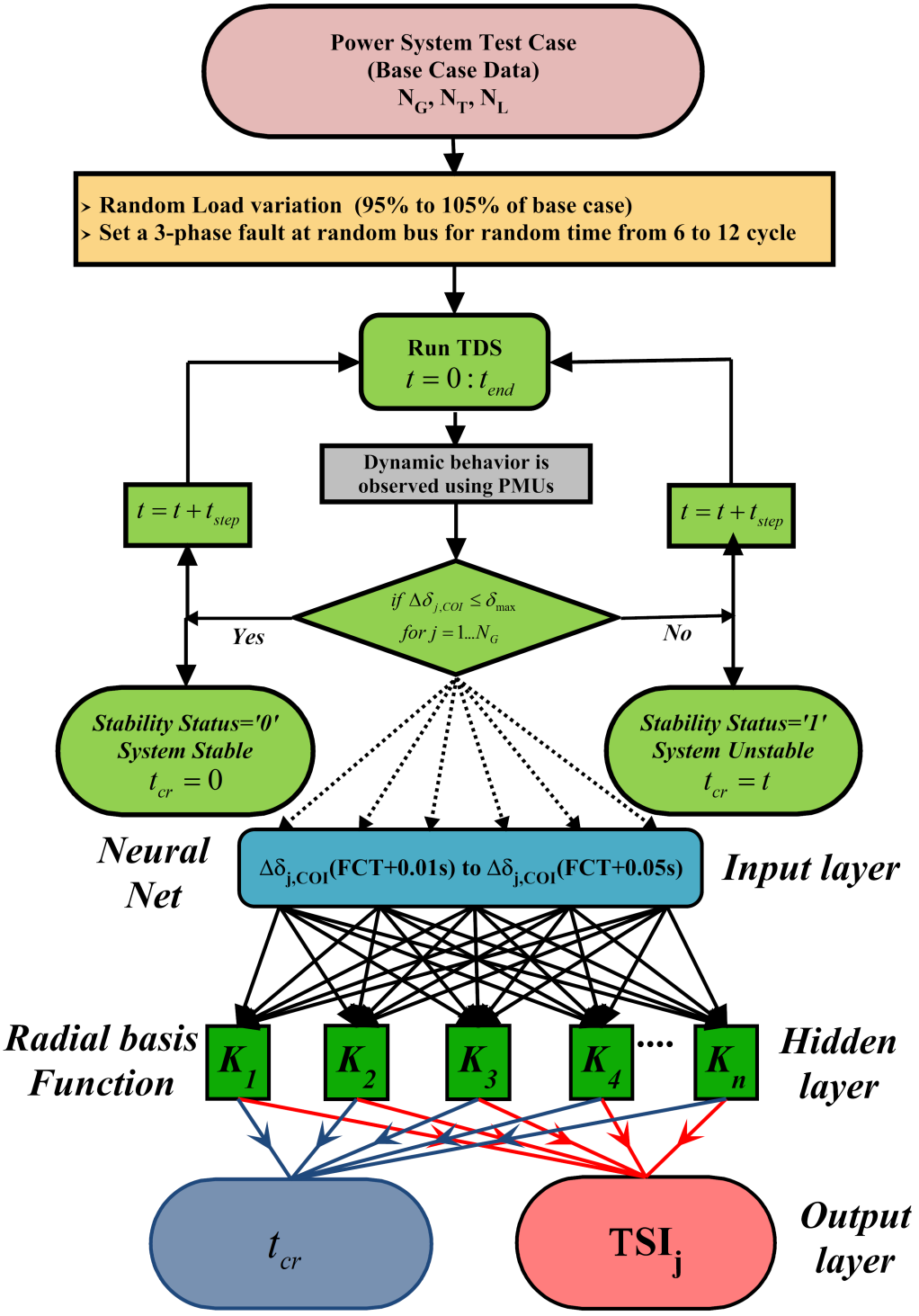

FIGURE 5.4: Flow chart of the proposed scheme

a vector of features' values is fed into each of k-neurons in the hidden layer, then the output yielded by each hidden neuron is fed into all neurons in the output layer, and finally all outputs of output neurons are the network's output Y with the j^{th} element being computed by

$$y_j = \sum_{i=1}^{k} w_{ji} \exp\left(-\frac{\|X - C\|^2}{2\sigma^2}\right) + w_{j0} \qquad j = 1, 2, \ldots, N \tag{5.10}$$

Where k is the number of hidden neuron, w_{ji} is the connection weight linking the i^{th} hidden neuron to the j^{th} output neuron, w_{j0} is the bias of the j^{th} output neuron, and C_i and δ_i are the i^{th} hidden neuron's center and its activation function's width respectively.

For on-line TSA, the off-line data is generated for the given set of credible contingencies by randomly varying the real and reactive loads, the real and reactive power generations of all the generators are set to optimal point of the base case. In this thesis, we propose a supervised architecture that is based on the rotor angle values of the generator after fault clearing time i.e. (FCT+0.01s to FCT+0.05s) and predict the values of TSI and out of step time for different cases. The dimension of feature vector for this approach is $5 \times N_G$ and output vector is $N_G + 1$ i.e. the time and the values of TSI of each generator. Radial basis function is used to build ANN. The transfer function of RBFNN is shown in Equation 5.10.

$$Input\,Vector\,[x_n] = \begin{bmatrix} \delta_G(FCT + 0.01s) \\ \delta_G(FCT + 0.02s) \\ \delta_G(FCT + 0.03s) \\ \delta_G(FCT + 0.04s) \\ \delta_G(FCT + 0.05s) \end{bmatrix}_{G=1}^{G=N_G} \tag{5.11}$$

A flow chart showing the process is depicted in Figure 5.4. The values are normalized between 0 and 1. The potential input features vector for this architecture is defined in Equation 5.11.

The target for RBFNN output is the TSI values, calculated from final values of the generator rotor angle at the end of the simulation and time at which any generators' rotor angle trajectory cross δ_{max}. These are defined as target vector as

given by Equation 5.12.

$$Output\,[Y] = \begin{bmatrix} TSI_G \\ t_{cr} \end{bmatrix}_{G=1}^{G=N_G} \tag{5.12}$$

Where $N_G = 1, 2, ..N_G; N_G$ represents the total no. of generators. Ranking of generators can be found from their corresponding generator TSI values'. Further this ranking can be used in the process of preventive and corrective control action.

5.4 Proposed Real Time Coherency Identification

Real-time coherency identification becomes a complex problem when the system is subjected to a large disturbance and rotors swing continuously. The coherent generators may change their group in the subsequent cycles and form different groups finally. Large groups may separate into smaller groups or vice versa, smaller groups may combine to form a larger group. The initiation of proper counter corrective measure is based on the coherency information. This action can be effective if it is taken in stipulated time. Hence, early detection of coherent groups after disturbance is critical and can prevent the system from cascaded failures resulting in blackouts. In proposed work, the classical criterion for two generators is computed as follows:

$$TSI_i - TSI_j \leq \lambda \tag{5.13}$$

Where TSI_i and TSI_j are the TSI values of the generators i and j respectively, predicted by RBFNN. λ is the maximum permissible deviation of rotor angles for a pair of generators at the considered time step. Identification of coherent group is a time dependent exercise that depends on the prediction and measurement time. In this work end time of TDS is considered for the coherency identification.

In this study, the identification of the coherent group of generators is obtained by predicting the rotor angle values at the end of the simulation with five consecutive cycles data consisting of rotor angle after fault clearing which is obtained at central

control location through PMUs. With these predicted rotor angle values, the real-time transient stability state is obtained using Equation 5.13.

5.5 Simulation Results

The proposed strategy is tested on three global standard benchmark systems, namely IEEE 10-generator 39-bus New England system, 16-generator 68-bus and 50-generator 145-bus power networks. All the TDS simulations are carried out using MATLAB [249], MATPOWER [275], PSAT Version 2.1.10 [276] and PST [277] with Intel Core(TM) i3-3110M platform with 2.40 GHz and 6 GB RAM. The symmetrical fault with ground is initiated at random time from 0.01s to 0.12s and cleared at 0.2s by randomly perturbing the real and reactive loads on all the load buses and real and reactive power generation at the generator buses. System total load is varied from 95% to 105% of base case load [278]. Fault is simulated with a large number of operating cases. Simulation time is selected as per Kundur et.al [35]. Gaussian spread parameter for RBFNN is taken 0.55. After observing the TDS, RBFNNs are constructed as per the Section 5.3.

5.5.1 Training and Testing Data Generation

The real and reactive loads are varied from 95% to 105% of the base case in steps of 2.5% and for each topology 100 patterns are generated by randomly varying all loads, which covers a wide range of scenarios. The dynamic simulation is performed for 3 seconds and 5 seconds for 10-generator, 39-bus & 16-generator, 68-bus system and 50-generator, 145-bus test system respectively. Rotor angles values of all the generators at the end of simulation is observed. The off-line data is generated by considering the following assumption [102]:

(i) A classical machine model is considered, where machine is represented by a constant voltage behind their direct axis transient reactance.

(ii) The loads are modeled as constant impedance with pre-fault steady state values.

(iii) The inertia constant of machines remains constant during transient period.

(iv) The mechanical power input to machine is considered constant during transient period and taken equal to pre-fault electrical power output of the machine.

(v) Damping or asynchronous power is negligible.

Thus total 500 patterns are generated for different contingencies. The online TSA is done by post-disturbance data of rotor angle trajectories. The RBFNN is used for mapping the nonlinear relationship of post-fault rotor angle trajectory values to the TSI values which are replica of the post-fault behavior of the generator. The fault applied at different locations, hence the load situated close to the fault affect the rotor angles of machines and the system stability close to that disturbance only and do not affect much the rotor angle of machines far from that disturbance.

5.5.2 Determination of Transient Stability Assessment using Proposed TSI

The transient stability state of each case is analyses based on the swing of rotor angles obtained by the numerical routines for 3s for small system and 5s for large power system as per [35]. The determination of TSA using proposed index is obtained on the basis of the following steps:

Step 1 The proposed TSI provides an index based on the generator rotor angle deviate from the COI.

Step 2 A threshold value or critical value for TSI is obtained by the boundary value of relative rotor angle deviation from COI, which is $\delta_{\max}$ for transient instability following a disturbance. For this study, $\delta_{\max}$ is taken as 120^0 which decides the critical value for TSI. The critical value of TSI for this system is taken as "1".

Step 3 For any generating unit having TSI$\leq$1 indicates that the machine will remain in synchronism with rest of the system. All such machines are called non-critical machines.

TABLE 5.1: Validation of RBFNN for 10 Generator 39 Bus System Case- 3-ϕ fault at bus-4 and cleared by opening the breakers to isolate line 4-14

		Fault Duration							
		0.2s	**0.18s**	**0.17s**	**0.14s**	**0.15s**	**0.13s**	**0.10s**	**0.08s**
$\Delta\delta_{COI}$		1563.6279	1138.8126	118.1225	109.2366	102.0193	90.1906	75.9733	67.8471
TDS	TSI	**1.8575**	**1.8093**	0.9921	0.9530	0.9190	0.8582	0.7753	0.7224
	t_{cr}	0.73	0.82	-	-	-	-	-	-
RBFNN	TSI	**1.8575**	**1.8093**	0.9921	0.9530	0.9190	0.8582	0.7753	0.7224
	t_{cr}	0.73	0.82	-	-	-	-	-	-

Step 4 For any generating machine having TSI>1, indicates that the machine will lose synchronism with rest of the system making insecure. The rotor angle of such machines continues to increase without bound with respect to COI following a disturbance on the system. All such generator are called critical generators.

Step 5 Generator status is indicated as "0" and "1" for non-critical and critical machines respectively. If any generator becomes critical by going out of step or losing synchronism, it will make the system transiently unstable represented as "1", otherwise the system will remain in synchronism and is transiently secure represented as "0".

Step 6 The TSI value is the target for proposed RBFNN. The Power system transient stability status is depended on the predicted value of TSI.

Step 7 The ranking of critical machines which going "Out-of-step" for each case can be obtained by ranking their TSI values in decreasing order of their severity.

5.5.3 Validation of proposed RBFNN

After training, in order to check how well the trained RBFNNs act under different simulated fault scenarios, the results of RBFNNs are validated by different test patterns with change in fault duration from 0.05s to 0.2s. The performance of trained RBFNNs in evaluation of system stability is determined by predicting accurate value of TSI and 'out of step' time. The validation of simulation results is shown in Tables 5.1, 5.2, 5.3 and 5.4.

Table 5.1 is shown for 10-generator 39-bus power system at base case random load variation and three-phase fault at bus-4 simulated at different fault initiated times from 0.001s to 0.12s and cleared at 0.2s by opening the breakers to isolate line 4-14. The state of transient stability for all generators is determined by observing rotor angle swings ($\Delta\delta_{COI}$) in the time interval. As per this table, for fault duration 0.2s, the maximum rotor angle deviation value among all the working generators is 1563.6279^0 at the end of simulation and corresponding to this value, TSI is calculated as 1.8575. The predicted maximum TSI value among the all TSI values by proposed RBFNN is also 1.8575 with 100% accuracy. Same comparison is shown in critical time prediction as TDS provide the 0.73s at which system lose his synchronism (i.e. anyone generators' rotor swing cross the maximum rotor angle limit $\delta_{\max}$). The predicted value by the proposed RBFNN is also 0.73. So the proposed RBFNN provide the information with high accuracy. Table 5.2 is shown other samples of validation result for 10-generator 39-bus power system.

In Table 5.3, validation results of twelve 3-phase fault simulation cases are exhibited for 16 generator 68 bus power system. This system has 16 generators and 86 transmission lines. Bus no. 65 is taken as slack bus for this system. Bold values of the TSI represent that these are more than the stability boundary value (i.e. 1) and considered as unstable system operating scenarios.

In Table 5.4 validation results of eight 3-phase fault simulation cases are exhibited for 50 generator 145 bus large power system. This system has 50 generators and 453 transmission lines. Bus no. 145 is taken as slack bus for this system. The results of proposed TSI are compared with the predefine Rotor Trajectory Index (RTI) [199] for 50-generator 145-bus power system. The following conclusions can be drawn from the results shown in Tables 5.2, 5.3 and 5.4.

- Validation results are taken for three different small to large size of power systems.
- Bold faced values represent the unstable cases. As fault time increases, final value of the rotor angle of the generators increases, so accordingly values of TSI are also increasing.

TABLE 5.2: Validation of RBFNN for 10 Generator 39 Bus System

Faulted Bus	**Line Trip**			**Fault Duration**							
				0.2s	**0.19s**	**0.18s**	**0.17s**	**0.15s**	**0.13s**	**0.10s**	**0.08s**
26	26-28	$\Delta\delta_{COI}$		6868.3757	6789.0313	6677.5301	6587.5834	6538.4365	5928.3965	4388.5204	99.4900
		TDS	TSI	**1.9657**	**1.9653**	**1.9647**	**1.9642**	**1.9640**	**1.9603**	**1.9468**	0.9066
			t_{cr}	0.3	0.3	0.32	0.34	0.36	0.45	0.66	-
		RBFNN	TSI	**1.9657**	**1.9653**	**1.9647**	**1.9642**	**1.9640**	**1.9603**	**1.9468**	0.9066
			t_{cr}	0.3	0.3	0.32	0.34	0.36	0.45	0.66	-
1	1-2	$\Delta\delta_{COI}$		76.7031	76.0331	74.5554	73.0982	71.6626	67.4724	63.4625	60.9007
		TDS	TSI	0.7799	0.7757	0.7664	0.7571	0.7478	0.7198	0.6918	0.6733
			t_{cr}	-	-	-	-	-	-	-	-
		RBFNN	TSI	0.7799	0.7757	0.7664	0.7571	0.7478	0.7198	0.6918	0.6733
			t_{cr}	-	-	-	-	-	-	-	-
10	10-13	$\Delta\delta_{COI}$		1876.5154	1679.1253	1182.3090	108.9813	100.6634	82.5404	69.1256	62.6888
		TDS	TSI	**1.8798**	**1.8666**	**1.8157**	0.9519	0.9124	0.8151	0.7310	0.6863
			t_{cr}	0.47	0.50	0.64	-	-	-	-	-
		RBFNN	TSI	**1.8798**	**1.8666**	**1.8157**	0.9519	0.9124	0.8151	0.7310	0.6863
			t_{cr}	0.47	0.50	0.64	-	-	-	-	-
26	26-27	$\Delta\delta_{COI}$		6751.0253	6706.4219	6606.0261	6524.6319	6333.9943	5196.6723	105.5658	88.8525
		TDS	TSI	**1.9651**	**1.9648**	**1.9643**	**1.9639**	**1.9628**	**1.9549**	0.9360	0.8509
			t_{cr}	0.30	0.31	0.33	0.35	0.37	0.49	-	-
		RBFNN	TSI	**1.9651**	**1.9648**	**1.9643**	**1.9639**	**1.9628**	**1.9549**	0.9360	0.8509
			t_{cr}	0.30	0.31	0.33	0.35	0.37	0.49	-	-
11	11-10	$\Delta\delta_{COI}$		1590.6022	1489.9770	1173.8111	445.8569	105.9833	86.6269	73.3731	66.0079
		TDS	TSI	**1.8597**	**1.8509**	**1.8145**	**1.5759**	0.9380	0.8385	0.7589	0.7097
			t_{cr}	0.54	0.61	0.93	1.76	-	-	-	-
		RBFNN	TSI	**1.9002**	**1.8936**	**1.8662**	**1.8342**	**1.7530**	0.9235	0.8220	0.7558
			t_{cr}	0.54	0.61	0.93	1.76	-	-	-	-
15	15-14	$\Delta\delta_{COI}$		2284.0305	2135.9274	1673.2968	1327.2819	851.8398	102.9432	83.7361	72.8908
		TDS	TSI	**1.9028**	**1.8984**	**1.8868**	**1.8729**	**1.8518**	0.9221	0.8358	0.7816
			t_{cr}	0.56	0.58	0.61	0.66	0.72	-	-	-
		RBFNN	TSI	**1.9028**	**1.8984**	**1.8868**	**1.8729**	**1.8518**	0.9221	0.8358	0.7816
			t_{cr}	0.56	0.58	0.61	0.66	0.72	-	-	-
23	23-24	$\Delta\delta_{COI}$		2348.7140	2241.0926	1999.7930	1768.2721	1498.9728	102.6568	86.1467	76.9875
		TDS	TSI	**1.9144**	**1.9126**	**1.9084**	**1.9037**	**1.8984**	**1.8722**	**1.1176**	0.8638
			t_{cr}	0.35	0.36	0.39	0.43	0.49	-	-	-
		RBFNN	TSI	**1.9144**	**1.9126**	**1.9084**	**1.9037**	**1.8984**	**1.8722**	**1.1176**	0.8638
			t_{cr}	0.35	0.36	0.39	0.43	0.49	-	-	-
16	16-21	$\Delta\delta_{COI}$		2683.6445	2627.3948	2499.6986	2371.7772	2243.3410	1758.1365	151.9760	91.2287
		TDS	TSI	**1.9445**	**1.9438**	**1.9419**	**1.9374**	**1.9251**	**1.9162**	**1.8363**	**1.6776**
			t_{cr}	0.37	0.38	0.40	0.43	0.47	0.63	2.60	-
		RBFNN	TSI	**1.9445**	**1.9438**	**1.9419**	**1.9374**	**1.9251**	**1.9162**	**1.8363**	**1.6776**
			t_{cr}	0.37	0.38	0.40	0.43	0.47	0.63	2.60	-
21	21-22	$\Delta\delta_{COI}$		4201.2378	4149.8285	4009.9856	3711.1352	3082.4815	2742.7729	1345.8358	624.4026
		TDS	TSI	**1.9516**	**1.9510**	**1.9496**	**1.9480**	**1.9463**	**1.9392**	**1.9245**	**1.8968**
			t_{cr}	0.40	0.41	0.44	0.46	0.50	0.63	0.84	1.61
		RBFNN	TSI	**1.9516**	**1.9510**	**1.9496**	**1.9480**	**1.9463**	**1.9392**	**1.9245**	**1.8968**
			t_{cr}	0.40	0.41	0.44	0.46	0.50	0.63	0.84	1.61

TABLE 5.3: Validation of RBFNN for 16 Generator 68 Bus System

Faulted Bus	Line Trip			Fault Duration							
				0.2s	**0.19s**	**0.18s**	**0.17s**	**0.15s**	**0.13s**	**0.10s**	**0.08s**
1	1-2	$\Delta\delta_{COI}$		140.5938	97.9984	57.0529	45.7158	42.5461	35.1102	29.6074	26.7331
		TDS	TSI	**1.0790**	0.8991	0.6445	0.5517	0.5235	0.4527	0.3958	0.3644
			t_{cr}	2.92	-	-	-	-	-	-	-
		RBFNN	TSI	**1.0790**	0.8991	0.6445	0.5517	0.5235	0.4527	0.3958	0.3644
			t_{cr}	2.92	-	-	-	-	-	-	-
2	2-3	$\Delta\delta_{COI}$		550.1039	478.5804	127.7585	58.8519	55.4807	46.7603	39.3890	34.9710
		TDS	TSI	**1.6418**	**1.5991**	**1.0313**	0.6581	0.6323	0.5608	0.4943	0.4513
			t_{cr}	1.97	2.09	2.95	-	-	-	-	-
		RBFNN	TSI	**1.6418**	**1.5991**	**1.0313**	0.6581	0.6323	0.5608	0.4943	0.4513
			t_{cr}	1.97	2.09	2.95	-	-	-	-	-
3	3-4	$\Delta\delta_{COI}$		496.2599	403.8139	78.8826	50.9888	48.2174	40.7603	34.1494	30.0520
		TDS	TSI	**1.6106**	**1.5418**	0.7933	0.5964	0.5733	0.5071	0.4431	0.4006
			t_{cr}	1.97	2.16	-	-	-	-	-	-
		RBFNN	TSI	**1.6106**	**1.5418**	0.7933	0.5964	0.5733	0.5071	0.4431	0.4006
			t_{cr}	1.97	2.16	-	-	-	-	-	-
16	16-21	$\Delta\delta_{COI}$		1302.9898	1278.1314	1218.1421	1153.1635	1084.6288	845.2869	347.4556	52.7786
		TDS	TSI	**1.8313**	**1.8283**	**1.8206**	**1.8115**	**1.8008**	**1.7514**	**1.4866**	0.6109
			t_{cr}	0.77	0.79	0.84	0.9	0.98	1.32	2.29	-
		RBFNN	TSI	**1.8313**	**1.8283**	**1.8206**	**1.8115**	**1.8008**	**1.7514**	**1.4866**	0.6109
			t_{cr}	0.77	0.79	0.84	0.9	0.98	1.32	2.29	-
2	2-25	$\Delta\delta_{COI}$		2091.3002	2043.6280	2046.3803	1822.2056	1740.2696	1133.6961	298.4052	51.3435
		TDS	TSI	**1.8915**	**1.8891**	**1.8892**	**1.8764**	**1.8710**	**1.8086**	**1.4264**	0.5993
			t_{cr}	0.91	0.93	0.99	1.06	1.14	1.54	2.53	-
		RBFNN	TSI	**1.8915**	**1.8891**	**1.8892**	**1.8764**	**1.8710**	**1.8086**	**1.4264**	0.5993
			t_{cr}	0.91	0.93	0.99	1.06	1.14	1.54	2.53	-
41	41-40	$\Delta\delta_{COI}$		424.4145	422.6583	418.6192	414.7074	410.9022	399.9143	389.1017	381.6658
		TDS	TSI	**1.5592**	**1.5577**	**1.5544**	**1.5512**	**1.5479**	**1.5384**	**1.5286**	**1.5216**
			t_{cr}	0.96	0.97	1	1.03	1.06	1.16	1.26	1.32
		RBFNN	TSI	**1.5592**	**1.5577**	**1.5544**	**1.5512**	**1.5479**	**1.5384**	**1.5286**	**1.5216**
			t_{cr}	0.96	0.97	1	1.03	1.06	1.16	1.26	1.32
16	16-21	$\Delta\delta_{COI}$		1302.9898	1278.1314	1218.1421	1153.1635	1084.6288	845.2869	347.4556	52.7786
		TDS	TSI	**1.8313**	**1.8283**	**1.8206**	**1.8115**	**1.8008**	**1.7514**	**1.4866**	0.6109
			t_{cr}	0.77	0.79	0.84	0.9	0.98	1.32	2.29	-
		RBFNN	TSI	**1.8313**	**1.8283**	**1.8206**	**1.8115**	**1.8008**	**1.7514**	**1.4866**	0.6109
			t_{cr}	0.77	0.79	0.84	0.9	0.98	1.32	2.29	-
17	17-27	$\Delta\delta_{COI}$		967.6763	933.5432	821.9137	705.2774	530.4347	42.7556	34.7953	30.3601
		TDS	TSI	**1.7793**	**1.7722**	**1.7452**	**1.7092**	**1.6310**	0.5254	0.4496	0.4038
			t_{cr}	1.33	1.38	1.51	1.71	1.99	-	-	-
		RBFNN	TSI	**1.7793**	**1.7722**	**1.7452**	**1.7092**	**1.6310**	0.5254	0.4496	0.4038
			t_{cr}	1.33	1.38	1.51	1.71	1.99	-	-	-
6	6-7	$\Delta\delta_{COI}$		716.0124	657.7357	494.5285	247.3862	36.1956	22.7305	21.3072	20.2139
		TDS	TSI	**1.7129**	**1.6914**	**1.6095**	**1.3467**	0.4635	0.3185	0.3016	0.2883
			t_{cr}	1.63	1.75	1.99	2.55	-	-	-	-
		RBFNN	TSI	**1.7129**	**1.6914**	**1.6095**	**1.3467**	0.4635	0.3185	0.3016	0.2883
			t_{cr}	1.63	1.75	1.99	2.55	-	-	-	-
16	16-17	$\Delta\delta_{COI}$		2119.5177	2078.9901	1966.2547	1851.9994	1727.0409	1567.0138	933.7024	371.5190
		TDS	TSI	**1.8928**	**1.8909**	**1.8850**	**1.8783**	**1.8701**	**1.8577**	**1.7722**	**1.5117**
			t_{cr}	0.79	0.81	0.84	0.89	0.93	1.11	1.52	2.18
		RBFNN	TSI	**1.8928**	**1.8909**	**1.8850**	**1.8783**	**1.8701**	**1.8577**	**1.7722**	**1.5117**
			t_{cr}	0.79	0.81	0.84	0.89	0.93	1.11	1.52	2.18
6	6-11	$\Delta\delta_{COI}$		804.7924	757.3365	633.5803	489.7843	276.0723	23.4235	21.6277	20.5814
		TDS	TSI	**1.7405**	**1.7264**	**1.6815**	**1.6064**	**1.3940**	0.3266	0.3054	0.2928
			t_{cr}	1.49	1.56	1.77	2	2.49	-	-	-
		RBFNN	TSI	**1.7405**	**1.7264**	**1.6815**	**1.6064**	**1.3940**	0.3266	0.3054	0.2928
			t_{cr}	1.49	1.56	1.77	2	2.49	-	-	-
23	23-24	$\Delta\delta_{COI}$		1042.1528	1007.0655	918.0170	800.7383	677.7291	63.9766	24.2660	21.0804
		TDS	TSI	**1.7935**	**1.7871**	**1.7688**	**1.7393**	**1.6991**	0.6955	0.3364	0.2988
			t_{cr}	1.19	1.3	1.41	1.53	1.7	-	-	-
		RBFNN	TSI	**1.7935**	**1.7871**	**1.7688**	**1.7393**	**1.6991**	0.6955	0.3364	0.2988
			t_{cr}	1.19	1.3	1.41	1.53	1.7	-	-	-

TABLE 5.4: Validation of RBFNN for 50-Generator 145 Bus System

Contingency	Faulted Bus	Line Trip			Fault Duration 0.2s	0.19s	0.17s	0.15s	0.13s	0.10s	0.08s
-	12	12-13	$\Delta\delta_{COI}$		2188.5436	2128.5802	2574.1369	1604.5680	78.8749	79.7281	75.0774
			RTI [199]		1.7223	1.7135	1.7615	1.6652	**0.6098**	**0.5025**	0.4476
			TDS	TSI	**1.8980**	**1.8944**	**1.9136**	**1.8744**	0.7864	0.8001	0.7721
				t_{cr}	0.27	0.28	0.31	0.34	0.45	-	-
			RBFNN	TSI	**1.8980**	**1.8944**	**1.9136**	**1.8744**	0.7864	0.8001	0.7721
				t_{cr}	0.27	0.28	0.31	0.34	0.45	-	-
-	12	12-25	$\Delta\delta_{COI}$		2228.6108	2162.7646	2660.7237	1884.4057	76.0739	80.4512	75.9326
			RTI [199]		1.7219	1.7146	1.7616	1.6792	**0.6157**	**0.5059**	0.4504
			TDS	TSI	**1.8978**	**1.8949**	**1.9137**	**1.8803**	0.7760	0.8027	0.7751
				t_{cr}	0.27	0.27	0.31	0.33	0.43	1.01	-
			RBFNN	TSI	**1.8978**	**1.8949**	**1.9137**	**1.8803**	0.7760	0.8027	0.7751
				t_{cr}	0.27	0.27	0.31	0.33	0.43	1.01	-
-	14	14-16	$\Delta\delta_{COI}$		70.4598	71.8058	79.9185	80.5176	77.5328	72.8295	69.7868
			RTI [199]		**0.6441**	**0.6282**	**0.5664**	**0.5406**	0.4752	0.4209	0.3888
			TDS	TSI	0.7399	0.7487	0.7995	0.8031	0.7850	0.7554	0.7354
				t_{cr}	0.4	0.41	0.52	0.69	-	-	-
			RBFNN	TSI	0.7399	0.7487	0.7995	0.8031	0.7850	0.7554	0.7354
				t_{cr}	0.4	0.41	0.52	0.69	-	-	-
-	33	33-39	$\Delta\delta_{COI}$		80.5139	80.2122	78.3334	77.2337	73.7625	70.3893	68.2840
			RTI [199]		**0.5080**	**0.5014**	0.4722	0.4586	0.4206	0.3862	0.3646
			TDS	TSI	0.8031	0.8013	0.7899	0.7832	0.7614	0.7394	0.7253
				t_{cr}	0.85	0.93	-	-	-	-	-
			RBFNN	TSI	0.8031	0.8013	0.7899	0.7832	0.7614	0.7394	0.7253
				t_{cr}	0.85	0.93	-	-	-	-	-
N-1 Line 6-12	6	6-7	$\Delta\delta_{COI}$		83.0865	83.0069	82.2879	82.0701	81.8073	81.9486	82.0530
			RTI [199]		**0.5078**	**0.5045**	0.4882	0.4806	0.4598	0.4418	0.4310
			TDS	TSI	0.8182	0.8178	0.8136	0.8123	0.8107	0.8116	0.8122
				t_{cr}	0.7	0.72	-	-	-	-	-
			RBFNN	TSI	0.8182	0.8178	0.8136	0.8123	0.8107	0.8116	0.8122
				t_{cr}	0.7	0.72	-	-	-	-	-
N-2 Lines 25-27 & 67-97	6	6-7	$\Delta\delta_{COI}$		86.3749	86.2021	85.1305	84.7669	84.1389	83.9855	83.9250
			RTI [199]		**0.5227**	**0.5190**	**0.5010**	0.4927	0.4700	0.4503	0.4386
			TDS	TSI	0.8371	0.8361	0.8300	0.8279	0.8243	0.8234	0.8231
				t_{cr}	0.63	0.64	0.76	-	-	-	-
			RBFNN	TSI	0.8371	0.8361	0.8300	0.8279	0.8243	0.8234	0.8231
				t_{cr}	0.63	0.64	0.76	-	-	-	-
N-3 Lines 12-14; 33-50 & 67-97	6	6-7	$\Delta\delta_{COI}$		84.0297	83.9009	82.9847	82.6923	82.2565	82.2969	82.3578
			RTI [199]		**0.5180**	**0.5144**	0.4966	0.4884	0.4657	0.4462	0.4345
			TDS	TSI	0.8237	0.8230	0.8176	0.8159	0.8134	0.8136	0.8140
				t_{cr}	0.65	0.67	-	-	-	-	-
			RBFNN	TSI	0.8237	0.8230	0.8176	0.8159	0.8134	0.8136	0.8140
				t_{cr}	0.65	0.67	-	-	-	-	-
N-4 Lines 1-2; 1-6; 40-44 & 119-130	6	6-7	$\Delta\delta_{COI}$		90.4421	90.1063	88.3558	87.6975	86.2132	85.2444	84.7527
			RTI [199]		**0.5408**	**0.5366**	**0.5158**	**0.5062**	0.4795	0.4563	0.4423
			TDS	TSI	0.8595	0.8577	0.8481	0.8445	0.8362	0.8307	0.8279
				t_{cr}	0.6	0.61	0.69	0.74	-	-	-
			RBFNN	TSI	0.8595	0.8577	0.8481	0.8445	0.8362	0.8307	0.8279
				t_{cr}	0.6	0.61	0.69	0.74	-	-	-

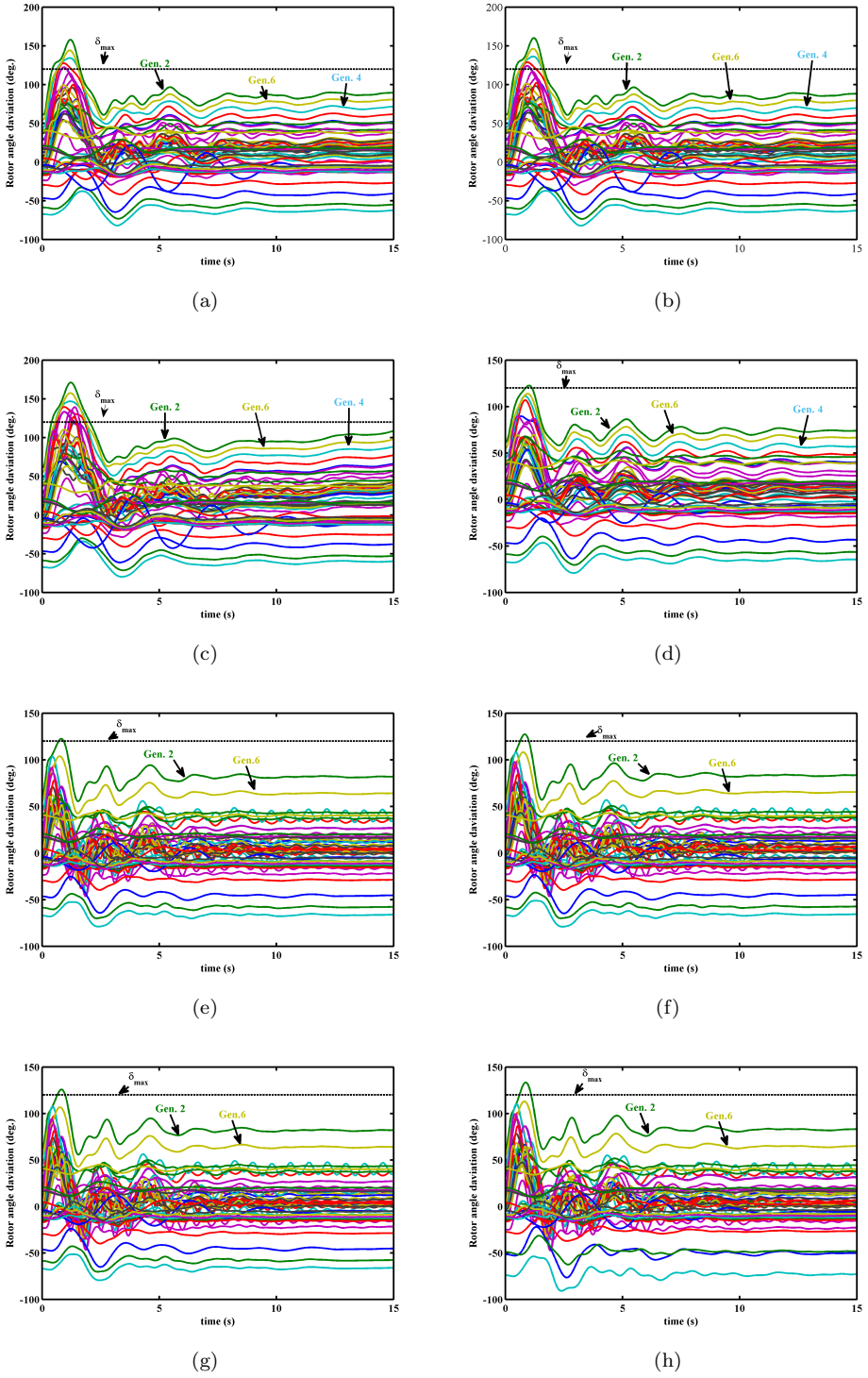

FIGURE 5.5: Rotor angle with respect to COI of applied contingencies (Table 5.4) for validation the RBFNN (50 Generator 145 Bus system)

- During long time fault scenario, system goes early "out of step" as compared to less time unstable scenario.
- Results obtained from the proposed RBFNN are almost same as results obtained from the TDS.
- For large 50-generator, 145-bus power system Table 5.4 shows the same cases as in Ref. [199] for comparison the proposed method with contemporary approach.
- For some operating conditions (Red colored in Table 5.4) classification results obtained from RTI and TSI are conflicting. For example first case in Table 5.4, is shown for base case loading condition and 3-phase fault at bus-12 simulated at different fault initiated times from 0.001s to 0.12s and cleared at 0.2s by opening the breakers to isolate line 12-13. For fault duration 0.13s the maximum value among all the generators of the system at the end of simulation is 78.8749^0, corresponding this value TSI is calculated as 0.7864 (< 1; i.e. stable) and value of RTI [199] is calculated 0.6098 (> 0.5; i.e. unstable). "Out of step" time t_{cr} is 0.45s for this case. It is observed from this investigation that due to disturbance, rotor angle of a generator or group of generators going out of step at time 0.45s, but TSI value is less then one (< 1), it means at the end of simulation all generators rotor angle are under the value of maximum permissible rotor angle limit(δ_{max}). So this case represent the first swing instability case [35]. For these type of cases RTI fails to identify the system health accurately.
- Graphical representation of the relative rotor angles curves for the grey highlighted cases (in Table 5.4) are also shown in Figure 5.5. However, these results are in favor of the proposed TSI prediction. To verify the stability, these cases are simulated for 15s and further system is found stable.

In the following section the robustness and effectiveness of proposed RBFNNs are evaluated by some unseen critical operating conditions.

5.5.4 Testing of proposed RBFNN

After validation, the trained RBFNNs are evaluated using 100 unseen operating scenarios for all three power systems. The test results prove the accuracy of trained RBFNNs prediction of stability status in the form of TSI and 'out of step' time for all tested fault scenarios. To demonstrate the effectiveness of the proposed method, six typical severe contingencies have been taken into consideration as described in Table 5.5 for studies.

5.5.4.1 10-Generator 39-Bus Power System

To exhibit the accuracy of the proposed technique three simulation results cases A, B and C out of 100 cases are selected randomly. Generator G-10 is considered as slack generator during simulations. A comparison between the proposed RBFNN and TDS is done for every operating case. Tables 5.6 , 5.9 and 5.12 exhibit the comparison of results for case-A, case-B and case-C respectively. These tables show the calculated TSI values as per the actual rotor angle deviation extracted from the TDS and TSI values predicted from RBFNN for comparison. Stability status, rank and coherent group of individual generator can be obtained by using the predicted TSI. After the evaluation of these simulation cases, the control action can be initiated to achieve stability.

Case-A: 3-phase fault at bus 25 cleared by opening the line 25-26 at 96.13% load of base case

Case-A is shown for 96.13% random load variation and three-phase fault at bus-25 initiated at 0.06s and cleared at 0.2s by opening the breakers to isolate line 25-26.

TABLE 5.5: Applied credible contingencies for testing of the proposed RBFNN

Power System	Case	Fault Type	Location of Fault	Tripped Line	Fault Duration	System Load
10 Generator 39 Bus	Case A	3-phase fault	Bus 25	Line 25-26	8 cycles	96.13%
	Case B	3-phase fault	Bus 28	Line 28-29	9 cycles	98.65%
	Case C	3-phase fault	Bus 2	Line 2-25	10 cycles	105.45%
16 Generator 68 Bus	Case D	3-phase fault	Bus 16	Line 16-19	10 cycles	98.09%
	Case E	3-phase fault	Bus 26	Line 26-28	11 cycles	101.58%
50 Generator 145 Bus	Case F	3-phase fault	Bus 66	Line 66-111	9 cycles	102.71%

TABLE 5.6: Comparison of results obtained from RBFNN with TDS results for Case A

Generator Number	**Actual (from TDS)**			**Predicted (from RBFNN)**		**Error**
	$\Delta\delta_{COI}$ **(deg.)**	**TSI**	t_{cr} **(s)**	t_{cr} **(s)**	**TSI**	
G-1	-0.4639254	-0.0078	1.15s	1.12s	-0.0077	-0.0001
G-2	289.52215	1.4140			1.4406	-0.0266
G-3	282.43238	1.4036			1.4293	-0.0257
G-4	298.21439	1.4261			1.4253	0.0008
G-5	281.26626	1.4019			1.4187	-0.0168
G-6	270.50497	1.3854			1.3656	0.0198
G-7	290.46514	1.4153			1.4109	0.0044
G-8	252.60779	1.3559			1.3784	-0.0225
G-9	1393.141	1.8414			1.8629	-0.0215

The state of T/S for all generators is determined by observing rotor angle swings in the time interval. As per Tables 5.6 and 5.7, the rotor angle deviation value of G-9 is 1393.141^0 and corresponding to this value, TSI is calculated as 1.8414. The predicted value of TSI for G-9 by proposed RBFNN is 1.8629 with -0.0215 error. Since this value is the largest as compared to predicted TSI of other generators, it is considered as the most advanced generator and holds the top rank in generator criticality list.

The generator G-1 which possesses minimum value of TSI, is considered as the least advanced generator and holds bottom rank in the generator criticality list. According to the predicted TSI, 3 coherent groups are formed. The difference of TSI values of any two generators are exhibited in Table 5.8. Bold and normal text represents the difference between stable and unstable generators. TSI difference of generators G-2, G-3, G-4, G-5, G-6, G-7 and G-8 fall in a narrow range and differ considerably from G-1 and G-9, hence generators G-1 and G-9 are assigned to different groups while generators G-2, G-3, G-4, G-5, G-6, G-7 and G-8 are assigned to a single group. For verifying the results obtained from proposed RBFNN, rotor angle trajectories are obtained from TDS.

Figure 5.6 shows relative rotor angle of all the generators with respect to COI. As per this figure the rotor swing of G-9 rises above the threshold value causing it to lose synchronism. This generator is going out of step with the rest of the generators creating the whole system transiently unstable. The predicted value of critical time

TABLE 5.7: Real time transient stability state and coherency identification of system for Case A

Generator	TSI	Gen. Stability Status		Rank	Coherent Group	System Status	Control Action (PG)
G-1	-0.0077	0	Stable	9	1		Generation Increasing
G-2	1.4406	1	Unstable	2	2	Unstable	-
G-3	1.4293	1	Unstable	3	2		-
G-4	1.4253	1	Unstable	4	2		-
G-5	1.4187	1	Unstable	5	2		-
G-6	1.3656	1	Unstable	8	2		-
G-7	1.4109	1	Unstable	6	2		-
G-8	1.3784	1	Unstable	7	2		-
G-9	1.8629	1	Unstable	1	3		Generation Decreasing

TABLE 5.8: Coherent group identification Case A (10-Generator 39-Bus System)

Generator Number	G-1	G-2	G-3	G-4	G-5	G-6	G-7	G-8	G-9
G-1	0.00	1.45	1.44	1.43	1.43	1.37	1.42	1.39	1.87
G-2	1.45	**0.00**	**0.01**	**0.02**	**0.02**	**0.08**	**0.03**	**0.06**	**0.42**
G-3	1.44	**0.01**	**0.00**	**0.00**	**0.01**	**0.06**	**0.02**	**0.05**	**0.43**
G-4	1.43	**0.02**	**0.00**	**0.00**	**0.01**	**0.06**	**0.01**	**0.05**	**0.44**
G-5	1.43	**0.02**	**0.01**	**0.01**	**0.00**	**0.05**	**0.01**	**0.04**	**0.44**
G-6	1.37	**0.08**	**0.06**	**0.06**	**0.05**	**0.00**	**0.05**	**0.01**	**0.50**
G-7	1.42	**0.03**	**0.02**	**0.01**	**0.01**	**0.05**	**0.00**	**0.03**	**0.45**
G-8	1.39	**0.06**	**0.05**	**0.05**	**0.04**	**0.01**	**0.03**	**0.00**	**0.48**
G-9	1.87	**0.42**	**0.43**	**0.44**	**0.44**	**0.50**	**0.45**	**0.48**	**0.00**

by RBFNN for generator G-9 is same as observed from the TDS results. To make the system stable for this case, the proposed method suggests rescheduling of the generating units as preventive control action show in Table 5.6.

Case-B: 3-phase fault at bus 28 cleared by opening the line 28-29 at 98.65% load of base case

Case-B is shown for 98.65% random load variation and three-phase fault at bus-28 initiated at 0.05s and cleared at 0.2s by opening the breakers to isolate line 28-29. The state of T/S for all the generators is determined by observing rotor angle swings in the time interval. Tables 5.9 and 5.19 show the rotor angle deviation value of G-9 is 7785.094^0 and corresponding to this value, TSI is calculated as 1.9696.

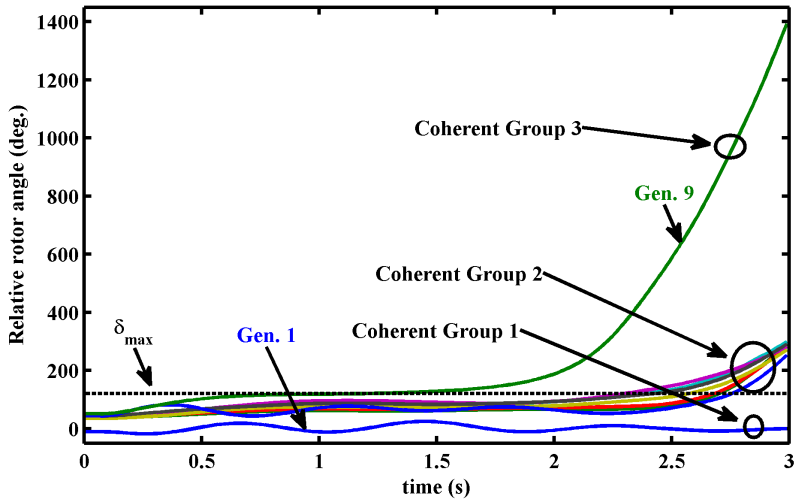

FIGURE 5.6: Rotor angle trajectories with respect to COI for testing the RBFNN (Case A)

TABLE 5.9: Comparison of results obtained from RBFNN with TDS results for Case B

Generator Number	Actual (from TDS)			Predicted (from RBFNN)		Error
	$\Delta\delta_{COI}$ (deg.)	TSI	t_{cr} (s)	t_{cr} (s)	TSI	
G-1	-356.5579	-1.0146	0.35s	0.35s	-1.0229	0.0084
G-2	-296.0258	-1.3634			-1.4596	0.0961
G-3	-289.2804	-1.4178			-1.4051	-0.0127
G-4	-269.8961	-1.6011			-1.5720	-0.0291
G-5	-258.9550	-1.7272			-1.6821	-0.0451
G-6	-284.5444	-1.4586			-1.4774	0.0189
G-7	-272.0028	-1.5789			-1.5912	0.0123
G-8	-294.2849	-1.3771			-1.4083	0.0312
G-9	7785.0943	1.9696			1.9854	-0.0158

The predicted value of TSI for G-9 by the proposed RBFNN is 1.9854 with -0.0158 error and considered as the most advanced generator and this generator holds the first rank in generator criticality list. The generator G-5 which possesses minimum value of TSI, is considered as least advanced generator and holds bottom rank in the generator criticality list. According to the predicted TSI, two coherent groups are formed as per Table 5.11. For verifying the results obtained from proposed RBFNN, rotor angle trajectories are obtained from TDS. Figure 5.7 shows relative rotor angle of all the generators with respect to COI. As per this figure the rotor

TABLE 5.10: Real time transient stability state and coherency identification of system for Case B

Generator	TSI	Gen. Stability Status		Rank	Coherent Group	System Status	Control Action (PG)
G-1	-1.0229	0	Stable	2	1		-
G-2	-1.4596	0	Stable	3	1		-
G-3	-1.4051	0	Stable	5	1		-
G-4	-1.5720	0	Stable	7	1		-
G-5	-1.6821	0	Stable	9	1		Generation Increasing
G-6	-1.4774	0	Stable	6	1		-
G-7	-1.5912	0	Stable	8	1		-
G-8	-1.4083	0	Stable	4	1		-
G-9	1.9854	1	Unstable	1	2		Generation Decreasing

TABLE 5.11: Coherent group identification Case B (10-Generator 39-Bus System)

Generator Number	G-1	G-2	G-3	G-4	G-5	G-6	G-7	G-8	G-9
G-1	**0.00**	**0.44**	**0.38**	**0.55**	**0.66**	**0.45**	**0.57**	**0.39**	3.01
G-2	**0.44**	**0.00**	**0.05**	**0.11**	**0.22**	**0.02**	**0.13**	**0.05**	3.44
G-3	**0.38**	**0.05**	**0.00**	**0.17**	**0.28**	**0.07**	**0.19**	**0.00**	3.39
G-4	**0.55**	**0.11**	**0.17**	**0.00**	**0.11**	**0.09**	**0.02**	**0.16**	3.56
G-5	**0.66**	**0.22**	**0.28**	**0.11**	**0.00**	**0.20**	**0.09**	**0.27**	3.67
G-6	**0.45**	**0.02**	**0.07**	**0.09**	**0.20**	**0.00**	**0.11**	**0.07**	3.46
G-7	**0.57**	**0.13**	**0.19**	**0.02**	**0.09**	**0.11**	**0.00**	**0.18**	3.58
G-8	**0.39**	**0.05**	**0.00**	**0.16**	**0.27**	**0.07**	**0.18**	**0.00**	3.39
G-9	3.01	3.44	3.39	3.56	3.67	3.46	3.58	3.39	0.00

swing of G-9 rises above the threshold value causing it to lose synchronism. This generator is going out of step with the rest of the generators creating the whole system transiently unstable.

Case-C: 3-phase fault at bus 2 cleared by opening the line 2-25 at 105.45% load of base case

Case-C is shown for 105.45% random load variation and three-phase fault at bus-2 initiated at 0.033s and cleared at 0.2s by opening the breakers to isolate line 2-25. The state of T/S for all generators is determined by observing rotor angle swings in the time interval. Tables 5.12 and 5.13 show the rotor angle deviation value of G-9 is 3587.0864^0 and corresponding to this value, TSI is calculated as 1.9351. The

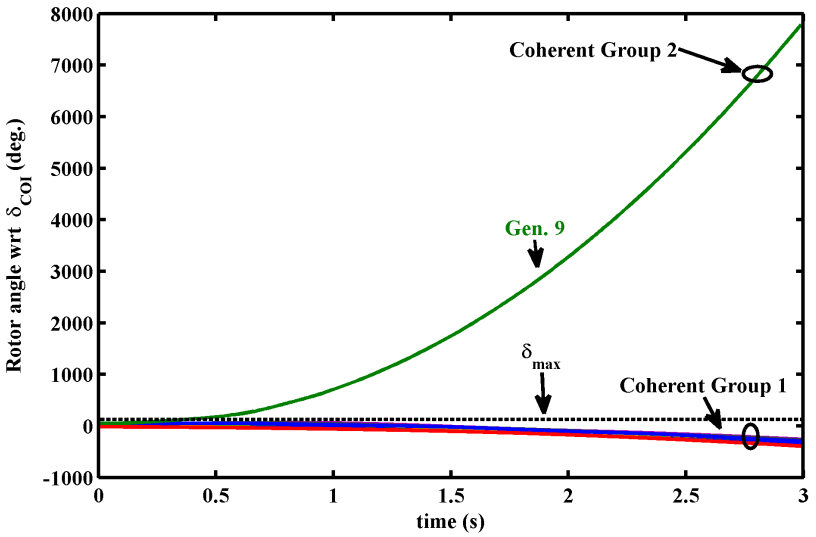

FIGURE 5.7: Rotor angle trajectories with respect to COI for testing the RBFNN (Case B)

predicted value of TSI for G-9 by the proposed RBFNN is 1.931 with 0.0041 error. Since this value is the largest as compared to predicted TSI of other generators and hence G-9 is considered as the most advanced generator and holds the top rank in generator criticality list. The generator G-1 which possesses minimum value of TSI, is considered as the least advanced generator and holds bottom rank in the generator criticality list. According to the predicted TSI, three coherent groups are formed. The difference of TSI values of any two generators are exhibited in Table 5.14. TSI difference of generators G-2, G-3, G-4, G-5, G-6 and G-7 fall in a narrow range and hence are assigned in a single group. TSI difference between G-8 and G-9 is also very small so both are assigned in the same group. G-1 is a single member of a another group.

For verifying the results obtained from proposed RBFNN, rotor angle trajectories are obtained from TDS. Figure 5.8 shows relative rotor angle of all the generators with respect to COI. As per this figure the rotor swing of G-8 and G-9 rise above the threshold value causing them to lose synchronism. These generators are going out of step with the rest of the generators creating the whole system transiently unstable.

Inspecting the results of unseen test cases of 10-generator 39-bus power system, RBFNN shows promising results

TABLE 5.12: Comparison of results obtained from RBFNN with TDS results for Case C

Generator Number	Actual (from TDS)			Predicted (from RBFNN)		Error
	$\Delta\delta_{COI}$ (deg.)	TSI	t_{cr} (s)	t_{cr} (s)	TSI	
G-1	-830.69873	-0.3377	0.66s	0.68s	-0.3330	-0.0047
G-2	1483.3509	1.8503			1.8324	0.0179
G-3	1475.9222	1.8496			1.8563	-0.0067
G-4	1437.6333	1.8459			1.8278	0.0181
G-5	1418.6196	1.8440			1.8488	-0.0047
G-6	1414.9456	1.8436			1.8247	0.0189
G-7	1432.5759	1.8454			1.8088	0.0366
G-8	3549.0626	1.9346			1.9230	0.0116
G-9	3578.0864	1.9351			1.9310	0.0041

TABLE 5.13: Real time transient stability state and coherency identification of system for Case C

Generator	TSI	Gen. Stability Status		Rank	Coherent Group	System Status	Control Action (PG)
G-1	-0.3330	0	Stable	9	1		Generation Increasing
G-2	1.8324	1	Unstable	5	2	Unstable	-
G-3	1.8563	1	Unstable	3	2		-
G-4	1.8278	1	Unstable	6	2		-
G-5	1.8488	1	Unstable	4	2		-
G-6	1.8247	1	Unstable	7	2		-
G-7	1.8088	1	Unstable	8	2		-
G-8	1.9230	1	Unstable	2	3		-
G-9	1.9310	1	Unstable	1	3		Generation Decreasing

TABLE 5.14: Coherent group identification Case C (10-Generator 39-Bus System)

Generator Number	G-1	G-2	G-3	G-4	G-5	G-6	G-7	G-8	G-9
G-1	0.00	2.17	2.19	2.16	2.18	2.16	2.14	2.26	2.26
G-2	2.17	**0.00**	**0.02**	**0.00**	**0.02**	**0.01**	**0.02**	**0.09**	**0.10**
G-3	2.19	**0.02**	**0.00**	**0.03**	**0.01**	**0.03**	**0.05**	**0.07**	**0.07**
G-4	2.16	**0.00**	**0.03**	**0.00**	**0.02**	**0.00**	**0.02**	**0.10**	**0.10**
G-5	2.18	**0.02**	**0.01**	**0.02**	**0.00**	**0.02**	**0.04**	**0.07**	**0.08**
G-6	2.16	**0.01**	**0.03**	**0.00**	**0.02**	**0.00**	**0.02**	**0.10**	**0.11**
G-7	2.14	**0.02**	**0.05**	**0.02**	**0.04**	**0.02**	**0.00**	**0.11**	**0.12**
G-8	2.26	**0.09**	**0.07**	**0.10**	**0.07**	**0.10**	**0.11**	**0.00**	**0.01**
G-9	2.26	**0.10**	**0.07**	**0.10**	**0.08**	**0.11**	**0.12**	**0.01**	**0.00**

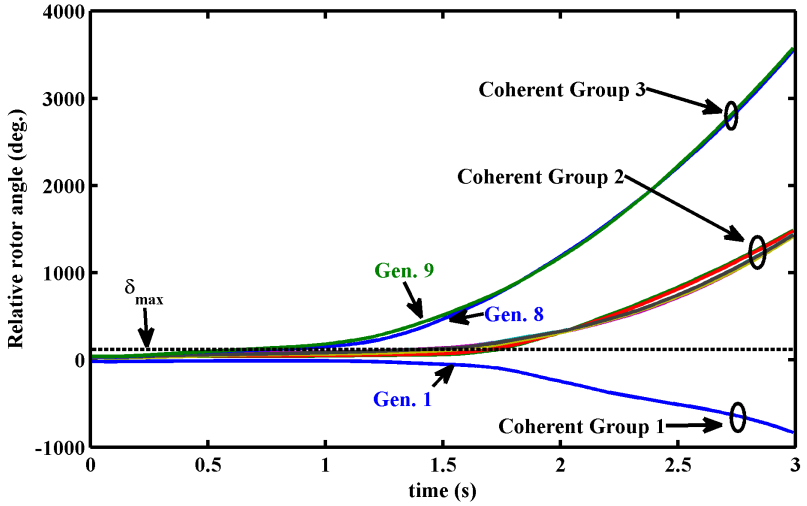

FIGURE 5.8: Rotor angle trajectories with respect to COI for testing the RBFNN (Case C)

5.5.4.2 16-Generator 68-Bus Power System

To exhibit the accuracy of the proposed technique two simulation results out of 100 cases are opted randomly. Generator G-13 is considered as slack generator during simulations. The particulars of the simulation are given in Table 5.5. A comparison between the proposed RBFNN and TDS is done for every operating case. Tables 5.15 and 5.18 show the comparison result of case-D and case-E respectively.

Case-D: 3-phase fault at bus 16 cleared by opening the line 16-19 at 98.09% load of base case

Case-D is shown for 98.09% random load variation and three-phase fault at bus-16 initiated at 0.03s and cleared at 0.2s by opening the breakers to isolate line 16-19. The state of T/S for all generators is determined by observing rotor angle swings with respect to COI in the time interval. As per Tables 5.15 and 5.16, the rotor angle deviation value of G-9 is 3587.0864^0 and corresponding to this value, TSI is calculated as 1.9351. Proposed RBFNN predicts the TSI value for G-9 to be 1.931 with 0.0041 error. Since this value is the highest as compared to predicted TSI of other generators. It is considered as the most advanced generator and this generator holds the top rank in generator criticality list. The generator G-1 which possesses

minimum value of TSI, is considered as least advanced generator and assigned the bottom rank in the generator criticality list.

According to the predicted TSI, three coherent groups are formed as shown in Table 5.17. As per Table 5.17, TSI difference of generators G-1, G-2, G-3, G-4, G-5, G-6, G-7 & G-8 and generators G-10, G-11, G-12, G-14, G-15 & G-16 fall in a narrow range. hence these generators are assigned in two different groups respectively. Generator G-9 is a single member of another group. For verifying the results obtained from the proposed RBFNN, rotor angle trajectories are obtained from TDS. Figure 5.9 shows relative rotor angle of all the generators with respect to COI. As per this figure, the rotor swing of G-9 rises above the threshold value causing it to lose synchronism. This generator is going out of step with the rest of the generators creating the whole system transiently unstable.

TABLE 5.15: Comparison of results obtained from RBFNN with TDS results for Case D

Generator	**Actual (from TDS)**			**Predicted (from RBFNN)**		**Error**
Number	$\Delta\delta_{COI}$ **(deg.)**	**TSI**	t_{cr} **(s)**	t_{cr} **(s)**	**TSI**	
G-1	449.74906	1.5788	0.39	0.36	1.5720	0.0068
G-2	399.12219	1.5377			1.5215	0.0162
G-3	416.89244	1.5530			1.5247	0.0283
G-4	412.64503	1.5494			1.5259	0.0235
G-5	381.09065	1.5210			1.5198	0.0012
G-6	390.32984	1.5297			1.5040	0.0257
G-7	402.89754	1.5410			1.5369	0.0041
G-8	417.15404	1.5532			1.5397	0.0135
G-9	5704.635	1.9588			1.9982	-0.0394
G-10	35.400151	0.4556			0.4563	-0.0007
G-11	53.144779	0.6139			0.6073	0.0066
G-12	36.029549	0.4618			0.4536	0.0082
G-14	0.2296741	0.0038			0.0037	0.0001
G-15	-26.129243	-0.5567			-0.5324	-0.0243
G-16	5.9748284	0.0949			0.0955	-0.0007

TABLE 5.16: Real time transient stability state and coherency identification of system for Case D

Generator	TSI	Gen. Stability Status		Rank	Coherent Group	System Status	Control Action (PG)
G-1	1.5720	1	Unstable	2	2		-
G-2	1.5215	1	Unstable	7	2		-
G-3	1.5247	1	Unstable	6	2		-
G-4	1.5259	1	Unstable	5	2		-
G-5	1.5198	1	Unstable	8	2		-
G-6	1.5040	1	Unstable	9	2		-
G-7	1.5369	1	Unstable	4	2		-
G-8	1.5397	1	Unstable	3	2	Unstable	-
G-9	1.9982	1	Unstable	1	3		Generation Decreasing
G-10	0.4563	0	Stable	11	1		-
G-11	0.6073	0	Stable	10	1		-
G-12	0.4536	0	Stable	12	1		-
G-14	0.0037	0	Stable	14	1		-
G-15	-0.5324	0	Stable	15	1		Generation Increasing
G-16	0.0955	0	Stable	13	1		-

TABLE 5.17: Coherent group identification Case D (16 Generator 68 Bus System)

Generator Number	G-1	G-2	G-3	G-4	G-5	G-6	G-7	G-8	G-9	G-10	G-11	G-12	G-14	G-15	G-16
G-1	**0.00**	**0.05**	**0.05**	**0.05**	**0.05**	**0.07**	**0.04**	**0.03**	**0.43**	1.12	0.96	1.12	1.57	2.10	1.48
G-2	**0.05**	**0.00**	**0.00**	**0.00**	**0.00**	**0.02**	**0.02**	**0.02**	**0.48**	1.07	0.91	1.07	1.52	2.05	1.43
G-3	**0.05**	**0.00**	**0.00**	**0.00**	**0.00**	**0.02**	**0.01**	**0.02**	**0.47**	1.07	0.92	1.07	1.52	2.06	1.43
G-4	**0.05**	**0.00**	**0.00**	**0.00**	**0.01**	**0.02**	**0.01**	**0.01**	**0.47**	1.07	0.92	1.07	1.52	2.06	1.43
G-5	**0.05**	**0.00**	**0.00**	**0.01**	**0.00**	**0.02**	**0.02**	**0.02**	**0.48**	1.06	0.91	1.07	1.52	2.05	1.42
G-6	**0.07**	**0.02**	**0.02**	**0.02**	**0.02**	**0.00**	**0.03**	**0.04**	**0.49**	1.05	0.90	1.05	1.50	2.04	1.41
G-7	**0.04**	**0.02**	**0.01**	**0.01**	**0.02**	**0.03**	**0.00**	**0.00**	**0.46**	1.08	0.93	1.08	1.53	2.07	1.44
G-8	**0.03**	**0.02**	**0.02**	**0.01**	**0.02**	**0.04**	**0.00**	**0.00**	**0.46**	1.08	0.93	1.09	1.54	2.07	1.44
G-9	**0.43**	**0.48**	**0.47**	**0.47**	**0.48**	**0.49**	**0.46**	**0.46**	**0.00**	1.54	1.39	1.54	1.99	2.53	1.90
G-10	1.12	1.07	1.07	1.07	1.06	1.05	1.08	1.08	1.54	0.00	0.15	0.00	0.45	0.99	0.36
G-11	0.96	0.91	0.92	0.92	0.91	0.90	0.93	0.93	1.39	0.15	0.00	0.15	0.60	1.14	0.51
G-12	1.12	1.07	1.07	1.07	1.07	1.05	1.08	1.09	1.54	0.00	0.15	0.00	0.45	0.99	0.36
G-14	1.57	1.52	1.52	1.52	1.52	1.50	1.53	1.54	1.99	0.45	0.60	0.45	0.00	0.54	0.09
G-15	2.10	2.05	2.06	2.06	2.05	2.04	2.07	2.07	2.53	0.99	1.14	0.99	0.54	0.00	0.63
G-16	1.48	1.43	1.43	1.43	1.42	1.41	1.44	1.44	1.90	0.36	0.51	0.36	0.09	0.63	0.00

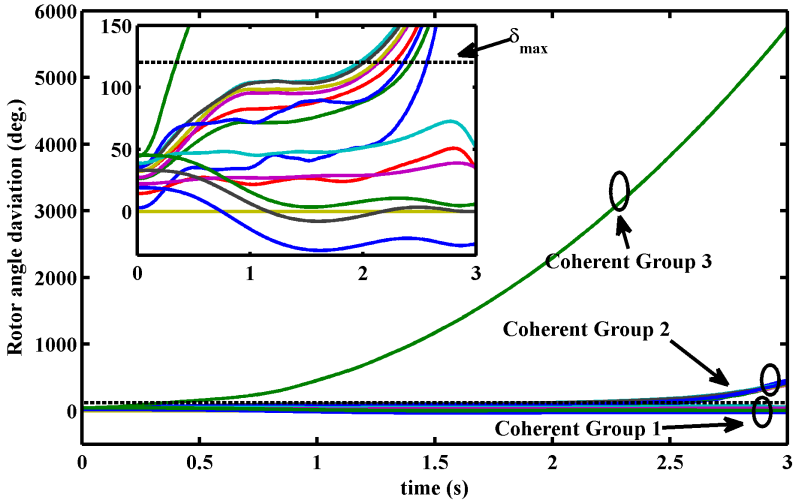

FIGURE 5.9: Rotor angle trajectories with Respect to COI for Testing the RBFNN (Case D)

Case-E: 3-phase fault at bus 26 cleared by opening the line 26-28 at 101.58% load of base case

Case-E is shown for 101.58% random load variation and three-phase fault at bus-26 initiated at 0.016s and cleared at 0.2s by opening the breakers to isolate line 26-28. The state of T/S for all generators is determined by observing rotor angle swings in the time interval. As per Tables 5.18 and 5.19, the rotor angle deviation value of G-4 is 3193.1033^0 and corresponding to this value, TSI is calculated as 1.9276. The predicted values of TSI for G-4 by Proposed RBFNN is 1.9120 with 0.0155 error. Since this value is the highest as compared to predicted TSI of other generators and hence G-4 is considered as the most advanced generator and holds the top rank in generator criticality list. The generator G-1 which possesses minimum value of TSI, is considered as the least advanced generator and holds bottom rank in the generator criticality list. According to the predicted TSI, two coherent groups are formed as shown in Table 5.20. As per Table 5.20, TSI difference of generators G-1, G-2, G-3, G-6, G-7, G-8, G-9, G-10, G-11, G-12, G-14, G-15 and G-16 falls in a narrow range and are assigned in a single group. Generators G-4 and G-5 show similar behavior and form a different coherent group.

For verifying the results obtained from proposed RBFNN, rotor angle trajectories are obtained from TDS. Figure 5.10 shows relative rotor angle of all the generators

TABLE 5.18: Comparison of results obtained from RBFNN with TDS results for Case E

Generator Number	Actual (from TDS)			Predicted (from RBFNN)		Error
	$\Delta\delta_{COI}$ (deg.)	TSI	t_{cr} (s)	t_{cr} (s)	TSI	
G-1	16.114969	0.2368	0.37s	0.45s	0.2359	0.0009
G-2	44.079747	0.5373			0.5371	0.0002
G-3	51.502401	0.6006			0.5902	0.0104
G-4	3193.1033	1.9276			1.9120	0.0155
G-5	3182.5211	1.9273			1.9078	0.0195
G-6	47.738578	0.5692			0.5580	0.0112
G-7	52.372944	0.6077			0.5998	0.0079
G-8	51.625608	0.6016			0.5916	0.0100
G-9	64.030763	0.6959			0.6936	0.0023
G-10	25.942528	0.3555			0.3507	0.0048
G-11	49.168546	0.5813			0.5761	0.0052
G-12	29.832123	0.3982			0.3916	0.0066
G-14	45.456811	0.5495			0.5415	0.0080
G-15	30.66806	0.4071			0.4045	0.0026
G-16	55.512377	0.6326			0.6291	0.0035

TABLE 5.19: Real time transient stability state and coherency identification of system for Case E

Generator	TSI	Gen. Stability Status		Rank	Coherent Group	System Status	Control Action (PG)
G-1	0.2359	0	Stable	15	1		Generation Increasing
G-2	0.5371	0	Stable	11	1		-
G-3	0.5902	0	Stable	7	1		-
G-4	1.9120	1	Unstable	1	2		Generation Decreasing
G-5	1.9078	1	Unstable	2	2	Unstable	-
G-6	0.5580	0	Stable	9	1		-
G-7	0.5998	0	Stable	5	1		-
G-8	0.5916	0	Stable	6	1		-
G-9	0.6936	0	Stable	3	1		-
G-10	0.3507	0	Stable	14	1		-
G-11	0.5761	0	Stable	8	1		-
G-12	0.3916	0	Stable	13	1		-
G-14	0.5415	0	Stable	10	1		-
G-15	0.4045	0	Stable	12	1		-
G-16	0.6291	0	Stable	4	1		-

TABLE 5.20: Coherent group identification Case E (16 Generator 68 Bus System)

Generator Number	G-1	G-2	G-3	G-4	G-5	G-6	G-7	G-8	G-9	G-10	G-11	G-12	G-14	G-15	G-16
G-1	0.00	0.30	0.35	1.68	1.67	0.32	0.36	0.36	0.46	0.11	0.34	0.16	0.31	0.17	0.39
G-2	0.30	0.00	0.05	1.37	1.37	0.02	0.06	0.05	0.16	0.19	0.04	0.15	0.00	0.13	0.09
G-3	0.35	0.05	0.00	1.32	1.32	0.03	0.01	0.00	0.10	0.24	0.01	0.20	0.05	0.19	0.04
G-4	1.68	1.37	1.32	0.00	0.00	1.35	1.31	1.32	1.22	1.56	1.34	1.52	1.37	1.51	1.28
G-5	1.67	1.37	1.32	0.00	0.00	1.35	1.31	1.32	1.21	1.56	1.33	1.52	1.37	1.50	1.28
G-6	0.32	0.02	0.03	1.35	1.35	0.00	0.04	0.03	0.14	0.21	0.02	0.17	0.02	0.15	0.07
G-7	0.36	0.06	0.01	1.31	1.31	0.04	0.00	0.01	0.09	0.25	0.02	0.21	0.06	0.20	0.03
G-8	0.36	0.05	0.00	1.32	1.32	0.03	0.01	0.00	0.10	0.24	0.02	0.20	0.05	0.19	0.04
G-9	0.46	0.16	0.10	1.22	1.21	0.14	0.09	0.10	0.00	0.34	0.12	0.30	0.15	0.29	0.06
G-10	0.11	0.19	0.24	1.56	1.56	0.21	0.25	0.24	0.34	0.00	0.23	0.04	0.19	0.05	0.28
G-11	0.34	0.04	0.01	1.34	1.33	0.02	0.02	0.02	0.12	0.23	0.00	0.18	0.03	0.17	0.05
G-12	0.16	0.15	0.20	1.52	1.52	0.17	0.21	0.20	0.30	0.04	0.18	0.00	0.15	0.01	0.24
G-14	0.31	0.00	0.05	1.37	1.37	0.02	0.06	0.05	0.15	0.19	0.03	0.15	0.00	0.14	0.09
G-15	0.17	0.13	0.19	1.51	1.50	0.15	0.20	0.19	0.29	0.05	0.17	0.01	0.14	0.00	0.22
G-16	0.39	0.09	0.04	1.28	1.28	0.07	0.03	0.04	0.06	0.28	0.05	0.24	0.09	0.22	0.00

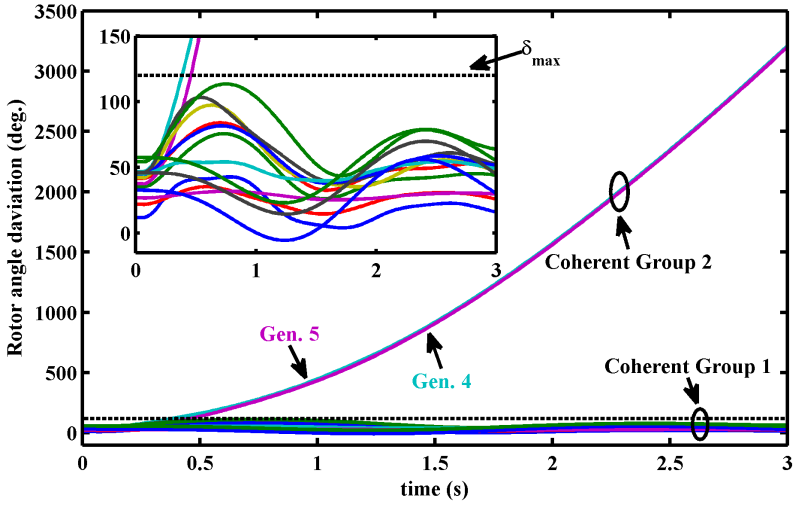

FIGURE 5.10: Rotor angle trajectories with respect to COI for Testing the RBFNN (Case E)

with respect to COI. This figure clearly shows that the rotor swing of G-4 and G-5 rise above the threshold value causing them to lose synchronism. These generators are going out of step with the rest of the generators creating the whole system transiently unstable. Inspecting the results of unseen test cases on 16-generator 68-bus power system, RBFNN shows promising results.

5.5.4.3 50-Generator 145-Bus Power System

To exhibit the accuracy of the proposed technique, one simulation result out of 100 cases is opted randomly. Generator G-50 is considered as slack generator during simulations. System reliability is a major concern for the system operator in case of a large power system. Information about the generator stability status helps, the operator to initiate the preventive control action under a severe contingency. Due to presence of large number of generators in this network, proposed TSI is mainly concern for collective generator behavior rather than the individual. Simulation time is taken 5s for 50-generator 145-bus power system study [35].

Case-F: 3-phase fault at bus 66 cleared by opening the line 66-111 at 102.71% load of base case

Case-F is shown for 102.71% random load variation and three-phase fault on bus-66 initiated at 0.05s and cleared at 0.2s by opening the breakers to isolate line 66-111. The state of T/S for all generators is determined by observing rotor angle swings in the time interval. Table 5.21 shows the comparison results of case-F. This table shows the calculated TSI values as per the actual rotor angle deviation extracted from the TDS and TSI values predicted from RBFNN for comparison. Stability status and coherent groups can be obtained by using the predicted TSI.

As per Table 5.22, A total of 29 generators are found to be unstable as per the predicted value of TSI by the proposed method. The rotor angle deviation with respect to COI of G-11 & G-13 are 6626.4578^0 & 6815.5048^0 respectively and corresponding to these values, TSI is calculated as 1.9644 & 1.9654 respectively. These values are more than other generators' TSI values, which causes, all the remaining generators to lose synchronism. The generators can be broadly classified into two coherent groups as per Table 5.23. For verifying the results obtained from proposed RBFNN, rotor angle trajectories are obtained from TDS. Figure 5.11 shows relative rotor angles of all the generators with respect to COI. As per this figure, the rotor swing of G-11 and G-13 rise above the threshold value causing them to lose synchronism. These generators are going out of step with the rest of the generators creating the whole system transiently unstable.

TABLE 5.21: Comparison of results obtained from RBFNN with TDS results for Case F

Generator Number	Actual (from TDS)			Predicted (from RBFNN)		Error
	$\Delta\delta_{COI}$ (deg.)	TSI	t_{cr} (s)	t_{cr} (s)	TSI	
G-1	4685.9119	1.9501	0.33s	0.32s	1.9466	0.0034
G-2	5450.2676	1.9569			1.9212	0.0357
G-3	4696.7871	1.9502			1.9275	0.0226
G-4	4711.2624	1.9503			1.9220	0.0284
G-5	4685.8738	1.9501			1.9438	0.0062
G-6	5469.2310	1.9571			1.9356	0.0214
G-7	2183.9087	1.8958			1.8942	0.0017
G-8	4606.2025	1.9492			1.9177	0.0315
G-9	4917.6160	1.9524			1.9241	0.0282
G-10	4905.0037	1.9522			1.9192	0.0331
G-11	6626.4576	1.9644			1.9508	0.0137
G-12	4655.0564	1.9497			1.9463	0.0034
G-13	6815.5048	1.9654			1.9510	0.0144
G-14	4650.4077	1.9497			1.9332	0.0165
G-15	2190.9092	1.8961			1.8640	0.0322
G-16	2975.0030	1.9225			1.9184	0.0040
G-17	4639.4518	1.9496			1.9361	0.0135
G-18	4604.3121	1.9492			1.9246	0.0246
G-19	4658.4264	1.9498			1.9318	0.0180
G-20	4640.5572	1.9496			1.9270	0.0225
G-21	4640.0090	1.9496			1.9137	0.0359
G-22	4643.1270	1.9496			1.9204	0.0292
G-23	-741.8773	-0.3859			-0.3792	-0.0067
G-24	4630.1413	1.9495			1.9180	0.0315
G-25	4616.6907	1.9493			1.9202	0.0292
G-26	4584.0339	1.9490			1.9271	0.0219
G-27	4642.4976	1.9496			1.9126	0.0370
G-28	-822.3096	-0.3417			-0.3414	-0.0004
G-29	-824.5393	-0.3406			-0.3406	-0.0001
G-30	-820.1698	-0.3428			-0.3395	-0.0033
G-31	-821.6824	-0.3420			-0.3387	-0.0033
G-32	-884.7573	-0.3138			-0.3098	-0.0041
G-33	4577.4674	1.9489			1.9468	0.0021
G-34	4598.5326	1.9491			1.9253	0.0239
G-35	4606.6540	1.9492			1.9148	0.0344
G-36	-875.6192	-0.3176			-0.3165	-0.0011
G-37	-878.7781	-0.3163			-0.3126	-0.0037
G-38	-842.0115	-0.3324			-0.3274	-0.0050
G-39	-808.5386	-0.3486			-0.3445	-0.0040
G-40	-829.8976	-0.3381			-0.3320	-0.0061
G-41	-747.0314	-0.3828			-0.3762	-0.0066
G-42	-774.3038	-0.3668			-0.3667	-0.0001
G-43	-768.1189	-0.3703			-0.3703	0.0000
G-44	-787.4977	-0.3596			-0.3567	-0.0028
G-45	-765.7697	-0.3716			-0.3647	-0.0070
G-46	-820.9077	-0.3424			-0.3373	-0.0052
G-47	-828.0272	-0.3390			-0.3347	-0.0043
G-48	-822.7289	-0.3415			-0.3406	-0.0009
G-49	-820.9416	-0.3424			-0.3357	-0.0067

TABLE 5.22: Real time transient stability state and coherency identification of system for Case F

Generator Number	TSI	Gen. Stability Status		Coherent Group	System Status	Control Action (PG)
G-1	1.9466	Unstable	1	2		-
G-2	1.9212	Unstable	1	2		-
G-3	1.9275	Unstable	1	2		-
G-4	1.9220	Unstable	1	2		-
G-5	1.9438	Unstable	1	2		-
G-6	1.9356	Unstable	1	2		-
G-7	1.8942	Unstable	1	2		-
G-8	1.9177	Unstable	1	2		-
G-9	1.9241	Unstable	1	2		-
G-10	1.9192	Unstable	1	2		-
G-11	1.9508	Unstable	1	2		Generation Decreasing
G-12	1.9463	Unstable	1	2		-
G-13	1.9510	Unstable	1	2		Generation Decreasing
G-14	1.9332	Unstable	1	2		-
G-15	1.8640	Unstable	1	2		-
G-16	1.9184	Unstable	1	2		-
G-17	1.9361	Unstable	1	2		-
G-18	1.9246	Unstable	1	2		-
G-19	1.9318	Unstable	1	2		-
G-20	1.9270	Unstable	1	2		-
G-21	1.9137	Unstable	1	2		-
G-22	1.9204	Unstable	1	2		-
G-23	-0.3792	Stable	0	1		-
G-24	1.9180	Unstable	1	2		-
G-25	1.9202	Unstable	1	2	Unstable	-
G-26	1.9271	Unstable	1	2		-
G-27	1.9126	Unstable	1	2		-
G-28	-0.3414	Stable	0	1		-
G-29	-0.3406	Stable	0	1		-
G-30	-0.3395	Stable	0	1		-
G-31	-0.3387	Stable	0	1		-
G-32	-0.3098	Stable	0	1		-
G-33	1.9468	Unstable	1	2		-
G-35	1.9148	Unstable	1	2		-
G-36	-0.3165	Stable	0	1		-
G-37	-0.3126	Stable	0	1		-
G-38	-0.3274	Stable	0	1		-
G-39	-0.3445	Stable	0	1		-
G-40	-0.3320	Stable	0	1		-
G-41	-0.3762	Stable	0	1		Generation Increasing
G-42	-0.3667	Stable	0	1		-
G-43	-0.3703	Stable	0	1		Generation Increasing
G-44	-0.3567	Stable	0	1		-
G-45	-0.3647	Stable	0	1		-
G-46	-0.3373	Stable	0	1		-
G-47	-0.3347	Stable	0	1		-
G-48	-0.3406	Stable	0	1		-
G-49	-0.3357	Stable	0	1		-

TABLE 5.23: Coherent group identification Case F (50 Generator 145 Bus System)

	G-1	G-2	G-3	G-4	G-5	G-6	G-7	G-8	G-9	G-10	G-11	G-12	G-13	G-14	G-15	G-16	G-17	G-18	G-19	G-20	G-21	G-22	G-23	G-24	G-25	G-26	G-27	G-28	G-29	G-30	G-31	G-32	G-33	G-34	G-35	G-36	G-37	G-38	G-39	G-40	G-41	G-42	G-43	G-44	G-45	G-46	G-47	G-48	G-49
G-1	0.0	0.0	0.0	0.0	0.0	0.0	0.1	0.0	0.0	0.0	0.0	0.0	0.0	0.0	0.1	0.0	0.0	0.0	0.0	0.0	0.0	0.0	2.3	0.0	0.0	0.0	0.0	2.3	2.3	2.3	2.3	2.3	0.0	0.0	0.0	2.3	2.3	2.3	2.3	2.3	2.3	2.3	2.3	2.3	2.3	2.3	2.3	2.3	2.3
G-2	0.0	0.0	0.0	0.0	0.0	0.0	0.0	0.0	0.0	0.0	0.0	0.0	0.0	0.0	0.1	0.0	0.0	0.0	0.0	0.0	0.0	0.0	2.3	0.0	0.0	0.0	0.0	2.3	2.3	2.3	2.3	2.2	0.0	0.0	0.0	2.2	2.2	2.2	2.3	2.3	2.3	2.3	2.3	2.3	2.3	2.3	2.3	2.3	2.3
G-3	0.0	0.0	0.0	0.0	0.0	0.0	0.0	0.0	0.0	0.0	0.0	0.0	0.0	0.0	0.1	0.0	0.0	0.0	0.0	0.0	0.0	0.0	2.3	0.0	0.0	0.0	0.0	2.3	2.3	2.3	2.3	2.2	0.0	0.0	0.0	2.2	2.2	2.3	2.3	2.3	2.3	2.3	2.3	2.3	2.3	2.3	2.3	2.3	2.3
G-4	0.0	0.0	0.0	0.0	0.0	0.0	0.0	0.0	0.0	0.0	0.0	0.0	0.0	0.0	0.1	0.0	0.0	0.0	0.0	0.0	0.0	0.0	2.3	0.0	0.0	0.0	0.0	2.3	2.3	2.3	2.3	2.2	0.0	0.0	0.0	2.2	2.2	2.2	2.3	2.3	2.3	2.3	2.3	2.3	2.3	2.3	2.3	2.3	2.3
G-5	0.0	0.0	0.0	0.0	0.0	0.0	0.0	0.0	0.0	0.0	0.0	0.0	0.0	0.0	0.1	0.0	0.0	0.0	0.0	0.0	0.0	0.0	2.3	0.0	0.0	0.0	0.0	2.3	2.3	2.3	2.3	2.3	0.0	0.0	0.0	2.3	2.3	2.3	2.3	2.3	2.3	2.3	2.3	2.3	2.3	2.3	2.3	2.3	2.3
G-6	0.0	0.0	0.0	0.0	0.0	0.0	0.0	0.0	0.0	0.0	0.0	0.0	0.0	0.0	0.1	0.0	0.0	0.0	0.0	0.0	0.0	0.0	2.3	0.0	0.0	0.0	0.0	2.3	2.3	2.3	2.3	2.2	0.0	0.0	0.0	2.3	2.2	2.3	2.3	2.3	2.3	2.3	2.3	2.3	2.3	2.3	2.3	2.3	2.3
G-7	0.1	0.0	0.0	0.0	0.0	0.0	0.0	0.0	0.0	0.0	0.0	0.1	0.1	0.0	0.0	0.0	0.0	0.0	0.0	0.0	0.0	0.0	2.3	0.0	0.0	0.0	0.0	2.2	2.2	2.2	2.2	2.2	0.1	0.0	0.0	2.2	2.2	2.2	2.2	2.2	2.3	2.3	2.3	2.3	2.2	2.2	2.2	2.2	2.2
G-8	0.0	0.0	0.0	0.0	0.0	0.0	0.0	0.0	0.0	0.0	0.0	0.0	0.0	0.0	0.1	0.0	0.0	0.0	0.0	0.0	0.0	0.0	2.3	0.0	0.0	0.0	0.0	2.3	2.3	2.3	2.3	2.2	0.0	0.0	0.0	2.2	2.2	2.2	2.3	2.2	2.3	2.3	2.3	2.3	2.3	2.3	2.3	2.3	2.3
G-9	0.0	0.0	0.0	0.0	0.0	0.0	0.0	0.0	0.0	0.0	0.0	0.0	0.0	0.0	0.1	0.0	0.0	0.0	0.0	0.0	0.0	0.0	2.3	0.0	0.0	0.0	0.0	2.3	2.3	2.3	2.3	2.2	0.0	0.0	0.0	2.2	2.2	2.3	2.3	2.3	2.3	2.3	2.3	2.3	2.3	2.3	2.3	2.3	2.3
G-10	0.0	0.0	0.0	0.0	0.0	0.0	0.0	0.0	0.0	0.0	0.0	0.0	0.0	0.0	0.1	0.0	0.0	0.0	0.0	0.0	0.0	0.0	2.3	0.0	0.0	0.0	0.0	2.3	2.3	2.3	2.3	2.2	0.0	0.0	0.0	2.2	2.2	2.3	2.3	2.3	2.3	2.3	2.3	2.3	2.3	2.3	2.3	2.3	2.3
G-11	0.0	0.0	0.0	0.0	0.0	0.0	0.0	0.0	0.0	0.0	0.0	0.0	0.0	0.0	0.1	0.0	0.0	0.0	0.0	0.0	0.0	0.0	2.3	0.0	0.0	0.0	0.0	2.3	2.3	2.3	2.3	2.2	0.0	0.0	0.0	2.2	2.2	2.3	2.3	2.3	2.3	2.3	2.3	2.3	2.3	2.3	2.3	2.3	2.3
G-12	0.0	0.0	0.0	0.0	0.0	0.0	0.1	0.0	0.0	0.0	0.0	0.0	0.0	0.0	0.1	0.0	0.0	0.0	0.0	0.0	0.0	0.0	2.3	0.0	0.0	0.0	0.0	2.3	2.3	2.3	2.3	2.3	0.0	0.0	0.0	2.3	2.3	2.3	2.3	2.3	2.3	2.3	2.3	2.3	2.3	2.3	2.3	2.3	2.3
G-13	0.0	0.0	0.0	0.0	0.0	0.0	0.1	0.0	0.0	0.0	0.0	0.0	0.0	0.0	0.1	0.0	0.0	0.0	0.0	0.0	0.0	0.0	2.3	0.0	0.0	0.0	0.0	2.3	2.3	2.3	2.3	2.3	0.0	0.0	0.0	2.3	2.3	2.3	2.3	2.3	2.3	2.3	2.3	2.3	2.3	2.3	2.3	2.3	2.3
G-14	0.0	0.0	0.0	0.0	0.0	0.0	0.0	0.0	0.0	0.0	0.0	0.0	0.0	0.0	0.1	0.0	0.0	0.0	0.0	0.0	0.0	0.0	2.3	0.0	0.0	0.0	0.0	2.3	2.3	2.3	2.3	2.2	0.0	0.0	0.0	2.2	2.2	2.3	2.3	2.3	2.3	2.3	2.3	2.3	2.3	2.3	2.3	2.3	2.3
G-15	0.1	0.1	0.1	0.1	0.1	0.1	0.0	0.1	0.1	0.1	0.1	0.1	0.1	0.1	0.0	0.1	0.1	0.1	0.1	0.1	0.0	0.1	2.2	0.1	0.1	0.1	0.0	2.2	2.2	2.2	2.2	2.2	0.1	0.1	0.1	2.2	2.2	2.2	2.2	2.2	2.2	2.2	2.2	2.2	2.2	2.2	2.2	2.2	2.2
G-16	0.0	0.0	0.0	0.0	0.0	0.0	0.0	0.0	0.0	0.0	0.0	0.0	0.0	0.0	0.1	0.0	0.0	0.0	0.0	0.0	0.0	0.0	2.3	0.0	0.0	0.0	0.0	2.3	2.3	2.3	2.3	2.2	0.0	0.0	0.0	2.2	2.2	2.3	2.3	2.3	2.3	2.3	2.3	2.3	2.3	2.3	2.3	2.3	2.3
G-17	0.0	0.0	0.0	0.0	0.0	0.0	0.0	0.0	0.0	0.0	0.0	0.0	0.0	0.0	0.1	0.0	0.0	0.0	0.0	0.0	0.0	0.0	2.3	0.0	0.0	0.0	0.0	2.3	2.3	2.3	2.3	2.2	0.0	0.0	0.0	2.3	2.2	2.3	2.3	2.3	2.3	2.3	2.3	2.3	2.3	2.3	2.3	2.3	2.3
G-18	0.0	0.0	0.0	0.0	0.0	0.0	0.0	0.0	0.0	0.0	0.0	0.0	0.0	0.0	0.1	0.0	0.0	0.0	0.0	0.0	0.0	0.0	2.3	0.0	0.0	0.0	0.0	2.3	2.3	2.3	2.3	2.2	0.0	0.0	0.0	2.2	2.2	2.3	2.3	2.3	2.3	2.3	2.3	2.3	2.3	2.3	2.3	2.3	2.3
G-19	0.0	0.0	0.0	0.0	0.0	0.0	0.0	0.0	0.0	0.0	0.0	0.0	0.0	0.0	0.1	0.0	0.0	0.0	0.0	0.0	0.0	0.0	2.3	0.0	0.0	0.0	0.0	2.3	2.3	2.3	2.3	2.2	0.0	0.0	0.0	2.2	2.2	2.3	2.3	2.3	2.3	2.3	2.3	2.3	2.3	2.3	2.3	2.3	2.3
G-20	0.0	0.0	0.0	0.0	0.0	0.0	0.0	0.0	0.0	0.0	0.0	0.0	0.0	0.0	0.1	0.0	0.0	0.0	0.0	0.0	0.0	0.0	2.3	0.0	0.0	0.0	0.0	2.3	2.3	2.3	2.3	2.2	0.0	0.0	0.0	2.2	2.2	2.3	2.3	2.3	2.3	2.3	2.3	2.3	2.3	2.3	2.3	2.3	2.3

Continued Table 5.17
Coherent group identification Case F (50 Generator 145 Bus System)

	G-1	G-2	G-3	G-4	G-5	G-6	G-7	G-8	G-9	G-10	G-11	G-12	G-13	G-14	G-15	G-16	G-17	G-18	G-19	G-20	G-21	G-22	G-23	G-24	G-25	G-26	G-27	G-28	G-29	G-30	G-31	G-32	G-33	G-34	G-35	G-36	G-37	G-38	G-39	G-40	G-41	G-42	G-43	G-44	G-45	G-46	G-47	G-48	G-49
G-21	0.0	0.0	0.0	0.0	0.0	0.0	0.0	0.0	0.0	0.0	0.0	0.0	0.0	0.0	0.0	0.0	0.0	0.0	0.0	0.0	0.0	0.0	2.3	0.0	0.0	0.0	0.0	2.3	2.3	2.3	2.3	2.2	0.0	0.0	0.0	2.2	2.2	2.2	2.3	2.2	2.3	2.3	2.3	2.3	2.3	2.3	2.2	2.3	2.2
G-22	0.0	0.0	0.0	0.0	0.0	0.0	0.0	0.0	0.0	0.0	0.0	0.0	0.0	0.0	0.1	0.0	0.0	0.0	0.0	0.0	0.0	0.0	2.3	0.0	0.0	0.0	0.0	2.3	2.3	2.3	2.3	2.2	0.0	0.0	0.0	2.2	2.2	2.2	2.3	2.3	2.3	2.3	2.3	2.3	2.3	2.3	2.3	2.3	2.3
G-23	2.3	2.3	2.3	2.3	2.3	2.3	2.3	2.3	2.3	2.3	2.3	2.3	2.3	2.3	2.2	2.3	2.3	2.3	2.3	2.3	2.3	2.3	0.0	2.3	2.3	2.3	2.3	0.0	0.0	0.0	0.0	0.1	2.3	2.3	2.3	0.1	0.1	0.1	0.0	0.0	0.0	0.0	0.0	0.0	0.0	0.0	0.0	0.0	0.0
G-24	0.0	0.0	0.0	0.0	0.0	0.0	0.0	0.0	0.0	0.0	0.0	0.0	0.0	0.0	0.1	0.0	0.0	0.0	0.0	0.0	0.0	0.0	2.3	0.0	0.0	0.0	0.0	2.3	2.3	2.3	2.3	2.2	0.0	0.0	0.0	2.2	2.2	2.2	2.3	2.3	2.3	2.3	2.3	2.3	2.3	2.3	2.3	2.3	2.3
G-25	0.0	0.0	0.0	0.0	0.0	0.0	0.0	0.0	0.0	0.0	0.0	0.0	0.0	0.0	0.1	0.0	0.0	0.0	0.0	0.0	0.0	0.0	2.3	0.0	0.0	0.0	0.0	2.3	2.3	2.3	2.3	2.2	0.0	0.0	0.0	2.2	2.2	2.2	2.3	2.3	2.3	2.3	2.3	2.3	2.3	2.3	2.3	2.3	2.3
G-26	0.0	0.0	0.0	0.0	0.0	0.0	0.0	0.0	0.0	0.0	0.0	0.0	0.0	0.0	0.1	0.0	0.0	0.0	0.0	0.0	0.0	0.0	2.3	0.0	0.0	0.0	0.0	2.3	2.3	2.3	2.3	2.2	0.0	0.0	0.0	2.2	2.2	2.3	2.3	2.3	2.3	2.3	2.3	2.3	2.3	2.3	2.3	2.3	2.3
G-27	0.0	0.0	0.0	0.0	0.0	0.0	0.0	0.0	0.0	0.0	0.0	0.0	0.0	0.0	0.0	0.0	0.0	0.0	0.0	0.0	0.0	0.0	2.3	0.0	0.0	0.0	0.0	2.3	2.3	2.3	2.3	2.2	0.0	0.0	0.0	2.2	2.2	2.2	2.3	2.2	2.3	2.3	2.3	2.3	2.2	2.2	2.3	2.2	2.2
G-28	2.3	2.3	2.3	2.3	2.3	2.3	2.2	2.3	2.3	2.3	2.3	2.3	2.3	2.3	2.2	2.3	2.3	2.3	2.3	2.3	2.3	2.3	0.0	2.3	2.3	2.3	2.3	0.0	0.0	0.0	0.0	0.0	2.3	2.3	2.3	0.0	0.0	0.0	0.0	0.0	0.0	0.0	0.0	0.0	0.0	0.0	0.0	0.0	0.0
G-29	2.3	2.3	2.3	2.3	2.3	2.3	2.2	2.3	2.3	2.3	2.3	2.3	2.3	2.3	2.2	2.3	2.3	2.3	2.3	2.3	2.3	2.3	0.0	2.3	2.3	2.3	2.3	0.0	0.0	0.0	0.0	0.0	2.3	2.3	2.3	0.0	0.0	0.0	0.0	0.0	0.0	0.0	0.0	0.0	0.0	0.0	0.0	0.0	0.0
G-30	2.3	2.3	2.3	2.3	2.3	2.3	2.2	2.3	2.3	2.3	2.3	2.3	2.3	2.3	2.2	2.3	2.3	2.3	2.3	2.3	2.3	2.3	0.0	2.3	2.3	2.3	2.3	0.0	0.0	0.0	0.0	0.0	2.3	2.3	2.3	0.0	0.0	0.0	0.0	0.0	0.0	0.0	0.0	0.0	0.0	0.0	0.0	0.0	0.0
G-31	2.3	2.3	2.3	2.3	2.3	2.3	2.2	2.3	2.3	2.3	2.3	2.3	2.3	2.3	2.2	2.3	2.3	2.3	2.3	2.3	2.3	2.3	0.0	2.3	2.3	2.3	2.3	0.0	0.0	0.0	0.0	0.0	2.3	2.3	2.3	0.0	0.0	0.0	0.0	0.0	0.0	0.0	0.0	0.0	0.0	0.0	0.0	0.0	0.0
G-32	2.3	2.2	2.2	2.2	2.3	2.2	2.2	2.2	2.2	2.2	2.2	2.3	2.3	2.2	2.2	2.2	2.2	2.2	2.2	2.2	2.2	2.2	0.1	2.2	2.2	2.2	2.2	0.0	0.0	0.0	0.0	0.0	2.3	2.2	2.2	0.0	0.0	0.0	0.0	0.0	0.1	0.1	0.1	0.0	0.1	0.0	0.0	0.0	0.0
G-33	0.0	0.0	0.0	0.0	0.0	0.0	0.1	0.0	0.0	0.0	0.0	0.0	0.0	0.0	0.1	0.0	0.0	0.0	0.0	0.0	0.0	0.0	2.3	0.0	0.0	0.0	0.0	2.3	2.3	2.3	2.3	2.3	0.0	0.0	0.0	2.3	2.3	2.3	2.3	2.3	2.3	2.3	2.3	2.3	2.3	2.3	2.3	2.3	2.3
G-34	0.0	0.0	0.0	0.0	0.0	0.0	0.0	0.0	0.0	0.0	0.0	0.0	0.0	0.0	0.1	0.0	0.0	0.0	0.0	0.0	0.0	0.0	2.3	0.0	0.0	0.0	0.0	2.3	2.3	2.3	2.3	2.2	0.0	0.0	0.0	2.2	2.2	2.2	2.3	2.3	2.3	2.3	2.3	2.3	2.3	2.3	2.3	2.3	2.3
G-35	0.0	0.0	0.0	0.0	0.0	0.0	0.0	0.0	0.0	0.0	0.0	0.0	0.0	0.0	0.1	0.0	0.0	0.0	0.0	0.0	0.0	0.0	2.3	0.0	0.0	0.0	0.0	2.3	2.3	2.3	2.3	2.2	0.0	0.0	0.0	2.2	2.2	2.2	2.3	2.2	2.3	2.3	2.3	2.3	2.2	2.2	2.3	2.2	2.2
G-36	2.3	2.2	2.2	2.2	2.3	2.3	2.2	2.2	2.2	2.2	2.2	2.3	2.3	2.2	2.2	2.2	2.3	2.2	2.2	2.2	2.2	2.2	0.1	2.2	2.2	2.2	2.2	0.0	0.0	0.0	0.0	0.0	2.3	2.2	2.2	0.0	0.0	0.0	0.0	0.0	0.1	0.1	0.1	0.0	0.0	0.0	0.0	0.0	0.0
G-37	2.3	2.2	2.2	2.2	2.3	2.2	2.2	2.2	2.2	2.2	2.2	2.3	2.3	2.2	2.2	2.2	2.2	2.2	2.2	2.2	2.2	2.2	0.1	2.2	2.2	2.2	2.2	0.0	0.0	0.0	0.0	0.0	2.3	2.2	2.2	0.0	0.0	0.0	0.0	0.0	0.1	0.1	0.1	0.0	0.1	0.0	0.0	0.0	0.0
G-38	2.3	2.2	2.3	2.2	2.3	2.3	2.2	2.2	2.3	2.2	2.3	2.3	2.3	2.3	2.2	2.2	2.3	2.3	2.3	2.3	2.2	2.2	0.1	2.2	2.2	2.3	2.2	0.0	0.0	0.0	0.0	0.0	2.3	2.3	2.2	0.0	0.0	0.0	0.0	0.0	0.0	0.0	0.0	0.0	0.0	0.0	0.0	0.0	0.0
G-39	2.3	2.3	2.3	2.3	2.3	2.3	2.2	2.3	2.3	2.3	2.3	2.3	2.3	2.3	2.2	2.3	2.3	2.3	2.3	2.3	2.3	2.3	0.0	2.3	2.3	2.3	2.3	0.0	0.0	0.0	0.0	0.0	2.3	2.3	2.3	0.0	0.0	0.0	0.0	0.0	0.0	0.0	0.0	0.0	0.0	0.0	0.0	0.0	0.0
G-40	2.3	2.3	2.3	2.3	2.3	2.3	2.2	2.2	2.3	2.3	2.3	2.3	2.3	2.3	2.2	2.3	2.3	2.3	2.3	2.3	2.2	2.3	0.0	2.3	2.3	2.3	2.2	0.0	0.0	0.0	0.0	0.0	2.3	2.3	2.2	0.0	0.0	0.0	0.0	0.0	0.0	0.0	0.0	0.0	0.0	0.0	0.0	0.0	0.0
G-41	2.3	2.3	2.3	2.3	2.3	2.3	2.3	2.3	2.3	2.3	2.3	2.3	2.3	2.3	2.2	2.3	2.3	2.3	2.3	2.3	2.3	2.3	0.0	2.3	2.3	2.3	2.3	0.0	0.0	0.0	0.0	0.1	2.3	2.3	2.3	0.1	0.1	0.0	0.0	0.0	0.0	0.0	0.0	0.0	0.0	0.0	0.0	0.0	0.0
G-42	2.3	2.3	2.3	2.3	2.3	2.3	2.3	2.3	2.3	2.3	2.3	2.3	2.3	2.3	2.2	2.3	2.3	2.3	2.3	2.3	2.3	2.3	0.0	2.3	2.3	2.3	2.3	0.0	0.0	0.0	0.0	0.1	2.3	2.3	2.3	0.1	0.1	0.0	0.0	0.0	0.0	0.0	0.0	0.0	0.0	0.0	0.0	0.0	0.0
G-43	2.3	2.3	2.3	2.3	2.3	2.3	2.3	2.3	2.3	2.3	2.3	2.3	2.3	2.3	2.2	2.3	2.3	2.3	2.3	2.3	2.3	2.3	0.0	2.3	2.3	2.3	2.3	0.0	0.0	0.0	0.0	0.1	2.3	2.3	2.3	0.1	0.1	0.0	0.0	0.0	0.0	0.0	0.0	0.0	0.0	0.0	0.0	0.0	0.0
G-44	2.3	2.3	2.3	2.3	2.3	2.3	2.3	2.3	2.3	2.3	2.3	2.3	2.3	2.3	2.2	2.3	2.3	2.3	2.3	2.3	2.3	2.3	0.0	2.3	2.3	2.3	2.3	0.0	0.0	0.0	0.0	0.0	2.3	2.3	2.3	0.0	0.0	0.0	0.0	0.0	0.0	0.0	0.0	0.0	0.0	0.0	0.0	0.0	0.0
G-45	2.3	2.3	2.3	2.3	2.3	2.3	2.3	2.3	2.3	2.3	2.3	2.3	2.3	2.3	2.2	2.3	2.3	2.3	2.3	2.3	2.3	2.3	0.0	2.3	2.3	2.3	2.3	0.0	0.0	0.0	0.0	0.1	2.3	2.3	2.3	0.0	0.1	0.0	0.0	0.0	0.0	0.0	0.0	0.0	0.0	0.0	0.0	0.0	0.0
G-46	2.3	2.3	2.3	2.3	2.3	2.3	2.2	2.3	2.3	2.3	2.3	2.3	2.3	2.3	2.2	2.3	2.3	2.3	2.3	2.3	2.3	2.2	0.0	2.3	2.3	2.3	2.2	0.0	0.0	0.0	0.0	0.0	2.3	2.3	2.3	0.0	0.0	0.0	0.0	0.0	0.0	0.0	0.0	0.0	0.0	0.0	0.0	0.0	0.0
G-47	2.3	2.3	2.3	2.3	2.3	2.3	2.2	2.3	2.3	2.3	2.3	2.3	2.3	2.3	2.2	2.3	2.3	2.3	2.3	2.3	2.2	2.3	0.0	2.3	2.3	2.3	2.2	0.0	0.0	0.0	0.0	0.0	2.3	2.3	2.2	0.0	0.0	0.0	0.0	0.0	0.0	0.0	0.0	0.0	0.0	0.0	0.0	0.0	0.0
G-48	2.3	2.3	2.3	2.3	2.3	2.3	2.2	2.3	2.3	2.3	2.3	2.3	2.3	2.3	2.2	2.3	2.3	2.3	2.3	2.3	2.3	2.3	0.0	2.3	2.3	2.3	2.3	0.0	0.0	0.0	0.0	0.0	2.3	2.3	2.3	0.0	0.0	0.0	0.0	0.0	0.0	0.0	0.0	0.0	0.0	0.0	0.0	0.0	0.0
G-49	2.3	2.3	2.3	2.3	2.3	2.3	2.2	2.3	2.3	2.3	2.3	2.3	2.3	2.3	2.2	2.3	2.3	2.3	2.3	2.3	2.2	2.3	0.0	2.3	2.3	2.3	2.2	0.0	0.0	0.0	0.0	0.0	2.3	2.3	2.3	0.0	0.0	0.0	0.0	0.0	0.0	0.0	0.0	0.0	0.0	0.0	0.0	0.0	0.0

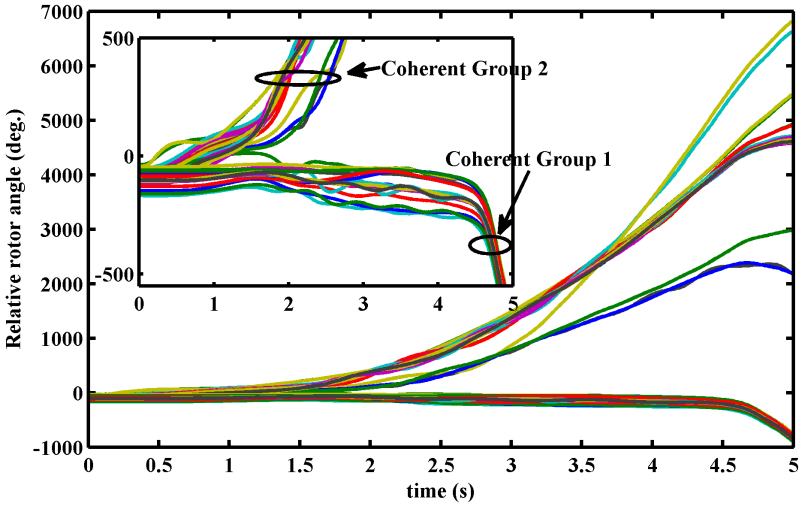

FIGURE 5.11: Rotor angle trajectories with respect to COI for testing the RBFNN (Case F)

Table **??** shows the performance evaluation of the proposed RBFNN. It is found from the results that, the proposed method gives excellent performance for prediction of TSI with high accuracy.

The following interpretations can be drawn from the results shown in this section.

- The relative rotor angle rather than absolute angles are monitored to test stability and instability.
- The proposed TSI provides an index of how much the generator rotor angle deviates from the COI.

TABLE 5.24: Performance evaluation of proposed RBFNN

System	Number of Features	Number of Sample		Average error in TSI Prediction	Prediction Accuracy (%)	Total Training Time (s)	Testing Time/Sample (s)
		Training Set	Testing Set				
10 Gen. 39 bus	50	400	100	0.01	**99.58**	3.256	6.451×10-4
16 Gen. 68 bus	80	400	100	0.009	**99.64**	5.462	6.241×10-4
50 Gen. 145 bus	250	400	100	0.015	**99.05**	7.241	6.151×10-4

- The proposed RBFNN model presented excellent performance on unseen load samples. The proposed RBFNN model requires only post fault rotor angle deviation of the generators as input.

- The trained RBFNN gives more then 99% prediction accuracy for all different size of power systems.

- The identification of the post-fault generators' transient stability status, criticality rank and coherent group in real time within a few cycles is possible by using proposed RBFNN.

- The ranking of critical generator can be examined by ranking their TSI values in decreasing order of their severity. Hence, a generator is most advance/critical generator if its having highest value of TSI and it is the first machine to loose synchronism. It can be concluded from the results that ranking of generator carries important information about generation control strategies like generator rescheduling.

- For this study, coherent groups are predicted at the end of the simulation time, however RBFNN can be trained for any desired time instant for the prediction.

- The simulation results represent monitoring, assessment and prediction capability of the proposed scheme. After observing the results, it can be concluded that system coherency plays an important role in the assessment of stability. Similar behavior generators can be represented as a single equivalent generator as shown in Tables 5.8, 5.11, 5.14, 5.17, 5.20 and 5.23 by using different colors.

- Post fault assessment of stability and identification of coherent groups for small power systems can be relatively simple. In case of moderate and large power system it can be a daunting task requiring greater simulation time. Hence, simulation time is kept 3s and 5s for moderate and large power networks respectively.

- The proposed RBFNN-based method is capable of predicting any unseen operating condition independent of system topology with very less computation time. This indicated their suitability for online security evaluation of power systems.

TABLE 5.25: Comparison results for transient stability assessment of IEEE 39-bus System

Type of ANN	**No. of Input Features**	**Number of Test Samples**	**Accuracy (%)**
MSVM [156]	26	221	91.40
PNN [279]	31	73	93.22
BPN [279]	15	73	92.36
GRNN [279]	15	73	98.95
SPCM [255]	23	110	90.91
MLS [255]	23	110	85.45
MLP [255]	23	110	81.82
RBFNN [Proposed]	**50**	**100**	**99.58**

TABLE 5.26: Comparison results for transient stability assessment of IEEE 145-Bus System

Type of ANN	**No. of Input Features**	**Number of Test Samples**	**Accuracy (%)**
BPN [279]	80	106	83.96
PNN [279]	80	106	97.88
GRNN [279]	80	106	97.77
MLP [273]	-	200/600	78.50
SVM [273]	-	200/600	85.00
RBFNN [280]	-	15720	96.05
RBFNN [Proposed]	**250**	**100**	**99.05**

A comparison of results is presented in term of type of ANN used, number of input features, number of test sample and prediction accuracy. From the Tables 5.25 and 5.26, it may be observed that the proposed method gives better results than the existing methods.

The proposed method of online TSA is straight forward method to identify the generator stability state. It can be implemented in EMS by continuously monitoring the security state of the system for different contingency under different operating conditions. Whenever the system is found to be unstable for anticipated operating conditions for probable contingency the preventive control action can be applied. Thus the proposed unified TSA scheme can provide vital solution to identify the generator criticality and instability problem to the operator at EMS.

5.6 Summary

The system stability assessment is a paramount importance in the dynamic operating scenario of power system. Any mechanism that helps the system operator to take intelligent decisions for ensuring the grid stability is a beneficial tool. In this chapter, an application of RBFNN has been explored to predict the system stability status in order to help in finalizing the control decisions. A more robust and reliable method for assessment of transient stability at EMS has been proposed and the application results are presented for different size of three systems as IEEE 39-bus system, IEEE 68-bus system and IEEE-145 bus system. Based on this chapter following conclusions may be drawn:

1. A fast and effective Radial Basis Function Neural Network (RBFNN) based approach has been proposed for online TSA of power system for varied operating conditions.

2. A new index TSI, based on rotor angle deviation of the generators has been proposed in this chapter. This index has been employed to do the assessment of system stability, to rank the generators as per the criticality and for identification of the candidate generators for application of the control actions such as generation rescheduling and coherent group identification.

3. The proposed method is based on the predicting the TSI values of the generators using RBFNN to assess the transient stability of the system.

4. A supervised learning architecture based on RBFNN has been proposed to evaluate the system stability under wide range of operating conditions, contingencies and faults.

5. Both informations about ranking obtained from the TSI value of each generating unit and TSI based coherent group information are important for selecting the units for change the generation during generation rescheduling as preventive control action.

6. The validation and testing of proposed architecture has been performed over three power systems. It has been observed that during validation and testing phase,

the performance of this engine is promising. The validation of the performance has been carried out with the help of nonlinear TDS.

7. For all the unseen operating cases the average error in predicting the TSI values using RBFNN is very less.

8. The proposed method is found to be significantly easier to implement than previous assessment methods, resulting high accuracy in assessment and prediction.

In following chapter enhancement of transient stability with the help of meta–heuristic optimization algorithm will be discuss in details.

Chapter 6

An Intelligent Grey Wolf Optimizer for Transient Stability and Security Constraints Optimal Power Flow

[*This chapter presents the design and implementation of Improved Grey Wolf Optimization (IGWO) for the TSSCOPF. The IGWO is implemented in order to reschedule the generator with minimum fuel cost such that the stability is maximized. In order to identify the efficiency of the proposed IGWO algorithm, the results obtained are compared with the other state-of-the-art algorithms.*]

6.1 Introduction

In chapter 4 and chapter 5 two important aspects of the power system security assessment methods, namely the static security assessment method with contingency ranking & classification and Transient Stability Assessment (TSA) with coherency identification have been discussed. These assessment approaches help in identifying the secure and insecure states of the power system. These approaches allow the

Independent System Operator (ISO) to achieve better performance analysis and determine the various capabilities of the power system in an online or offline mode. In the efficient power system operation, to supply the required amount of active and reactive power at constant frequency and with a stable voltage level continually, system stability assessment and enhancement is required. In the case of critical situations, the ISO need to know how to prevent the system from collapse. Therefore, control actions are required to activate proper counter-measures, which have a stability improving impact on the power system.

Due to deregulation in power system, it is required to transmit large amount of electrical power over long distances in day-ahead electricity markets. The contingencies associated with power system operation and high demand of power with complex control hierarchy pushed systems to operate at their stability boundaries [281]. In this milieu, instability of power system has become major issues, which must be taken care of by suitable techniques. This has given rise to a new methodology known as Transient Stability and Security Constrained Optimal Power Flow (TSSCOPF) problem, which is a highly nonlinear, non-convex, and multidimensional optimization problem [282]. In general, TSSCOPF is extension of Optimal Power Flow (OPF) with additional rotor angle and line flow inequality constraints. It considers optimal, secure and stable operations simultaneously.

TSSCOPF is, however, a nonlinear optimization problem with both algebraic and differential equations in the time domain. As a special requirement of the system, the initial or feasible operating point should withstand the disturbance and can move to a new stable equilibrium state after the clearance of the fault without disturbing the equality and the inequality constraints. Due to huge dimension of the TSSCOPF problem, it is really a tough exercise to deal with this type of problem. For a given power system configuration, although the number of possible contingencies are numerous, there are few critical contingencies that may cause instability.

In order to achieve this objective, variant of a new meta heuristic algorithm Grey Wolf Optimizer (GWO) namely, Intelligent Grey Wolf Optimizer (IGWO) is employed to reschedule the generator with minimum increase in fuel cost, such that the transient severity is minimized. In order to prove the efficacy of the IGWO algorithm, the results obtained on IEEE-30 bus test system and IEEE 39-bus 10

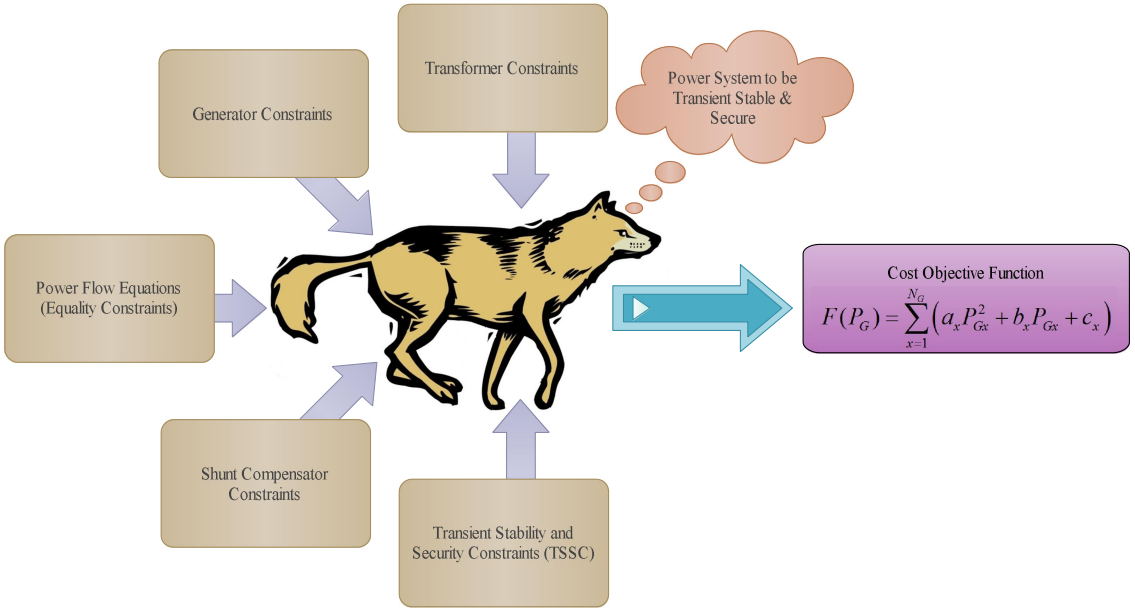

FIGURE 6.1: Block diagram representation of TSSCOPF problem with IGWO

generator, are compared with other state-of-the-art algorithms namely GA [121], PSO [121], ABC [124], CABC [124], WOA [125] and CWOA [125] algorithms.

6.2 Problem Formulation

The power network is a complex system, having three parts performing generation, transmission and distribution of electric power. It is required from the ISO to operate the system by using minimum resources incorporating stability and security constraints.

6.2.1 Optimal Power Flow

Optimal Power Flow (OPF) problem formulation is concerned with the optimal setting of control variables for the steady state performance study of power system with respect to a predefine objective function subjected to various equality and inequality constraints [213]. The main goal of the OPF problem is to minimize the total fuel cost while satisfying all the equality and the inequality constraints.

Mathematically, OPF problem may be represented as:

$$\text{Min } f(i,j) \tag{6.1}$$

$$\text{subject to : } \left.\begin{matrix} m(i,j)=0 \\ n(i,j)\leq 0 \end{matrix}\right\}$$

Where the above objective function $f(i,j)$ is taken as the total production cost, the equality constraints $m(i,j)$ are taken as the power flow equations and the inequality constraints $n(i,j)$ are taken as static and dynamic constraints as transmission line loading constraints, generator capacity constraints, security and transient stability constraints.

The vector of dependent variables i may be represented by 6.2.

$$i^T = [P_{G_{slack}}, V_{L_1}, ..., V_{L_{NL}}, Q_{G_1}, ..., Q_{G_{NG}}, S_{L_1}, ..., S_{L_{NT}}] \tag{6.2}$$

Where P_{G_slack} is the slack bus power, V_L is the load bus voltages, Q_G indicates the reactive power outputs of the generators, S_L indicates the transmission line flows, N_L is the number of load buses, N_G is the number of generator buses and NTL is the number of transmission lines. Similarly, the vector of control variables j may be written by Equation 6.3.

$$j^T = [P_{G_2}, .., P_{G_{NG}}, V_{G_1}, .., V_{G_{NG}}, T_1, .., T_{NT}, Q_{C_1}, .., Q_{C_{NC}}] \tag{6.3}$$

Where NT is the number of tap changing transformers and NC is the number of shunt VAR compensators, V_G is the terminal voltage at the generator buses, P_G is the active power output of the generators, T_i is the tap setting of the tap changing transformers and Q_C is the output of shunt VAR compensator.

6.2.2 Objective Function

The objective function can be described by the concepts such as production cost, social welfare, and fuel cost. In an interconnected power system, the production cost is given by the fuel cost curve approximated as the quadratic function of generated

active power output. In this case, the total production, minimization is taken in to consideration as the objective of TSSCOPF problem and it is expressed mathematically in Equation 6.4 [123].

$$F(P_G) = \sum_{x=1}^{N_G} \left(a_x P_{Gx}^2 + b_x P_{Gx} + c_x\right) \tag{6.4}$$

Where $F(P_G)$ is the total generating cost, a_x, b_x and c_x are the fuel cost coefficients of the generator x, P_{Gx} is the active power generation of the unit x, N_G is the total number of generator buses.

6.2.3 Constraints in OPF Problem with Security and Transient Stability

Security and Transient Stability constrained OPF can be considered as a conventional OPF with additional inequality constraints imposed by the transmission line loading limits and the rotor angle limits. The power flow should meets the steady state constraints related to solution of the conventional OPF problem and dynamic constraints imposed on the rotor angle during the transient period under undesirable conditions. The OPF problem has two categories of constraints (viz. the equality constraint and the inequality constraint). These two types of constraints are, sequentially, described below:

6.2.3.1 Equality Constraints (Power Flow Constraints)

The power flow equations form the equality constraints as shown in Equation 6.5.

$$\begin{cases} P_{G_x} - P_{D_x} - V_x \sum\limits_{y=1}^{N_B} V_y \left(G_{xy}\cos\delta_{xy} + B_{xy}\sin\delta_{xy}\right) = 0 \\ Q_{G_x} + Q_{C_x} - Q_{D_x} - V_x \sum\limits_{y=1}^{N_B} V_y \left(G_{xy} sin\delta_{xy} - B_{xy} cos\delta_{xy}\right) = 0 \end{cases} \tag{6.5}$$

Where N_B is the total number of system buses; P_{G_x} and Q_{G_x} are active and reactive power outputs, respectively of the generator x. P_{D_x} and Q_{D_x} are total active and reactive power loads respectively of bus x. V_x and V_y are the voltage of

the buses x and y respectively. Q_{C_x} is shunt reactive source at bus x. G_{xy}, B_{xy} and δ_{xy}, respectively, are the transfer conductance, the susceptance and the phase difference of voltage, between buses x and y.

6.2.3.2 Inequality Constraints (Static and Dynamic Constraints)

- *Generator Constraints*

  Generator voltage, active power outputs and reactive power outputs of bus x should lie between their respective lower and upper limits, as shown in equation 6.6.

$$\left.\begin{aligned} V_{G_x}^{\min} \leq V_{G_x} \leq V_{G_x}^{\max}, \quad x = 1, 2, \ldots, N_G \\ P_{G_x}^{\min} \leq P_{G_x} \leq P_{G_x}^{\max}, \quad x = 1, 2, \ldots, N_G \\ Q_{G_x}^{\min} \leq Q_{G_x} \leq Q_{G_x}^{\max}, \quad x = 1, 2, \ldots, N_G \end{aligned}\right\} \tag{6.6}$$

  where V_{Gx}^{min}; V_{Gx}^{max} are the minimum and the maximum generator voltage, respectively, of bus x, P_{Gx}^{min}; P_{Gx}^{max} are the minimum and the maximum active power output, respectively, of bus x and Q_{Gx}^{min}; Q_{Gx}^{max} are the minimum and the maximum reactive power output, respectively, of bus x.

- *Transformer Constraints*

  Transformer tap settings are bounded by their respective upper and lower limits as shown in Equation 6.7 .

$$T_x^{\min} \leq T_x \leq T_x^{\max}, \quad x = 1, 2, \ldots, N_T \tag{6.7}$$

  where T_x^{min}; T_x^{max} are the minimum and the maximum tap setting limits, respectively, of transformer x and N_T is the number of regulating transformers.

- *Shunt Compensator Constraints*

  Reactive power injections at buses are restricted by their respective maximum and minimum limits as shown in Equation 6.8.

$$Q_{C_x}^{\min} \leq Q_{C_x} \leq Q_{C_x}^{\max}, \quad x = 1, 2, \ldots, N_C \tag{6.8}$$

where Q_{Cx}^{min}; Q_{Cx}^{max} are the minimum and the maximum VAR injection limits, respectively, of the shunt compensator x and N_C is the number of shunt compensators.

- *Security Constraints*
  These include transmission line loadings and voltages at load buses are represented by the Equations 6.9 and 6.10 respectively.

$$V_{L_x}^{\min} \leq V_{L_x} \leq V_{L_x}^{\max}, \quad x = 1, 2, \ldots, N_L \tag{6.9}$$

$$S_{L_x} = \sqrt{P_{L_x}^2 + Q_{L_x}^2} \leq S_{L_x}^{\max}, \quad x = 1, 2, \ldots, N_{TL} \tag{6.10}$$

  where V_{Lx}^{min} ; V_{Lx}^{max} are the minimum and the maximum load voltage, respectively, of load bus x, S_{Lx} ; S_{Lx}^{max} are the apparent power flow and the maximum apparent power flow limit, respectively, through branch x, N_L is the number of load buses and N_{TL} is the number of transmission lines.

6.2.4 Transient Stability Assessment and Constraints

TSA of power system is required to find whether system can maintain synchronism during disturbance or not [283]. This decision is taken by monitoring the trajectories of rotor angles during a perturbation period. The swing equation shows the transient behavior of the system. If the trajectories of rotor angle of either single generator or a group of generators are found to have continuous increment without limit with reference to remaining machines, then the system is unstable. Another phenomenon, if rotor angles of all participating system generators remain bounded within their respective permissible limits, then system is stable [33, 102]. The transient stability constraints of TSSCOPF problem constitute a set of differential algebraic equations [33] that may be solved by time-domain technique. The swing equation set of the generator x can be represented by the Equations 6.11, 6.12 and 6.13.

$$\frac{d\delta_x}{dt} = \Delta\omega_x \tag{6.11}$$

$$\frac{d\Delta\omega_x}{dt} = \frac{1}{M_x}\left(P_{mx} - P_{ex} - D_x\Delta\omega_x\right) \tag{6.12}$$

$$M_x \frac{d^2\delta_x}{dt^2} = (P_{mx} - P_{ex}) \tag{6.13}$$

In the Equation 6.12, M_x is moment of inertia of generator x, P_{mx} and P_{ex} are mechanical power input and electrical power outputs, respectively of the generator x. D_x and $\Delta\omega_x$ are damping coefficient and rotor speed deviation, respectively of the generator x. δ_x is rotor angle of generator x.

The generator rotor angle deviation with respect to the rotor angle of slack generator δ_{slack} is expressed in the form of inequality constraints, as stated in Equations 6.14 and 6.15 [121].

$$\delta^{\min} \leq |\Delta\delta_x| \leq \delta^{\max} \tag{6.14}$$

where

$$\Delta\delta_x = |\delta_x - \delta_{slack}| \;\; x = 1, 2, ..., (N_G - 1) \tag{6.15}$$

For this work maximum allowable value of relative rotor angle for secure operation $\delta^{\max}$ is taken as 120^0 [271–273].

6.2.5 Formulation of TSSCOPF Problem

The formulation of the TSSCOPF problem is summarized according to the equality and inequality constraints which are defined in sections 6.2.3.1 and 6.2.3.2 respectively.

For the equality constraints, the power balance based on Newton-Raphson method is met by the power flow constraints in Equation 6.5, while the swing equation in Equations 6.11 and 6.12 are satisfied by the time-domain simulation based on the Euler method.

For the inequality constraints, the penalty function is adopted to deal with all operating limits as given in Equations 6.6 to 6.10. The penalty function for limit violation of any variable can be defined as follows [284]:

$$h(\lambda_i) = \begin{cases} \lambda_i - {\lambda_i}^{\max} & if \quad \lambda_i > {\lambda_i}^{\max} \\ {\lambda_i}^{\min} - \lambda_i & if \quad \lambda_i < {\lambda_i}^{\min} \\ 0 & if \;\; {\lambda_i}^{\min} \leq \lambda_i \leq {\lambda_i}^{\max} \end{cases} \tag{6.16}$$

Where $h(\lambda_i)$ represents the penalty function of variable λ_i: ${\lambda_i}^{\min}$ and ${\lambda_i}^{\max}$ are the lower Eand upper limits of the variable λ_i. λ_i represent the variables expressed in Equations 6.6 to 6.10, but the penalty value for Equation 6.14 is kept constant. The penalty functions reflect the violation of the inequality constraints and is assigned a high cost of penalty for a candidate point far away from the feasible region.

In order to enforce all inequality constraints mentioned above, the objective function as shown in Equation 6.4 is added with the penalty functions of active power generation of slack bus, reactive power generation, load bus voltage magnitude, transient stability limit, and transmission line loading. The fitness value is calculated by Equation 6.17.

$$F_i = F(P_G) + \mathrm{P} \tag{6.17}$$

Where P for penalty describes as

$$P = K_p[h(P_{slack})] + K_Q \sum_{i=1}^{N_G} h(Q_{gi}) + K_V \sum_{i=1}^{N_l} h(V_{Li}) + K_T \sum_{i=1}^{N_G} h(\Delta\delta_i) + K_S \sum_{i=1}^{N_{line}} h(S_i)$$

Where $h(P_{slack})$, $h(Q_{gi})$, $h(V_{Li})$, $h(\Delta\delta_i)$ and $h(S_i)$ are penalty functions of active power output of slack bus, the reactive power output of the generator, load bus voltage magnitude, relative rotor angle and transmission line loading respectively, Ks are the corresponding penalty weights. N_l is the total number of load buses.

6.3 Procedure of IGWO to solve TSSCOPF Problem

To inculcate IGWO based TSSCOPF following steps are used:

Step 1 Initialize the grey wolf population (N), maximum number of iterations (T_{max}) and dimension of the problem (Dim).

Step 2 Initialize a, A, C.

Step 3 Create a 3-phase fault.

Step 4 Under the created operating scenario, violation of limits of transmission line power flow, voltage magnitude at the load bus bar and slack bus unit need to be considered. To include these violations, a penalty-function approach is used as shown in Equation 6.17.

Step 5 Compute the augmented objective function and obtain the fuel cost and active powers of the generators and compute the transient stability using the time-domain method. These are taken as the initial solutions. Calculate the fitness of each search agent.
X_α = the best search agent.
X_β = the second best search agent.
X_δ = the third best search agent.

Step 6 Set generation $t = 1$.

Step 7 Update the position of each search agent by using Equation 3.5.

Step 8 Update a, A, C.

Step 9 Calculate the fitness of each search agent and Update X_α, X_β and X_δ according to the best solution.

Step 10 If $t < T_{max}$ Set generation $t = t + 1$ and go to step 7. Otherwise X_α is the best solution.

6.4 Simulation Results

This section presents application of the proposed IGWO based solution of Transient stability and security constrained optimal power flow (TSSCOPF) problem on two test systems namely IEEE 30-bus 6-generator system and the New England 39-bus 10-generator system. A classical generator model and a constant impedance model are taken into consideration for the synchronous generator and the loads [123], respectively. All the simulations are carried out using MATLAB [249], with Intel Core i3, 2.5 GHz, 6 GB RAM. The software used for transient stability analysis is in Ref. [285].

6.4.1 Test Case A: IEEE 30-Bus 6-Generator Test System

The IEEE 30-bus 6-generator system, consists of 6 generating units interconnected with 41 transmission lines and 4 transformers. The single-line diagram and system data of this power system are given in Appendix A. The system data such as bus data, line data, and initial values of control variables are taken from [275]. The fuel cost coefficients data and the rating of generators are the same as in [124]. The total load demand for this test system are P_{Load} = 189.2 MW and Q_{Load} = 107.2 MAVr at 100 MVA base. Two widely used case studies, including the base load condition, are used to exhibit the comparison of proposed approach with the contemporary approaches. A single consisting of a three phase fault occurs near at bus 2 of line 2-5 at $t = 0s$ is considered. The study is implemented for two different fault clearing time given in Ref. [121, 124, 284].

- **Case A.1:** A 3-phase to ground fault is considered near bus 2 and in-between lines 2-5 and is cleared after 0.18s. Here integration time step is 0.1s.
- **Case A.2:** A 3-phase to ground fault is considered near bus 2 and in-between lines 2-5 and is cleared after 0.35s. Here integration time step is 0.01s.

For both the cases, number of iteration for simulation is considered as 100. Furthermore, the results of the GWO and IGWO algorithms are obtained after carrying out 30 independent run for different cases.

Case A.1: A 3-phase to ground fault is considered near bus 2 and in-between lines 2-5 and is cleared after 0.18s

The study is shown with base case loading and 3-ϕ fault near bus-2 and in-between the line 2-5. Fault clearing time (FCT) is taken as 0.18s. The optimal parameters obtained by the both GWO and IGWO algorithms for the production cost minimization objective function are presented in Table 6.1. This table also includes the results obtained by GA [121], PSO [121], ABC [124], CABC [124], WOA [125] and CWOA [125] algorithms.

TABLE 6.1: Best control variables and production cost for IEEE 30-Bus system (Case A.1)

Parameter	**GA** [**121**]	**PSO** [**121**]	**ABC** [**124**]	**CABC** [**124**]	**WOA** [**125**]	**CWOA** [**125**]	**GWO**	**IGWO**
PG1 (MW)	41.88	43.63	40.5512	41.4823	41.6772	42.3443	43.7621	44.1780
PG2 (MW)	56.38	58.05	51.9248	55.3017	57.1053	56.789	59.2737	58.2334
PG13 (MW)	22.94	23.29	18.9168	17.0909	18.3953	17.923	14.7302	18.5019
PG22 (MW)	37.63	32.49	23.811	20.8952	21.3213	18.9767	23.1303	22.842
PG23 (MW)	16.7	17.04	16.801	17.0019	17.5919	20.8343	17.0989	17.0411
PG27 (MW)	16.53	17.54	40	40.4145	35.9138	35.1727	33.5374	30.6481
T6-9 (p.u.)	1.01	1.01	-	-	0.95	0.97	1.0672	1.0198
T6-10 (p.u.)	0.95	0.96	-	-	1.01	0.99	0.9275	1.0129
T4-12 (p.u.)	1	1.01	-	-	1	0.96	0.9745	0.9934
T28-27 (p.u.)	0.97	0.97	-	-	0.97	1.01	1.052	0.9965
VG1 (p.u.)	-	-	0.9858	0.9723	1.0213	1.0241	1.05	1.05
VG2 (p.u.)	-	-	0.978	0.9738	1.0335	1.0234	1.0473	1.0482
VG13 (p.u.)	-	-	1.0601	1.0785	1.0205	1.0069	1.0494	1.0498
VG22 (p.u.)	-	-	1.0191	1.0241	1.0262	1.0133	1.038	1.0383
VG23 (p.u.)	-	-	1.04	1.034	1.043	1.0102	1.049	1.0424
VG27 (p.u.)	-	-	1.0639	1.061	1.04	1.0382	1.05	1.0499
PL (MW)	-	-	-	-	-	-	2.3329	2.2321
Minimum Cost ($/h)	594.3117	585.736	577.78	577.63	576.4648	577.6347	574.2187	**573.9821**

- means not reported in the referred literature

The production cost calculated by using optimal parameters using Equation 6.4. By inspecting the calculated production costs obtained by different algorithms, it may be observed that the production cost 573.98 $\$/h$ which is obtained by using proposed IGWO parameters is the minimum. The comparative convergence analysis, obtained by both GWO and the proposed IGWO, is shown in Figure 6.2. This figure presents that IGWO based objective function value for this case converges smoothly and reaches the near global optimal value. The relative rotor angle trajectories are also shown in Figures 6.3 and 6.4 as obtained by using GWO and IGWO. It may be observed from these figures all the generators are stable and the rotor angles of all the generators do not cross the value δ^{max}.

Moreover, the statistical comparison of best, worst and mean fuel cost values as obtained using different algorithms are listed in Table 6.2.

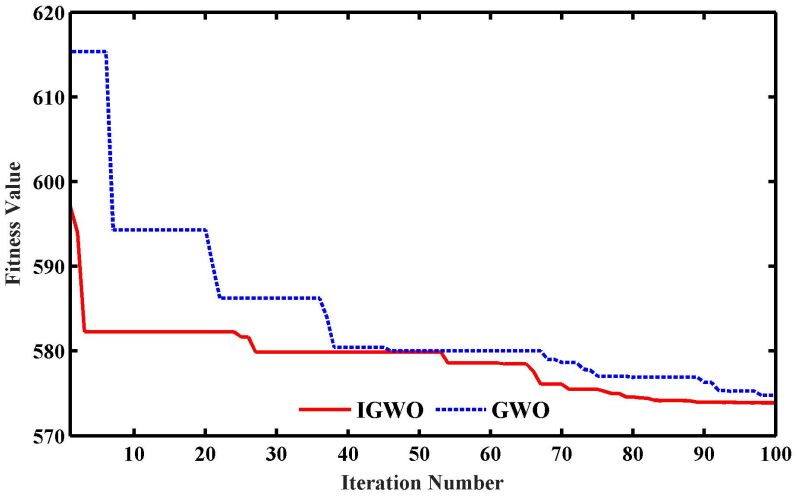

FIGURE 6.2: Variation of fitness value against iteration for Case A.1

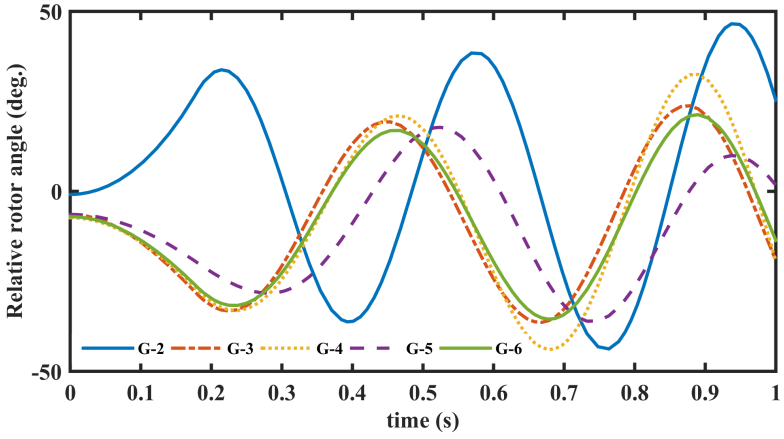

FIGURE 6.3: Relative rotor angles obtained by the GWO for Case A.1

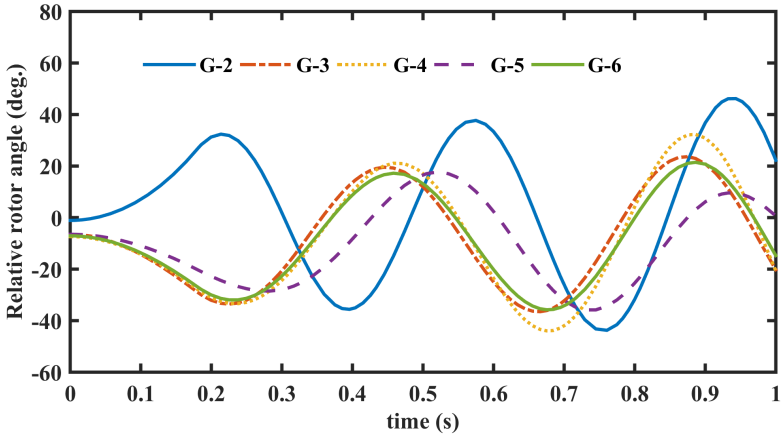

FIGURE 6.4: Relative rotor angles obtained by the IGWO for Case A.1

Table 6.2: Comparative results of IEEE 30-Bus system for Case A.1

Cost($/h)	**GA [121]**	**PSO [121]**	**ABC [124]**	**CABC [124]**	**WOA [125]**	**CWOA [125]**	**GWO**	**IGWO**
Minimum	585.62	585.17	577.78	577.63	576.46	577.634	574.21	**573.98**
Maximum	585.71	585.69	583.9	580.83	587.08	582.78	583.67	**579.11**
Average	585.66	585.34	580.84	579.23	568.98	565.92	577.74	**576.84**

Case A.2: A 3-phase to ground fault is considered near bus 2 and in-between lines 2-5 and is cleared after 0.35s

The study is shown with base case loading and 3-ϕ fault near bus-2 and in-between the line 2-5. Fault clearing time (FCT) is taken as 0.35s. The optimal parameters

Table 6.3: Best control variables and production cost for IEEE 30-Bus system (Case A.2)

Parameter	**EPNN [121]**	**ABC [124]**	**CABC [124]**	**WOA [125]**	**CWOA [125]**	**GWO**	**IGWO**
PG1 (MW)	48.95	40.6796	42.7411	41.6443	42.3443	45.857	48.2694
PG2 (MW)	38.41	55.00	54.7034	55.4773	56.789	48.2536	48.8317
PG13 (MW)	23.34	15.4663	14.8287	15.9703	17.923	17.0005	19.8346
PG22 (MW)	24.65	22.1919	24.3374	21.3843	18.9767	25.3365	23.8431
PG23 (MW)	17.61	19.9917	17.9055	18.5905	20.8343	18.8316	16.7253
PG27 (MW)	38.99	38.8263	37.6754	39.0933	35.1727	36.3593	34.155
T6-9 (p.u.)	1.01	-	-	0.98	0.97	0.9243	0.9424
T6-10 (p.u.)	0.98	-	-	1.01	0.99	0.9681	0.9309
T4-12 (p.u.)	1.03	-	-	1.04	0.96	0.946	0.9496
T28-27 (p.u.)	1.04	-	-	1.01	1.01	0.9944	0.9309
VG1 (p.u.)	0.99	0.97	0.9733	1.0273	1.0241	0.9903	0.9727
VG2 (p.u.)	0.99	0.9715	0.9653	1.0466	1.0234	1.0168	0.9726
VG13 (p.u.)	1.07	1.0752	1.062	1.0078	1.0069	1.0488	1.0485
VG22 (p.u.)	0.99	1.0187	1.0106	1.01	1.0133	1.04	1.0255
VG23 (p.u.)	1.02	1.0264	1.0242	1.0366	1.0102	1.0421	1.03
VG27 (p.u.)	1.05	1.0643	1.0685	1.0007	1.0382	1.0467	1.0489
PL (MW)	-	-	-	-	-	2.3954	2.4513
Minimum Cost ($/h)	585.102	577.71	577.47	577.3819	577.2578	577.2002	**576.9377**

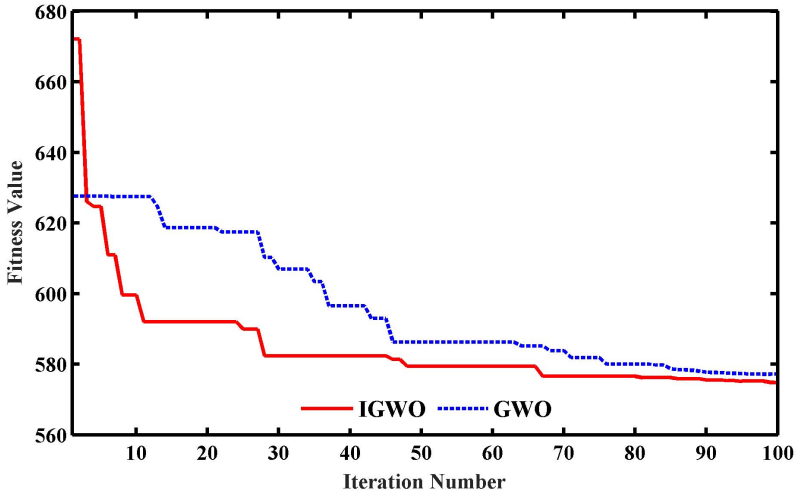

FIGURE 6.5: Variation of fitness value against iteration for Case A.2

obtained by the both GWO and IGWO algorithms for the production cost minimization objective function are presented in Table 6.3. This table also includes the results obtained by EPNN [121], ABC [124], CABC [124], WOA [125] and CWOA [125] algorithms.

The production cost is calculated by using optimal parameters using Equation 6.4. By inspecting the calculated production costs obtained by different algorithms it is observed that the production cost 576.9377 $\$/h$ which is obtained by using proposed IGWO parameters is the minimum. The comparative convergence analysis, obtained by both GWO and the proposed IGWO, is shown in Figure 6.5. This figure presents that IGWO based objective function value for this case converges smoothly and reaches the near global optimal value. The relative rotor angle trajectories are also shown in Figures 6.6 and 6.7 by using GWO and IGWO respectively. As seen from these figures all the generators are stable and the rotor angles of all the generators do not cross the value δ^{max}. Moreover, the statistical comparison of best, worst and mean fuel cost values as obtained using different algorithms are listed in Table 6.4.

6.4.2 Test Case B: IEEE 39-Bus 10-Generator System

The IEEE 39-bus test system, consisting of ten generating units interconnected with forty-six transmission lines. The single-line diagram and system data of this power

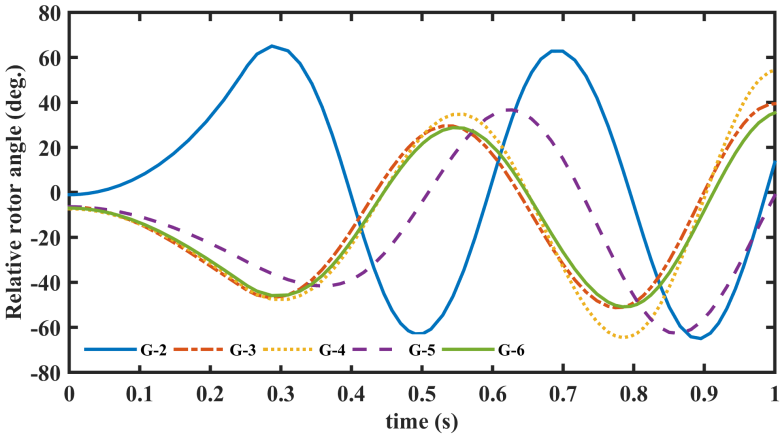

FIGURE 6.6: Relative rotor angles obtained by the GWO for Case A.2

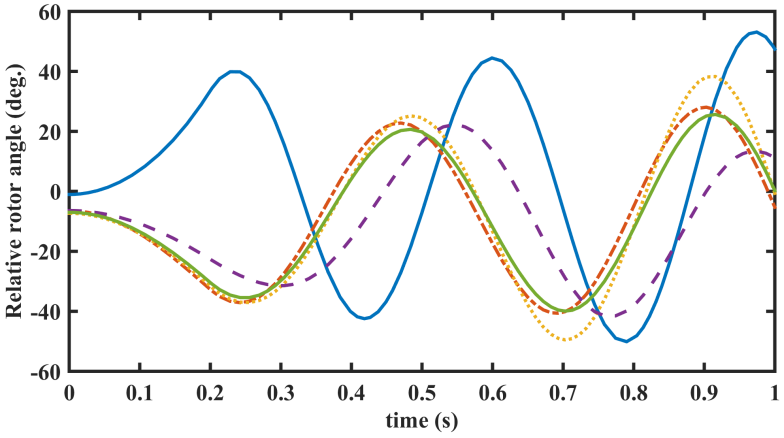

FIGURE 6.7: Relative rotor angles obtained by the IGWO for Case A.2

TABLE 6.4: Comparative results of IEEE 30-Bus system for Case A.2

Cost ($/h)	**EP [121]**	**EPNN [121]**	**ABC [124]**	**CABC [124]**	**WOA [125]**	**CWOA [125]**	**GWO**	**IGWO**
Minimum	585.15	585.12	577.71	577.47	577.3819	577.257	577.20	**576.93**
Maximum	586.86	586.73	583.26	580.74	-	-	583.48	**579.87**
Average	585.83	585.84	580.21	579.10	-	-	578.79	**577.69**

TABLE 6.5: Cost-coefficient data of 10-Generator 39-Bus System

Generator	**Bus**	**For Cases B.1 & B.2 as per Ref. [221, 287]**			**For Case B.3 as per Ref. [250]**		
Number	**Number**	α_i	β_i	γ_i	α_i	β_i	γ_i
1	30	0.0193	6.9	0	0.01	0.3	0.2
2	31	0.0111	3.7	0	0.01	0.3	0.2
3	32	0.0104	2.8	0	0.01	0.3	0.2
4	33	0.0088	4.7	0	0.01	0.3	0.2
5	34	0.0128	2.8	0	0.01	0.3	0.2
6	35	0.0094	3.7	0	0.01	0.3	0.2
7	36	0.0099	4.8	0	0.01	0.3	0.2
8	37	0.0113	3.6	0	0.01	0.3	0.2
9	38	0.0071	3.7	0	0.01	0.3	0.2
10	39	0.0065	3.9	0	0.01	0.3	0.2

system are given in Appendix A. The system data such as bus data, line data, and initial values of control variables are taken from [286]. The fuel cost coefficients data and the rating of generators are the same as in [221, 275, 287]. The upper and lower limits of all the bus voltages magnitudes are available in [275]. The total load demand for the operating condition considered for this test system are $P_{Load} = 6098$ MW and $Q_{Load} = 1409$ MVAr. Three widely used case studies, including the base load condition, are used to exhibit the comparison of proposed approach with the contemporary approaches.

- **Case B.1:** A 3-phase to ground fault is considered near bus 29 and in-between lines 28-29 and is cleared after 0.1s [218].
- **Case B.2:** A 3-phase to ground fault is considered near bus 17 and in-between lines 17-18 and is cleared after 0.2s [124, 221].
- **Case B.3:** A 3-phase to ground fault is considered near bus 17 and in-between lines 17-18 and is cleared after 0.2s [124].

The fuel cost coefficient data and the rating of the generators are considered as given in [221, 287] for case studies B.1 and B.2, whereas for case B.3, these values are taken from [250] as shown in Table 6.5. For these cases, population size and maximum number of iterations for optimization are considered as 50 and 100 respectively. Furthermore, the results of the GWO and IGWO algorithms are obtained after carrying out 30 independent run for different cases.

Case B.1: A 3-phase to ground fault is considered near bus 29 and in-between lines 28-29 and is cleared after 0.1s

The study is shown with base case loading and 3-ϕ fault near bus-29 and in-between the line 28-29. Fault clearing time (FCT) is taken as 0.1s. The optimal parameters obtained by the both GWO and IGWO algorithms for the production cost minimization objective function are presented in Table 6.6. This table also includes the results obtained by Dynamic Simulation Algorithm (DSA) [288], generator Classical Model(CM) [289], generator Detailed Model (DM) [289], algorithms.

The production cost is calculated by using optimal parameters using Equation 6.4. By inspecting the calculated production costs obtained by different algorithms it is observed that the production cost 60906.32 $\$/h$ which is obtained by using proposed

Table 6.6: Best control variables and production cost for IEEE 39-Bus system (Case B.1)

Parameter	**DSA [288]**	**CM [289]**	**DM [289]**	**GWO**	**IGWO**
PG30 (MW)	247.83	248.73	249.45	226.27	235.47
PG31 (MW)	577.23	577.84	578.36	558.11	549.93
PG32 (MW)	653.41	654.47	654.35	613.28	627.82
PG33 (MW)	643.28	645.00	641.76	629.68	619.26
PG34 (MW)	517.78	518.82	517.41	506.42	499.73
PG35 (MW)	662.46	664.32	660.73	630.07	635.26
PG36 (MW)	569.59	571.37	568.18	544.63	547.51
PG37 (MW)	543.88	547.81	547.69	518.58	525.40
PG38 (MW)	774.54	752.02	754.61	798.71	785.37
PG39 (MW)	1000.35	995.60	1003.18	1100.00	1100.00
V30(p.u.)	0.98	1.01	1.01	1.014	1.014
V31(p.u.)	1.07	1.08	1.08	1.04	1.05
V32(p.u.)	1.00	1.02	1.02	1.04	1.05
V33(p.u.)	1.01	1.01	1.01	1.05	1.05
V34(p.u.)	1.01	1.02	1.02	1.04	1.05
V35(p.u.)	1.06	1.06	1.06	1.05	1.05
V36(p.u.)	1.08	1.09	1.09	1.04	1.05
V37(p.u.)	1.01	1.04	1.04	1.04	1.03
V38(p.u.)	1.05	1.03	1.03	1.05	1.05
V39(p.u.)	1.01	1.05	1.05	1.04	1.02
Minimum Cost($/h)	61799.68	61600.76	61597.76	60912.81	**60906.32**
Maximum Cost($/h)	-	-	-	60984.22	**61243.33**
Average Cost($/h)	-	-	-	66941.25	**61064.78**

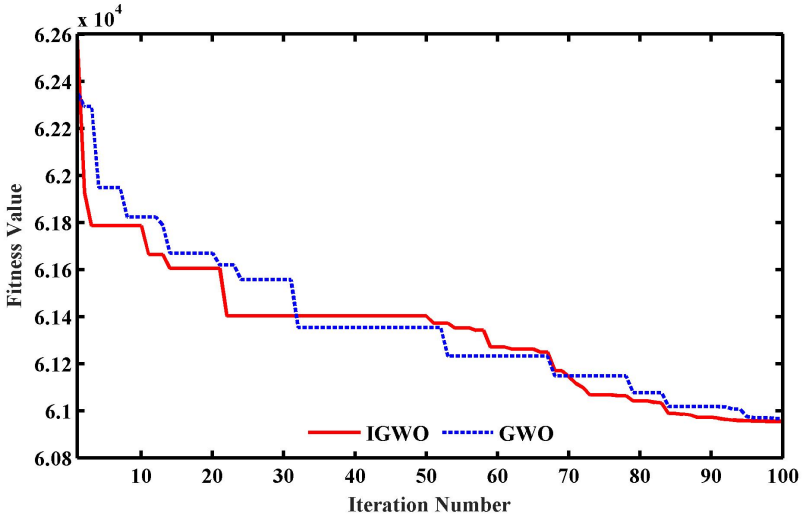

FIGURE 6.8: Variation of fitness value against iteration for Case B.1

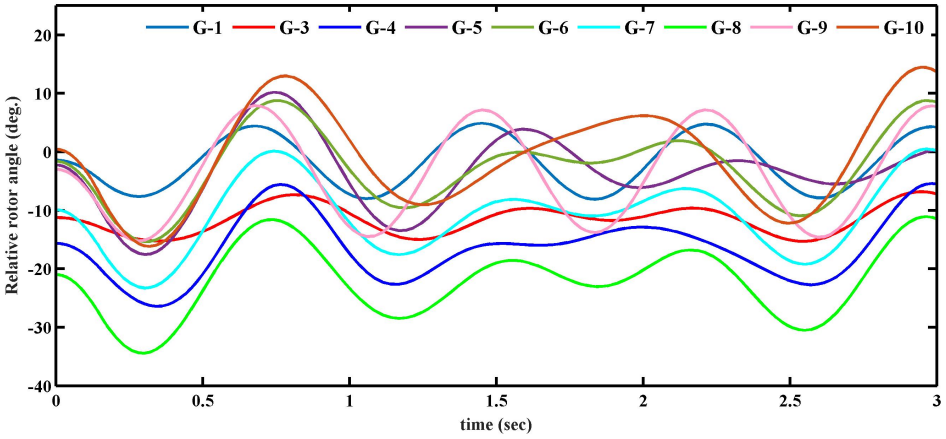

FIGURE 6.9: Relative rotor angles obtained by IGWO for Case B.1

IGWO parameters is the minimum. The comparative convergence analysis, obtained by both GWO and the proposed IGWO, is shown in Figure 6.8. This figure presents that IGWO based objective function value for this case converges smoothly and reaches the near global optimal value. The relative rotor angle trajectories are also shown in Figure 6.9 by using IGWO. As seen from this figure all the generators are stable and the rotor angles of all the generators do not cross the value δ^{max}.

Case B.2: A 3-phase to ground fault is considered near bus 17 and in-between lines 17-18 and is cleared after 0.2s

The study is shown with base case loading and 3-ϕ fault near bus-17 and in-between the line 17-18. Fault clearing time (FCT) is taken as 0.2s. The optimal parameters obtained by the both GWO and IGWO algorithms for the production cost minimization objective function are presented in Table 6.7. This table also includes the results obtained by TS [221], ABC [124], CABC [124], WOA [290] and CWOA [290] algorithms. The comparative convergence analysis, obtained by both GWO and the proposed IGWO, is shown in Figure 6.10. This figure presents that IGWO based objective function value for this case converges smoothly and reaches the near global optimal value.

Table 6.7: Best control variables and production cost for IEEE 39-Bus system (Case B.2)

Parameter	**TS [221]**	**ABC [124]**	**CABC [124]**	**WOA [290]**	**CWOA [290]**	**GWO**	**IGWO**
PG30 (MW)	243.61	313.03	300.00	329.60	306.89	226.24	242.98
PG31 (MW)	568.34	616.15	570.30	527.49	520.56	551.78	562.68
PG32 (MW)	643.81	610.23	653.26	601.54	616.80	630.07	641.80
PG33 (MW)	644.57	617.57	600.00	647.77	600.76	612.02	629.26
PG34 (MW)	243.58	455.23	443.87	400.44	395.67	499.80	507.35
PG35 (MW)	658.27	602.95	645.14	605.55	645.78	641.10	655.09
PG36 (MW)	565.44	507.08	503.38	513.34	510.12	533.96	562.49
PG37 (MW)	538.17	600.00	600.00	568.86	598.46	534.27	533.69
PG38 (MW)	533.19	702.48	719.36	778.89	801.56	797.71	807.38
PG39 (MW)	1200.00	1110.00	1100.00	1168.69	1149.68	1098.84	983.09
V30(p.u.)	-	1.00	1.01	1.01	1.02	1.04	1.00
V31(p.u.)	-	1.01	1.00	1.00	1.02	1.05	1.05
V32(p.u.)	-	1.02	1.01	1.02	1.03	1.03	1.05
V33(p.u.)	-	1.03	1.03	0.99	1.01	1.04	1.05
V34(p.u.)	-	1.01	1.02	0.97	1.04	1.03	1.05
V35(p.u.)	-	1.03	1.03	1.02	1.00	1.05	1.05
V36(p.u.)	-	1.03	1.03	1.00	1.00	1.02	1.05
V37(p.u.)	-	1.02	1.02	1.01	0.98	1.04	1.03
V38(p.u.)	-	1.03	1.04	1.02	1.01	1.05	1.05
V39(p.u.)	-	0.95	0.96	0.99	1.00	1.00	1.01
Cost($/h)	62261.28	61485.48	61369.19	61126.23	61106.27	60917.17	**60783.22**

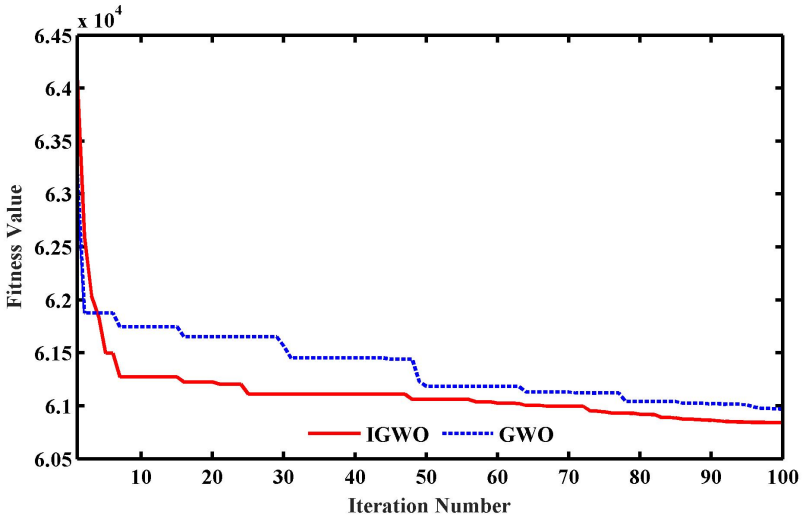

FIGURE 6.10: Variation of fitness value against iteration for Case B.2

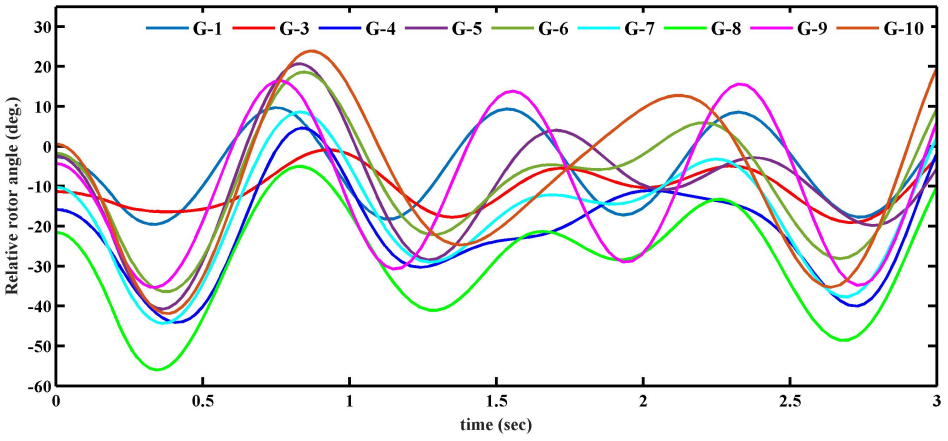

FIGURE 6.11: Relative rotor angles obtained by IGWO for Case B.2

TABLE 6.8: Comparative Results of IEEE 39-bus Test System for Case B.2

Cost ($/h)	TS [221]	ABC [124]	CABC [124]	WOA [290]	CWOA [290]	GWO	IGWO
Minimum	62261.28	61485.48	61369.19	61126.23	61106.27	60917.17	**60783.22**
Maximum	-	61703.42	61602.53	61198.23	61176.67	61134.71	**61091.46**
Average	-	61594.45	61485.86	61132.55	61126.67	61094.63	**60984.44**

The production cost is calculated by using optimal parameters using Equation 6.4. By inspecting the calculated production costs obtained by different algorithms it is observed that the production cost 60783.22 $\$/h$ which is obtained by using proposed IGWO parameters is the minimum. The relative rotor angle trajectories are also shown in Figure 6.11 by using IGWO. As seen from this figure all the generators are stable and the rotor angles of all the generators do not cross the value δ^{max}. Moreover, the statistical comparison of best, worst and mean fuel cost values as obtained using different algorithms are listed in Table 6.8.

Case B.3: A 3-phase to ground fault is considered near bus 17 and in-between lines 17-18 and is cleared after 0.2s

The study is shown with base case loading and 3-ϕ fault near bus-17 and in-between the line 17-18. Fault clearing time (FCT) is taken as 0.2s. The optimal parameters obtained by the both GWO and IGWO algorithms for the production cost minimization objective function are presented in Table 6.9. This table also includes the results obtained by ABC [124], CABC [124], WOA [290] and CWOA [290] algorithms.

The production cost is calculated by using optimal parameters using Equation 6.4. By inspecting the calculated production costs obtained by different algorithms it is observed that the production cost 35256.50 $\$/h$ which is obtained by using proposed

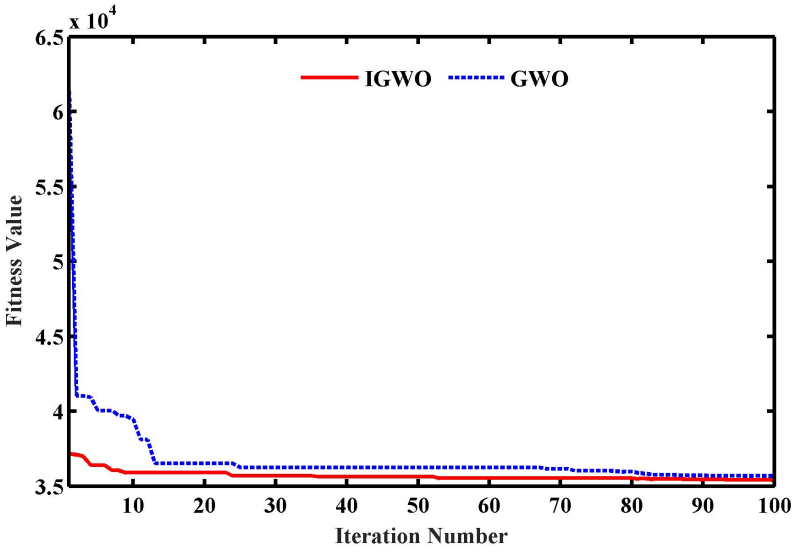

FIGURE 6.12: Variation of fitness value against iteration for Case B.3

IGWO parameters is the minimum. The comparative convergence analysis, obtained by both GWO and the proposed IGWO, is shown in Figure 6.12. This figure presents that IGWO based objective function value for this case converges smoothly and reaches the near global optimal value. The relative rotor angle trajectories are also shown in Figure 6.13 by using IGWO. As seen from this figure all the generators

TABLE 6.9: Best control variables and production cost for IEEE 39-Bus system (Case B.3)

Parameter	**ABC [124]**	**CABC [124]**	**WOA [290]**	**CWOA [290]**	**GWO**	**IGWO**
PG30 (MW)	336.96	350.00	393.60	364.56	569.02	574.84
PG31 (MW)	562.59	564.26	525.56	529.89	586.12	574.30
PG32 (MW)	549.17	577.14	560.19	587.78	582.10	576.21
PG33 (MW)	627.34	600.00	612.34	609.98	569.95	557.32
PG34 (MW)	489.38	491.62	445.56	446.62	508.00	508.00
PG35 (MW)	535.59	556.22	525.55	555.55	588.68	566.71
PG36 (MW)	577.91	564.63	567.61	543.78	573.67	554.28
PG37 (MW)	580.68	568.49	610.45	598.23	562.35	545.17
PG38 (MW)	759.98	763.34	745.68	788.67	596.36	717.60
PG39 (MW)	1119.70	1100.00	1149.70	1109.26	989.56	951.37
V30(p.u.)	1.03	1.00	1.03	1.03	0.95	0.95
V31(p.u.)	1.05	0.98	1.02	1.01	0.99	1.04
V32(p.u.)	0.99	1.01	1.01	1.02	0.98	1.00
V33(p.u.)	1.05	1.06	1.00	1.01	0.97	1.01
V34(p.u.)	1.02	1.06	1.00	1.00	1.01	1.00
V35(p.u.)	1.05	1.06	1.01	0.96	1.02	0.99
V36(p.u.)	1.03	1.06	0.99	0.99	0.98	0.98
V37(p.u.)	1.01	1.01	0.99	1.00	0.95	0.96
V38(p.u.)	0.95	1.06	1.05	1.01	1.05	1.05
V39(p.u.)	1.03	1.00	1.00	0.97	0.95	0.96
Cost($/h)	36058.69	35869.23	35930.45	35857.71	35680.63	**35256.50**

TABLE 6.10: Comparative results of IEEE 39-Bus 10-Generator system for Case B.3

Cost ($/h)	**ABC [124]**	**CABC [124]**	**WOA [290]**	**CWOA [290]**	**GWO**	**IGWO**
Minimum	36058.69	35869.23	35930.45	35857.71	35680.63	**35256.50**
Maximum	36678.11	36258.53	36882.78	36987.09	35874.44	**35604.01**
Average	36368.4	36063.88	36828.45	36619.34	35617.61	**35403.46**

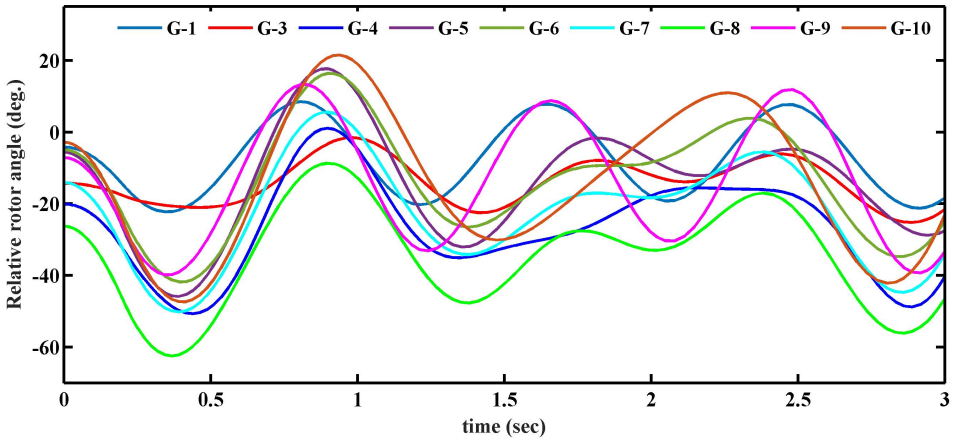

FIGURE 6.13: Relative rotor angles obtained by IGWO for Case B.3

are stable and the rotor angles of all the generators do not cross the value δ^{max}. Moreover, the statistical comparison of best, worst and mean fuel cost values as obtained using different algorithms are listed in Table 6.10.

The following interpretations can be drawn from the results shown in this section:

- The optimal setting of control variables obtained from the both GWO and proposed IGWO for fuel cost minimization.
- The results obtained from proposed IGWO-TSSCOPF are compared with the other obtained results offered by different published techniques for both IEEE 30-bus 6-generator system and IEEE 39-bus 10-generator system.
- It is observed from the comparison that the total cost from IGWO is less than that obtained by all other published algorithms for both IEEE 30-bus 6-generator system and IEEE 39-bus 10-generator system..
- Moreover, the statical comparison of best, worst and mean fuel cost values of different algorithms are listed in results. From the statical results, it is clear that the difference among the best, worst and mean objective cost values, as obtained by IGWO, are very much insignificant.
- It is observed from the results the worst value of IGWO is even much batter than the best values obtained by the other indicated methods.

- Results clearly suggest that the proposed IGWO-TSSCOPF method produces similar results in most of the trials and robustness of the proposed method is thus proved.

6.5 Summary

Applications of meta-heuristic algorithms in power engineering have increased in recent years. The meta-heuristic paradigms are able to solve complex power engineering problems and help to find a optimal solution. In this chapter the applications of the proposed IGWO is exhibited in the area of optimal power flow with respect to both system security constraints and transient stability constraints and the application results are presented for two systems as IEEE 30-bus system and IEEE 39-bus system. Based on this chapter following conclusions may be drawn:

1. An OPF problem has been developed as a constrained optimization problem by incorporating different stability constraints i.e. transmission, generation and stability constrains.

2. Penalty factor based approach has been employed in order to enforce all inequality constraints.

3. The solution obtained by the proposed IGWO-TSSCOPF have been compared with those obtained by other heuristic methods in the literature.

4. It has been observed that, the performance of the proposed method is promising. The validation of the performance has been carried out with the help of nonlinear TDS.

5. The application results reveal that proposed method effectively reduces the generation cost by considering the stability and security of the power system.

Chapter 7

Conclusions and Future Scope

[In this chapter the major research findings of the work done by the author are summarized and suggestions have also been made to extend the current research work.]

The objective of this chapter is to summarize the main contributions and findings of the work carried out in this thesis and to suggest scope for future research work in this area. In the deregulated and competitive scenario of power system, the operation of modern power systems has become complicated. This thesis focuses on the most important aspects related to power system stability, particularly security assessment, dynamic stability assessment and their enhancement.

Chapter 3 of this thesis has presented an improved version of Grey Wolf Optimizer (GWO), named as Intelligent Grey Wolf Optimizer (IGWO). In this chapter an efficient sinusoidal function has been employed to improve the bridging mechanism between the exploration and exploitation phase of GWO. Exploration and exploitation capabilities of GWO are enhanced with this newly developed mechanism. Further, opposition based learning concept has been employed in initialization phase of the GWO along with this sinusoidal bridging mechanism. The combined effect of these two modifications is positive and the implication of these modifications can be observed through the results on various benchmarking functions. The performance of the proposed variant has been validated on standard 22 benchmark functions of different properties and nature. The effectiveness of the proposed algorithm IGWO

is throughly investigated and presented. The conclusions drawn from this work are summarized below.

1. There is a scope of improvement in existing meta-heuristic techniques for many complex optimization problems. The developed IGWO perform better than its previous model and the existing meta-heuristic models for the standard 22 benchmark functions.

2. The modifications suggested in order to improved GWO algorithm are effectively contributing towards enhancing the convergence, accuracy and efficiency of the algorithm.

3. Proposed opposition based modification, disperses tentative solutions near the promising region so virtually reduces search space of meta-heuristics. This feature makes the algorithms more efficient.

4. The obtained results reveals that the proposed variant IGWO shows promising results on majority of the benchmark functions. The superiority of this variant has been validated by optimal values of standard deviation, mean and p-value less than the significance level.

In Chapter 4 of this thesis the application of ANN approaches for online static security assessment and contingency analysis of power systems has been investigated. Attempt has been made to employ supervised learning architecture for ranking and classification of the probable contingencies. In supervised learning approaches feature selection process is very critical because these approaches are employed for online applications. By considering this fact meta-heuristic based distinct feature selection approach has been proposed and the application results are presented for two systems namely IEEE 30-bus system and IEEE 39-bus system. Two different ANN-based architectures i.e. Radial Basis Function Neural Network (RBFNN) and Feed Forward Neural Network (FFNN) have been investigated for online contingency classification. The RBFNN and FFNN have been trained using some selected features offered by the proposed IGWO based feature selection method. A large number of load patterns have been generated by randomly perturbing the real and reactive loads on all the buses to generate a data set that is representative of all possible operating conditions. For each operating condition, a contingency is simulated.

Two Performance Indices (PIs) as PI_{MVA} and PI_{VQ} have been used to classify the contingency into different critical and non-critical classes. A supervised learning approach to fast and accurate power system security assessment and contingency analysis has been proposed in this chapter. Work has been done to improve the classification accuracy and reduce the computational complexity by incorporating the IGWO based feature selection method. The suitability of the proposed model for contingency analysis as a decision making tool for online application at the EMS has been investigated. Following conclusions are drawn from this chapter:

1. For feature selection task, new version of GWO algorithm named as IGWO has been proposed and employed for performing feature selection task. It has been observed that the proposed IGWO based feature selection technique shows promising results, when it is compared with previously published approaches.

2. The results of comparative study for two power systems show that the proposed RBFNN yields results with higher accuracy in comparison to the existing contemporary approaches.

3. The overall accuracy of the test results for unseen samples highlights the capability and the suitability of the proposed approach for online application at EMS.

4. The proposed method is also capable of contingency ranking under uncertain loading condition.

5. The proposed RBFNN method gives excellent accuracy (more than 99%) for contingency classification even with a very small feature subset. Therefore, proposed RBFNN-based method may serve as a promising tool for online contingency classification.

Chapter 5, of the thesis is devoted for online assessment of transient stability of power system. A supervised learning algorithm is investigated for the stability identification which is fast and accurate. In this chapter, a new index named Transient Stability Index (TSI) is proposed for identification of the stability status of individual generator in term of its synchronism. The proposed index is based on the Time Domain Simulation (TDS) of the swing equation. An application of the RBFNN

has been investigated for the online identification of generator criticality and TSA of the system for set of probable contingencies. The RBFNN is trained by taking the wide ranging dataset consisting of the randomly varied real and reactive loads at all the buses. The TSI values of all the generators and "Out of Step" time of system are obtained from the trained RBFNN for the unseen operating conditions. The effectiveness of the proposed scheme for online TSA is tested on IEEE 10-generator 39-bus New England system, IEEE 68-bus 16 generator and IEEE 50-generator 145-bus power systems at different loading levels with random perturbations. Thus the proposed unified TSA scheme can provide vital solution to identify the generator criticality and instability problem to the operator at EMS. From this chapter following conclusions can be drawn:

1. A fast and highly accurate RBFNN based transient stability assessment of power system has been carried out for different size small to large power systems considering different operating conditions for the probable contingencies.

2. The online prediction of transient instability within a few cycles from Fault Clearing Time (FCT) is determined.

3. Proposed TSI has been employed to do the assessment of system stability, to rank the generators as per the criticality and for identification of the candidate generators for application of the control actions such as coherent group identification and generator rescheduling.

4. The proposed method is based on the prediction of TSI values of each generator for unseen operating condition using RBFNN for a given contingency and through the predicted value of TSI the stability of the system is assessed.

5. For all the unseen operating cases the average error in predicting the TSI using RBFNN is very less and the proposed RBFNN is able to classify stability rapidly with high accuracy.

6. Both informations about ranking obtained from the TSI value of each generating unit and TSI based coherent group information are important for selecting the units for change the generation during generation rescheduling as preventive control action.

7. The proposed RBFNN based method provides better results than the existing methods and they are independent of minor changes in topology of power systems.

In Chapter 6, the applications of the proposed IGWO is exhibited in the area of optimal power flow with respect to both system security constraints and transient stability constraints. An OPF problem has been developed as a constrained optimization problem by incorporating different stability constraints i.e. transmission, generation and stability constrains. Penalty factor based approach has been employed in order to enforce all inequality constraints. The solutions obtained by the proposed IGWO-TSSCOPF have been compared with those obtained by other heuristic methods in the literature. The validation of the performance has been carried out with the help of nonlinear TDS. The application results have been presented for two systems as IEEE 30-bus system and IEEE 39-bus system. It has been observed that, the performance of this proposed method is promising. Based on this chapter, following conclusions may be drawn:

1. Penalty factor based objective function reduces handling of constraints and make the problem simple by considering all inequality constraints.

2. Proposed opposition based modification, disperses tentative solutions near the promising region so virtually reduces the problem search space of meta-heuristics. This feature makes the algorithm more efficient.

3. The statistical analysis reveals that TSSCOPF using proposed IGWO algorithm is improved to a good degree of optima searching ability.

4. The solution obtained by the proposed IGWO-TSSCOPF have been compared with those obtained by other heuristic methods in the literature. It has been observed that, the performance of this proposed method is promising. The validation of the performance has been carried out with the help of nonlinear TDS.

5. The application results reveal that proposed method effectively reduces the generation cost by considering the stability and security of the power system.

Salient Contributions

Major contributions of the thesis may be summarized as below:

1. Developed the improved version of the Grey Wolf Optimizer (GWO) named Intelligent Grey Wolf Optimizer (IGWO) to solve large-scale complex optimization problems and tested over standard 22 benchmark functions.

2. Explored two applications of the IGWO to solve dimension reduction (feature selection) problem for supervised learning engine and Transient Stability and Security Constrained Optimal Fower Flow (TSSCOPF) problem for enhancing the stability and security of the power system.

3. Proposed appropriate modification in scalar Performance Indices (PIs) for contingency analysis and static security assessment.

4. Developed a new Transient Stability Index (TSI) to identify the stability status of each generator in terms of their synchronism.

5. Investigated different ANN architectures for fast and accurate contingency analysis, online static security assessment and online transient stability assessment capable of performing well under uncertain loading condition while handling the contingencies.

6. Proposed a unified approach for contingency analysis, online static security assessment, online transient stability assessment and security & stability enhancement of power systems.

Future Research Scope

Now a days power systems are very complex and having a large number of components at all the levels i.e. generation, transmission and distribution. So a unified scheme is required for monitoring and control of system against the power system instabilities. The online assessment of the power system stability is a key issue for the operator. This thesis attempts to address major issues like contingency analysis, static security assessment, transient stability assessment and TSSCOPF as a

method of enhancement of transient stability and security of power systems. The following are suggestions for future research direction in these areas:

1. The present research work is focused around the conventional generation resources. However, the problem may be extended with the inclusion of renewable energy resources with the conventional generation resources.

2. In this work, only ANN based supervised learning engines have been employed. This may be extended to compare various other computational intelligence methods like Deep Learning Programming. This may lead to a new solution for more accurate and fast assessment of power system stability.

3. In this work, focus is on the assessment part of the stability alone. Therefore the methods of preventive control and emergency control can be investigated.

4. This work can be extended for voltage stability assessment and control, and the preventive and emergency control for voltage instability can also be investigated.

Appendix A

Test Systems

The single-line diagrams, bus, line and other data of various test systems considered for simulation during thesis work are given in this appendix.

A.1 IEEE 30-Bus, 6-Generator Test System

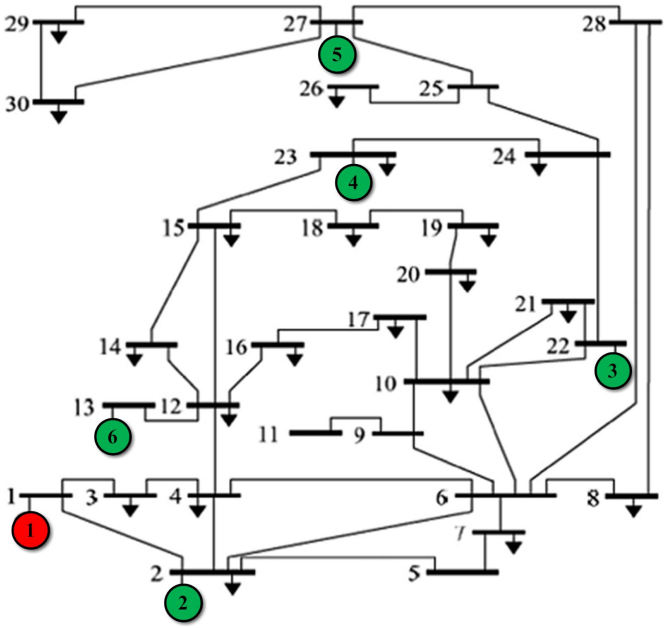

FIGURE A.1: Single line diagram of IEEE 30-Bus System

TABLE A.1: Bus data of IEEE 30-Bus, 6-Generator System

Bus No.	**Active Load**, P_d **(MW)**	**Reactive Load**, Q_d **(MVAr)**	V_m **(p.u.)**	V_θ **(degree)**
1	0	0	1	0
2	21.7	12.7	1	-0.41549
3	2.4	1.2	0.983138	-1.52207
4	7.6	1.6	0.980093	-1.79473
5	0	0	0.982406	-1.86382
6	0	0	0.973184	-2.26696
7	22.8	10.9	0.967355	-2.65184
8	30	30	0.960624	-2.72577
9	0	0	0.980506	-2.99693
10	5.8	2	0.984404	-3.37494
11	0	0	0.980506	-2.99693
12	11.2	7.5	0.985468	-1.53691
13	0	0	1	1.476163
14	6.2	1.6	0.976677	-2.30804
15	8.2	2.5	0.980229	-2.31184
16	3.5	1.8	0.977396	-2.64449
17	9	5.8	0.976865	-3.39234
18	3.2	0.9	0.96844	-3.47839
19	9.5	3.4	0.965287	-3.9582
20	2.2	0.7	0.969166	-3.87102
21	17.5	11.2	0.993383	-3.48839
22	0	0	1	-3.39273
23	3.2	1.6	1	-1.58923
24	8.7	6.7	0.988566	-2.63146
25	0	0	0.990215	-1.68999
26	3.5	2.3	0.972194	-2.13935
27	0	0	1	-0.82844
28	0	0	0.974715	-2.26593
29	2.4	0.9	0.979597	-2.1285
30	10.6	1.9	0.967883	-3.04152

TABLE A.2: Technical limits of generators of IEEE 30-Bus, 6-Generator System

Generator Number	**Bus Number**	P_G **(MW)**	Q_G **(MVAr)**	$P_{G,max}$ **(MW)**	$P_{G,min}$ **(MW)**	$Q_{G,max}$ **(MVAr)**	$Q_{G,min}$ **(MVAr)**
1	1	25.9738	-0.99848	80	0	150	-20
2	2	60.97	31.99898	80	0	60	-20
3	22	21.59	39.56997	50	0	62.5	-15
4	27	26.91	10.54051	55	0	48.7	-15
5	23	19.2	7.950952	30	0	40	-10
6	13	37	11.35288	40	0	44.7	-15

TABLE A.3: Line data of IEEE 30-Bus, 6-Generator System

Line number	**From Bus**	**To bus**	**Line Resistance (p.u.)**	Line **Reactance (p.u.)**	**Line Charging Susptance (p.u.)**	**MVA Rating**
1	1	2	0.02	0.06	0.03	130
2	1	3	0.05	0.19	0.02	130
3	2	4	0.06	0.17	0.02	65
4	3	4	0.01	0.04	0	130
5	2	5	0.05	0.2	0.02	130
6	2	6	0.06	0.18	0.02	65
7	4	6	0.01	0.04	0	90
8	5	7	0.05	0.12	0.01	70
9	6	7	0.03	0.08	0.01	130
10	6	8	0.01	0.04	0	32
11	6	9	0	0.21	0	65
12	6	10	0	0.56	0	32
13	9	11	0	0.21	0	65
14	9	10	0	0.11	0	65
15	4	12	0	0.26	0	65
16	12	13	0	0.14	0	65
17	12	14	0.12	0.26	0	32
18	12	15	0.07	0.13	0	32
19	12	16	0.09	0.2	0	32
20	14	15	0.22	0.2	0	16
21	16	17	0.08	0.19	0	16
22	15	18	0.11	0.22	0	16
23	18	19	0.06	0.13	0	16
24	19	20	0.03	0.07	0	32
25	10	20	0.09	0.21	0	32
26	10	17	0.03	0.08	0	32
27	10	21	0.03	0.07	0	32
28	10	22	0.07	0.15	0	32
29	21	22	0.01	0.02	0	32
30	15	23	0.1	0.2	0	16
31	22	24	0.12	0.18	0	16
32	23	24	0.13	0.27	0	16
33	24	25	0.19	0.33	0	16
34	25	26	0.25	0.38	0	16
35	25	27	0.11	0.21	0	16
36	28	27	0	0.4	0	65
37	27	29	0.22	0.42	0	16
38	27	30	0.32	0.6	0	16
39	29	30	0.24	0.45	0	16
40	8	28	0.06	0.2	0.02	32
41	6	28	0.02	0.06	0.01	32

TABLE A.4: Generator cost data of IEEE 30-Bus, 6-Generator System

Generator Number	α_i	β_i	γ_i
1	0.02	2	0
2	0.0175	1.75	0
3	0.0625	1	0
4	0.00834	3.25	0
5	0.025	3	0
6	0.025	3	0

A.2 IEEE 39-Bus, 10-Generator New England Test System

IEEE 39 Bus, 10 Generator New England Test System [278] consists of 39 buses, 46 transmission lines, 10 generators, 29 loads and 12 transformers. It is 345 kV dynamic test system. The bus voltage magnitude limits are $V^{min} = 0.94$ p.u. and $V^{max} = 1.06$ p.u.. Bus no. 39 is taken as slack bus.

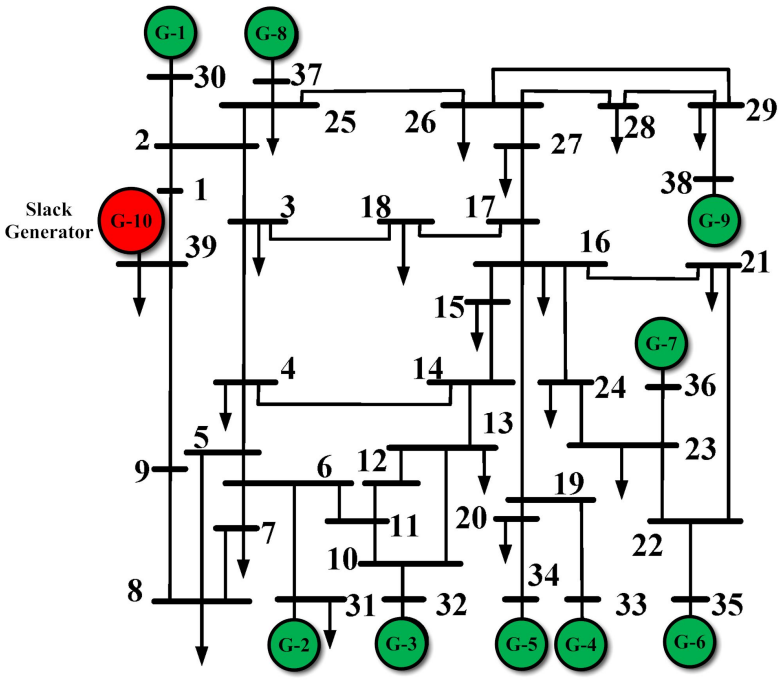

FIGURE A.2: Single line diagram of IEEE 39-Bus, 10-Generator New England System

TABLE A.5: Bus data of IEEE 39-Bus, 10- Generator System

Bus No.	**Active Load** P_d **(MW)**	**Reactive Load** Q_d **(MVAr)**	**Voltage** V_m **(p.u.)**	V_θ **(degree)**
1	97.6	44.2	1.039384	-13.5366
2	0	0	1.048494	-9.78527
3	322	2.4	1.030708	-12.2764
4	500	184	1.00446	-12.6267
5	0	0	1.006006	-11.1923
6	0	0	1.008226	-10.4083
7	233.8	84	0.998397	-12.7556
8	522	176.6	0.997872	-13.3358
9	6.5	-66.6	1.038332	-14.1784
10	0	0	1.017843	-8.17088
11	0	0	1.013386	-8.93697
12	8.53	88	1.000815	-8.99882
13	0	0	1.014923	-8.92993
14	0	0	1.012319	-10.7153
15	320	153	1.016185	-11.3454
16	329	32.3	1.03252	-10.0333
17	0	0	1.034237	-11.1164
18	158	30	1.031573	-11.9862
19	0	0	1.050107	-5.41007
20	680	103	0.991011	-6.82118
21	274	115	1.032319	-7.62875
22	0	0	1.050143	-3.18312
23	247.5	84.6	1.045145	-3.38128
24	308.6	-92.2	1.038001	-9.91376
25	224	47.2	1.057683	-8.36924
26	139	17	1.052561	-9.43877
27	281	75.5	1.038345	-11.3622
28	206	27.6	1.050374	-5.92836
29	283.5	26.9	1.050115	-3.16987
30	0	0	1.0499	-7.37047
31	9.2	4.6	0.982	0
32	0	0	0.9841	-0.18844
33	0	0	0.9972	-0.19317
34	0	0	1.0123	-1.63112
35	0	0	1.0494	1.776507
36	0	0	1.0636	4.468437
37	0	0	1.0275	-1.5829
38	0	0	1.0265	3.892818
39	1104	250	1.03	-14.5353

TABLE A.6: Line data of IEEE 39-Bus, 10-Generator System

Line Number	From Bus	To bus	Line Resistance (p.u.)	Line Reactance (p.u.)	Line Charging Susptance (p.u.)	MVA Rating
1	1	2	0.0035	0.0411	0.6987	600
2	1	39	0.001	0.025	0.75	1000
3	2	3	0.0013	0.0151	0.2572	500
4	2	25	0.007	0.0086	0.146	500
5	2	30	0	0.0181	0	900
6	3	4	0.0013	0.0213	0.2214	500
7	3	18	0.0011	0.0133	0.2138	500
8	4	5	0.0008	0.0128	0.1342	600
9	4	14	0.0008	0.0129	0.1382	500
10	5	6	0.0002	0.0026	0.0434	1200
11	5	8	0.0008	0.0112	0.1476	900
12	6	7	0.0006	0.0092	0.113	900
13	6	11	0.0007	0.0082	0.1389	480
14	6	31	0	0.025	0	1800
15	7	8	0.0004	0.0046	0.078	900
16	8	9	0.0023	0.0363	0.3804	900
17	9	39	0.001	0.025	1.2	900
18	10	11	0.0004	0.0043	0.0729	600
19	10	13	0.0004	0.0043	0.0729	600
20	10	32	0	0.02	0	900
21	12	11	0.0016	0.0435	0	500
22	12	13	0.0016	0.0435	0	500
23	13	14	0.0009	0.0101	0.1723	600
24	14	15	0.0018	0.0217	0.366	600
25	15	16	0.0009	0.0094	0.171	600
26	16	17	0.0007	0.0089	0.1342	600
27	16	19	0.0016	0.0195	0.304	600
28	16	21	0.0008	0.0135	0.2548	600
29	16	24	0.0003	0.0059	0.068	600
30	17	18	0.0007	0.0082	0.1319	600
31	17	27	0.0013	0.0173	0.3216	600
32	19	20	0.0007	0.0138	0	900
33	19	33	0.0007	0.0142	0	900
34	20	34	0.0009	0.018	0	900
35	21	22	0.0008	0.014	0.2565	900
36	22	23	0.0006	0.0096	0.1846	600
37	22	35	0	0.0143	0	900
38	23	24	0.0022	0.035	0.361	600
39	23	36	0.0005	0.0272	0	900
40	25	26	0.0032	0.0323	0.531	600
41	25	37	0.0006	0.0232	0	900
42	26	27	0.0014	0.0147	0.2396	600
43	26	28	0.0043	0.0474	0.7802	600
44	26	29	0.0057	0.0625	1.029	600
45	28	29	0.0014	0.0151	0.249	600
46	29	38	0.0008	0.0156	0	1200

TABLE A.7: Technical limits of generators of IEEE 39-Bus, 10- Generator System

Generator Number	**Bus Number**	P_G **(MW)**	Q_G **(MVAr)**	$P_{G,max}$ **(MW)**	$P_{G,min}$ **(MW)**	$Q_{G,max}$ **(MVAr)**	$Q_{G,min}$ **(MVAr)**
1	30	250	161.762	1040	0	400	140
2	31	677.871	221.574	646	0	300	-100
3	32	650	206.965	725	0	300	150
4	33	632	108.293	652	0	250	0
5	34	508	166.688	508	0	167	0
6	35	650	210.661	687	0	300	-100
7	36	560	100.165	580	0	240	0
8	37	540	-1.36945	564	0	250	0
9	38	830	21.7327	865	0	300	-150
10	39	1000	78.4674	1100	0	300	-100

TABLE A.8: Dynamic data of generators of IEEE 39-Bus, 10-Generator System

Generator Number	**xd (pu)**	**x'd (pu)**	**T'do (sec)**	**xq (pu)**	**x'q (pu)**	**T'qo (sec)**	**H (sec)**
1	1.00	0.31	10.20	0.69	0.31	1.50	4.20
2	2.95	0.697	6.56	2.82	0.697	1.50	3.03
3	2.495	0.531	5.70	2.37	0.531	1.50	3.58
4	2.62	0.436	5.69	2.58	0.436	1.50	2.86
5	6.70	1.32	5.40	6.20	1.32	0.44	2.60
6	2.54	0.50	7.30	2.41	0.5	0.40	3.48
7	2.95	0.49	5.66	2.92	0.49	1.50	2.64
8	2.90	0.57	6.70	2.80	0.57	0.41	2.43
9	2.106	0.57	4.79	2.05	0.57	1.96	3.45
10	0.20	0.06	7.00	0.19	0.06	0.70	50.00

TABLE A.9: Cost coefficient data of 10-Generator 39-Bus System

Generator Number	**Bus Number**	**As per Ref. [221, 287]**			**As per Ref. [250]**		
		α_i	β_i	γ_i	α_i	β_i	γ_i
1	30	0.0193	6.9	0	0.01	0.3	0.2
2	31	0.0111	3.7	0	0.01	0.3	0.2
3	32	0.0104	2.8	0	0.01	0.3	0.2
4	33	0.0088	4.7	0	0.01	0.3	0.2
5	34	0.0128	2.8	0	0.01	0.3	0.2
6	35	0.0094	3.7	0	0.01	0.3	0.2
7	36	0.0099	4.8	0	0.01	0.3	0.2
8	37	0.0113	3.6	0	0.01	0.3	0.2
9	38	0.0071	3.7	0	0.01	0.3	0.2
10	39	0.0065	3.9	0	0.01	0.3	0.2

A.3 IEEE 68-Bus, 16-Generator Test System

TABLE A.10: Bus data of IEEE 68-Bus, 16-Generator System

Bus No.	Bus Type	Voltage V_m	Voltage Angle V_θ	Generator		Load	
				P_g	Q_g	P_d	Q_d
1	3	1	0	0	0	2.527	1.1856
2	3	1	0	0	0	0	0
3	3	1	0	0	0	3.22	0.02
4	3	1	0	0	0	5	1.84
5	3	1	0	0	0	0	0
6	3	1	0	0	0	0	0
7	3	1	0	0	0	2.34	0.84
8	3	1	0	0	0	5.22	1.77
9	3	1	0	0	0	1.04	1.25
10	3	1	0	0	0	0	0
11	3	1	0	0	0	0	0
12	3	1	0	0	0	0.09	0.88
13	3	1	0	0	0	0	0
14	3	1	0	0	0	0	0
15	3	1	0	0	0	3.2	1.53
16	3	1	0	0	0	3.29	0.32
17	3	1	0	0	0	0	0
18	3	1	0	0	0	1.58	0.3
19	3	1	0	0	0	0	0
20	3	1	0	0	0	6.8	1.03
21	3	1	0	0	0	2.74	1.15
22	3	1	0	0	0	0	0
23	3	1	0	0	0	2.48	0.85
24	3	1	0	0	0	3.09	-0.92
25	3	1	0	0	0	2.24	0.47
26	3	1	0	0	0	1.39	0.17
27	3	1	0	0	0	2.81	0.76
28	3	1	0	0	0	2.06	0.28
29	3	1	0	0	0	2.84	0.27
30	3	1	0	0	0	0	0
31	3	1	0	0	0	0	0
32	3	1	0	0	0	0	0
33	3	1	0	0	0	1.12	0

Continued on next page

Table A.10 – *Continued from previous page*

Bus No.	**Bus Type**	**Voltage** V_m	**Voltage Angle** V_θ	**Generator**		**Load**	
				P_g	Q_g	P_d	Q_d
34	3	1	0	0	0	0	0
35	3	1	0	0	0	0	0
36	3	1	0	0	0	1.02	-0.1946
37	3	1	0	0	0	60	3
38	3	1	0	0	0	0	0
39	3	1	0	0	0	2.67	0.126
40	3	1	0	0	0	0.6563	0.2353
41	3	1	0	0	0	10	2.5
42	3	1	0	0	0	11.5	2.5
43	3	1	0	0	0	0	0
44	3	1	0	0	0	2.6755	0.0484
45	3	1	0	0	0	2.08	0.21
46	3	1	0	0	0	1.507	0.285
47	3	1	0	0	0	2.0312	0.3259
48	3	1	0	0	0	2.412	0.022
49	3	1	0	0	0	1.64	0.29
50	3	1	0	0	0	1	-1.47
51	3	1	0	0	0	3.37	-1.22
52	3	1	0	0	0	24.7	1.23
53	2	1	0	2.5	0	0	0
54	2	1	0	5.45	0	0	0
55	2	1	0	6.5	0	0	0
56	2	1	0	6.32	0	0	0
57	2	1	0	5.052	0	0	0
58	2	1	0	7	0	0	0
59	2	1	0	5.6	0	0	0
60	2	1	0	5.4	0	0	0
61	2	1	0	8	0	0	0
62	2	1	0	5	0	0	0
63	2	1	0	10	0	0	0
64	2	1	0	13.5	0	0	0
65	1	1	0	35.91	0	0	0
66	2	1	0	17.85	0	0	0
67	2	1	0	10	0	0	0
68	2	1	0	40	0	0	0

Bus type: (1) Slack Bus, (2) Generator bus, (3) Load bus

TABLE A.11: Line data of IEEE 68-Bus, 16-Generator System

Line No.	From Bus	To bus	Line Resistance (p.u.)	Line Reactance (p.u.)	Line Charging Susptance (p.u.)	MVA Rating
1	1	2	0.0035	0.0411	0.6987	0
2	1	30	0.0008	0.0074	0.48	0
3	2	3	0.0013	0.0151	0.2572	0
4	2	25	0.007	0.0086	0.146	0
5	2	53	0	0.0181	0	1.025
6	3	4	0.0013	0.0213	0.2214	0
7	3	18	0.0011	0.0133	0.2138	0
8	4	5	0.0008	0.0128	0.1342	0
9	4	14	0.0008	0.0129	0.1382	0
10	5	6	0.0002	0.0026	0.0434	0
11	5	8	0.0008	0.0112	0.1476	0
12	6	7	0.0006	0.0092	0.113	0
13	6	11	0.0007	0.0082	0.1389	0
14	6	54	0	0.025	0	1.07
15	7	8	0.0004	0.0046	0.078	0
16	8	9	0.0023	0.0363	0.3804	0
17	9	30	0.0019	0.0183	0.29	0
18	10	11	0.0004	0.0043	0.0729	0
19	10	13	0.0004	0.0043	0.0729	0
20	10	55	0	0.02	0	1.07
21	12	11	0.0016	0.0435	0	1.06
22	12	13	0.0016	0.0435	0	1.06
23	13	14	0.0009	0.0101	0.1723	0
24	14	15	0.0018	0.0217	0.366	0
25	15	16	0.0009	0.0094	0.171	0
26	16	17	0.0007	0.0089	0.1342	0
27	16	19	0.0016	0.0195	0.304	0
28	16	21	0.0008	0.0135	0.2548	0
29	16	24	0.0003	0.0059	0.068	0
30	17	18	0.0007	0.0082	0.1319	0

Continued on next page

Table A.11 – *Continued from previous page*

Line No.	From Bus	To bus	Line Resistance (p.u.)	Line Reactance (p.u.)	Line Charging Susptance (p.u.)	MVA Rating
31	17	27	0.0013	0.0173	0.3216	0
32	19	20	0.0007	0.0138	0	1.06
33	19	56	0.0007	0.0142	0	1.07
34	20	57	0.0009	0.018	0	1.009
35	21	22	0.0008	0.014	0.2565	0
36	22	23	0.0006	0.0096	0.1846	0
37	22	58	0	0.0143	0	1.025
38	23	24	0.0022	0.035	0.361	0
39	23	59	0.0005	0.0272	0	0
40	25	26	0.0032	0.0323	0.531	0
41	25	60	0.0006	0.0232	0	1.025
42	26	27	0.0014	0.0147	0.2396	0
43	26	28	0.0043	0.0474	0.7802	0
44	26	29	0.0057	0.0625	1.029	0
45	28	29	0.0014	0.0151	0.249	0
46	29	61	0.0008	0.0156	0	1.025
47	9	30	0.0019	0.0183	0.29	0
48	9	36	0.0022	0.0196	0.34	0
49	9	36	0.0022	0.0196	0.34	0
50	36	37	0.0005	0.0045	0.32	0
51	34	36	0.0033	0.0111	1.45	0
52	35	34	0.0001	0.0074	0	0.946
53	33	34	0.0011	0.0157	0.202	0
54	32	33	0.0008	0.0099	0.168	0
55	30	31	0.0013	0.0187	0.333	0
56	30	32	0.0024	0.0288	0.488	0
57	1	31	0.0016	0.0163	0.25	0
58	31	38	0.0011	0.0147	0.247	0
59	33	38	0.0036	0.0444	0.693	0
60	38	46	0.0022	0.0284	0.43	0

Continued on next page

Table A.11 – *Continued from previous page*

Line No.	From Bus	To bus	Line Resistance (p.u.)	Line Reactance (p.u.)	Line Charging Susptance (p.u.)	MVA Rating
61	46	49	0.0018	0.0274	0.27	0
62	1	47	0.0013	0.0188	1.31	0
63	47	48	0.0025	0.0268	0.4	0
64	47	48	0.0025	0.0268	0.4	0
65	48	40	0.002	0.022	1.28	0
66	35	45	0.0007	0.0175	1.39	0
67	37	43	0.0005	0.0276	0	0
68	43	44	0.0001	0.0011	0	0
69	44	45	0.0025	0.073	0	0
70	39	44	0	0.0411	0	0
71	39	45	0	0.0839	0	0
72	45	51	0.0004	0.0105	0.72	0
73	50	52	0.0012	0.0288	2.06	0
74	50	51	0.0009	0.0221	1.62	0
75	49	52	0.0076	0.1141	1.16	0
76	52	42	0.004	0.06	2.25	0
77	42	41	0.004	0.06	2.25	0
78	41	40	0.006	0.084	3.15	0
79	31	62	0	0.026	0	1.04
80	32	63	0	0.013	0	1.04
81	36	64	0	0.0075	0	1.04
82	37	65	0	0.0033	0	1.04
83	41	66	0	0.0015	0	1
84	42	67	0	0.0015	0	1
85	52	68	0	0.003	0	1
86	1	27	0.0320	0.32	0.41	1

TABLE A.12: Dynamic data of generators of IEEE 68-Bus, 16-Generator System

Generator Number	xd (pu)	x'd (pu)	T'do (sec)	xq (pu)	x'q (pu)	T'qo (sec)	H (sec)
1	0.969	0.248	12.6	0.6	0.25	0.035	3.4
2	1.8	0.42529	6.56	1.7207	0.3661	1.5	4.9494
3	1.8	0.38309	5.7	1.7098	0.36072	1.5	4.9623
4	1.8	0.29954	5.69	1.7725	0.27481	1.5	4.1629
5	1.8	0.36	5.4	1.6909	0.32727	0.44	4.7667
6	1.8	0.35433	7.3	1.7079	0.3189	0.4	4.9107
7	1.8	0.29898	5.66	1.7817	0.27458	1.5	4.3267
8	1.8	0.35379	6.7	1.7379	0.31034	0.41	3.915
9	1.8	0.48718	4.79	1.7521	0.42735	1.96	4.0365
10	1.8	0.48675	9.37	1.2249	0.47929	1.5	2.9106
11	1.8	0.25312	4.1	1.7297	0.21094	1.5	2.0053
12	1.8	0.55248	7.4	1.6931	0.49901	1.5	5.1791
13	1.8	0.33446	5.9	1.7392	0.30405	1.5	4.0782
14	1.8	0.285	4.1	1.73	0.25	1.5	3
15	1.8	0.285	4.1	1.73	0.25	1.5	3
16	1.8	0.35899	7.8	1.6888	0.30337	1.5	4.45

A.4 IEEE 145-Bus, 50-Generator Test System

TABLE A.13: Bus data of IEEE 145-Bus, 50-Generator System

Bus No.	Bus Type	Voltage V_m	Voltage Angle V_θ	Base kV	Generator P_g	Generator Q_g	Load P_d	Load Q_d
1	3	1.081	-4.32	500	0	0	0	0
2	3	1.0809	-4.39	500	0	0	0	0
3	3	1.1015	-4.02	25.7	0	0	0	0
4	3	1.1015	-4.02	25.7	0	0	0	0
5	3	1.1018	-4.02	25.7	0	0	0	0
6	3	1.0433	-7.84	500	0	0	0	0
7	3	1.0763	3.21	500	0	0	0	0
8	3	1.1137	1.15	100	0	0	0	0
9	3	1.0396	-8.05	500	0	0	0	0
10	3	1.0396	-8.05	500	0	0	0	0
11	3	1.0937	-10.66	100	0	0	0	0
12	3	1.0389	-8.77	500	0	0	0	0
13	3	1.0982	-11.43	100	0	0	0	0
14	3	1.0385	-9.18	500	0	0	0	0
15	3	1.0683	-9.81	100	0	0	0	0

Continued on next page

Table A.13 – *Continued from previous page*

Bus	Bus	Voltage	Voltage Angle	Base	Generator		Load	
No.	Type	V_m	V_θ	kV	P_g	Q_g	P_d	Q_d
16	3	1.0686	-9.86	100	0	0	0	0
17	3	1.0012	-9.44	500	0	0	0	0
18	3	1.0746	-10.88	100	0	0	0	0
19	3	1.0708	-10.96	100	0	0	0	0
20	3	1.1131	-10.96	100	0	0	0	0
21	3	1.1086	-11.24	100	0	0	0	0
22	3	1.0311	-3.88	500	0	0	0	0
23	3	1.0979	-5.51	100	0	0	0	0
24	3	1.0272	2.3	500	0	0	0	0
25	3	1.038	-9.87	500	0	0	0	0
26	3	1.0894	-11.37	100	0	0	0	0
27	3	1.0389	-13.07	500	0	0	0	0
28	3	1.0762	-15.28	100	0	0	0	0
29	3	1.0746	-15.44	100	0	0	0	0
30	3	1.0731	-5.35	100	0	0	0	0
31	3	1.0905	-11.81	100	0	0	0	0
32	3	1.0937	-10.66	100	0	0	0	0
33	3	1.1392	-4.06	220	0	0	0	0
34	3	1.1387	-4	220	0	0	45.05	46.56
35	3	1.139	-4.08	220	0	0	49.19	27.53
36	3	1.1385	-3.82	220	0	0	0	0
37	3	1.1235	-6.23	220	0	0	0	0
38	3	1.1306	-5.29	220	0	0	0	0
39	3	1.127	-7.92	220	0	0	0	0
40	3	1.1269	-7.92	220	0	0	0	0
41	3	1.1188	-10.43	100	0	0	0	0
42	3	1.1188	-10.45	100	0	0	0	0
43	3	1.1189	-10.4	220	0	0	0	0
44	3	1.1189	-10.42	220	0	0	0	0
45	3	1.1173	-11.41	220	0	0	0	0
46	3	1.1173	-11.41	220	0	0	0	0
47	3	1.1275	-6.73	100	0	0	0	0
48	3	1.1278	-6.71	100	0	0	0	0
49	3	1.1279	-6.7	220	0	0	0	0
50	3	1.1276	-6.72	220	0	0	0	0
51	3	1.1124	-10.16	220	0	0	58.45	28.44

Continued on next page

Table A.13 – *Continued from previous page*

Bus	Bus	Voltage	Voltage Angle	Base	Generator		Load	
No.	**Type**	V_m	V_θ	**kV**	P_g	Q_g	P_d	Q_d
52	3	1.1118	-11.13	100	0	0	0	0
53	3	1.1118	-11.13	100	0	0	0	0
54	3	1.1131	-11.79	100	0	0	0	0
55	3	1.1131	-11.79	100	0	0	0	0
56	3	1.1072	-9.94	100	0	0	0	0
57	3	1.1072	-9.94	100	0	0	0	0
58	3	1.1067	-9.76	100	0	0	76.3	-10.8
59	3	1.1165	-10.84	100	0	0	0	0
60	2	1.137	-6.37	100	0.51	0.3292	0	0
61	3	1.1144	-11.89	220	0	0	0	0
62	3	1.0566	-14.47	100	0	0	0	0
63	3	1.1109	-13.98	100	0	0	0	0
64	3	1.098	-9.29	100	0	0	0	0
65	3	1.098	-9.29	100	0	0	0	0
66	3	1.1129	1.32	100	0	0	102.2	26.7
67	2	1.09	-5.66	100	14.86	2.852	0	0
68	3	1.2086	-30.99	100	0	0	0	-7.41
69	3	1.0968	-10.42	100	0	0	0	0
70	3	0.9998	-14.17	100	0	0	0	56.63
71	3	1.0275	-14.26	100	0	0	0	-21.2
72	3	1.1007	-11.19	100	0	0	0	0
73	3	1.0975	-11.06	100	0	0	0	0
74	3	1.0973	-11.46	100	0	0	81.9	43.7
75	3	1.1179	-15.19	100	0	0	0	0
76	3	1.0209	5.54	100	0	0	0	0
77	3	0.988	6.72	100	0	0	0	0
78	3	1.074	-5.19	100	0	0	89	26.8
79	2	1.052	-9.51	100	2.502	-0.1595	9.1	3
80	2	1.069	-8.21	100	0.47	-0.1506	17.1	5
81	3	1.1304	-25.86	100	0	0	82.2	-93.1
82	2	0.975	-18.66	100	0.7	0.1715	2.1	1.1
83	3	1.0985	-5.38	100	0	0	0	0
84	3	1.1156	-9.44	100	0	0	24.3	8.2
85	3	1.1165	-13.05	100	0	0	27.4	0.3
86	3	1.0567	-14.01	100	0	0	0	0
87	3	1.0652	-7.17	100	0	0	0	0

Continued on next page

Table A.13 – *Continued from previous page*

Bus	Bus	Voltage	Voltage Angle	Base	Generator		Load	
No.	Type	V_m	V_θ	kV	P_g	Q_g	P_d	Q_d
88	3	1.1094	-8.35	100	0	0	69	20.9
89	2	1.066	3.68	100	6.73	1.3639	0.6	0.2
90	2	0.95	-7.35	100	0.22	-0.0387	4.6	1.5
91	2	1	-9.28	100	0.64	-0.0154	0	0
92	3	0.9561	-12.75	100	0	0	0	31.02
93	2	1	-1.92	18.5	7	3.7381	100.4	73.2
94	2	1.02	-0.74	100	3	0.1905	15.4	7.6
95	2	0.92	18.88	100	1.31	0.1012	6.7	2.2
96	2	1	-8.98	100	0.6	0.2111	0	0
97	2	0.967	-4.34	100	1.4	0.4563	0	0
98	2	0.97	5.19	100	4.26	-0.3273	0	0
99	2	1	1.1	18.0	2	-0.0836	10.46	5.23
100	2	1.014	0.7	100	1.7	0.5872	0	0
101	2	1.039	-6.09	100	3.109	1.4866	17.8	4.5
102	2	1.019	-4.76	100	20.4	4.889	37.6	9.2
103	2	1	1.51	100	1.35	0.0496	0	0
104	2	1.0059	13.68	100	20	5	30.2	7.6
105	2	1.007	-2.8	100	16.2	3.8834	96	167.4
106	2	1.005	-2.75	100	10.8	2.0936	64	16
107	3	1.0211	-13.57	100	0	0	-17.5	-12.8
108	2	1.014	-14.03	100	8	0.7728	0	0
109	2	0.915	-18.46	100	0.52	-0.1555	0	0
110	2	1	-1.31	18.5	7	5.1984	100.4	73.2
111	2	1	7.97	100	20	5.6372	60.4	1166
112	2	1.037	-6.26	100	3	1.4011	18.6	4.6
113	3	0.978	-4.39	24.0	0	0	0	0
114	3	0.978	-4.39	24.0	0	0	0	0
115	2	1.049	-15.61	100	24.93	1.4272	683.5	184.7
116	2	1.043	-16.86	100	27.13	6.3184	792.6	315.5
117	2	1.03	-15.32	100	26.27	2.5854	485.3	71.4
118	2	1.01	-17.79	100	42.2	6.6038	651.9	328.4
119	2	1.013	-59.41	100	89.54	47.4848	2094	3774
120	3	1.0331	-51.6	100	0	0	-408	175.1
121	2	1.046	-20.2	100	29.97	-1.6022	237.7	-17.3
122	2	1	-2.79	100	10.09	1.7404	29.2	7
123	3	1.0171	-33.12	100	0	0	-84	-19

Continued on next page

Table A.13 – *Continued from previous page*

Bus No.	Bus Type	Voltage V_m	Voltage Angle V_θ	Base kV	Generator P_g	Generator Q_g	Load P_d	Load Q_d
124	2	1	-1.89	100	30.05	5.6919	94.1	780.3
125	3	1.0084	-32.59	100	0	0	-712	-319
126	3	1.0524	-73.9	100	0	0	-333	-160
127	3	1.007	-36.4	100	0	0	-546	-72
128	2	1.025	-39.71	100	129.63	26.1082	4075	703.5
129	3	0.9802	-73.07	100	0	0	-482	-122
130	2	1.057	-51.87	100	59.37	18.3496	4328	944.3
131	2	1.042	-24.32	100	283	74.7304	21840	4320
132	2	1.042	-7.24	100	30.95	6.3342	491.9	110.2
133	3	1.0922	-11.6	100	0	0	-83	-36.3
134	2	1.044	-10.82	100	2.0626	7.40214	223.09	740.2
135	2	1.107	29.04	100	59.82	15.6484	4298	1264
136	2	1.083	4.39	100	5.195	0.005	529.51	13552
137	2	1.064	-72.73	100	1.2068	2.45076	129.46	260.8
138	3	1.1138	12.01	100	0	0	-363	-188
139	2	1.04	-10.56	100	568.34	0.0065	57718	13936
140	2	1.05	-26.16	100	231.23	67.1047	24775	6676
141	2	1.053	-9.12	100	3.7911	0.0052	327.99	11361
142	2	1.155	-10.73	100	244.49	54.9612	17737	3934
143	2	1.031	-13.66	100	52.54	21.5863	4672	1709
144	2	0.997	-8.58	100	113.97	26.8685	9602	2203
145	1	1.052	5.02	100	141.1862	29.8715	9173	1555

Bus type: (1) Slack Bus, (2) Generator bus, (3) Load bus

TABLE A.14: Line data of IEEE 145-Bus, 50- Generator System

Line Number	From Bus	To bus	Line Resistance (p.u.)	Line Reactance (p.u.)	Line Charging Susptance (p.u.)
1	1	2	0.00003	0.0008	0.0632
2	1	2	0.00003	0.0008	0.0632
3	1	3	0.00900	0.1718	0
4	1	4	0.00900	0.1718	0
5	1	5	0.00890	0.1697	0
6	1	6	0.00194	0.0209	2.3792
7	1	33	0.00010	0.006	0
8	1	93	0.00020	0.0138	0

Continued on next page

Table A.14 – *Continued from previous page*

Line Number	From Bus	To bus	Line Resistance (p.u.)	Line Reactance (p.u.)	Line Charging Susptance (p.u.)
9	1	93	0.00020	0.0138	0
10	2	6	0.00194	0.0209	2.3792
11	2	113	0.00000	0.0148	0
12	2	114	0.00018	0.0145	0
13	3	33	0.00020	0.0221	0
14	4	33	0.00020	0.0221	0
15	5	33	0.00020	0.0219	0
16	6	7	0.00129	0.0139	1.4652
17	6	9	0.00016	0.0017	0.1752
18	6	10	0.00016	0.0017	0.1752
19	6	12	0.00020	0.0021	0.8776
20	7	8	0.01120	0.1516	0
21	7	66	0.00015	0.0097	0
22	7	104	0.00036	0.019	0
23	7	104	0.00041	0.0174	0
24	8	66	0.00020	0.0299	0
25	8	66	0.00020	0.0221	0
26	9	11	0.02170	0.3062	0
27	9	69	0.00040	0.0188	0
28	10	32	0.02700	0.3041	0
29	10	69	0.00040	0.0187	0
30	11	69	0.00020	0.0262	0
31	12	13	0.02230	0.3099	0
32	12	13	0.02370	0.316	0
33	12	13	0.02370	0.316	0
34	12	14	0.00096	0.0091	0.8556
35	12	14	0.00096	0.0091	0.8556
36	12	25	0.00051	0.0055	0.625
37	12	25	0.00051	0.0055	0.625
38	12	72	0.00030	0.0189	0
39	12	72	0.00030	0.019	0
40	12	72	0.00030	0.019	0
41	13	72	0.00020	0.026	0
42	13	72	0.00030	0.0262	0
43	13	72	0.00020	0.026	0
44	14	15	0.04150	0.3996	0

Continued on next page

Table A.14 – *Continued from previous page*

Line Number	From Bus	To bus	Line Resistance (p.u.)	Line Reactance (p.u.)	Line Charging Susptance (p.u.)
45	14	16	0.01000	0.1669	0
46	14	17	0.00339	0.0367	3.4582
47	14	17	0.00352	0.0367	3.4516
48	14	58	0.00020	0.0097	0
49	15	58	0.00020	0.0255	0
50	16	58	0.00020	0.022	0
51	17	18	0.31810	1.315	0
52	17	19	0.00000	0.847	0
53	17	20	0.00000	0.8676	0
54	17	21	0.00950	0.1615	0
55	17	22	0.00228	0.0276	2.6204
56	17	59	0.00010	0.0071	0
57	18	59	0.00020	0.0298	0
58	19	59	0.00000	0.0629	0
59	20	59	0.00000	0.0638	0
60	21	59	0.00020	0.0329	0
61	22	23	0.00000	0.3787	0
62	22	24	0.00173	0.0208	1.9648
63	22	30	0.00000	0.3066	0
64	22	78	0.00000	0.0268	0
65	22	83	0.00000	0.0349	0
66	23	83	0.00040	0.0595	0
67	23	83	0.00030	0.0597	0
68	24	76	0.00020	0.0088	0
69	24	77	0.00230	0.0603	0
70	25	26	0.00600	0.1375	0
71	25	27	0.00230	0.0266	3.0508
72	25	27	0.00230	0.0266	3.0508
73	25	31	0.00820	0.1648	0
74	25	73	0.00030	0.0172	0
75	25	74	0.00040	0.0179	0
76	26	73	0.00030	0.0267	0
77	27	28	0.11530	0.7453	0
78	27	29	0.01630	0.2618	0
79	27	75	0.00016	0.01	0
80	28	75	0.00020	0.029	0

Continued on next page

Table A.14 – *Continued from previous page*

Line Number	From Bus	To bus	Line Resistance (p.u.)	Line Reactance (p.u.)	Line Charging Susptance (p.u.)
81	29	75	0.00020	0.0269	0
82	30	78	0.00000	0.0335	0
83	31	74	0.00030	0.0279	0
84	32	69	0.00020	0.0265	0
85	33	34	0.00006	0.0009	0.0006
86	33	35	0.00006	0.0009	0.0006
87	33	37	0.00996	0.0707	0.1116
88	33	38	0.00995	0.0693	0.111
89	33	39	0.00850	0.0699	0.1006
90	33	40	0.00849	0.0698	0.1004
91	33	49	0.00560	0.0493	0.0778
92	33	50	0.00560	0.0493	0.0778
93	33	110	0.00024	0.0157	0
94	33	110	0.00023	0.0156	0
95	34	36	0.00025	0.0022	0.0006
96	36	99	0.00080	0.0455	0
97	37	87	0.00093	0.0442	0
98	37	88	0.00310	0.1651	0
99	38	88	0.00310	0.1638	0
100	39	43	0.00602	0.0495	0.0712
101	39	84	0.00722	0.2786	0
102	40	44	0.00603	0.0496	0.0714
103	40	84	0.00729	0.2756	0
104	41	42	0.00050	0.1514	0
105	41	43	0.00001	0.0009	0.0006
106	42	44	0.00001	0.0009	0.0006
107	43	46	0.00618	0.0508	0.0732
108	44	45	0.00618	0.0508	0.0732
109	45	61	0.00445	0.0366	0.0526
110	45	85	0.00000	0.26	0
111	46	61	0.00445	0.0366	0.0526
112	46	85	0.00000	0.2592	0
113	47	48	0.01000	0.2306	0
114	47	50	0.00001	0.0009	0.0006
115	47	87	0.08310	0.401	0
116	48	49	0.00001	0.0009	0.0006

Continued on next page

Table A.14 – *Continued from previous page*

Line Number	From Bus	To bus	Line Resistance (p.u.)	Line Reactance (p.u.)	Line Charging Susptance (p.u.)
117	48	87	0.09980	0.436	0
118	49	51	0.00898	0.079	0.1248
119	50	51	0.00898	0.079	0.1248
120	51	52	0.00290	0.0279	0.0466
121	51	53	0.00290	0.0279	0.0466
122	51	56	0.00759	0.0483	0.0712
123	51	57	0.00759	0.0483	0.0712
124	52	53	0.00670	0.3911	0
125	52	54	0.00470	0.0293	0.0462
126	53	55	0.00470	0.0293	0.0462
127	54	55	0.05530	0.9289	0
128	54	61	0.00141	0.0087	0.0138
129	55	61	0.00141	0.0087	0.0138
130	56	57	0.00900	0.3895	0
131	56	58	0.00190	0.012	0.0178
132	57	58	0.00190	0.012	0.0178
133	58	59	0.66740	2.2175	0
134	58	72	0.03020	0.2364	0
135	58	87	0.08630	0.3906	0
136	58	98	0.01310	0.1765	0
137	58	100	0.11930	1.269	0
138	58	103	0.84160	5.5383	0
139	59	60	0.18030	5.9659	0
140	59	72	0.86130	3.0485	0
141	59	79	0.00990	0.2644	0
142	59	80	0.28760	2.3898	0
143	59	89	0.34210	9.0571	0
144	59	92	0.00700	0.5678	0
145	59	94	0.70410	5.9885	0
146	59	98	0.10600	0.5845	0
147	59	100	0.01830	0.2016	0
148	59	103	0.03680	0.3341	0
149	59	107	0.03720	0.8834	0
150	60	135	1.83100	9.7964	0
151	60	79	0.03750	1.1068	0
152	60	80	0.06550	2.6441	0

Continued on next page

Table A.14 – *Continued from previous page*

Line Number	From Bus	To bus	Line Resistance (p.u.)	Line Reactance (p.u.)	Line Charging Susptance (p.u.)
153	60	90	0.02010	1.5135	0
154	60	92	0.26400	3.7139	0
155	60	94	0.00120	0.0775	0
156	60	95	0.08550	0.9926	0
157	60	138	0.36390	1.7936	0
158	61	62	0.03620	0.2608	0
159	61	62	0.04720	0.5438	0
160	61	63	0.00812	0.0782	0.1318
161	61	63	0.00812	0.0782	0.1318
162	61	64	0.00242	0.0318	0.0568
163	61	65	0.00242	0.0318	0.0568
164	61	86	0.00132	0.032	0
165	61	86	0.00110	0.037	0
166	61	86	0.00110	0.037	0
167	62	86	0.00360	0.0501	0
168	62	86	0.00130	0.0838	0
169	63	64	0.01470	0.2825	0
170	63	65	0.01470	0.2813	0
171	63	66	0.00560	0.09	0
172	63	67	0.03210	0.2785	0
173	63	69	0.01070	0.1571	0
174	63	102	0.01060	0.1583	0
175	63	102	0.01060	0.1576	0
176	63	102	0.01070	0.1604	0
177	63	102	0.01040	0.1542	0
178	63	116	0.38970	6.8588	0
179	63	117	0.00300	0.056	0
180	63	118	0.01250	0.2425	0
181	63	124	0.12650	2.022	0
182	64	65	0.00130	0.1674	0
183	64	66	0.00390	0.0684	0
184	64	67	0.02330	0.212	0
185	64	69	0.00750	0.1196	0
186	64	97	0.43360	8.2923	0
187	64	124	0.10410	1.5375	0
188	65	66	0.00390	0.0682	0

Continued on next page

Table A.14 – *Continued from previous page*

Line Number	From Bus	To bus	Line Resistance (p.u.)	Line Reactance (p.u.)	Line Charging Susptance (p.u.)
189	65	67	0.02330	0.2111	0
190	65	69	0.00750	0.1191	0
191	65	97	0.42920	8.2582	0
192	65	124	0.10320	1.5312	0
193	66	67	0.00810	0.0675	0
194	66	68	2.47300	2.472	0
195	66	69	0.00280	0.0381	0
196	66	97	0.11190	2.6432	0
197	66	111	0.00000	0.0264	0
198	66	111	0.00057	0.0266	0
199	66	111	0.00000	0.0273	0
200	66	111	0.00057	0.0264	0
201	66	124	0.02830	0.4902	0
202	67	68	3.44300	3.7172	0
203	67	69	0.00610	0.055	0
204	67	97	0.00630	0.1166	0
205	67	119	0.22130	9.3918	0
206	67	120	0.00340	1.7847	0
207	67	121	0.00820	1.17	0
208	67	122	0.00470	0.4473	0
209	67	124	0.00030	0.0065	0
210	67	125	0.00620	0.2519	0
211	67	132	0.31940	4.3566	0
212	68	69	0.69200	0.6984	0
213	69	70	0.00850	0.3333	0
214	69	71	0.00750	0.312	0
215	69	72	0.00130	0.01	0
216	69	73	0.00980	0.0747	0
217	69	74	0.01350	0.0741	0
218	69	97	0.06740	1.5849	0
219	69	101	0.01740	0.2188	0
220	69	112	0.01750	0.2201	0
221	69	124	0.02670	0.3986	0
222	70	71	0.48910	2.6613	0
223	70	72	0.00620	0.1216	0
224	70	73	0.04240	0.9125	0

Continued on next page

Table A.14 – *Continued from previous page*

Line Number	From Bus	To bus	Line Resistance (p.u.)	Line Reactance (p.u.)	Line Charging Susptance (p.u.)
225	70	74	0.00320	0.9138	0
226	70	101	0.12480	1.0409	0
227	70	112	0.12570	1.0471	0
228	71	72	0.00600	0.1138	0
229	71	73	0.04090	0.8541	0
230	71	74	0.00180	0.8553	0
231	71	101	0.15920	1.2303	0
232	71	112	0.16030	1.2377	0
233	72	73	0.00150	0.0275	0
234	72	74	0.00280	0.0274	0
235	72	98	0.01380	0.2417	0
236	72	100	0.13370	1.7384	0
237	72	101	0.00020	0.0802	0
238	72	103	1.02240	7.5945	0
239	72	112	0.00020	0.0806	0
240	73	74	0.00070	0.0393	0
241	73	75	0.01470	0.2581	0
242	73	81	0.01220	0.3068	0
243	73	82	0.00360	2.0169	0
244	73	91	0.02710	0.5732	0
245	73	96	0.02450	0.4805	0
246	73	101	0.00440	0.6014	0
247	73	105	0.00070	0.0325	0
248	73	105	0.00070	0.0325	0
249	73	105	0.00060	0.0295	0
250	73	108	0.01820	0.5832	0
251	73	109	0.05240	3.0059	0
252	73	112	0.00430	0.605	0
253	73	121	0.02680	1.7653	0
254	74	75	0.02150	0.3277	0
255	74	81	0.03330	0.4631	0
256	74	82	0.00980	1.9859	0
257	74	91	0.04130	0.7511	0
258	74	96	0.43500	7.6901	0
259	74	101	0.03440	0.6005	0
260	74	106	0.00300	0.0335	0

Continued on next page

Table A.14 – *Continued from previous page*

Line Number	From Bus	To bus	Line Resistance (p.u.)	Line Reactance (p.u.)	Line Charging Susptance (p.u.)
261	74	106	0.00050	0.0328	0
262	74	108	0.01870	0.4544	0
263	74	109	0.10040	3.4697	0
264	74	112	0.03450	0.6042	0
265	74	121	0.03480	1.3757	0
266	75	82	0.07770	1.125	0
267	75	91	0.22550	3.1442	0
268	75	96	0.45160	4.631	0
269	75	108	0.00420	0.1049	0
270	75	109	0.10460	1.4465	0
271	75	121	0.01780	0.3172	0
272	76	77	0.00020	0.016	0
273	76	89	0.00110	0.0221	0
274	79	80	0.04400	0.0991	0
275	79	90	0.05060	2.471	0
276	79	92	0.00170	0.3032	0
277	79	94	0.12750	1.1195	0
278	79	95	0.30500	6.4154	0
279	79	107	0.07860	1.414	0
280	80	90	0.46580	5.8756	0
281	80	92	0.11920	1.5053	0
282	80	94	0.46000	2.6475	0
283	82	91	0.23490	2.4188	0
284	82	108	0.07420	0.7278	0
285	82	109	0.00710	0.2634	0
286	82	121	0.18920	2.2054	0
287	83	89	0.05820	0.3855	0
288	89	103	1.07300	4.1433	0
289	90	92	0.13800	8.2959	0
290	90	94	0.06890	1.0717	0
291	91	96	0.12240	4.2463	0
292	91	108	0.10780	0.6994	0
293	91	109	0.26990	4.2634	0
294	91	121	0.29240	2.121	0
295	92	94	0.28830	3.7717	0
296	92	107	0.01760	3.0227	0

Continued on next page

Table A.14 – *Continued from previous page*

Line Number	From Bus	To bus	Line Resistance (p.u.)	Line Reactance (p.u.)	Line Charging Susptance (p.u.)
297	94	95	0.05340	0.996	0
298	94	138	0.11250	1.8385	0
299	95	138	0.07320	0.6389	0
300	96	108	0.82150	6.1143	0
301	97	124	0.37930	1.9557	0
302	98	100	0.00630	0.3269	0
303	98	103	0.05440	1.4358	0
304	100	103	0.02490	0.4891	0
305	101	112	0.01380	0.361	0
306	102	117	0.00030	0.019	0
307	102	118	0.02670	0.3222	0
308	108	109	0.08250	1.2713	0
309	108	121	0.00090	0.0431	0
310	109	121	0.18810	3.8499	0
311	115	116	0.00080	0.0291	0
312	115	117	0.00920	0.2222	0
313	115	118	0.00440	0.0677	0
314	115	143	0.10170	0.4924	0
315	116	117	0.00191	0.0288	0
316	116	118	0.00100	0.044	0
317	116	143	0.21870	1.2896	0
318	117	118	0.00080	0.0081	0
319	117	143	0.08340	0.6854	0
320	118	131	0.89250	6.2385	0
321	118	132	0.69670	8.143	0
322	118	143	0.00110	0.0231	0
323	119	120	0.00100	0.0236	0
324	119	121	0.01100	0.2901	0
325	119	122	0.60130	5.8941	0
326	119	124	0.26180	3.394	0
327	119	125	0.00820	0.2595	0
328	119	126	0.00153	0.0179	0
329	119	127	0.11720	1.3932	0
330	119	128	0.00540	0.0516	0
331	119	129	0.00340	0.0642	0
332	119	130	0.00220	0.0163	0

Continued on next page

Table A.14 – *Continued from previous page*

Line Number	From Bus	To bus	Line Resistance (p.u.)	Line Reactance (p.u.)	Line Charging Susptance (p.u.)
333	119	131	0.00440	0.0242	0
334	119	132	0.41370	2.4027	0
335	119	144	0.85110	3.8358	0
336	120	121	0.00090	0.0779	0
337	120	122	0.06100	0.9305	0
338	120	123	0.04660	0.5011	0
339	120	124	0.02590	0.4722	0
340	120	125	0.00020	0.0555	0
341	120	127	0.00200	0.1818	0
342	120	128	0.00290	0.0743	0
343	120	129	0.02290	0.4911	0
344	120	130	0.16740	1.0675	0
345	120	131	0.06870	0.4516	0
346	120	132	0.02550	0.4566	0
347	121	122	0.01080	0.483	0
348	121	123	0.17120	1.9482	0
349	121	124	0.00600	0.3494	0
350	121	125	0.00000	0.0124	0
351	121	127	0.02040	0.8338	0
352	121	128	0.02780	0.3095	0
353	121	129	0.45450	4.254	0
354	121	131	0.21830	1.5066	0
355	121	132	0.13080	1.3815	0
356	122	123	0.58400	4.8609	0
357	122	124	0.00090	0.0552	0
358	122	125	0.00690	0.1583	0
359	122	131	0.24330	1.935	0
360	122	132	0.01870	0.2572	0
361	122	133	0.09800	0.9821	0
362	122	143	0.03120	0.4888	0
363	123	124	0.22300	1.967	0
364	123	125	0.08210	0.6062	0
365	123	131	0.17830	1.2535	0
366	123	132	0.13550	1.2041	0
367	124	125	0.00170	0.0949	0
368	124	128	1.15300	8.2513	0

Continued on next page

Table A.14 – *Continued from previous page*

Line Number	From Bus	To bus	Line Resistance (p.u.)	Line Reactance (p.u.)	Line Charging Susptance (p.u.)
369	124	131	0.10620	0.8185	0
370	124	132	0.00940	0.1612	0
371	124	133	0.03420	1.1798	0
372	124	143	0.00780	0.7607	0
373	125	127	0.07910	0.9851	0
374	125	128	0.06200	0.5991	0
375	125	129	0.42170	3.9702	0
376	125	130	1.97400	8.4854	0
377	125	131	0.12510	0.6939	0
378	125	132	0.05360	0.5086	0
379	127	128	0.00260	0.124	0
380	127	129	0.03920	1.1082	0
381	128	129	0.00100	0.0207	0
382	128	130	1.10000	2.9924	0
383	128	131	1.55900	4.0869	0
384	130	131	0.00270	0.0154	0
385	130	132	0.65090	3.031	0
386	130	144	0.75320	3.0664	0
387	131	132	0.00320	0.0411	0
388	131	133	1.07700	5.5285	0
389	131	143	0.05880	0.4055	0
390	131	144	0.00220	0.0151	0
391	132	133	0.09160	0.8229	0
392	132	143	0.00490	0.0965	0
393	132	144	0.11080	0.9827	0
394	133	143	0.36000	2.6309	0
395	134	131	0.40420	0.9144	0
396	134	136	0.06980	0.6428	0
397	134	139	0.03530	0.166	0
398	134	141	0.02300	0.1179	0
399	134	142	0.02630	0.1167	0
400	134	144	0.01450	0.0435	0
401	134	145	0.00340	0.0216	0
402	135	95	0.34480	3.4845	0
403	135	136	0.00310	0.0178	0
404	135	138	0.00840	0.1729	0

Continued on next page

Table A.14 – *Continued from previous page*

Line Number	From Bus	To bus	Line Resistance (p.u.)	Line Reactance (p.u.)	Line Charging Susptance (p.u.)
405	135	141	0.12900	0.6993	0
406	136	115	0.01200	0.0855	0
407	136	116	1.20000	4.2655	0
408	136	117	2.96900	9.0875	0
409	136	118	0.57490	1.6206	0
410	136	138	0.15810	0.5485	0
411	136	139	0.00590	0.0293	0
412	136	140	2.40300	9.378	0
413	136	141	0.00260	0.0175	0
414	136	142	0.04670	0.1709	0
415	136	143	1.76200	3.4549	0
416	136	145	0.00490	0.0539	0
417	137	139	0.01830	0.0936	0
418	137	140	2.22900	8.0228	0
419	137	145	0.08520	0.4071	0
420	139	140	0.00540	0.0239	0
421	139	141	0.00830	0.046	0
422	139	142	0.31020	1.267	0
423	139	145	0.00090	0.008	0
424	140	145	0.10880	0.48	0
425	141	115	0.00070	0.0131	0
426	141	116	0.15680	0.7448	0
427	141	117	0.37020	1.382	0
428	141	118	0.04140	0.1439	0
429	141	131	0.23310	0.8129	0
430	141	132	1.62800	7.0936	0
431	141	142	0.00180	0.0105	0
432	141	143	0.07020	0.1778	0
433	141	144	0.07560	0.2441	0
434	141	145	0.00380	0.0358	0
435	142	115	0.01660	0.1563	0
436	142	116	0.69160	2.6302	0
437	142	117	0.55960	2.2284	0
438	142	118	0.01850	0.1037	0
439	142	119	0.27420	1.8611	0
440	142	120	0.60430	7.353	0

Continued on next page

Table A.14 – *Continued from previous page*

Line Number	From Bus	To bus	Line Resistance (p.u.)	Line Reactance (p.u.)	Line Charging Susptance (p.u.)
441	142	122	0.25890	2.1732	0
442	142	124	0.17360	2.1347	0
443	142	125	1.09000	8.616	0
444	142	130	0.36080	1.8618	0
445	142	131	0.00130	0.0157	0
446	142	132	0.00550	0.081	0
447	142	133	1.63600	9.1725	0
448	142	143	0.00380	0.0187	0
449	142	144	0.00200	0.0229	0
450	142	145	0.07380	0.438	0
451	143	144	0.48630	2.3282	0
452	144	145	0.38350	1.2052	0

TABLE A.15: Dynamic data of generators of IEEE 145-Bus, 50-Generator System

Generator Number	Bus Number	xd (pu)	x'd (pu)	T'do (sec)	xq (pu)	x'q (pu)	T'qo (sec)	H (sec)
1	93	1.75	0.42700	8.5	1.72	0.65	1.24	6.47
2	104	2.39	0.28700	10	2.31	0.34	1.5	3.14
3	105	2.18	0.39600	6.615	2.08	0.6	1.5	4.43
4	106	2.18	0.39600	6.615	2.08	0.6	1.5	4.43
5	110	1.75	0.42700	8.5	1.72	0.65	1.24	6.47
6	111	2.39	0.28700	10	2.31	0.34	1.5	3.14
7	60	0	0.47690	0	0	0	0	1.41
8	67	0	0.02130	0	0	0	0	52.18
9	79	0	0.12920	0	0	0	0	6.65
10	80	0	0.66480	0	0	0	0	1.29
11	82	0	0.52910	0	0	0	0	2.12
12	89	0	0.05850	0	0	0	0	20.56
13	90	0	1.60000	0	0	0	0	0.76
14	91	0	0.37180	0	0	0	0	1.68
15	94	0	0.08390	0	0	0	0	17.34
16	95	0	0.16190	0	0	0	0	5.47
17	96	0	0.48240	0	0	0	0	2.12
18	97	0	0.21250	0	0	0	0	5.49
19	98	0	0.07950	0	0	0	0	13.96

Continued on next page

Table A.15 – *Continued from previous page*

Generator Number	**Bus Number**	**xd (pu)**	**x'd (pu)**	**T'do (sec)**	**xq (pu)**	**x'q (pu)**	**T'qo (sec)**	**H (sec)**
20	99	0	0.11460	0	0	0	0	17.11
21	100	0	0.13860	0	0	0	0	7.56
22	101	0	0.09240	0	0	0	0	12.28
23	102	1.81	0.30000	7.8	1.76	0.61	0.9	3.53
24	103	0	0.10630	0	0	0	0	8.16
25	108	0	0.02480	0	0	0	0	30.43
26	109	0	0.20290	0	0	0	0	2.66
27	112	0	0.09240	0	0	0	0	12.28
28	115	0	0.00240	0	0	0	0	97.33
29	116	0	0.00220	0	0	0	0	105.50
30	117	0	0.00170	0	0	0	0	102.16
31	118	0	0.00140	0	0	0	0	162.74
32	119	0	0.00020	0	0	0	0	348.22
33	121	0	0.00170	0	0	0	0	116.54
34	122	0	0.00890	0	0	0	0	39.24
35	124	0	0.00170	0	0	0	0	116.86
36	128	0	0.00010	0	0	0	0	503.87
37	130	0	0.00100	0	0	0	0	230.90
38	131	0	0.00010	0	0	0	0	1101.72
39	132	0	0.00160	0	0	0	0	120.35
40	134	0	0.00003	0	0	0	0	802.12
41	135	0	0.00080	0	0	0	0	232.63
42	136	0	0.00001	0	0	0	0	2018.17
43	137	0	0.00040	0	0	0	0	469.32
44	139	0	0.00010	0	0	0	0	2210.20
45	140	0	0.00030	0	0	0	0	889.19
46	141	0	0.00010	0	0	0	0	1474.22
47	142	0	0.00030	0	0	0	0	950.80
48	143	0	0.00230	0	0	0	0	204.30
49	144	0	0.00040	0	0	0	0	443.22
50	145	0	0.00180	0	0	0	0	518.08

Publications

Following papers have been published/accepted out of this thesis work:

A. International Journals

1. Bhanu Pratap Soni, Akash Saxena, Vikas Gupta and S.L. Surana, "Identification of Generator Criticality and Transient Instability by Supervising Real-Time Rotor Angle Trajectories employing RBFNN", *ISA Transactions Elsevier*, Vol. 83, pp. 66–88, 2018.
2. Akash Saxena, Bhanu Pratap Soni, Rajesh Kumar and Vikas Gupta, "Intelligent Grey Wolf Optimizer–Development and Application for Strategic Bidding in Uniform Price Spot Energy Market", *Applied Soft Computing Elsevier*, Vol. 69, pp.1–13, 2018.
3. Bhanu Pratap Soni, Akash Saxena, Vikas Gupta, S.L. Surana, "Assessment of Transient Stability through Coherent Machine Identification by Using Least-Square Support Vector Machine", *Modeling and Simulation in Engineering Hindawi*, 2018.
4. Bhanu Pratap Soni, Akash Saxena, Vikas Gupta, S.L. Surana, "Transient Stability Oriented Assessment and Preventive Control Action for Deregulated Power System", *The Journal of Engineering, IET*, Vol. 18, pp. 5345–5350, 2019.
5. Bhanu Pratap Soni, Akash Saxena, Vikas Gupta, "A Least Square Support Vector Machine-based Approach for Contingency Classification and Ranking in a Large Power System", *Cogent Engineering, Taylor & Francis*, Vol. 3, No. 1, 2016

B. International Conferences

1. Bhanu Pratap Soni, Akash Saxena, and Vikas Gupta, "Support Vector Machine based Approach for Accurate Contingency Ranking in Power System", *In India Conference (INDICON), 2015 Annual IEEE*, pp. 1-5. IEEE, 2015.

2. Bhanu Pratap Soni, Akash Saxena, Vikas Gupta, "Application of Support Vector Machines for Fast and Accurate Contingency Ranking in Large Power System", In *Information Systems Design and Intelligent Applications*, pp. 327-335, Springer, New Delhi, 2016.

3. Bhanu Pratap Soni, Akash Saxena, Vikas Gupta, "Supervised Learning Paradigm Based on Least Square Support Vector Machine for Contingency Ranking in a Large Power System", In *Proceedings of the International Congress on Information and Communication Technology*, pp. 531-539. Springer Singapore, 2016.

4. Bhanu Pratap Soni, Akash Saxena, and Vikas Gupta, "Online Identification of Coherent Generators in Power System by using SVM", *IEEE 2017 4th International Conference on Power, Control & Embedded Systems (ICPCES)*, Allahabad, India, 2017, pp.1-5.

5. Bhanu Pratap Soni, Akash Saxena, Vikas Gupta, Rajesh Kumar, S.L. Surana, "Application of ANN for Stability Assessment of Large Power System by Post-fault Rotor Angle Measurements", *IEEE International Conference Engineer Infinite (e-TechNxt-2018) ELECRAMA-2018*, Gr. Noida, India, March 2018, pp.1-5.

6. Bhanu Pratap Soni, Akash Saxena, Rajesh Kumar, Vikas Gupta, S.L. Surana, "Application of Intelligent Grey Wolf Optimizer for Transient Stability Constrained Optimal Power Flow", *8th IEEE India International Conference on Power Electronics, IICPE-2018*, Jaipur, India, Dec. 2018, pp.1-5.

Bibliography

[1] T. C. Elliott, "Standard handbook of powerplant engineering," 1989.

[2] E. C. Portante, S. F. Folga, J. A. Kavicky, and L. T. Malone, "Simulation of the september 8, 2011, san diego blackout," in *Proceedings of the Winter Simulation Conference 2014*. IEEE, 2014, pp. 1527–1538.

[3] M. Papic, "Pacific southwest blackout on september 8, 2011 at 15: 27," in *IEEE PES General Meeting*, 2013.

[4] W. Lin, Y. Tang, H. Sun, Q. Guo, H. Zhao, and B. Zeng, "Blackout in brazil power grid on february 4, 2011 and inspirations for stable operation of power grid," *Dianli Xitong Zidonghua(Automation of Electric Power Systems)*, vol. 35, no. 9, pp. 1–5, 2011.

[5] V. A. Miranda and A. V. Oliveira, "Airport slots and the internalization of congestion by airlines: An empirical model of integrated flight disruption management in brazil," *Transportation Research Part A: Policy and Practice*, vol. 116, pp. 201–219, 2018.

[6] L. L. Lai, H. T. Zhang, S. Mishra, D. Ramasubramanian, C. S. Lai, and F. Y. Xu, "Lessons learned from july 2012 indian blackout," 2012.

[7] Y. Tang, G. Bu, and J. Yi, "Analysis and lessons of the blackout in indian power grid on july 30 and 31, 2012," in *Zhongguo Dianji Gongcheng Xuebao(Proceedings of the Chinese Society of Electrical Engineering)*, vol. 32, no. 25. Chinese Society for Electrical Engineering, 2012, pp. 167–174.

[8] J. J. Romero, "Blackouts illuminate india's power problems," *IEEE spectrum*, vol. 49, no. 10, pp. 11–12, 2012.

[9] P. T. Son and N. Voropai, "The major outage in south vietnam in 2013: The nature of blackout, security measures and strategy of national power system modernization," 2015.

[10] P. Gomes, "New strategies to improve bulk power system security: lessons learned from large blackouts," in *IEEE Power Engineering Society General Meeting, 2004.* IEEE, 2004, pp. 1703–1708.

[11] N. Leelawat, C. Mateo, S. Gaspay, A. Suppasri, and F. Imamura, "Filipinos' views on the disaster information for the 2013 super typhoon haiyan in the philippines," *Int J Sustain Future Hum Secur*, vol. 2, no. 2, pp. 61–73, 2014.

[12] N. Phuangpornpitak and S. Tia, "Opportunities and challenges of integrating renewable energy in smart grid system," *Energy Procedia*, vol. 34, pp. 282–290, 2013.

[13] M. A. Kabir, M. M. H. Sajeeb, M. N. Islam, and A. H. Chowdhury, "Frequency transient analysis of countrywide blackout of bangladesh power system on 1st november, 2014," in *2015 International Conference on Advances in Electrical Engineering (ICAEE)*. IEEE, 2015, pp. 267–270.

[14] S. Masood, "Rebels tied to blackout across most of pakistan," *New York Times*, vol. 25, 2015.

[15] O. P. Veloza and F. Santamaria, "Analysis of major blackouts from 2003 to 2015: Classification of incidents and review of main causes," *The Electricity Journal*, vol. 29, no. 7, pp. 42–49, 2016.

[16] B. Liu, B. Zhou, D. Jiang, Z. Yu, X. Yang, and X. Ma, "Distributed accommodation for distributed generation–from the view of power system blackouts," in *Advances in Green Energy Systems and Smart Grid*. Springer, 2018, pp. 236–246.

[17] L. Baojie, L. Jinbo, L. Hongjie *et al.*, "Analysis of turkey blackout on march 31 2015 and lessons on china power grid," *Proc. CSEE*, vol. 36, pp. 5788–5795, 2016.

[18] Y. Shao, Y. Tang, J. Yi, and A. WANG, "Analysis and lessons of blackout in turkey power grid on march 31, 2015," *Autom. Electr. Power Syst*, vol. 40, pp. 9–14, 2016.

[19] G. Liang, S. R. Weller, J. Zhao, F. Luo, and Z. Y. Dong, "The 2015 ukraine blackout: Implications for false data injection attacks," *IEEE Transactions on Power Systems*, vol. 32, no. 4, pp. 3317–3318, 2016.

[20] J. E. Sullivan and D. Kamensky, "How cyber-attacks in ukraine show the vulnerability of the us power grid," *The Electricity Journal*, vol. 30, no. 3, pp. 30–35, 2017.

[21] Z. Sheng-jie, H. Bing, W. Li-fu, and G. Liang-tao, "Enlightenments of the ukraine blackout to cyber security of global energy interconnection," *Electr. Power Inf. Commun. Technol*, vol. 14, pp. 77–83, 2016.

[22] K. Lee, E. Miguel, and C. Wolfram, "Experimental evidence on the demand for and costs of rural electrification," National Bureau of Economic Research, Tech. Rep., 2016.

[23] T. Bambaravanage, S. Kumarawadu, and A. Rodrigo, "Comparison of three under-frequency load shedding schemes referring to the power system of sri lanka," *Engineer: Journal of the Institution of Engineers, Sri Lanka*, vol. 49, no. 1, 2016.

[24] R. Yan, T. K. Saha, F. Bai, H. Gu *et al.*, "The anatomy of the 2016 south australia blackout: a catastrophic event in a high renewable network," *IEEE Transactions on Power Systems*, vol. 33, no. 5, pp. 5374–5388, 2018.

[25] I. Dobson and D. E. Newman, "Cascading blackout overall structure and some implications for sampling and mitigation," *International Journal of Electrical Power & Energy Systems*, vol. 86, pp. 29–32, 2017.

[26] T. A. R. EnergíA, "Ose dice que se solucionaron fallas," Technical Report, 26 August 2017. Available online: http://www. elpais. com . . . , Tech. Rep.

[27] J. F. Hauer, N. B. Bhatt, K. Shah, and S. Kolluri, "Performance of" wams east" in providing dynamic information for the north east blackout of august 14, 2003," in *IEEE Power Engineering Society General Meeting, 2004.* IEEE, 2004, pp. 1685–1690.

[28] A. Muir and J. Lopatto, "Final report on the august 14, 2003 blackout in the united states and canada: Causes and recommendations," 2004.

[29] G. Andersson, P. Donalek, R. Farmer, N. Hatziargyriou, I. Kamwa, P. Kundur, N. Martins, J. Paserba, P. Pourbeik, J. Sanchez-Gasca *et al.*, "Causes of the 2003 major grid blackouts in north america and europe, and recommended means to improve system dynamic performance," *IEEE transactions on Power Systems*, vol. 20, no. 4, pp. 1922–1928, 2005.

[30] S. Larsson and A. Danell, "The black-out in southern sweden and eastern denmark, september 23, 2003." in *2006 IEEE PES Power Systems Conference and Exposition.* IEEE, 2006, pp. 309–313.

[31] S. Corsi and C. Sabelli, "General blackout in italy sunday september 28, 2003, h. 03: 28: 00," in *IEEE Power Engineering Society General Meeting, 2004.* IEEE, 2004, pp. 1691–1702.

[32] A. Berizzi, "The italian 2003 blackout," in *IEEE Power Engineering Society General Meeting, 2004.* IEEE, 2004, pp. 1673–1679.

[33] P. Kundur, "Power system stability and control," *McGraw-Hill*, vol. 7, 1994.

[34] H. Haes Alhelou, M. E. Hamedani-Golshan, T. C. Njenda, and P. Siano, "A survey on power system blackout and cascading events: Research motivations and challenges," *Energies*, vol. 12, no. 4, p. 682, 2019.

[35] P. Kundur, J. Paserba, V. Ajjarapu, G. Andersson, A. Bose, C. Canizares, N. Hatziargyriou, D. Hill, A. Stankovic, C. Taylor *et al.*, "Definition and classification of power system stability ieee/cigre joint task force on stability terms and definitions," *IEEE transactions on Power Systems*, vol. 19, no. 3, pp. 1387–1401, 2004.

[36] G. S. Vassell, "The northeast blackout of 1965," *Public Utilities Fortnightly;(United States)*, vol. 126, no. 8, 1990.

[37] B. F. Wollenberg, "In my view-from blackout to blackout-1965 to 2003: how far have we come with reliability?" *IEEE Power and Energy Magazine*, vol. 2, no. 1, pp. 88–86, 2004.

[38] M. Pai and P. W. Sauer, "Stability analysis of power systems by lyapunov's direct method," *IEEE Control Systems Magazine*, vol. 9, no. 1, pp. 23–27, 1989.

[39] S. Singh and S. Srivastava, "Improved voltage and reactive power distribution factors for outage studies," *IEEE Transactions on Power systems*, vol. 12, no. 3, pp. 1085–1093, 1997.

[40] M. Lauby, "Evaluation of a local dc load flow screening method for branch contingency selection of overloads," *IEEE transactions on power systems*, vol. 3, no. 3, pp. 923–928, 1988.

[41] T. Medicherla and S. Rastogi, "A voltage-criterion based contingency selection technique," *IEEE Transactions on Power Apparatus and Systems*, no. 9, pp. 3523–3531, 1982.

[42] C. Castro, A. Bose, E. Handschin, and W. Hoffmann, "Comparison of different screening techniques for the contingency selection function," *International Journal of Electrical Power & Energy Systems*, vol. 18, no. 7, pp. 425–430, 1996.

[43] K. S. Swarup and G. Sudhakar, "Neural network approach to contingency screening and ranking in power systems," *Neurocomputing*, vol. 70, no. 1-3, pp. 105–118, 2006.

[44] S. Singh, L. Srivastava, and J. Sharma, "Fast voltage contingency screening and ranking using cascade neural network," *Electric Power Systems Research*, vol. 53, no. 3, pp. 197–205, 2000.

[45] L. Srivastava, S. Singh, and J. Sharma, "A hybrid neural network model for fast voltage contingency screening and ranking," *International Journal of Electrical Power & Energy Systems*, vol. 22, no. 1, pp. 35–42, 2000.

[46] R. Singh and L. Srivastava, "Line flow contingency selection and ranking using cascade neural network," *Neurocomputing*, vol. 70, no. 16-18, pp. 2645–2650, 2007.

[47] D. Devaraj, B. Yegnanarayana, and K. Ramar, "Radial basis function networks for fast contingency ranking," *International journal of electrical power & energy systems*, vol. 24, no. 5, pp. 387–393, 2002.

[48] J. Refaee, M. Mohandes, and H. Maghrabi, "Radial basis function networks for contingency analysis of bulk power systems," *IEEE Transactions on Power Systems*, vol. 14, no. 2, pp. 772–778, 1999.

[49] T. Jain, L. Srivastava, and S. Singh, "Fast voltage contingency screening using radial basis function neural network," *IEEE Transactions on Power Systems*, vol. 18, no. 4, pp. 1359–1366, 2003.

[50] S. Chakrabarti and B. Jeyasurya, "An enhanced radial basis function network for voltage stability monitoring considering multiple contingencies," *Electric power systems Research*, vol. 77, no. 7, pp. 780–787, 2007.

[51] R. Misra and S. Singh, "Steady-state security analysis using artificial neural network," *Electric Power Components and Systems*, vol. 32, no. 11, pp. 1063–1081, 2004.

[52] S. Ghosh and B. Chowdhury, "Design of an artificial neural network for fast line flow contingency ranking," *International Journal of Electrical Power & Energy Systems*, vol. 18, no. 5, pp. 271–277, 1996.

[53] K. S. Swarup, "Artificial neural network using pattern recognition for security assessment and analysis," *Neurocomputing*, vol. 71, no. 4-6, pp. 983–998, 2008.

[54] R. Fischl, M. Kam, J.-C. Chow, and S. Ricciardi, "Screening power system contingencies using a back-propagation trained multiperceptron," in *Circuits and Systems, 1989., IEEE International Symposium on.* IEEE, 1989, pp. 486–489.

[55] R. Thomas, E. Sakk, K. Hashemi, B. Ku, and H. Chiang, "On-line security classification using an artificial neural network," in *Circuits and Systems, 1990., IEEE International Symposium on.* IEEE, 1990, pp. 2921–2924.

[56] S. Weerasooriya, M. El-Sharkawi, M. Damborg, and R. Marks, "Towards static-security assessment of a large-scale power system using neural networks," in *IEE Proceedings C-Generation, Transmission and Distribution*, vol. 139, no. 1. IET, 1992, pp. 64–70.

[57] S. Weerasooriya and M. El-Sharkawi, "Feature selection for static security assessment using neural networks," in *Circuits and Systems, 1992. ISCAS'92. Proceedings., 1992 IEEE International Symposium on*, vol. 4. IEEE, 1992, pp. 1693–1696.

[58] S. Ankaliki, A. Kulkarni, and T. Ananthapadmanabha, "Multi layer feed forward neural network for contingency evaluation of bulk power system," in *International Conference on Computational Intelligence and Multimedia Applications (ICCIMA 2007)*, vol. 1. IEEE, 2007, pp. 232–236.

[59] J. Souza, M. Do Coutto Filho, and M. T. Schilling, "Fast contingency selection through a pattern analysis approach," *Electric Power Systems Research*, vol. 62, no. 1, pp. 13–19, 2002.

[60] K. Lo, L. Peng, J. Macqueen, A. Ekwue, and D. Cheng, "Fast real power contingency ranking using a counterpropagation network," *IEEE Transactions on Power Systems*, vol. 13, no. 4, pp. 1259–1264, 1998.

[61] S. Chauhan, "Fast real power contingency ranking using counter propagation network: feature selection by neuro-fuzzy model," *Electric power systems research*, vol. 73, no. 3, pp. 343–352, 2005.

[62] M. Pandit, L. Srivastava, and J. Sharma, "Contingency ranking for voltage collapse using parallel self-organizing hierarchical neural network," *International journal of electrical power & energy systems*, vol. 23, no. 5, pp. 369–379, 2001.

[63] K. S. Swarup and P. B. Corthis, "Ann approach assesses system security," *IEEE Computer Applications in Power*, vol. 15, no. 3, pp. 32–38, 2002.

[64] K. Swarup and P. B. Corthis, "Power system static security assessment using self-organizing neural network." *Journal of the Indian Institute of Science*, vol. 86, no. 4, p. 327, 2013.

[65] D. Niebur and A. J. Germond, "Power system static security assessment using the kohonen neural network classifier," in *Power Industry Computer Application Conference, 1991. Conference Proceedings.* IEEE, 1991, pp. 270–277.

[66] M. Pandit, L. Srivastava, and J. Sharma, "Two-phase neural network based estimation of degree of insecurity of power system," *Computers & Electrical Engineering*, vol. 29, no. 4, pp. 489–503, 2003.

[67] ——, "Ann based voltage contingency screening and ranking using a novel feature selection technique," *Journal-Institution Of Engineers India Part El Electrical Engineering Division*, pp. 154–160, 2003.

[68] G. Joya, F. García-Lagos, and F. Sandoval, "Contingency evaluation and monitorization using artificial neural networks," *Neural Computing and Applications*, vol. 19, no. 1, pp. 139–150, 2010.

[69] M. Mohammadi and G. B. Gharehpetian, "Application of multi-class support vector machines for power system on-line static security assessment using dt-based feature and data selection algorithms," *Journal of Intelligent & Fuzzy Systems*, vol. 20, no. 3, pp. 133–146, 2009.

[70] M. Mohammadi and G. Gharehpetian, "Power system on-line static security assessment by using multi-class support vector machines," *Journal of Applied Sciences*, vol. 8, no. 12, pp. 2226–2233, 2008.

[71] M. Mohammadi and G. B. Gharehpetian, "Application of multi-class support vector machines for power system on-line static security assessment," *International Review of Electrical Engineering (IREE)*, vol. 3, no. 3, pp. 532–542, 2008.

[72] K. Niazi, C. Arora, and S. Surana, "Power system security evaluation using ann: feature selection using divergence," *Electric Power Systems Research*, vol. 69, no. 2-3, pp. 161–167, 2004.

[73] B. D. A. Selvi and N. Kamaraj, "Categorizing power system stability using clustering based support vector machines," *International Journal of Soft Computing*, vol. 2, no. 4, pp. 544–548, 2007.

[74] D. Devaraj, J. P. Roselyn, and R. U. Rani, "Artificial neural network model for voltage security based contingency ranking," *Applied Soft Computing*, vol. 7, no. 3, pp. 722–727, 2007.

[75] M. Boudour and A. Hellal, "Combined use of unsupervised and supervised learning for large-scale power system static security assessment," *International Journal of Power and Energy Systems*, vol. 26, no. 2, p. 157, 2006.

[76] I. Kamwa, R. Grondin, and L. Loud, "Time-varying contingency screening for dynamic security assessment using intelligent-systems techniques," *IEEE Transactions on Power Systems*, vol. 16, no. 3, pp. 526–536, 2001.

[77] Y. Mansour, A. Chang, J. Tamby, E. Vaahedi, B. Corns, and M. El-Sharkawi, "Large scale dynamic security screening and ranking using neural networks," *IEEE Transactions on Power Systems*, vol. 12, no. 2, pp. 954–960, 1997.

[78] Y. Mansour, E. Vaahedi, and M. A. El-Sharkawi, "Dynamic security contingency screening and ranking using neural networks," *IEEE Transactions on Neural Networks*, vol. 8, no. 4, pp. 942–950, 1997.

[79] C. Fu and A. Bose, "Contingency ranking based on severity indices in dynamic security analysis," *IEEE Transactions on power systems*, vol. 14, no. 3, pp. 980–985, 1999.

[80] K. Chan, A. Edwards, R. Dunn, and A. Daniels, "On-line dynamic security contingency screening using artificial neural networks," *IEE Proceedings-Generation, Transmission and Distribution*, vol. 147, no. 6, pp. 367–372, 2000.

[81] N. P. Patidar and J. Sharma, "A hybrid decision tree model for fast voltage contingency screening and ranking," *International Journal of Emerging Electric Power Systems*, vol. 8, no. 4, 2007.

[82] N. Patidar and J. Sharma, "Fast voltage contingency analysis of power systems using model trees," *International Journal of Reliability and Safety*, vol. 2, no. 1-2, pp. 36–50, 2008.

[83] N. Hatziargyriou, G. Contaxis, and N. Sideris, "A decision tree method for on-line steady state security assessment," *IEEE Transactions on power systems*, vol. 9, no. 2, pp. 1052–1061, 1994.

[84] T. S. Sidhu and L. Cui, "Contingency screening for steady-state security analysis by using fft and artificial neural networks," *IEEE Transactions on Power Systems*, vol. 15, no. 1, pp. 421–426, 2000.

[85] M. Pandit, L. Srivastava, and J. Sharma, "Fast voltage contingency selection using fuzzy parallel self-organizing hierarchical neural network," *IEEE Transactions on power systems*, vol. 18, no. 2, pp. 657–664, 2003.

[86] ——, "Voltage contingency ranking using fuzzified multilayer perceptron," *Electric Power Systems Research*, vol. 59, no. 1, pp. 65–73, 2001.

[87] ——, "Cascade fuzzy neural network based voltage contingency screening and ranking," *Electric Power Systems Research*, vol. 67, no. 2, pp. 143–152, 2003.

[88] I. Musirin and T. A. Rahman, "Hybrid neural network topology (hnnt) for line outage contingency ranking," in *Power Engineering Conference, 2003. PECon 2003. Proceedings. National*. IEEE, 2003, pp. 220–224.

[89] C. Chang, T. Chung, and K. Lo, "Application of pattern recognition technique to power system security analysis and optimization," *IEEE transactions on power systems*, vol. 5, no. 3, pp. 835–841, 1990.

[90] M. Matos, N. Hatziargriou, and J. P. Lopes, "Multicontingency steady state security evaluation using fuzzy clustering techniques," *IEEE Transactions on Power Systems*, vol. 15, no. 1, pp. 177–183, 2000.

[91] D. Sobajic and Y.-H. Pao, "An artificial intelligence system for power system contingency screening," *IEEE transactions on power systems*, vol. 3, no. 2, pp. 647–653, 1988.

[92] K. T. Chaturvedi, M. Pandit, L. Srivastava, J. Sharma, and R. Bhatele, "Hybrid fuzzy-neural network-based composite contingency ranking employing fuzzy curves for feature selection," *Neurocomputing*, vol. 73, no. 1-3, pp. 506–516, 2009.

[93] A. H. A. Mohamed, Sheikh Maniruzzaman, "Static security assessment of a power system using genetic-based neural network," *Electric Power Components and Systems*, vol. 29, no. 12, pp. 1111–1121, 2001.

[94] S.-J. Huang, "Static security assessment of a power system using query-based learning approaches with genetic enhancement," *IEE Proceedings-Generation, Transmission and Distribution*, vol. 148, no. 4, pp. 319–325, 2001.

[95] S. Kalyani and K. S. Swarup, "Classifier design for static security assessment using particle swarm optimization," *Applied Soft Computing*, vol. 11, no. 1, pp. 658–666, 2011.

[96] S. N. Talukdar, "Iterative multistep methods for transient stability studies," *IEEE Transactions on Power Apparatus and Systems*, no. 1, pp. 96–102, 1971.

[97] C. Tang, C. Graham, M. El-Kady, and R. Alden, "Transient stability index from conventional time domain simulation," *IEEE Transactions on Power Systems*, vol. 9, no. 3, pp. 1524–1530, 1994.

[98] A. H. El-Abiad and K. Nagappan, "Transient stability regions of multimachine power systems," *IEEE Transactions on Power Apparatus and Systems*, no. 2, pp. 169–179, 1966.

[99] Y. Dong and H. Pota, "Fast transient stability assessment using large step-size numerical integration (power systems)," in *IEE Proceedings C-Generation, Transmission and Distribution*, vol. 138, no. 4. IET, 1991, pp. 377–383.

[100] C. Gear, "Simultaneous numerical solution of differential-algebraic equations," *IEEE transactions on circuit theory*, vol. 18, no. 1, pp. 89–95, 1971.

[101] M. Haque, "Novel method of finding the first swing stability margin of a power system from time domain simulation," *IEE Proceedings-Generation, Transmission and Distribution*, vol. 143, no. 5, pp. 413–419, 1996.

[102] P. M. Anderson and A. A. Fouad, *Power system control and stability*. John Wiley & Sons, 2008.

[103] M. Pavella, "Power system transient stability assessment–traditional vs modern methods," *Control Engineering Practice*, vol. 6, no. 10, pp. 1233–1246, 1998.

[104] G. Cai, K. Chan, W. Yuan, and G. Mu, "Identification of the vulnerable transmission segment and cluster of critical machines using line transient potential energy," *International Journal of Electrical Power & Energy Systems*, vol. 29, no. 3, pp. 199–207, 2007.

[105] D. Fang and A. David, "A normalized energy function for fast transient stability assessment," *Electric Power Systems Research*, vol. 69, no. 2-3, pp. 287–293, 2004.

[106] F. Rahimi, N. Balu, and M. Lauby, "Assessing online transient stability in energy management systems," *IEEE Computer Applications in Power*, vol. 4, no. 3, pp. 44–49, 1991.

[107] S. Zhao, H. Jia, D. Fang, Y. Jiang, and X. Kong, "Criterion to evaluate power system online transient stability based on adjoint system energy function," *IET Generation, Transmission Distribution*, vol. 9, no. 1, pp. 104–112, 2015.

[108] D. Z. Fang, L. Jing, and T. S. Chung, "Corrected transient energy function-based strategy for stability probability assessment of power systems," *IET Generation, Transmission Distribution*, vol. 2, no. 3, pp. 424–432, May 2008.

[109] X. Liao, K. Liu, H. Niu, J. Luo, Y. Li, and L. Qin, "An interval taylor-based method for transient stability assessment of power systems with uncertainties," *International Journal of Electrical Power & Energy Systems*, vol. 98, pp. 108–117, 2018.

[110] M. A. Pai, K. R. Padiyar, and C. Radhakrishna, "Transient stability analysis of multimachine ac/dc power systems via energy-function method," *IEEE Transactions on Power Apparatus and Systems*, vol. PAS-100, no. 12, pp. 5027–5035, Dec 1981.

[111] H.-D. Chang, C.-C. Chu, and G. Cauley, "Direct stability analysis of electric power systems using energy functions: theory, applications, and perspective," *Proceedings of the IEEE*, vol. 83, no. 11, pp. 1497–1529, Nov 1995.

[112] S. Krishna and K. Padiyar, "Transient stability assessment using artificial neural networks," in *Industrial Technology 2000. Proceedings of IEEE International Conference on*, vol. 1. IEEE, 2000, pp. 627–632.

[113] N. Amjady and S. F. Majedi, "Transient stability prediction by a hybrid intelligent system," *IEEE Transactions on Power Systems*, vol. 22, no. 3, pp. 1275–1283, 2007.

[114] K. Sanyal, "Transient stability assessment using artificial neural network," in *2004 IEEE International Conference on Electric Utility Deregulation, Restructuring and Power Technologies. Proceedings*, vol. 2. IEEE, 2004, pp. 633–637.

[115] I. M. El-Amin and A.-A. M. Al-Shams, "Transient stability assessment using artificial neural networks," *Electric power systems research*, vol. 40, no. 1, pp. 7–16, 1997.

[116] F. Tian, X. Zhou, Z. Yu, D. Shi, Y. Chen, and Y. Huang, "A preventive transient stability control method based on support vector machine," *Electric Power Systems Research*, vol. 170, pp. 286–293, 2019.

[117] H. Wei, L. Zongxiang, W. Shuang, W. Zhang, D. Yu, Y. Rui, and L. Baisi, "Real-time transient stability assessment in power system based on improved svm," *Journal of Modern Power Systems and Clean Energy*, vol. 7, no. 1, pp. 26–37, 2019.

[118] M. Chen, Q. Liu, S. Chen, Y. Liu, C.-H. Zhang, and R. Liu, "Xgboost-based algorithm interpretation and application on post-fault transient stability status prediction of power system," *IEEE Access*, vol. 7, pp. 13 149–13 158, 2019.

[119] Y. Yuan, J. Kubokawa, and H. Sasaki, "A solution of optimal power flow with multicontingency transient stability constraints," *IEEE Transactions on Power Systems*, vol. 18, no. 3, pp. 1094–1102, 2003.

[120] D. Gan, R. J. Thomas, and R. D. Zimmerman, "Stability-constrained optimal power flow," *IEEE Transactions on Power Systems*, vol. 15, no. 2, pp. 535–540, 2000.

[121] N. Mo, Z. Zou, K. Chan, and T. Pong, "Transient stability constrained optimal power flow using particle swarm optimisation," *IET Generation, Transmission & Distribution*, vol. 1, no. 3, pp. 476–483, 2007.

[122] A. G. Bakirtzis, P. N. Biskas, C. E. Zoumas, and V. Petridis, "Optimal power flow by enhanced genetic algorithm," *IEEE Transactions on power Systems*, vol. 17, no. 2, pp. 229–236, 2002.

[123] H. Cai, C. Chung, and K. Wong, "Application of differential evolution algorithm for transient stability constrained optimal power flow," *IEEE Transactions on Power Systems*, vol. 23, no. 2, pp. 719–728, 2008.

[124] K. Ayan, U. Kılıç, and B. Baraklı, "Chaotic artificial bee colony algorithm based solution of security and transient stability constrained optimal power flow," *International Journal of Electrical Power & Energy Systems*, vol. 64, pp. 136–147, 2015.

[125] D. Prasad, A. Mukherjee, and V. Mukherjee, "Transient stability constrained optimal power flow using chaotic whale optimization algorithm," in *Handbook of Neural Computation*. Elsevier, 2017, pp. 311–332.

[126] A. J. Wood, B. F. Wollenberg, and G. B. Sheblé, *Power generation, operation, and control*. John Wiley & Sons, 2013.

[127] B. Stott, O. Alsac, and A. J. Monticelli, "Security analysis and optimization," *Proceedings of the IEEE*, vol. 75, no. 12, pp. 1623–1644, 1987.

[128] H. Saadat, *Power systems analysis of Mcgraw-Hill series in electrical and computer engineering*. McGraw-Hill, New York, 2002.

[129] N. M. Peterson, W. F. Tinney, and D. W. Bree, "Iterative linear ac power flow solution for fast approximate outage studies," *IEEE Transactions on Power Apparatus and Systems*, no. 5, pp. 2048–2056, 1972.

[130] K. Mamandur and G. Berg, "Efficient simulation of line and transformer outages in power systems," *IEEE Transactions on Power Apparatus and Systems*, no. 10, pp. 3733–3741, 1982.

[131] M. Sachdev and S. Ibrahim, "A fast approximate technique for outage studies in power system planning and operation," *IEEE Transactions on Power Apparatus and Systems*, no. 4, pp. 1133–1142, 1974.

[132] B. Stott and O. Alsac, "Fast decoupled load flow," *IEEE transactions on power apparatus and systems*, no. 3, pp. 859–869, 1974.

[133] O. Alsac and B. Stott, "Optimal load flow with steady-state security," *IEEE transactions on power apparatus and systems*, no. 3, pp. 745–751, 1974.

[134] C.-Y. Lee and N. Chen, "Distribution factors of reactive power flow in transmission line and transformer outage studies," *IEEE Transactions on Power systems*, vol. 7, no. 1, pp. 194–200, 1992.

[135] G. Ejebe and B. Wollenberg, "Automatic contingency selection," *IEEE Transactions on Power Apparatus and Systems*, no. 1, pp. 97–109, 1979.

[136] T. Mikolinnas and B. Wollenberg, "An advanced contingency selection algorithm," *IEEE Transactions on Power Apparatus and Systems*, no. 2, pp. 608–617, 1981.

[137] G. Irisarri and A. Sasson, "An automatic contingency selection method for on-line security analysis," *IEEE transactions on power apparatus and systems*, no. 4, pp. 1838–1844, 1981.

[138] T. Halpin, R. Fischl, and R. Fink, "Analysis of automatic contingency selection algorithms," *IEEE transactions on power apparatus and systems*, no. 5, pp. 938–945, 1984.

[139] B. Stott, O. Alsac, and F. Alvarado, "Analytical and computational improvements in performance-index ranking algorithms for networks," *International Journal of Electrical Power & Energy Systems*, vol. 7, no. 3, pp. 154–160, 1985.

[140] I. Dabbaghchi and G. Irisarri, "Aep automatic contingency selector: branch outage impacts on load bus voltage profile," *IEEE transactions on power systems*, vol. 1, no. 2, pp. 37–44, 1986.

[141] M. Lauby, T. Mikolinnas, and N. Peppen, "Contingency selection of branch outage causing voltage problems," *IEEE Transactions on Power Apparatus and Systems*, no. 12, pp. 3899–3904, 1983.

[142] J. Zaborszky, K.-W. Whang, and K. Prasad, "Fast contingency evaluation using concentric relaxation," *IEEE Transactions on Power Apparatus and Systems*, no. 1, pp. 28–36, 1980.

[143] F. Albuyeh, A. Bose, and B. Heath, "Reactive power considerations in automatic contingency selection," *IEEE Transactions on Power Apparatus and Systems*, no. 1, pp. 107–112, 1982.

[144] F. Galiana, "Bound estimates of the severity of line outages in power system contingency analysis and ranking," *IEEE Transactions on Power Apparatus and Systems*, no. 9, pp. 2612–2624, 1984.

[145] K. Nara, K. Tanaka, H. Kodama, R. Shoults, M. Chen, P. Van Olinda, and D. Bertagnolli, "On-line contingency selection algorithm for voltage security analysis," *IEEE transactions on power apparatus and systems*, no. 4, pp. 846–856, 1985.

[146] V. Brandwajn, "Efficient bounding method for linear contingency analysis," *IEEE Transactions on Power Systems*, vol. 3, no. 1, pp. 38–43, 1988.

[147] V. Brandwajn and M. Lauby, "Complete bounding method for ac contingency screening," *IEEE Transactions on Power systems*, vol. 4, no. 2, pp. 724–729, 1989.

[148] R. Bacher and W. Tinney, "Faster local power flow solutions: the zero mismatch approach," *IEEE Transactions on Power Systems*, vol. 4, no. 4, pp. 1345–1354, 1989.

[149] J. Chow, R. Fischl, M. Kam, H. Yan, and S. Ricciardi, "An improved hopfield model for power system contingency classification," in *IEEE international symposium on circuits and systems*. IEEE, 1990, pp. 2925–2928.

[150] L. H. Hassan, M. Moghavvemi, H. A. Almurib, and O. Steinmayer, "Current state of neural networks applications in power system monitoring and control," *International Journal of Electrical Power & Energy Systems*, vol. 51, pp. 134–144, 2013.

[151] V. S. S. Vankayala and N. D. Rao, "Artificial neural networks and their applications to power systems—a bibliographical survey," *Electric power systems research*, vol. 28, no. 1, pp. 67–79, 1993.

[152] Y. Xu, Z. Y. Dong, J. H. Zhao, P. Zhang, and K. P. Wong, "A reliable intelligent system for real-time dynamic security assessment of power systems," *IEEE Transactions on Power Systems*, vol. 27, no. 3, pp. 1253–1263, 2012.

[153] K. Verma and K. Niazi, "Supervised learning approach to online contingency screening and ranking in power systems," *International Journal of Electrical Power & Energy Systems*, vol. 38, no. 1, pp. 97–104, 2012.

[154] B. P. Soni, A. Saxena, and V. Gupta, "A least square support vector machine-based approach for contingency classification and ranking in a large power system," *Cogent Engineering*, vol. 3, no. 1, p. 1137201, 2016.

[155] D. J. Sobajic and Y.-H. Pao, "Artificial neural-net based dynamic security assessment for electric power systems," *IEEE Transactions on Power Systems*, vol. 4, no. 1, pp. 220–228, 1989.

[156] S. Kalyani and K. S. Swarup, "Classification and assessment of power system security using multiclass svm," *IEEE Transactions on Systems, Man, and Cybernetics, Part C (Applications and Reviews)*, vol. 41, no. 5, pp. 753–758, 2010.

[157] M. La Scala, A. Bose, D. J. Tylavsky, and J. S. Chai, "A highly parallel method for transient stability analysis," *IEEE Transactions on Power Systems*, vol. 5, no. 4, pp. 1439–1446, 1990.

[158] L. Chen, Y. Min, F. Xu, and K.-P. Wang, "A continuation-based method to compute the relevant unstable equilibrium points for power system transient stability analysis," *IEEE Transactions on Power Systems*, vol. 24, no. 1, pp. 165–172, 2009.

[159] A. Fouad and S. Stanton, "Transient stability of a multi-machine power system part i: Investigation of system trajectories," *IEEE transactions on power apparatus and systems*, no. 7, pp. 3408–3416, 1981.

[160] R. T. Treinen, V. Vittal, and W. Kliemann, "An improved technique to determine the controlling unstable equilibrium point in a power system," *IEEE Transactions on Circuits and Systems I: Fundamental Theory and Applications*, vol. 43, no. 4, pp. 313–323, 1996.

[161] H.-D. Chiang, F. Wu, and P. Varaiya, "Foundations of direct methods for power system transient stability analysis," *IEEE Transactions on Circuits and systems*, vol. 34, no. 2, pp. 160–173, 1987.

[162] H.-D. Chiang and C.-C. Chu, "Theoretical foundation of the bcu method for direct stability analysis of network-reduction power system. models with small transfer conductances," *IEEE Transactions on Circuits and Systems I: Fundamental Theory and Applications*, vol. 42, no. 5, pp. 252–265, 1995.

[163] H.-D. Chiang, F. F. Wu, and P. P. Varaiya, "A bcu method for direct analysis of power system transient stability," *IEEE Transactions on Power Systems*, vol. 9, no. 3, pp. 1194–1208, 1994.

[164] M. La Scala, G. Lorusso, R. Sbrizzai, and M. Trovato, "A qualitative approach to the transient stability analysis [of power systems]," *IEEE transactions on power systems*, vol. 11, no. 4, 1996.

[165] V. Vittal, E. Zhou, C. Hwang, and A.-A. Fouad, "Derivation of stability limits using analytical sensitivity of the transient energy margin," *IEEE Transactions on Power Systems*, vol. 4, no. 4, pp. 1363–1372, 1989.

[166] M. Ribbens-Pavella and F. Evans, "Direct methods for studying dynamics of large-scale electric power systems—a survey," *Automatica*, vol. 21, no. 1, pp. 1–21, 1985.

[167] K. Padiyar, *Power system dynamics: stability and control*. John Wiley New York, 1996.

[168] Y. Xue, T. Van Cutsem, and M. Ribbens-Pavella, "A simple direct method for fast transient stability assessment of large power systems," *IEEE Transactions on Power Systems*, vol. 3, no. 2, pp. 400–412, 1988.

[169] H. Sawhney and B. Jeyasurya, "A feed-forward artificial neural network with enhanced feature selection for power system transient stability assessment," *Electric Power Systems Research*, vol. 76, no. 12, pp. 1047–1054, 2006.

[170] C. A. Jensen, M. A. El-Sharkawi, and R. J. Marks, "Power system security assessment using neural networks: feature selection using fisher discrimination," *IEEE Transactions on power systems*, vol. 16, no. 4, pp. 757–763, 2001.

[171] A. N. Izzri, A. Mohamed, and I. Yahya, "A new method of transient stability assessment in power systems using ls-svm," in *Research and Development, 2007. SCOReD 2007. 5th Student Conference on*. IEEE, 2007, pp. 1–6.

[172] N. A. Wahab, A. Mohamed, and A. Hussain, "Transient stability assessment of a power system using pnn and ls-svm methods," *Journal of applied sciences*, vol. 7, no. 21, pp. 3208–3216, 2007.

[173] N. I. A. Wahab, A. Mohamed, and A. Hussain, "Fast transient stability assessment of large power system using probabilistic neural network with feature reduction techniques," *Expert systems with applications*, vol. 38, no. 9, pp. 11 112–11 119, 2011.

[174] D. Marpaka, M. H. Thursby, and S. M. Aghili, "Artificial neural net based stability study of power systems," in *IEEE Proceedings of the SOUTHEASTCON'91*. IEEE, 1991, pp. 234–238.

[175] A. Del Angel, P. Geurts, D. Ernst, M. Glavic, and L. Wehenkel, "Estimation of rotor angles of synchronous machines using artificial neural networks and local pmu-based quantities," *Neurocomputing*, vol. 70, no. 16-18, pp. 2668–2678, 2007.

[176] A. G. Bahbah and A. A. Girgis, "New method for generators' angles and angular velocities prediction for transient stability assessment of multimachine power systems using recurrent artificial neural network," *IEEE Transactions on Power Systems*, vol. 19, no. 2, pp. 1015–1022, 2004.

[177] Q. Zhou, J. Davidson, and A. Fouad, "Application of artificial neural networks in power system security and vulnerability assessment," *IEEE Transactions on Power Systems*, vol. 9, no. 1, pp. 525–532, 1994.

[178] A. Hoballah and I. Erlich, "Transient stability assessment using ann considering power system topology changes," in *2009 15th International Conference on Intelligent System Applications to Power Systems*. IEEE, 2009, pp. 1–6.

[179] R. Ebrahimpour and E. K. Abharian, "E."an improved method in transient stability assessment of a power system using committee neural networks"," *IJCSNS*, vol. 9, no. 1, pp. 119–124, 2009.

[180] L. Chunyan, T. Biqiang, and C. Xiangyi, "On-line transient stability assessment using hybrid artificial neural network," in *Industrial Electronics and Applications, 2007. ICIEA 2007. 2nd IEEE Conference on*. IEEE, 2007, pp. 342–346.

[181] M. Silveira, A. Lotufo, and C. Minussi, "Transient stability analysis of electrical power systems using a neural network based on fuzzy artmap," in *Power Tech Conference Proceedings, 2003 IEEE Bologna*, vol. 3. IEEE, 2003, pp. 7–pp.

[182] N. Amjady, "Application of a new fuzzy neural network to transient stability prediction," in *Power Engineering Society General Meeting, 2005. IEEE*. IEEE, 2005, pp. 636–643.

[183] L. Moulin, A. A. Da Silva, M. El-Sharkawi, and R. J. Marks, "Support vector machines for transient stability analysis of large-scale power systems," *IEEE Transactions on Power Systems*, vol. 19, no. 2, pp. 818–825, 2004.

[184] A. Gavoyiannis, D. Vogiatzis, D. Georgiadis, and N. Hatziargyriou, "Combined support vector classifiers using fuzzy clustering for dynamic security assessment," in *Power Engineering Society Summer Meeting, 2001*, vol. 2. IEEE, 2001, pp. 1281–1286.

[185] B. Jayasekara and U. Annakkkage, "Transient security assessment using multivariate polynomial approximation," *Electric power systems research*, vol. 77, no. 5-6, pp. 704–711, 2007.

[186] E. M. Voumvoulakis and N. D. Hatziargyriou, "Decision trees-aided self-organized maps for corrective dynamic security," *IEEE Transactions on Power Systems*, vol. 23, no. 2, pp. 622–630, 2008.

[187] K. Sun, S. Likhate, V. Vittal, V. S. Kolluri, and S. Mandal, "An online dynamic security assessment scheme using phasor measurements and decision trees," *IEEE transactions on power systems*, vol. 22, no. 4, pp. 1935–1943, 2007.

[188] M. Haque and A. Rahim, "Determination of first swing stability limit of multimachine power systems through taylor series expansions," in *IEE Proceedings C (Generation, Transmission and Distribution)*, vol. 136, no. 6. IET, 1989, pp. 373–379.

[189] M. Ribbens-Pavella, P. Murthy, J. Horward, and J. Carpentier, "Transient stability index for online stability assessment and contingency evaluation," *International Journal of Electrical Power & Energy Systems*, vol. 4, no. 2, pp. 91–99, 1982.

[190] M. Abapour and M.-R. Haghifam, "Probabilistic transient stability assessment for on-line applications," *International Journal of Electrical Power & Energy Systems*, vol. 42, no. 1, pp. 627–634, 2012.

[191] D. Ernst, D. Ruiz-Vega, M. Pavella, P. M. Hirsch, and D. Sobajic, "A unified approach to transient stability contingency filtering, ranking and assessment," *IEEE Transactions on Power Systems*, vol. 16, no. 3, pp. 435–443, 2001.

[192] J. H. Chow, R. Galarza, P. Accari, and W. W. Price, "Inertial and slow coherency aggregation algorithms for power system dynamic model reduction," *IEEE Transactions on Power Systems*, vol. 10, no. 2, pp. 680–685, 1995.

[193] H. Kim, G. Jang, and K. Song, "Dynamic reduction of the large-scale power systems using relation factor," *IEEE Transactions on Power Systems*, vol. 19, no. 3, pp. 1696–1699, 2004.

[194] D. Chaniotis and M. Pai, "Model reduction in power systems using krylov subspace methods," *IEEE Transactions on Power Systems*, vol. 20, no. 2, pp. 888–894, 2005.

[195] G. Ramaswamy, G. Verghese, L. Rouco, C. Vialas, and C. DeMarco, "Synchrony, aggregation, and multi-area eigenanalysis," *IEEE Transactions on Power Systems*, vol. 10, no. 4, pp. 1986–1993, 1995.

[196] B. Marinescu, B. Mallem, and L. Rouco, "Large-scale power system dynamic equivalents based on standard and border synchrony," *IEEE Transactions on Power Systems*, vol. 25, no. 4, pp. 1873–1882, 2010.

[197] G. N. Ramaswamy, C. Evrard, G. C. Verghese, O. Fillatre, and B. C. Lesieutre, "Extensions, simplifications, and tests of synchronic modal equivalencing (sme)," *IEEE Transactions on Power Systems*, vol. 12, no. 2, pp. 896–905, 1997.

[198] A. Al Fuhaid, "Coherency identification for power systems," *International Journal of Electrical Power & Energy Systems*, vol. 9, no. 3, pp. 149–156, 1987.

[199] K. Verma and K. Niazi, "A coherency based generator rescheduling for preventive control of transient stability in power systems," *International Journal of Electrical Power & Energy Systems*, vol. 45, no. 1, pp. 10–18, 2013.

[200] X. Lei, D. Povh, and O. Ruhle, "Industrial approaches for dynamic equivalents of large power systems," in *Power Engineering Society Winter Meeting, 2002. IEEE*, vol. 2. IEEE, 2002, pp. 1036–1042.

[201] M. Jonsson, M. Begovic, and J. Daalder, "A new method suitable for real-time generator coherency determination," *IEEE Transactions on Power Systems*, vol. 19, no. 3, pp. 1473–1482, 2004.

[202] K. K. Anaparthi, B. Chaudhuri, N. F. Thornhill, and B. C. Pal, "Coherency identification in power systems through principal component analysis," *IEEE transactions on power systems*, vol. 20, no. 3, pp. 1658–1660, 2005.

[203] M. Ariff and B. C. Pal, "Coherency identification in interconnected power system—an independent component analysis approach," *IEEE Transactions on Power Systems*, vol. 28, no. 2, pp. 1747–1755, 2013.

[204] H. A. Alsafih and R. Dunn, "Determination of coherent clusters in a multi-machine power system based on wide-area signal measurements," in *Power and Energy Society General Meeting, 2010 IEEE*. IEEE, 2010, pp. 1–8.

[205] K. Mei, S. M. Rovnyak, and C.-M. Ong, "Clustering-based dynamic event location using wide-area phasor measurements," *IEEE Transactions on Power Systems*, vol. 23, no. 2, pp. 673–679, 2008.

[206] M. Davodi, H. Modares, E. Reihani, M. Davodi, and A. Sarikhani, "Coherency approach by hybrid pso, k-means clustering method in power system," in *Power and Energy Conference, 2008. PECon 2008. IEEE 2nd International*. IEEE, 2008, pp. 1203–1207.

[207] T. Nababhushana, K. Veeramanju *et al.*, "Coherency identification using growing self organizing feature maps [power system stability]," in *Energy Management and Power Delivery, 1998. Proceedings of EMPD'98. 1998 International Conference on*, vol. 1. IEEE, 1998, pp. 113–116.

[208] I. Kamwa, A. K. Pradhan, and G. Joós, "Automatic segmentation of large power systems into fuzzy coherent areas for dynamic vulnerability assessment," *IEEE Transactions on Power Systems*, vol. 22, no. 4, pp. 1974–1985, 2007.

[209] I. Kamwa, A. K. Pradhan, G. Joos, and S. Samantaray, "Fuzzy partitioning of a real power system for dynamic vulnerability assessment," *IEEE Transactions on Power Systems*, vol. 24, no. 3, pp. 1356–1365, 2009.

[210] S. Avdakovic, E. Becirovic, A. Nuhanovic, and M. Kusljugic, "Generator coherency using the wavelet phase difference approach," *IEEE Transactions on Power Systems*, vol. 29, no. 1, pp. 271–278, 2014.

[211] N. Senroy, "Generator coherency using the hilbert–huang transform," *IEEE Transactions on Power Systems*, vol. 23, no. 4, pp. 1701–1708, 2008.

[212] P. W. Sauer, K. Demaree, and M. Pai, "Stability limited load supply and interchange capability," *IEEE transactions on power apparatus and systems*, no. 11, pp. 3637–3643, 1983.

[213] J. Carpentier, "Optimal power flows," *International Journal of Electrical Power & Energy Systems*, vol. 1, no. 1, pp. 3–15, 1979.

[214] J. Sterling, M. Pai, and P. W. Sauer, "A methodology of secure and optimal operation of a power system for dynamic contingencies," *Electric machines and power systems*, vol. 19, no. 5, pp. 639–655, 1991.

[215] S. Singh and A. David, "Dynamic security in open power market dispatch," *Electric Power Components and Systems*, vol. 30, no. 3, pp. 315–330, 2002.

[216] D.-H. Kuo and A. Bose, "A generation rescheduling method to increase the dynamic security of power systems," *IEEE Transactions on Power Systems*, vol. 10, no. 1, pp. 68–76, 1995.

[217] M. La Scala, M. Trovato, and C. Antonelli, "On-line dynamic preventive control: an algorithm for transient security dispatch," *IEEE Transactions on Power Systems*, vol. 13, no. 2, pp. 601–610, 1998.

[218] A. Mukherjee, P. K. Roy, and V. Mukherjee, "Transient stability constrained optimal power flow using oppositional krill herd algorithm," *International Journal of Electrical Power & Energy Systems*, vol. 83, pp. 283–297, 2016.

[219] K. Y. Chan, K. Chan, S. Ling, H. H. Iu, and G. Pong, "Solving multi-contingency transient stability constrained optimal power flow problems with an improved ga," in *2007 IEEE Congress on Evolutionary Computation*. IEEE, 2007, pp. 2901–2908.

[220] Y. Xia, K. Chan, and M. Liu, "Direct nonlinear primal–dual interior-point method for transient stability constrained optimal power flow," *IEE Proceedings-Generation, Transmission and Distribution*, vol. 152, no. 1, pp. 11–16, 2005.

[221] T. B. Nguyen and M. Pai, "Dynamic security-constrained rescheduling of power systems using trajectory sensitivities," *IEEE Transactions on Power Systems*, vol. 18, no. 2, pp. 848–854, 2003.

[222] K. Shubhanga and A. Kulkarni, "Stability-constrained generation rescheduling using energy margin sensitivities," *IEEE Transactions on Power Systems*, vol. 19, no. 3, pp. 1402–1413, 2004.

[223] K. Holzinger, V. Palade, R. Rabadan, and A. Holzinger, "Darwin or lamarck? future challenges in evolutionary algorithms for knowledge discovery and data mining," in *Interactive Knowledge Discovery and Data Mining in Biomedical Informatics*. Springer, 2014, pp. 35–56.

[224] A. Holzinger, D. Blanchard, M. Bloice, K. Holzinger, V. Palade, and R. Rabadan, "Darwin, lamarck, or baldwin: Applying evolutionary algorithms to machine learning techniques," in *Proceedings of the 2014 IEEE/WIC/ACM International Joint Conferences on Web Intelligence (WI) and Intelligent Agent Technologies (IAT)-Volume 02*. IEEE Computer Society, 2014, pp. 449–453.

[225] S. Mirjalili, S. M. Mirjalili, and A. Lewis, "Grey wolf optimizer," *Advances in Engineering Software*, vol. 69, pp. 46–61, 2014.

[226] A. Saxena and S. Shekhawat, "Ambient air quality classification by grey wolf optimizer based support vector machine," *Journal of environmental and public health*, vol. 2017, 2017.

[227] E. Gupta and A. Saxena, "Grey wolf optimizer based regulator design for automatic generation control of interconnected power system," *Cogent Engineering*, vol. 3, no. 1, p. 1151612, 2016.

[228] L. K. Panwar, S. Reddy, A. Verma, B. Panigrahi, and R. Kumar, "Binary grey wolf optimizer for large scale unit commitment problem," *Swarm and Evolutionary Computation*, 2017.

[229] E. Emary, H. M. Zawbaa, and A. E. Hassanien, "Binary ant lion approaches for feature selection," *Neurocomputing*, vol. 213, pp. 54–65, 2016.

[230] T. Jayabarathi, T. Raghunathan, B. Adarsh, and P. N. Suganthan, "Economic dispatch using hybrid grey wolf optimizer," *Energy*, vol. 111, pp. 630–641, 2016.

[231] A. A. Heidari and P. Pahlavani, "An efficient modified grey wolf optimizer with lévy flight for optimization tasks," *Applied Soft Computing*, vol. 60, pp. 115–134, 2017.

[232] L. Li, L. Sun, J. Guo, J. Qi, B. Xu, and S. Li, "Modified discrete grey wolf optimizer algorithm for multilevel image thresholding," *Computational intelligence and neuroscience*, vol. 2017, 2017.

[233] M. Pradhan, P. K. Roy, and T. Pal, "Oppositional based grey wolf optimization algorithm for economic dispatch problem of power system," *Ain Shams Engineering Journal*, 2017.

[234] H. R. Tizhoosh, "Opposition-based learning: a new scheme for machine intelligence," in *Computational intelligence for modelling, control and automation, 2005 and international conference on intelligent agents, web technologies and internet commerce, international conference on*, vol. 1. IEEE, 2005, pp. 695–701.

[235] Q. Xu, L. Wang, N. Wang, X. Hei, and L. Zhao, "A review of opposition-based learning from 2005 to 2012," *Engineering Applications of Artificial Intelligence*, vol. 29, pp. 1–12, 2014.

[236] X. Yao, Y. Liu, and G. Lin, "Evolutionary programming made faster," *IEEE Transactions on Evolutionary computation*, vol. 3, no. 2, pp. 82–102, 1999.

[237] J. G. Digalakis and K. G. Margaritis, "On benchmarking functions for genetic algorithms," *International journal of computer mathematics*, vol. 77, no. 4, pp. 481–506, 2001.

[238] M. Molga and C. Smutnicki, "Test functions for optimization needs," *Test functions for optimization needs*, p. 101, 2005.

[239] X.-S. Yang, "Appendix a: test problems in optimization," *Engineering optimization*, pp. 261–266, 2010.

[240] S. Mirjalili and A. Lewis, "S-shaped versus v-shaped transfer functions for binary particle swarm optimization," *Swarm and Evolutionary Computation*, vol. 9, pp. 1–14, 2013.

[241] S. Mirjalili, S. M. Mirjalili, and X.-S. Yang, "Binary bat algorithm," *Neural Computing and Applications*, vol. 25, no. 3-4, pp. 663–681, 2014.

[242] F. Wilcoxon, "Individual comparisons by ranking methods," *Biometrics bulletin*, vol. 1, no. 6, pp. 80–83, 1945.

[243] S. Mirjalili and A. H. Gandomi, "Chaotic gravitational constants for the gravitational search algorithm," *Applied Soft Computing*, vol. 53, pp. 407–419, 2017.

[244] J. Kennedy, "Particle swarm optimization," in *Encyclopedia of machine learning*. Springer, 2011, pp. 760–766.

[245] E. Rashedi, H. Nezamabadi-Pour, and S. Saryazdi, "Gsa: a gravitational search algorithm," *Information sciences*, vol. 179, no. 13, pp. 2232–2248, 2009.

[246] R. Storn and K. Price, "Differential evolution–a simple and efficient heuristic for global optimization over continuous spaces," *Journal of global optimization*, vol. 11, no. 4, pp. 341–359, 1997.

[247] M. M. Mafarja and S. Mirjalili, "Hybrid whale optimization algorithm with simulated annealing for feature selection," *Neurocomputing*, vol. 260, pp. 302–312, 2017.

[248] N. S. Altman, "An introduction to kernel and nearest-neighbor nonparametric regression," *The American Statistician*, vol. 46, no. 3, pp. 175–185, 1992.

[249] I. MathWorks, *MATLAB: the language of technical computing. Desktop tools and development environment, version 7*. MathWorks, 2005, vol. 9.

[250] R. D. Zimmerman, C. E. Murillo-Sánchez, R. J. Thomas *et al.*, "Matpower: Steady-state operations, planning, and analysis tools for power systems research and education," *IEEE Transactions on power systems*, vol. 26, no. 1, pp. 12–19, 2011.

[251] J. Yang and V. Honavar, "Feature subset selection using a genetic algorithm," in *Feature extraction, construction and selection*. Springer, 1998, pp. 117–136.

[252] L.-Y. Chuang, H.-W. Chang, C.-J. Tu, and C.-H. Yang, "Improved binary pso for feature selection using gene expression data," *Computational Biology and Chemistry*, vol. 32, no. 1, pp. 29–38, 2008.

[253] F. Gomez, A. Rajapakse, and U. Annakkage, "Transient stability prediction algorithm based on post-fault recovery voltage measurements," in *Electrical Power & Energy Conference (EPEC), 2009 IEEE*. IEEE, 2009, pp. 1–6.

[254] P. Sekhar and S. Mohanty, "Classification and assessment of power system static security using decision tree and random forest classifiers," *International Journal of Numerical Modelling: Electronic Networks, Devices and Fields*, vol. 29, no. 3, pp. 465–474, 2016.

[255] S. Kalyani and K. Swarup, "Supervised fuzzy c-means clustering technique for security assessment and classification in power systems," *International Journal of Engineering, Science and Technology*, vol. 2, no. 3, pp. 175–185, 2010.

[256] Z. Y. Dong, J. H. Zhao, and D. J. Hill, "Numerical simulation for stochastic transient stability assessment," *IEEE Transactions on Power Systems*, vol. 27, no. 4, pp. 1741–1749, Nov 2012.

[257] "TSAT user's manual," *TSAT, Power-Tech Labs Inc., 2004.*

[258] W. Li and A. Bose, "A coherency based rescheduling method for dynamic security," *IEEE Transactions on Power Systems*, vol. 13, no. 3, pp. 810–815, 1998.

[259] I. Genc, R. Diao, V. Vittal, S. Kolluri, and S. Mandal, "Decision tree-based preventive and corrective control applications for dynamic security enhancement in power systems," *IEEE Transactions on Power Systems*, vol. 25, no. 3, pp. 1611–1619, 2010.

[260] S. Grillo, S. Massucco, A. Pitto, and F. Silvestro, "Indices for fast contingency ranking in large electric power systems," in *MELECON 2010-2010 15th IEEE Mediterranean Electrotechnical Conference*. IEEE, 2010, pp. 660–666.

[261] D. Hill, I. Hiskens, and I. Mareels, "Stability theory of differential/algebraic models of power systems," *Sadhana*, vol. 18, no. 5, pp. 731–747, 1993.

[262] F. Teymouri and T. Amraee, "An milp formulation for controlled islanding coordinated with under frequeny load shedding plan," *Electric Power Systems Research*, vol. 171, pp. 116–126, 2019.

[263] S. A. Siddiqui, K. Verma, K. R. Niazi, and M. Fozdar, "Real-time monitoring of post-fault scenario for determining generator coherency and transient stability through ann," *IEEE Transactions on Industry Applications*, vol. 54, no. 1, pp. 685–692, Jan 2018.

[264] F. Hashiesh, H. E. Mostafa, A.-R. Khatib, I. Helal, and M. M. Mansour, "An intelligent wide area synchrophasor based system for predicting and mitigating transient instabilities," *IEEE Transactions on Smart Grid*, vol. 3, no. 2, pp. 645–652, 2012.

[265] C. Cortes and V. Vapnik, "Support vector machine," *Machine learning*, vol. 20, no. 3, pp. 273–297, 1995.

[266] B. P. Soni, A. Saxena, and V. Gupta, "Support vector machine based approach for accurate contingency ranking in power system," in *India Conference (INDICON), 2015 Annual IEEE*. IEEE, 2015, pp. 1–5.

[267] F. R. Gomez, A. D. Rajapakse, U. D. Annakkage, and I. T. Fernando, "Support vector machine-based algorithm for post-fault transient stability status prediction using synchronized measurements," *IEEE Transactions on Power Systems*, vol. 26, no. 3, pp. 1474–1483, 2011.

[268] P. M. Vahdati, A. Kazemi, M. H. Amini, and L. Vanfretti, "Hopf bifurcation control of power system nonlinear dynamics via a dynamic state feedback controller–part i: Theory and modeling," *IEEE Transactions on Power Systems*, vol. 32, no. 4, pp. 3217–3228, 2017.

[269] Y. Li, W. Yuan, K. Chan, and M. Liu, "Coordinated preventive control of transient stability with multi-contingency in power systems using trajectory sensitivities," *International Journal of Electrical Power & Energy Systems*, vol. 33, no. 1, pp. 147–153, 2011.

[270] J. Yan, C.-C. Liu, and U. Vaidya, "Pmu-based monitoring of rotor angle dynamics," *IEEE Transactions on Power Systems*, vol. 26, no. 4, pp. 2125–2133, 2011.

[271] E. M. Voumvoulakis and N. D. Hatziargyriou, "A particle swarm optimization method for power system dynamic security control," *IEEE Transactions on Power Systems*, vol. 25, no. 2, pp. 1032–1041, 2010.

[272] R. Zárate-Miñano, T. Van Cutsem, F. Milano, and A. J. Conejo, "Securing transient stability using time-domain simulations within an optimal power flow," *IEEE Transactions on Power Systems*, vol. 25, no. 1, pp. 243–253, 2010.

[273] N. Amjady and S. Banihashemi, "Transient stability prediction of power systems by a new synchronism status index and hybrid classifier," *IET generation, transmission & distribution*, vol. 4, no. 4, pp. 509–518, 2010.

[274] D. Lowe and D. Broomhead, "Multivariable functional interpolation and adaptive networks," *Complex systems*, vol. 2, no. 3, pp. 321–355, 1988.

[275] R. D. Zimmerman, C. E. Murillo-Sánchez, and D. Gan, "Matpower: A matlab power system simulation package," *Manual, Power Systems Engineering Research Center, Ithaca NY*, vol. 1, 1997.

[276] F. Milano, "An open source power system analysis toolbox," *IEEE Transactions on Power systems*, vol. 20, no. 3, pp. 1199–1206, 2005.

[277] J. Chow, G. Rogers, and K. Cheung, "Power system toolbox," *Cherry Tree Scientific Software*, vol. 48, p. 53, 2000.

[278] "Power system test cases," http://www.ee.washington.edu/pstca/.

[279] S. Muknahallipatna and B. H. Chowdhury, "Input dimension reduction in neural network training-case study in transient stability assessment of large systems," in *Proceedings of International Conference on Intelligent System Application to Power Systems*. IEEE, 1996, pp. 50–54.

[280] E. M. Voumvoulakis and N. D. Hatziargyriou, "A particle swarm optimization method for power system dynamic security control," *IEEE Transactions on Power Systems*, vol. 25, no. 2, pp. 1032–1041, 2009.

[281] B. Y. Bagde, B. S. Umre, and K. R. Dhenuvakonda, "An efficient transient stability-constrained optimal power flow using biogeography-based algorithm," *International Transactions on Electrical Energy Systems*, vol. 28, no. 1, p. e2467, 2018.

[282] F. Capitanescu, J. M. Ramos, P. Panciatici, D. Kirschen, A. M. Marcolini, L. Platbrood, and L. Wehenkel, "State-of-the-art, challenges, and future trends in security constrained optimal power flow," *Electric Power Systems Research*, vol. 81, no. 8, pp. 1731–1741, 2011.

[283] B. P. Soni, A. Saxena, and V. Gupta, "Online identification of coherent generators in power system by using svm," in *Power, Control & Embedded Systems (ICPCES), 2017 4th International Conference on*. IEEE, 2017, pp. 1–5.

[284] K. Tangpatiphan and A. Yokoyama, "Evolutionary programming incorporating neural network for transient stability constrained optimal power flow," in *Power System Technology and IEEE Power India Conference, 2008. POWERCON 2008. Joint International Conference on*. IEEE, 2008, pp. 1–8.

[285] H. Saadat, *Power System Analysis*. WCB/McGraw-Hill, 1999.

[286] M. Pai, *Energy function analysis for power system stability*. Springer Science & Business Media, 2012.

[287] Y. Xu, Z. Y. Dong, K. Meng, J. H. Zhao, and K. P. Wong, "A hybrid method for transient stability-constrained optimal power flow computation," *IEEE Transactions on Power Systems*, vol. 27, no. 4, pp. 1769–1777, 2012.

[288] X. Tu, L.-A. Dessaint, and H. Nguyen-Duc, "Transient stability constrained optimal power flow using independent dynamic simulation," *IET Generation, Transmission & Distribution*, vol. 7, no. 3, pp. 244–253, 2013.

[289] H. Ahmadi, H. Ghasemi, A. Haddadi, and H. Lesani, "Two approaches to transient stability-constrained optimal power flow," *International Journal of Electrical Power & Energy Systems*, vol. 47, pp. 181–192, 2013.

[290] D. Prasad, A. Mukherjee, G. Shankar, and V. Mukherjee, "Application of chaotic whale optimisation algorithm for transient stability constrained optimal power flow," *IET Science, Measurement & Technology*, vol. 11, no. 8, pp. 1002–1013, 2017.

Author's Brief Biography

Bhanu Pratap Soni is currently pursuing Ph.D. degree in Electrical Engineering from Malaviya National Institute of Technology Jaipur. He received his M.Tech. (Honours) and B.Tech. (Honours) in Electrical Engineering form Rajasthan Technical University, Kota, India in 2014 and 2011 respectively. He published 09 papers in different journals and 13 papers presented in different international conferences. His current research interests include development and application of optimization algorithm, power system stability, artificial intelligence and machine learning.